Department of Mechanical Engineering

POST-COMBUSTION CARBON CAPTURE FOR COMBINED CYCLE GAS TURBINES

Abdul'Aziz Adamu Aliyu

October 2020

POST-COMBUSTION CARBON CAPTURE FOR COMBINED CYCLE GAS TURBINES

Abdul'Aziz Adamu Aliyu

Supervisors:

Professor Mohamed Pourkashanian ❘ Professor Derek Binns Ingham
Professor Lin Ma ❘ Dr. Kevin Hughes ❘ Dr. Muhammad Akram
Dr. Alastair Clements ❘ Dr. Maria Elena Diego de Paz

Thesis report is submitted to the
Energy Institute, Faculty Engineering, University of Sheffield
in fulfilment of the requirement for the degree of Doctor of Philosophy (PhD)

20 - 10 - 2020

It is with the warmest of gratitude and profound regards that I dedicate this thesis to my beloved parents

Dr and Mrs Adamu Aliyu

For their timeless love, inspiration and unconditional support to my siblings and I

Furthermore, I will also want to dedicate this thesis to my wife and son,

Saeeda Umar Kirfi and Adam Abdul'Aziz Adamu

for been supportive in times of overwhelming research pressure and difficulty.
Adam is 3 months old, so he doesn't really know what is going on, but I pray he grows up
to be righteous and successful in the future.

ACKNOWLEDGEMENTS

DECLARATION OF AUTHORSHIP

The candidate confirms that the work submitted is his own and that appropriate credit has been given where reference has been made to the work of others.

This copy has been supplied on the understanding that it is copyright material and that no quotation from the thesis may be published without proper acknowledgement

RESEARCH OUTPUT AND PRESENTATIONS

- Aliyu A. A, Hughes K, Ma L, Ingham B. D, Pourkashanian M. Process optimization of PACT CO_2 Capture Plant with 40 wt(%) MEA. [Poster presentation]. Exhibited at the IEAGHG-International Knowledge Centre CCS Summer School, Saskatchewan, Canada. 2019.

- Aliyu A. A, Clements A, Hughes K, Ma L, Ingham B. D, Pourkashanian M. Process optimization of PACT CO_2 Capture Plant with 40 wt(%) MEA. Evaluation of the PACT CO_2 Capture with twin absorber reactors. [Oral presentation]. UKCCSRC-ECR Winter School, Sheffield. 2019.

- Aliyu A. A, Clements A, Hughes K, Ma L, Ingham B. D, Pourkashanian M. Process optimization of PCC with 40 wt(%) MEA and twin absorber columns. [Poster presentation] UKCCSRC Network Conference. 2019.

- Aliyu A. A, Clements A, Hughes K, Ma L, Ingham B. D, Pourkashanian M. Experimental investigation into Selective Exhaust Gas Recirculation. [Oral presentation]. CCUS Development in the UK: A Contemporary Academic and Industrial Perspective. Coventry. 2018.

- Aliyu A. A, Clements A, Hughes K, Ma L, Ingham B. D, Pourkashanian M. Appraisal of the PACT CO_2 capture plant with 40wt% MEA and varying PHW temperature. [Poster presentation] UKCCSRC Bi-annual meeting, Cambridge. 2018.

- Aliyu A. A, Diego E. M, Hughes K, Ma L, Ingham B. D, Pourkashanian M. Process and system optimization of the Amine Capture Plant. [Poster presentation]. UKCCSRC-ECR Winter School, Nottingham, 2017

ABSTRACT

The Intergovernmental Panel on Climate Change (IPCC) have conveyed in their fifth assessment report that anthropogenic emissions and endeavours are responsible for approximately 100 % of global warming since 1950 [1] and electricity and heat generation account for 41 % of the 32.8 billion tons of global CO_2 emission from fossil fuel combustion in 2017 [2]. There is thus a sense of urgency to capture CO_2 from large point sources of fossil fuel combustion to limit global temperature rise. Natural gas combustion is envisaged to play a fundamental role towards a zero-carbon economy as opposed to coal and oil due to its low carbon content. However, capturing CO_2 from natural gas combustion, which emits about 6.7 billion tonnes of CO_2 in 2017 is challenging as it, bestows a parasitic energy penalty on Natural Gas Combined Cycle (NGCC) power plants. This is due to the low partial pressure of CO_2 in the flue gas of gas turbines, which necessitate that substantial reboiler heat duty is employed for solvent regeneration.

To address the aforementioned impasse, pertinent experimental campaigns at the UKCCSRC-PACT National Core Facility were carried out to simulate Selective-Exhaust Gas Recirculation (S-EGR) under the influence of 40 wt(%) of Monoethanolamine (MEA). This was to enhance the driving force behind CO_2 capture and to reduce the Specific Reboiler Duty (SRD), consequently counterweigh against the forfeit on the power plant's productivity. Furthermore, the impact of varying Pressurized Hot Water (PHW) temperature at the inlet of reboiler was studied. The influence of oxidative degradation of the amine solvent at 15 vol(%) of O_2 and 5 vol(%) of CO_2 has been experimentally investigated.

Results from these studies have demonstrated that Selective Exhaust Gas Recirculation (S-EGR) is favourable in reducing the solvent regeneration energy requirement by about 25 % at CO_2 concentration of 6.6 vol(%) prior to flue gas introduction in the Post-combustion Carbon Capture (PCC) system. PHW temperature at 125 °C was identified to give the lowest SRD by 6 % against the baseline SRD. Detection of Dissolved Oxygen (DO) peaks was observed as water from the water-wash column was transferred to the absorber column which may have a possible impact on the oxidative degradation of the amine solvent in the PCC system. The concentration of the Iron in the amine solvent, which is a key indicator of the solvent decay increased by approximately 10 times from 3.68 to 36.20 mg/l over a course of 545 hours of experimental operation. Results and recommendations from these studies will potentially reduce the solvent regeneration energy requirement of the next generation PCC technologies and facilitate the global deployment of such technologies towards decarbonisation of the fossil fuel combustion industries and strengthening the efforts of limiting global temperature increase.

CONTENTS

LIST OF FIGURES

LIST OF TABLES

NOMENCLATURE

M_{CO2}	kg/h	Mass of CO₂ Captured
n_{CO2}	%	Molar fraction of CO₂
n_{CC}^{CO2}	%	n_{CO2} in conc. CO₂ stream
n_{FG}^{CO2}	%	n_{CO2} in Flue Gas
T	^{O}C, K, F	Temperature
V	m^3	Volume
x_{CO2}^{rich}	-	Rich solvent CO₂ loading
x_{CO2}^{lean}	-	Lean solvent CO₂ loading
Δx_{reg}	-	Degree of regeneration

ACRONYMS

ACP	Amine Capture Plant
AMP	2-Amino-2-methyl-l-propanol
AR6	*IPPC's* **S**ixth **A**ssessment **R**eport
BECCS	Bio-Energy with Carbon Capture and Storage
CapEx	Capital Expenditure
CC	Carbon Capture
CCGT	Combined Cycle Gas Turbine
CO	Carbon-monoxide
COO	Carboxylate ion
COOH	Carboxylic acid
CW	Cooling water
CO_2	Carbon dioxide
CHP	Combined Heat and Power
CH_4	Methane
CxHy	Hydrocarbon (Fuel)
CCP	Carbon Capture Plant
CoE	Cost of Electricity
CCR	Carbon Capture Ready
CCS	Carbon Capture and Storage (Sequestration)
CCUS	Carbon Capture, Utilization and Storage
DEA	Diethanolamine
DECC	Department of Energy and Climate Change
DCC	Direct Contact Cooler

DOE	Department of Energy
EGR	Exhaust Gas Recirculation
ESA	Electrical Swing adsorption
ECBM	Enhanced Coal Bed Methane *recovery*
EOR	Enhanced Oil Recovery
FGD	Flue gas Desulphurization
GHG	Greenhouse Gas(es)
GT	Gas Turbine
GWPs	Global Warming Potentials
HCl	Hydrogen Chloride
HCO_3	Bicarbonate
HFC	Hydrofluorocarbons
HRSG	Heat Recovery Steam Generator
IEA	International Energy Agency
IEO	International Energy Outlook
IGCC	Integrated Gasification Carbon Capture
IR	Infrared Radiation
IPCC	Intergovernmental Panel on Climate Change
ISO	International Standard Organization
kg	Kilogramme
$kJmol^{-1}$	Kilojoule per mole
kWh	Kilowatt hour
LHV	Lower Heating Value
MEA	Monoethanolamine

MDEA	Methyldiethanolamine
mGT	Micro gas turbine
Mtpa	Mega ton per annum
MJ	Megajoule
MW	Molecular Weight
MWe	Megawatt of electricity
N_2	Nitrogen
NaOH	Sodium Hydroxide
NH_3	Ammonia
NOx	Oxides of Nitrogen
NG	Natural Gas
NGCC	Natural Gas Combined Cycle
OpEx	Operating Expenditure
PACT	Pilot-scale Advanced Capture Technology
PCC	Post Combustion Carbon Capture
PCPP	Pulverised Coal Power Plant
PFC	Perfluorocarbons
PHW	Pressurized Hot Water
PTSA	Pressure Temperature Swing Adsorption
PSA	Pressure Swing Adsorption
R&D	Research and Development
RD&D	Research, Development and Demonstration
S-EGR	Specific Exhaust Gas Recirculation
SF	Supplementary firing

SRD	Specific Reboiler Duty
ST	Steam Turbine
Tcf	Trillion Cubic Feet
TSA	Temperature Swing Adsorption
UNEP	United Nations Environmental Programme
USEPA	United States Environmental Protection Agency
UNFCCC	United Nations Framework Convention on Climate Change
UKCCSRC	United Kingdom Carbon Capture and Storage Research Centre
WMO	World Meteorological Organization
ΔF	Radiative forcing

CHAPTER I

GENERAL INTRODUCTION

1.1   SYNOPSIS

Sustainability of the human race in the 21st century and beyond requires clean energy to power every sector of the economy. Approximately 67.3% of the electricity generated across the globe in 2016 is from fossil fuel [3] (*concentrated organic compounds resident in the earth, formed from the decay of plants and animals under high temperature and pressure over millions of years ago* [4]) combustion with its consequential CO_2 production, which is widely wasted into the atmosphere. The combustion process for a 1 GW of NGCC power plant and a lit dining-table candle obeys the same chemical principle. Essentially, CO_2 and H_2O are produced when hydrocarbon (fuel) is burnt under the influence of air (oxidant). The chemical representation of the process is as follows [5]:

$$CxHy + \left(x + \frac{y}{4}\right)O_2 \rightarrow xCO_2 + \frac{y}{2}H_2O \qquad (1.1)$$
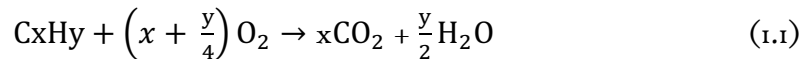
This chapter presents a synopsis of the global energy utilization and the resulting state of climate change phenomenon, which is partly as a result from increasing GHGs due to human indulgence on fossil fuel combustion and other heavy chemical processes to power the world's economy. The primary aims and objectives of the thesis are also presented in this chapter.

1.2   GREENHOUSE GASES

In 1896, a Swedish scientist, Svante Arrhenius asserted that emissions from fossil fuel combustion may be responsible for global warming. He later hypothesized the connexion between increased atmospheric CO_2 content with global temperature increase. Furthermore, Arrhenius suggested that a twofold increase in CO_2 content in the atmosphere will likely result in 5 °C temperature increase and expressed from his study that human activities are likely to be responsible for global warming [6]. This finding however received mixed reviews as the scientific community at the time maintained that human activities is insignificant to cause any dramatic change in the climatic system. The development of infrared spectroscopy in the 1940's further proved Arrhenius postulation

and in 1958 an American scientist, Charles Keeling utilized the technology at the time to take measurements and began generating a concentration curve of atmospheric CO2 in Antarctica and Mauna Loa. The global annual mean temperature began to rise sharply in the late 1980's, drumming fears of an impending global warming across a wide spectrum of intellectual community. Further studies conforming the link of GHGs and global warming eventually led to the formation of the Intergovernmental Panel on Climate Change (IPCC) in 1988 under the auspices of the United Nations Environmental Programme (UNEP) and World Meteorological Organization (WMO) to squarely address the challenges of climate change [6], [7].

In 1997, the Kyoto Protocol was adopted, charging parties to commit to the reduction of the designated six (6) greenhouse gases and their corresponding Global Warming Potentials (GWPs) namely CO2 (1), CH4 (28 – 36) , N2O (265 – 298), HFCs (1000's), PFCs (1000's) and SF6 (1000's) [8],[9]. CO2 is however, the chief greenhouse gas due to its sizeable amount released into the atmosphere and much longer atmospheric residency, thus accounts for the highest Radiative Forcing (ΔF) compared to the other GHGs as presented in Fig. 1.1.
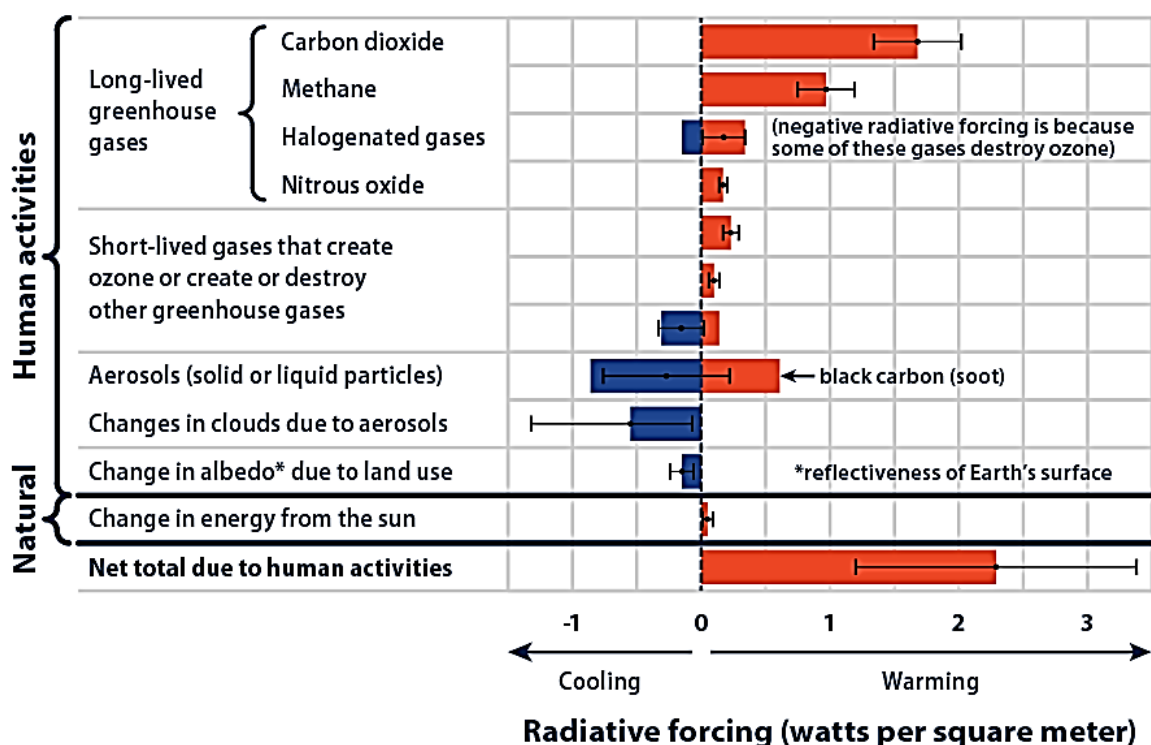
Fig. 1.1 Radioactive forcing [10].

The increase in the earth's energy budget due to GHGs absorbing Infrared Radiation (IR), technically increasing global warming signifies positive ΔF, whereas negative ΔF caused by e.g. aerosol particles results in the decrease in the earth's energy budget which causes net cooling [11]. Due to instantaneous nature of ΔF, future influences of GHGs cannot be adequately ascertained, as well as the nature of climate response to long-lived GHGs [11]. Shift in the net irradiance at the tropopause (climate sensitivity $[K/Wm^{-2}]$) is expressed as the ratio of the global mean surface temperature response (ΔT_S) to the ΔF, as represented below [12].

$$\Delta T_S / \Delta F = \Upsilon \qquad (1.2)$$

CH_4 for example is more potent than CO_2 but due to their lower anthropogenic introduction into the atmosphere, their RF (W/m^2) is lower than CO_2, which by atmospheric abundance surpasses all other GHGs. Note that water vapour is the most copious GHG, but hardly commands any RF authority due to its short-lived atmospheric residency [10].

About 65% of GHGs is CO_2 as demonstrated in the approximates of global GHG emissions as follows while electricity and heat production accounts to about a quarter of these emissions as shown in Fig 1.2 [15].
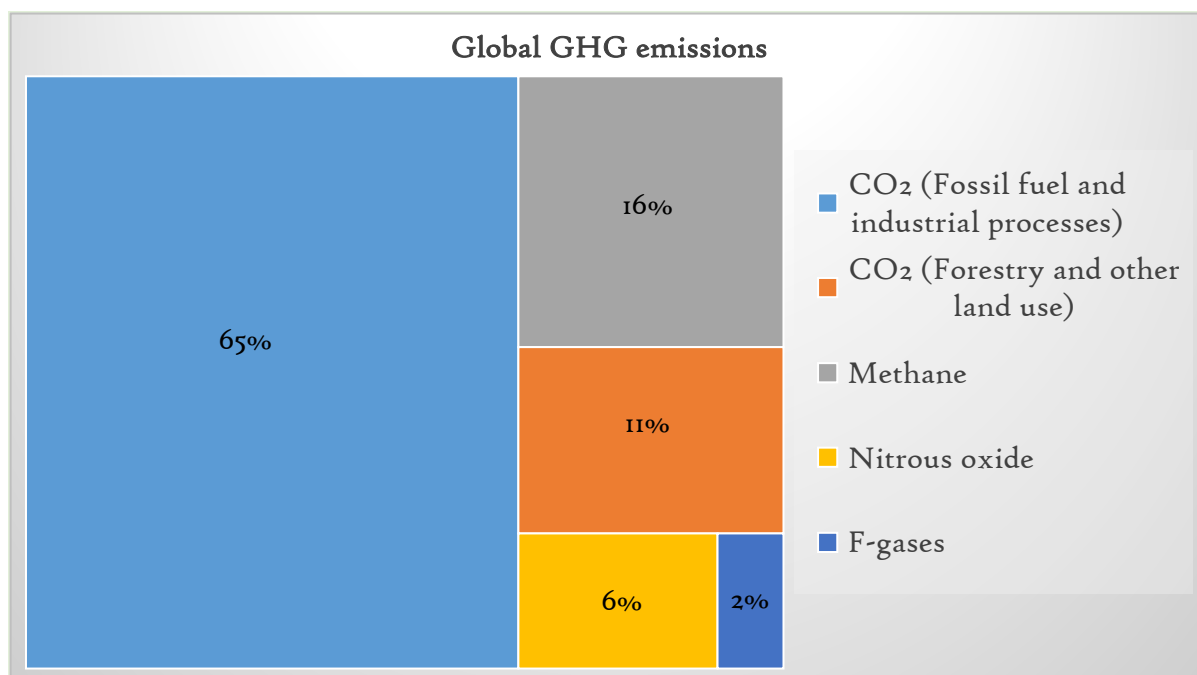
Fig. 1.2 Global GHG emissions [13]

The IPCC is currently working on its sixth appraisal and evaluation of national greenhouse gas inventories and its sixth assessment report (AR6), which is due in 2022 [14]. The efforts embarked by the United Nations Climate Change Agencies and the international communities underscores the magnitude of the consequences of climate change and are targeted towards an ambitious case scenario of limiting global temperature well below 2°C and subverting the impending negative consequence due to human induced activities of increasing GHGs into the atmosphere.

1.3   CLIMATE CHANGE

The dynamics resulting from the Earth's inbound ultraviolet and outbound infrared energies dictates the short and long-term temperature and pressure of its atmosphere. Increased retention of the outbound energy within the earth's atmosphere causes warming of the planet as represented in Fig 1.3.
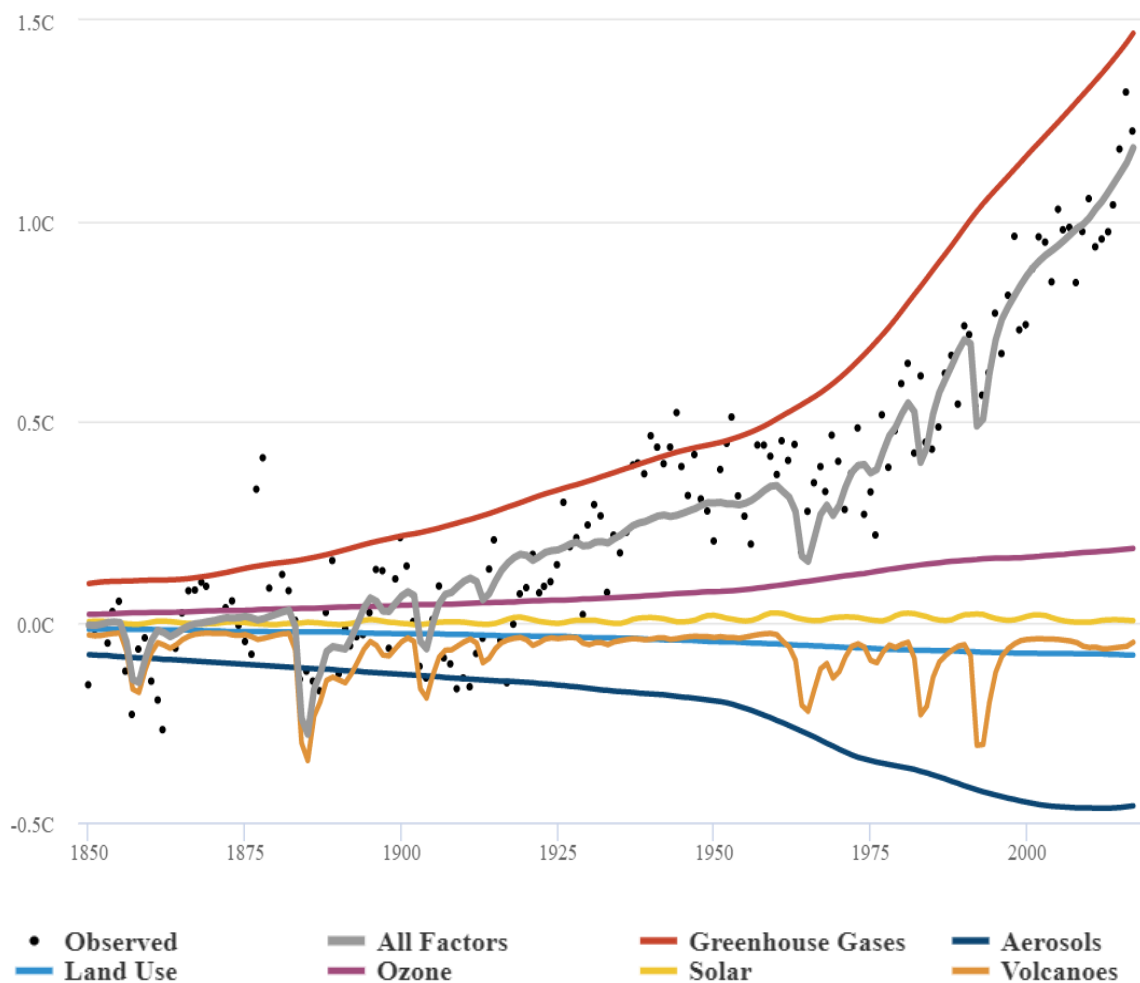
Fig 1.3 Global mean surface temperature (human and natural factors) from 1850 – 2017 [1]

4

The global warming potential is due to a cocktail of natural and anthropogenic occurrences, which include but not limited to deforestation, respiration, volcanic eruptions and emissions from chemical & energy industries. The consequential spectacle, called the greenhouse gas effect is further accelerated by the heat absorption potential of some GHGs lodged in the atmosphere [15],[16]. The Earth's climatic and weather conditions respond significantly to small shifts in its average temperature with potentially negative consequences [17],[18]. The CO_2 content in the atmosphere is at its highest in 650,000 years, global temperature has increased to about 1.7°F since 1880. Arctic and land ice is reported to decrease by 31.3%/decade and 287Gt/year respectively, and the sea level rise increase at 3.4mm/yr [18]. It is against this backdrop, among others that led the UNFCCC to first convene in 1992 towards addressing measures needed to stabilize the climate system. The Paris Agreement in 2016 was a sequel to previous Climate Change Conventions to further reinforce the resolve of the world to keep the "global temperature rise this century well below 2°C above pre-industrial levels and to pursue efforts to limit the temperature increase even lower to 1.5°C" [19]. Figures 1.4 and 1.5 strikingly demonstrates how the earth has warmth from the outset of industrial revolution to date [20].

Fig. 1.4.

| No data | 0 t | 50 million t | 500 million t | 5 billion t | 50 billion t | 100 billion t | 250 billion t | 400 billion t |
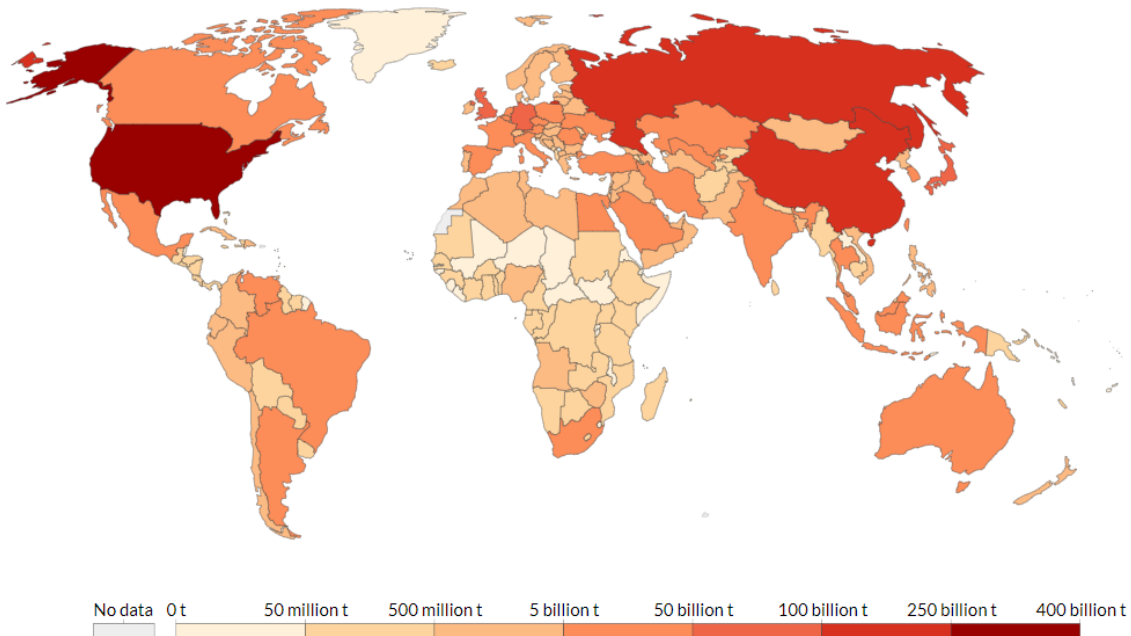
Fig. 1.5.

Figures 1.4 and 1.5 are cumulative CO_2 emission in 1751 and 2017 respectively.

Deployment of clean and sustainable energy systems based on its environmental friendliness, security of supply, smart distribution and at reasonably priced CoE eventually became imperative in achieving the main goal of decarbonizing planet earth among which power generating plants and other heavy chemical industries integrated with CCS are expected to make a noteworthy low-carbon transition.

1.4   GLOBAL ENERGY OUTLOOK

As the world's population is envisaged to increase and projected to reach 8.7 billion in 2035 [21], [22] so does energy consumption which is expected to increase by 34% in the same year, and these increases are suggestive to be synonymous to an increase in the world's economy within the growth time window [23]. Increasing hydrocarbon-based fuel combustion for energy generation to meet the needs of increasing population is evocative to higher CO_2 emissions if no credible actions are taken to address the global decarbonisation campaign in all its ramifications.

China and US produce 24.8% and 17.2% of the global electricity respectively, India (5.9%), Russia (4.4%), Japan (4.2%), Canada (2.7%), Germany (2.6%), France (2.2%), Brazil (2.3%) and Korea (2.2%) follow suit and these countries account to a staggering 66.7% global electricity production and about 66.7% of this production is from fossil fuel combustion [24], [3]. This information further underscores the need for a formidable transitional decarbonization course where CCS will play a crucial role. A visual representation of the electricity production is given in Fig 1.6, the *full data* can be accessed on the IEA energy statistics webpage [24]. Electricity per capita however takes a completely different trend due socio-economic dynamics of individual countries.

CO_2 emissions for individual countries normally depend on the energy mix utilization, population, socio-economic repute and political landscape of the country. The three primary polluters responsible for 2/3 of the total emissions from fossil fuel combustion, namely coal, oil and natural gas, and accounts for 46%, 36% and 19% of the carbon emissions, respectively [24].

Global electricity production in 2017 was 25 721 TWh, a 2.5% increase a year earlier and comprise mainly of fossil fuel (64.5%), biofuels and waste (2.3%), nuclear (10.2%), renewables (23%) [25],[26] among which the fuel combustion sector is responsible for at least two-third of the GHG emission [27]. A visual representation of electricity production is as follows and that of CO_2 emissions from fossil fuel combustion in Fig. 1.7.
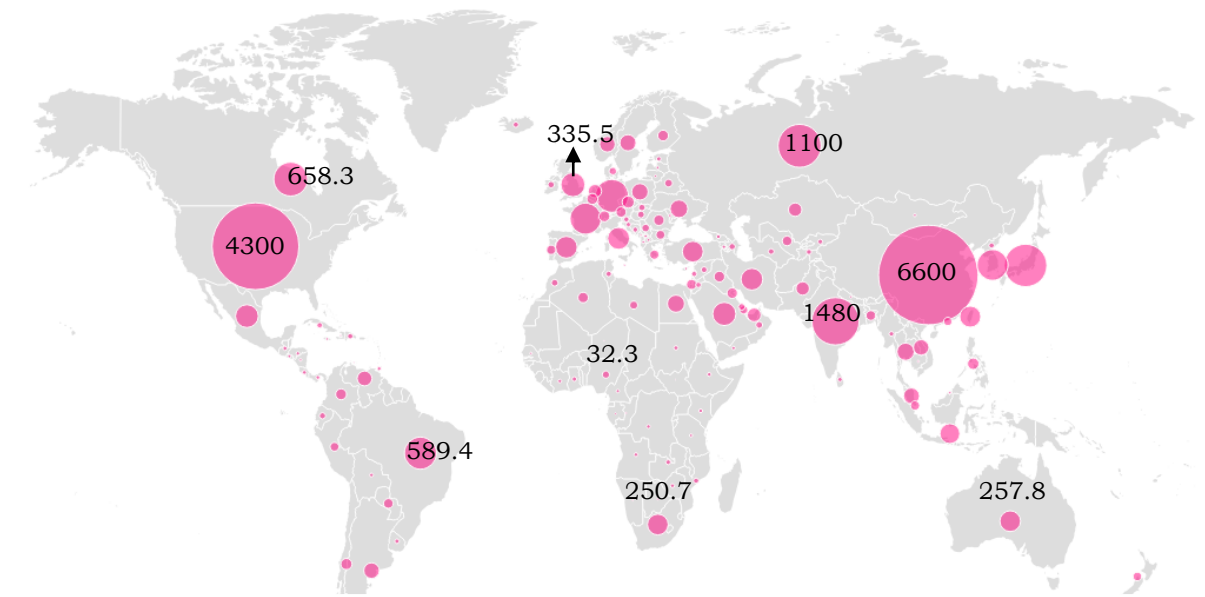
This map is without prejudice to the status of or sovereignty over any territory to the delimitation of international frontiers and boundaries and to the name of any territory, city or area

Fig. 1.6 Global electricity generation (25,082 TWh) 2016. Inset values (TWh) [24], [3].
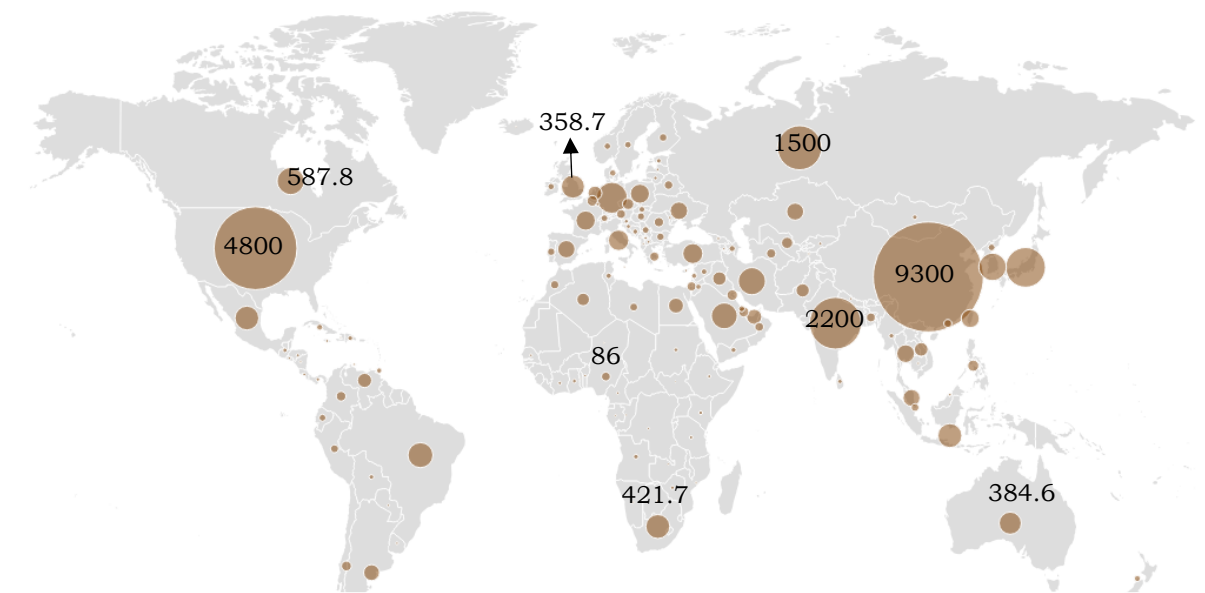
This map is without prejudice to the status of or sovereignty over any territory to the delimitation of international frontiers and boundaries and to the name of any territory, city or area

Fig. 1.7 Global CO2 emissions from fossil fuel combustion (~32 300Mt CO2) 2016 inset values (MtCO2) [24].

Gas powered plants in the UK have been asked to be prepared to be CO2 capture ready (CCR) in the event of impending legislative requirement and/or commercial viability [28].

8

This policy will lay a foundation for power plants to be fitted with a carbon capture capability in the near future and eventually lead to decarbonisation of fossil fuel combustion facilities. The chief culprit i.e. coal in global electricity generation sector (Fig 1.7) is planned to be discontinued to generate electricity in the near future. A global alliance called the 'Powering Past Coal Alliance' established in 2017 and aimed at effort towards phasing out of unabated coal power plants by 2030 (OECD), 2040 (China) and 2050 (rest of the world) [29].

On a positive turn of event, the International Energy Agency (IEA) reported in March, 2017 that in spite of global economic growth within the last three years, CO_2 emissions from the global energy industry has levelled within this time frame [30]. This development reflects the global efforts to decrease carbon emission is beginning to show encouraging results. Reassuringly, the UK has experienced a 38% decrease in GHG between 1990 to 2015 while its economy increased by 64%, this trend is a result of the ambitious binding 80% emission reduction target in the UK by 2050 [31].

1.5 SOLUTION TO CLIMATE CHANGE

10 billion people are projected to live on planet Earth by the end of the century and energy demand is expected to increase to 300%. To meet this demand and close the energy gap in the year 2100, the world is expected to demand an additional energy supply equivalent to 1,800 of the world's biggest dams or 23,000 nuclear power stations or 14 million wind turbines or 36 billion solar panels or 36,000 new fossil fuel powered stations. Deployment of these forms of energy at a measure aforementioned is at its infancy. Meanwhile, new fossil fuel reserves are being discovered across the globe every year worth trillions of dollars. The likelihood that governments and multinational oil companies are going to ignore these wealth buried underground is implausible especially with the maturing prospect of utilizing capturing CO_2 and utilizing it as a valuable raw material [32].

Technologizing green energy systems, as a climate change mitigation pathway is an option closely looked at; however, this avenue is unlikely to meet the 2°C Scenario because deployment of green energy systems at a scale and time required to meet the 2DS should have long been underway. Nuclear energy has been relegated down the line due to its long-term building and decommissioning issues, nuclear waste storage as well as risks of accidents. Geoengineering has been floated as a last resort technology, where massive

umbrellas will put into orbit to reflect solar radiation from reaching the Earth. This technology is however, unproven, costly and long-term consequences unknown. Behavioural change is worth implementing, however, this need a ground-breaking global collaboration between governments, the private sectors and individuals. This will make us to consume less meat, utilize less water as a result, less products, less energy, dispense less waste and travel less. There are 3 billion people in the world who are in the queue, waiting for their country's socio-economic indices to rise so that they can consume more, travel more and use more energy [32].

A rational conclusion in averting the consequences of global warming appears to be a mirage. Global conventions, commitments, international resolutions and politicking hasn't yielded the result that is expected and despondently, generations to come will have to bear the consequences of the actions of prior generations.

The world has approximately 3600GW of fossil fuel electricity generation capacity in 2014, and the closest competitor hydroelectric power capacity stands at 1000GW capacity and nuclear energy with about 400GW. Wind, solar, tidal, geothermal, biomass & waste forms of energy cumulatively account to approximately 600GW of installed capacity [3]. This stark statistical silhouette of global power generation capacity further signifies a huge gap to close if other forms of clean energy forms are to take over from fossil fuel.

It is worth noting to accentuate that CCS is a prerequisite mechanism for transitioning to greener forms of energy towards curbing the global temperature rise to 2°C. This will however not be viable without the complementary contribution of other sustainable forms of energy. A broad spectrum of clean energy assortment will correspondingly need to play an equally progressive role. This will include employment of all climate change mitigation processes and entail all forms of renewable energy, CHP, micro CHP, energy efficiency, improved insulation, smart metering, load shedding and nuclear energy. The fluctuation of harnessing most sustainable forms of energy and consequently higher CoE as compared to fossil fuel combustion has posed a major challenge to robust deployment of renewables, such as wind and solar.

The rational to slow deployment of clean energy is also partly due to the inability of energy producing conglomerates to desert their huge investments in fossil fuel generating plants for cleaner ones. This is not pragmatic from an economic point of view. Small shifts in investment for cleaner forms of energy appears to be cost-conscious way forward, however,

these small shifts tend to keep the CoE of cleaner energy higher due to the limited scale of production.

1.6   CCS: CONTEXT

Pacala and Socolow [33] in their 2004 technical review identified CCS among 15 different emission mitigation measures to combat global warming. Since then, the impetus for CCS has grown over time. Page [34], of the Global CCS Institute, noted in his 2016 address that pledges made by countries at the Paris Climate Change Convention are insufficient to tackle a temperature increase target of 2°C and therefore more emphasis is needed to fast track the deployment and commercialization of CCS.

The IEA projected in its 2010 CCS roadmap that 100 industrial-scale CCS projects are needed to be functional and an additional 3,300 by 2050 in its 'least-cost emission reduction pathway' to avert the cataclysmic penalties of global warming. For the global sustainable community to achieve reasonable targets of stabilizing the atmospheric CO_2 concentration, while producing energy from fossil fuel, Carbon Capture Utilization and Storage presents a huge opportunity towards meeting these targets.

Advancing and successful deploying CCS is accompanied by numerous challenges and requires expertise drawn from a number of inter-disciplinary applications, broadly including science, engineering, law and economics. Mitigation cost, technical maturity and diffusivity of CCS expertise to the developing world, and favorable policies are key to achieving the role CCS has to play in global emission reduction [35], [36].

The world's first full chain large-scale electricity generation CCS project was commissioned at Boundary Dam power station in Saskatchewan in 2014 (Fig. 1.8) and since then 43 large-scale CCS projects across the world are currently either in operation or about to be completed according to the Global CCS Institute and captioned in Fig. 1.8 [37],[40].
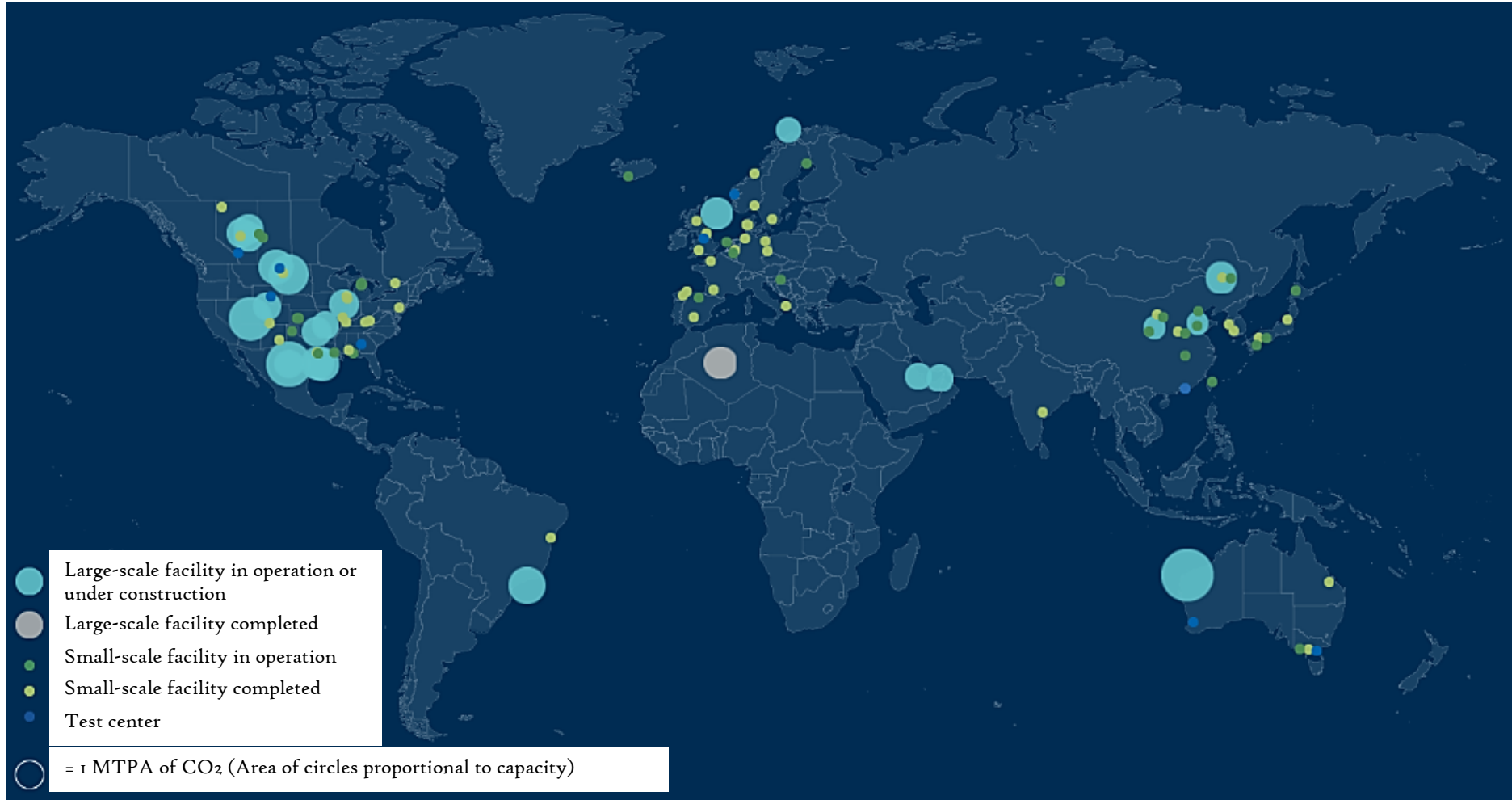
Fig 1.8   Commercial, 'pilot & demonstration' scale and test centres CCS facility across the world in 2018 [38].

It is a widely held view that three technological pathways are investigated for carbon capture; these include post, pre and oxy-fuel combustions carbon captures. The category of CCS technology employed depends on the process of fuel combustion.

1.7   CARBON CAPTURE AND STORAGE

Carbon Capture is broadly a 3-stage multifaceted process of firstly annexing, condensing and compressing CO_2 from industrial endeavors, transporting and eventually safely quarantining it in suitable geological formations for a very long term. Alternatively, the captured CO_2 can be utilized for enhanced oil recovery (EOR), Enhanced Coal Bed Methane recovery (ECBM), chemical and food processes.

1.7.1   POST-COMBUSTION CARBON CAPTURE

This is the carbon capture route where, as the name infers, CO_2 is captured and compressed at the tail-end of fuel combustion in a chemical process or energy generation industry. Fuel is combusted under the influence of air (oxidant) to generate thermal energy, the isentropic expansion at the turbine's outlet produces mechanical energy, which is converted to electricity. The gas-powered exhaust gas contains minute concentration of CO_2 of about 3% - 4%, which is subsequently channeled to a CCS plant for CO_2 capture [39],[40]. The low partial pressure of CO_2 in this case negates the efficiency of the CO_2 absorption process [41], and this will be discussed in Section 2.5.2 and 2.5.3. The level of maturity of the PCC technology is high due to its long-term utilization in the natural gas sweetening process and urea manufacturing industries and it is envisaged to be the earliest to be deployed in the carbon capture industry [40]. This technology also comes with an ease of retrofitting on an existing power plant [42], [43]. However, this ease comes with an electrical penalty that the PCC plant bestows on the power plant [43]. This translates into a rise in electricity production and the inevitable transfer of the incurred energy cost to the consumers, with the cost of electricity projected to sour to between 32% and 65%, as reported by Leung [41]. In another study using a supercritical 1200MWe (gross) PCC, the net electrical efficiency dropped from 45% (without capture) - 30% (with capture) and a corresponding increase in the CoE of 65% [44]. This factor has decelerated the market diffusivity of such technology, but ongoing RD&D is making PCC economical feasible and as a result salvaging the inertia of the industrial implementation of CCS.
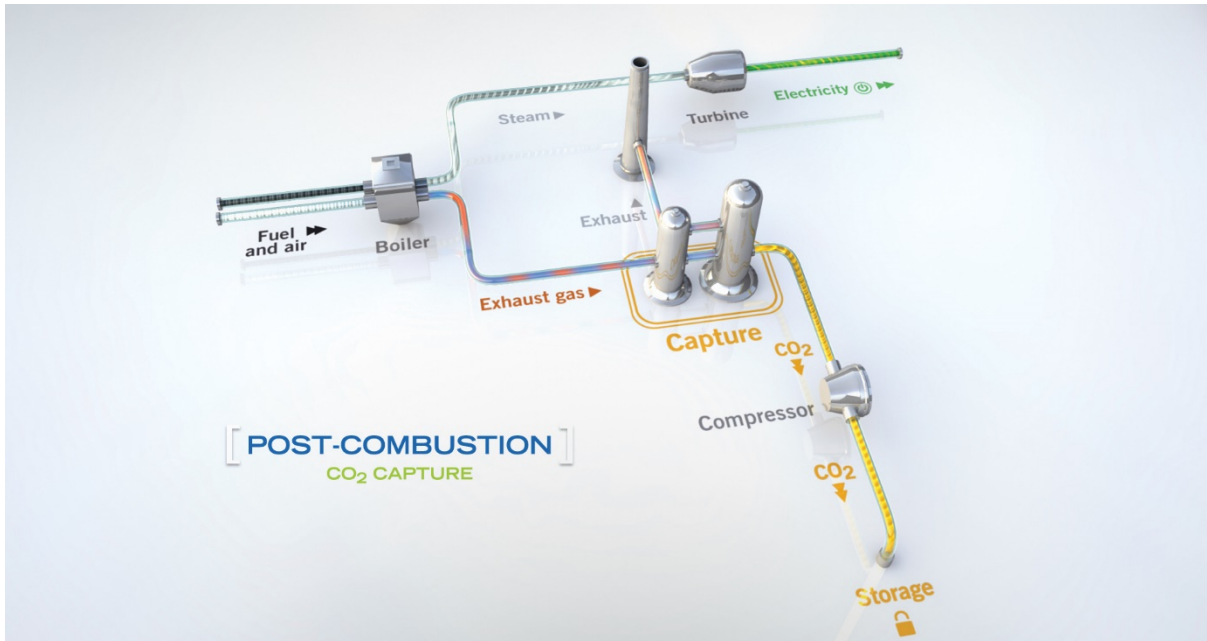
Fig. 1.9 Simplified schematic of the PCC [36].

Solvent loss, solvent degradation, almost clean flue gas requirement and of course the exorbitant solvent regeneration energy has made this process challenging for its employment in energy industries. This is in addition to its environmental as well as health concerns of amine emissions into the atmosphere. However, PCC has the advantage of dynamic operation.

The impetus of this research work was capitalized on the challenges of implementing PCC on a commercial scale. These challenges were borne out due to insufficient proficiency and expertise in lessening the solvent regeneration energy requirement of reactive absorption carbon capture. The copious energy intensity process of this capture is primarily due to low partial pressure of the CO_2 content in high volumetric flow of flue gas to be treated.

1.7.2   PRE-COMBUSTION CARBON CAPTURE

This is the carbon capture process that involves alienation of N_2 before combustion as diagrammatically represented in Fig 1.10 and the chemical equation presented as follows:

$$C_xH_y + xH_2O \longleftrightarrow xCO + (x + y/2)H_2 \tag{1.3}$$

$$C_xH_y + x/2O_2 \longleftrightarrow xCO + (y/2)H_2 \tag{1.4}$$
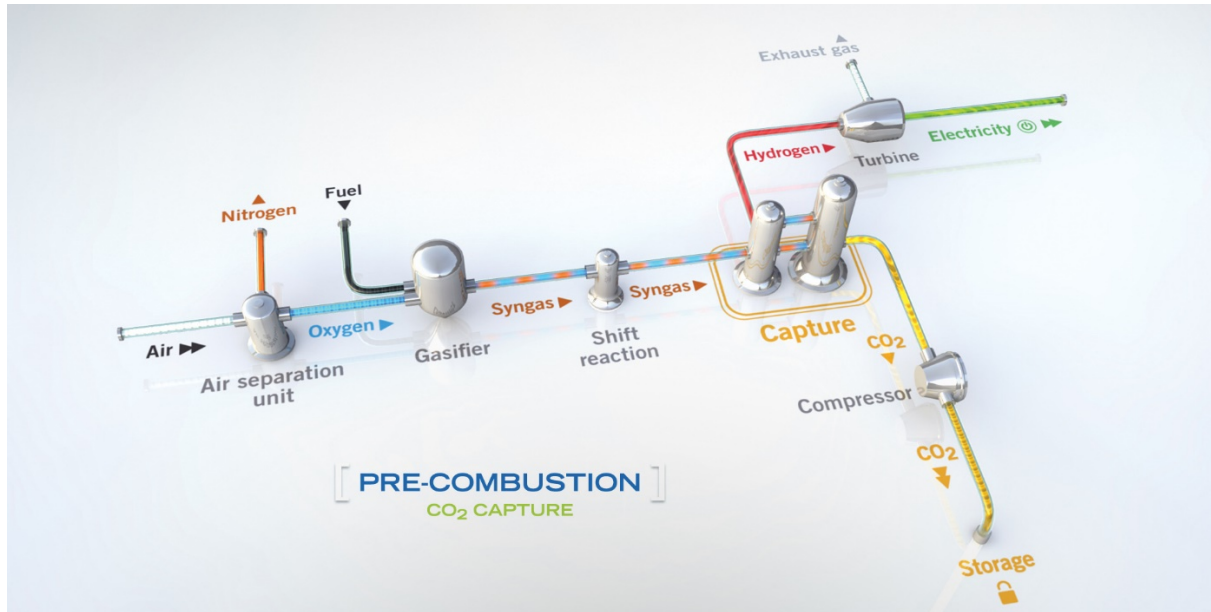
Fig. 1.10 Simplified schematic of the Precombustion Carbon Capture [36].

The primary fuel (CxHy) is then broken down by subjecting it to a temperature of more than 700°C under the influence of steam [xH2O](steam reforming: eq. (1.3)) or oxygen (partial oxidation or gasification in the case of liquid/gaseous fuel or solid fuel respectively: eq. (1.4)) to produce syngas (producer gas) which is mainly composed of CO and H2. The Water Gas Shift reaction follows to metamorphose CO to CO2 under the influence of steam as presented in eq. (1.5) [45], [36], [46], [47] as follows:

$$CO + H_2O \longleftrightarrow CO_2 + H_2 \tag{1.5}$$

The Water Gas Shift reaction product is then separated, H2 can be utilized to produce energy at the turbine and has the advantage of enhanced energy generation due to its high-temperature combustion capability and can be used in the fuel cells industry. Presented in fig 1.10 is a schematic representation of a Pre-Combustion Carbon Capture process [37], [46], [47].

For pre-combustion to be a commercial success, research on reducing the high cost of air separation unit, syngas generation, shift reaction, H2/CO2 separation processes and associated auxiliary operational cost must be addressed. Efficiency losses of between 8% - 16% has been reported from studies when pre-combustion is integrated with carbon capture [48]. Priorities of this research work is channelled towards addressing the challenges of post-combustion carbon capture due to its much better prospects of commercialisation.

1.7.3 OXYFUEL COMBUSTION CARBON CAPTURE

Enriched oxygen (95% O_2) serves as the primary oxidant for the combustion of fuel in oxy-fuel combustion, hence the reference name 'oxy-fuel'. This process was primarily suggested in 1982 (pre-IPCC) to enable the production of enriched CO_2 for EOR and for fuel efficiency in the chemical and process industries. This process permits a high combustion temperature as N_2 has been alienated from the air (which also reduces the amount of NOx emissions) before combustion. A simple schematic of the process is presented in Fig. 1.11 [37].
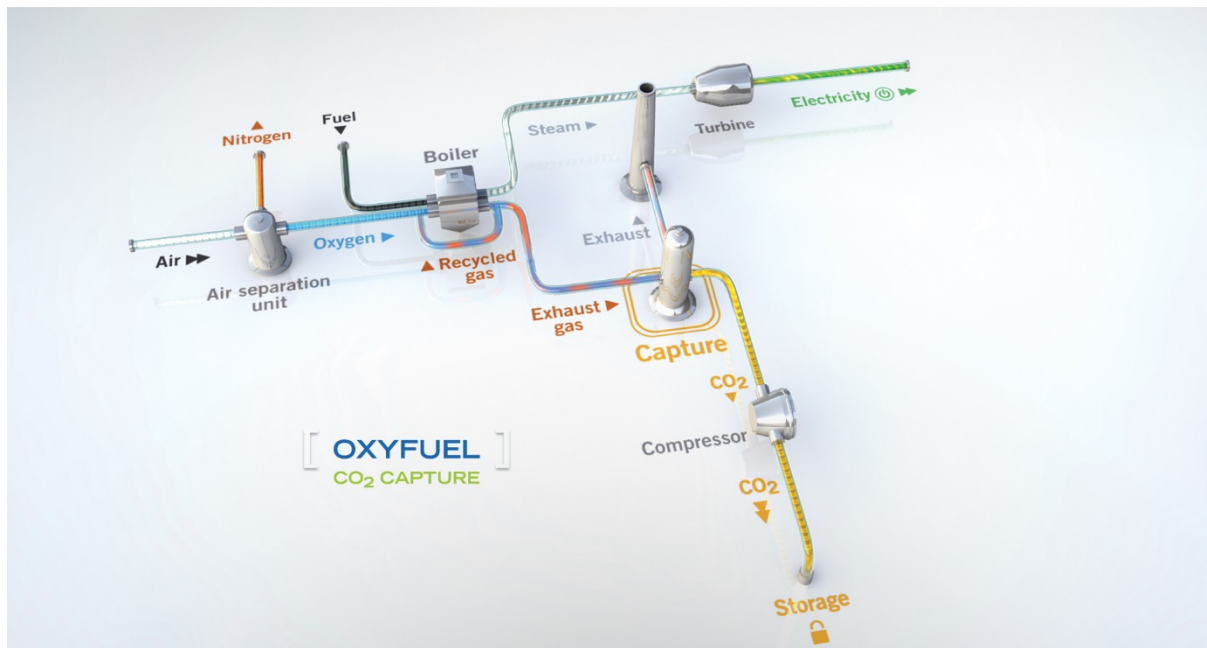
Fig. 1.11 Simplified schematic of an Oxy-fuel Combustion process [36].

This process has a key environmental advantage over post and pre-combustion as it releases 75% less exhaust gas by volume than air-fuelled combustion and mainly CO_2 and H_2O in its flue gas [49]. Drastic reduction in flue gas translates into less CO_2 emissions and as a result creates the opportunity to better utilize the residual heat energy that will otherwise be lost in the large volume of flue gas. In addition, this enables the miniaturizing of the flue gas processing system. Due to the high CO_2 concentration and partial pressure, the quarantining of CO_2 is better achieved via physical separation processes [44], [50].

The key standing challenge and research areas worth embarking on with regards to oxy-fuel combustion is the supply of a large volume oxygen at low economic implication. 250 tons/h of O_2 is needed to service a 1000MW power plant and cryogenic air separation

process serves this purpose, but at a very high economic cost as it is energy intensive despite the maturity of the technique [51]. Secondly, there's metallurgical constraints due to high thermal energy generated as a result of enriched O_2 combustion and the remedy is to increase the boiler's surface transfer area or recycle the FG to derate the combustion temperature, both are practically expensive to embarked on. This research work will concentrate on the most practically viable carbon capture technique with the shortest-term market penetration odds, as a result PCC has an overriding advantage over pre and oxy fuel combustion carbon capture.

1.8   PROLOGUE: MODELLING CCS TECHNOLOGIES

Reactive absorption of CO_2 with an aqueous solution of amine is a process where the CO_2 (gas phase) is absorbed by amine (liquid phase) via chemical reaction to form a fragile bonded intermediate compound, which can be reversed by applying thermal energy to produce almost pure streams of the original fluids, CO_2 and the amine solvent. The application of heat to reverse the process is daunting as it consumes a high amount of energy and de-rates the efficiency of a power plant when integrated together. MEA is utilised in this research work because it is a well-studied solvent, which is often used as a benchmark for more advance approaches, therefore can be used to optimise the capture process more independently of solvent choice [52].

Modelling of CCS systems is key to enable conceptual design of the entire CCS chain, operations and cost effectiveness of CCS technologies. This will potentially facilitate the deployment of CCS systems with better understanding of the results regarding operational optimisation, response to dynamic operations and reduction in energy consumption. However, models need to further be validated with experimental results on a pilot-scale to be validated and trusted in their application to full-scale cases. Efforts is pursued across the academia and industries to run more test campaigns in an effort to reduce conceivable risks in commercialisation of CCS plants [53],[54].

1.9   RESARCH PREMISE AND NOVELTY

As result of the low concentration of CO_2 i.e. about 4 vol(%) in the flue gas of gas turbines, significant reboiler heat duty of about 4 MJ is thus required to regenerate 1 kg of CO_2 from the rich solvent stream. The thermal energy utilized for CO_2 desorption is parasitic to the

low steam turbine of the NGCC and as a result derating the efficiency of the power plant and potentially increasing the CoE. How then can the high degree of difficulty and cost of CO_2 capture (i.e. the knowledge gap) be counteracted (i.e. the incentive) based on its low partial pressure.

Motivation: The enthusiasm and impetus of this research work has been driven primarily from the passion to contribute towards stabilizing the earth temperature rise via carbon capture and storage from energy production industry, which is responsible for a major share of global GHG emission into the atmosphere.

Gap: The market penetration of CCS is lethargic and at best slow due to primarily the high energy requirement needed to regenerate amine solvent in a reactive absorption CO_2 capture. There is as a result an expertise and skilled breach that must to be closed if CCS is going to be play a major role towards decarbonization of the global energy and heavy industrial sectors.

These gaps include but not limited to

- Prohibitive cost of the Operating and Capital Expenditure (OpEx and CapEx) and thermal energy consumption
- Technology: process optimization and intensifications to enhance operational efficiency e.g.
  - Solvent architecture designed to be highly CO_2 selective and regenerated under low thermal environment
  - Utilizing simulated centrifugal force in Rotating Packed Beds (RPB) to enhance CO_2 capture
  - Enhancing the CO_2 partial pressure to facilitate CO_2 capture via e.g. Exhaust Gas Recirculation (EGR), Selective Exhaust Gas Recirculation (S-EGR) and supplementary firing
- Retrofitting and integrating PCC technologies with existing power plants
- Performance of the PCC technology to dynamic changes in power loads.
- Evaluation and sustainability of Bio-Energy with Carbon Capture and Storage (BECCS)
- Regulatory, legal, Permitting and political frameworks to facilitate CCS
- Public perception and acceptance

The study gap this research is addressing is the high-energy utilization of the PCC for NGCC due to the role natural gas is projected to play in the transition to zero-carbon economy.

The knowledge gap addressed are bullet pointed as follows and these are considered to be amongst the most important because the thermodynamics has established that the lower the CO_2 concentration in the flue gas, the more expensive it is to capture the CO_2 [55], Hence, it is critical to lower the cost of the CO_2 capture if this technology is to make a noteworthy contribution to decarbonizing the fossil fuel combustion industries across the globe. The absorption capacity of MEA is 0.5 moles of CO_2 for every mole of amine, practically about 360gCO_2/kgMEA depending on the CO_2 capture operating conditions [56], Thus, increasing both the concentration of the amine solvent and the partial pressure of the CO_2 is expected to increase the performance of the CO_2 capture and reduce the high energy cost of the capture process. It is also important to study how different temperatures of the regeneration fluid influences the CO_2 capture so as to establish the optimization regime of the CO_2 capture processes with regards to the temperature of the regeneration fluid at the inlet of the reboiler unit. Furthermore, a slow but sure process is solvent degradation, and this restricts the solvent absorption capacity in the long term and as a consequence increases the cost of the long-term CO_2 capture process. The study of how the solvent behaves with the flue gas of the natural gas combustion will furnish vital information with regards to how best to address the solvent degradation and maintain the CO_2 capture performance. S-EGR is thus considered to be a novel technology that increases the partial pressure of the CO_2 in the flue gas with its consequential reduction in the solvent regeneration energy requirement.

A noteworthy reduction in the solvent regeneration energy requirement is achievable by increasing the solvent concentration as reported by Abu Zahra et al. (2007), where the simulation study he carried out achieved a reduction of the regeneration energy from 3.9 GJ/ton to 3.0 GJ/ton while increasing solvent concentration from 30 to 40 wt(%) MEA. Akram et al. (2020) reported a reduction of 14% in the NSRD from 30 to 40 wt(%) MEA. Thus there is a huge potential and knowledge gap to explore with regards to how S-EGR will fair under 40 wt(%) MEA and hence the impetus of using 40 wt(%) MEA in this research study.

- Simulating S-EGR to enhance the CO_2 content at the inlet of the absorber column to effectively expedite the driving forces for CO_2 capture under the influence of 40 wt(%) of MEA on a pilot-scale CO_2 capture plant.

- Evaluating the performance of CO_2 capture process under the influence of varying PHW temperature from 24 to 27 °C at 9.1 vol(%) of CO_2 in the flue gas

- Study of the performance of PCC under the impact of oxidative solvent degradation with 15.0 vol(%) of O_2 with twin absorber columns at a pilot-scale plant.

With regards to the study gap considered in this thesis and highlighted above, simulating S-EGR will make available knowledge in respect of the CO_2 concentration in the flue gas after recirculation that will achieve the highest energy savings and lowest operating expenditure. Further, evaluation of the different thermal temperature at the working fluid at the inlet of the reboiler will identify the PHW temperature that yields better value in operating a CO_2 capture process, because high and low thermal energy input will both increase SRD as a result of poor solvent regeneration and high reboiler duty. Solvent degrades under stress of CO_2 capture, thus, minimizing solvent decay will not only capture CO_2 and improve on the energy savings but reduce the associated cost of solvent management and disposal.

Novelty: A number of operational modifications has been worked on to reduce the low CO_2 partial presure in the flue gas of NGCC power plant, the novelty of this research work was sprouted based on preconcentrating the CO_2 in the flue gas agaisnt 40 wt(%) MEA to enhance a driving force for CO_2 mass transfer on a pilot-scale campaign. This innovative process is expected to reduce the major complexities associated with the major flue gas CO_2 enrichment techniques. Suites of different system and operating modifications on both experimental and simulation fronts has been embarked-on in this research endeavour to close the knowledge gaps.

1.10   OBJECTIVES OF THE RESEARCH

The underlying objective of this research project is to work towards reducing the regeneration energy requirement of amine-based CO_2 capture plants while concurrently reducing the parasitic energy impacted on a power plant.

- Investigate how varying partial pressure of CO_2 under the influence of 40wt.% MEA affect the performance of the PCC that include CO_2 capture efficiency and capture rate, CO_2 loadings, degree of solvent regeneration, temperature profiles in the absorption & stripping reactors and the SRD at a Pilot-scale CO_2 capture plant.
- Evaluate how different operating conditions i.e. Pressurized Hot Water (PHW) temperature affects the performance and emissions of PCC at a pilot-scale plant
- Examine how solvent degradation with 40 wt.% MEA affect the performance of the PCC using two absorber reactors.

The experimentation campaigns are carried out at the UKCCSRC Pilot-scale Advanced Capture Technology (PACT) National Core facility, Sheffield, UK. gCCS was utilized as the process modelling platform for validation of published experimental campaign at the PACT facility and geared towards design optimization campaigns of the Solvent-based CO_2 Capture Plant (SCCP). The results from this study is tailored towards facilitating PCC deployment across the globe.

1.11   SILHOUETTE OF THE THESIS

The primary motivation and enthusiasm behind this thesis is global warming which is caused via anthropogenic carbon emissions into the atmosphere by almost every aspect of human socio-economic enterprise. To address this challenge, the silhouette of this study is given as follows:

- Chapter 1 looks at how running the world's economy over the last century via fossil fuel has expedited and amplified global warming, the global energy outlook and technologies for CCS.
- Chapter 2 reports on the intricacies, advances and knowledge gaps while giving a critical review to Post-combustion Carbon Capture (PCC).
- Chapter 3 presents a detailed scheme of the experimental plan of the study campaigns carried out at the PACT facility with an aqueous solution of amine (MEA).
- Chapter 4 discusses the results of the experimental campaign of simulating Selective-Exhaust Gas Recirculation (S-EGR) ratios against 40wt% MEA.

- Chapter 5 presents and discusses on the pilot-scale experimental results and reviews the oxidative degradation of 40 wt.% MEA.

- Chapter 6 develops, presents and discusses a process modelling and simulation study on the validation of a published experimental campaign with varying CO_2 concentration against the case of 30 wt.% MEA and optimization studies based on a cocktail of different process parameters.

- Chapter 7 contains a discussion of the conclusions and further work.

CHAPTER II

LITERATURE REVIEW

INTRODUCTION

This chapter critically reviews and describes the background and principle of CO_2 capture via the medium of aqueous solution of amine and the challenges facing the commercialization of the PCC technology and gaps in knowledge to fill in to make it techno-economically viable. This chapter also discusses the development, advances and limitations of CO_2 capture technologies. A review of the current CO_2 capture projects across the globe is also highlighted.

2.1   BACKGORUND: AMINE CAPTURE SYSTEM

R. R. Bottoms [57] was credited with the development of the application of alkanolamines absorbents for acidic gases, the original schematic of the amine capture process patent (see Fig. 2.1) was granted on the 2nd of December in 1930 for this application, where Triethanolamine (TEA) became the first solvent to be utilized [58]. Monoethanolamine or 2-aminoethanol (MEA: $H_2NCH_2CH_2OH$ or RNH_2) will eventually be widely utilized for the capture of CO_2 and H_2S in process and chemical industries for decades and recently for the carbon capture from fossil fuel power plants. The low molecular weight of MEA, "resulting in high solution capacity at moderate concentrations", makes it easier to regenerate, its ability to capture CO_2 in relatively low concentrations and its state of alkalinity makes it suitable for capturing low CO_2 concentration in flue gases [57]. Post-combustion Carbon Capture with aqueous alkanoamines is as a result envisaged to earlier be commercially adopted than other forms of carbon capture technologies due to its high state of maturity and long track record of experience in the heavy chemical industries. However, MEA has its own share of drawbacks with regards to higher corrosive potential compared to other amines. 30% MEA concentration has been optimized and utilized in industries. However, Kohl and Reisenfeld, [57] reported that a concentration of higher than 20% renders the solvent increasingly corrosive, especially if the flue gas contains high content of acid gases. Vaporization loss is also a drawback of utilizing MEA for carbon capture; such a loss is however, counteracted via capturing the vaporized MEA by means of a simple water wash facility above the absorber column. MEA readiness to form

Carbonyl sulfide (COS) and Carbon disulphide (CS2) in an irreversible reaction that leads to chemical degradation of the solvent and therefore desulphurization becomes a key requirement of treating flue gas upstream of the gas inlet of the absorber reactor for coal combustion [57], [59]. Furthermore, thermal and oxidative degradation associated with MEA is a major challenge in PCC. Research is underway to fully understand the mechanism of solvent decay [57]. Suites of improved solvents, many of which are under patents, are currently utilized on experimental and pilot-scale campaigns, however, their full commercial success and utilization however remains to been seen [60].

2.2 PROCESS DESCRIPTION OF AN ACP

The Amine Capture Plant (ACP) utilizes the process of reactive absorption in a packed absorber column between aqueous alkanoamines and a stream of flue gas from the power plant or other industrial processes in a counter-current flow, which is based on Bottoms original design provided in Fig.2.1.
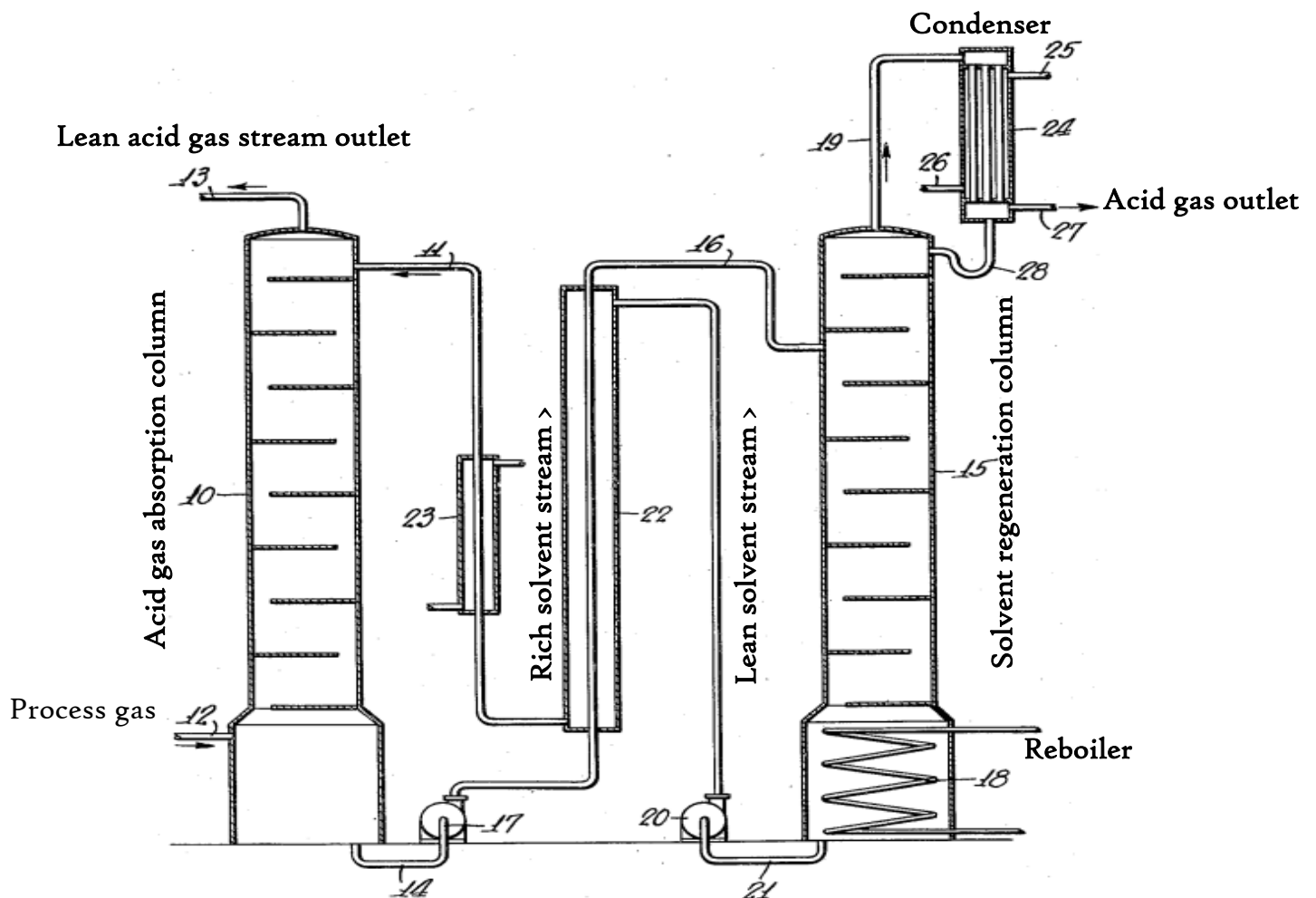
Fig 2.1: Bottom's patent application model of the process of separating acidic gas [58].

The prominence of electrolyte dissociation in aqueous solutions is influenced by chemical equilibrium. Electrolytes that undergo complete or partial dissociation are described as strong and weak electrolytes respectively. Weak electrolytes are of interest within the context of this study, i.e. MEA (weak organic base electrolyte) and CO_2 (weak acid electrolyte) which partially ionise or dissociate when reacting in aqueous solution as follows: [61],[62].

Ionization of H_2O:

$$H_2O \longleftrightarrow OH^- + H^+ \tag{2.1}$$

Dissociation of dissolved oxygen to carbonic acid:

$$CO_2 + H_2O \longleftrightarrow HCO_3^- + H^+ \tag{2.2}$$

Formation of bicarbonate

$$CO_2 + OH^- \longleftrightarrow HCO_3^- \tag{2.3}$$

Formation of carbamate

$$CO_2 + RNH_2. \longleftrightarrow RNH_2^+COO^- \tag{2.4}$$

Reversion of carbamate: Hydrolysis

$$RNH_2^+COO^- + H_2O \longleftrightarrow RNH_2 + HCO_3^- \tag{2.5}$$

Protonation of MEA

$$RNH_2 + H_3O^+ \longleftrightarrow RNH_3^+ + H_2O \tag{2.6}$$

Introducing the stable carbamate to heat energy forces a divorce between the amine $R\text{-}NH_2$ and CO_2 [62].

The CO_2 rich stream at the stripper gas outlet is condensed, compressed and stored whereas the regenerated amine is recycled back to the absorber. Packed columns are generally used for reactive absorption in an ACP as it can be utilized for small facilities, accommodate high L/G ratios and delivers higher purity CO_2 as oppose to plate or spray towers [57],[63].

The flue gas at a temperature of about 120 $^\circ$C downstream of a power plant is thermally quench to a temperature of about 40°c in a flash drum (DCC) before being introduced at

the base of the absorber. The flue rises upwards along the packed absorber column under a pressure of about 1 bar. Meanwhile the amine solvent introduced at the top of the column flows downward. The counter current flow enables the two different phases to chemically react as described in the absorption chemical reactions (Eq. 2.1 and 2.2), making it possible for CO_2 in the flue gas to be absorbed onto the aqueous solvent [57],[63],[64].

The rich cold solvent is harvested at the bottom of the absorber is passed through a rich-lean heat exchanger where it absorbs heat to reduce the energy requirement of solvent heating as it is introduced into the stripper liquid inlet, reducing the total specific reboiler duty (SRD) as a result. The downward flowing of the rich solvent in a counter-current direction with steam generated by partial evaporation of the aqueous amine solvent in the reboiler strips the CO_2 off the rich solvent. The steam generated by the reboiler will normally depend on the quality of stripped CO_2 required, makeup of solution and column height. Thermal energy generated fundamentally performs the following duties [65]:

i.   To supply sensible heat required to increase the temperature of the incoming cold rich solvent to that of the hot lean solvent departing at the bottom of the stripper.

ii.   To supply thermal energy necessary for the stripping off the CO_2 from the solvent.

iii.   To vaporize the water which acts as a carrier of the acid gas.

The CO_2, steam and carried-over amine solvent is thereafter routed to a condenser, dried CO_2 is thereafter compressed and stored for subsequent utilization whereas the carried over condensed fluid is returned back to the stripper as reflux, which is likely to result to a slight heat requirement in the packed stripper column. The regenerated amine at the base of the stripper is channelled back to the absorber via the same rich-lean heat exchanger, where it gives up some of its thermal energy to the rich lean solvent before being reintroduced into the absorber again. The cycle continues and the makeup solvent periodically introduced to compensate for the solvents lost in the process, via evaporation, thermal and oxidative decay. A water wash facility containing demineralized water located downstream of the absorber claims some of the emitted amine that trails along with the treated lean CO_2 stream to meet regulatory solvents emission requirement [57], [66], [67], [64]. Studies have reported the specific regeneration energy of about 3.6GJ/tCO_2, this thermal energy requirement translates into a fall of electrical efficiency of the power plant of approximately

11% - 12%, including CO_2 compression. The amine regeneration process demands about 75% of the total energy requirement of the ACP. Hence the focus on RD&D on reducing the SRD [65].

2.3 QUALITIES OF SOLVENT FOR CO₂ CAPTURE

Characteristically, the solvent utilized for CO_2 carbon capture needs to satisfy the following [43]:

i. Relatively high reactivity with CO_2, this factor will reduce L/G and consequentially the height of the absorber, making way for reduced CapEx and more importantly OpEx.

ii. The solvent needs to be regenerated with a relatively low energy requirement. Solvent regeneration is the key challenge of solvent-based CO_2 capture and addressing this factor will make an instrumental headway towards decarbonizing the power industry.

iii. Relatively high absorption capacity. This unequivocally reduces the solvent circulation flow rates and reduces the daily OpEx of the capture unit.

iv. High thermal permanence and low degradation of the solvent reduces waste of the solvent and its associated cost of disposal.

v. Ability to produce the solvent in a cost effective and environmentally friendly manner.

2.4 ACHILLES HEEL OF THE REACTIVE ABSORPTION CO₂ CAPTURE

Reactive absorption with aqueous MEA in an absorber-stripper configuration is the most expedient technology for PCC, however, the advantages of the traditional and accustomed ACP using MEA is eventually giving way for improved solvents grades, enhanced nano membranes technologies and improved system & operating conditions. These were necessitated due to limitations of the SCCP process; the key drawbacks are now highlighted below.

Energy penalty: Carbamate, the product of CO_2 and MEA absorption demands significant energy to break its bond due to the stable nature of the compound. Compression of CO_2 for subsequent transportation for storage or CO_2 utilization site also requires considerable energy. This energy derates the power plant's net efficiency and 7 - 11% efficiency penalty has been reported from studies when a NGCC is coupled to an ACP, $3.2 - 4.2$ MJ/kg of the

CO2 captured is consumed from which solvent regeneration accounts for about 70 % of the total energy requirement of the ACP [63]. A cocktail of system modifications and operating conditions across the length and breadth of the capture plant is under investigation to drastically reduce the consequential penalty on the power plant.

Loss of sorbent: It is not pragmatic to recover 100 % of the solvent from PCC process, solvent recycling over a protracted period of time leads to the forfeit of the solvent with regards to thermal & chemical degradation, vaporisation, leakage and entrainment [62]. Oxygen, oxides of sulphur in the flue gas are considered impurities as they are agents for reducing CO_2 absorption due to the production of heat stable salts after reacting with MEA [62]. This necessitates Flue Gas Desulphurization (FGD) treating flue gases from fuel combustions with high sulphur content.

Corrosion: Corrosion is a key factor affecting the dynamics of reactive absorption of CO_2 by amines, amines that host acid gases are known corrode the internal equipment of the CO_2 capture facility. Thus, the higher the amine concentration, the higher the CO_2 loading and the higher the operating temperature, the likelihood of facilitated corrosion. Corrosion has been studied to increase in the following order of amine type, MDEA→DEA→AMP→MEA. Corrosion inhibitors, lower MEA concentration, mild operating conditions and better facility designs reduces the severity of chemical weathering [43],[62].

Solvent Degradation: Three major amine solvent degradation routes have been identified in the literature, namely carbamate polymerization, thermal and oxidative degradations. Polymerization of carbamate normally takes places above 100 $^\circ$C. The standard absorption processes in industries and experimental modes usually takes place between 40 – 60°C, thereby greatly limiting such type of degradation [43]. Approximately 67% and 33% of thermal degradation takes place in the reboiler and stripper where operating temperature of the amine capture plant are at its highest [64]. Wang [43], Rezazadeh [63] and Akram [64] reported a temperature above 205°C, 130°C and 128°C triggers the severity of thermal degradation. Wang reported in his paper that oxidative degradation takes place at a temperature above 205°C, which is about 75°C above the values reported in similar peer reviewed studies [63, 65], but this value has not been substantiated in his reported result. His reported value is thermodynamically not sensible because this is likely to cause increased water and the amine solvent vaporization in the desorber beyond the practical

operation of the CO_2 capture process. Furthermore, this is likely to significantly increase the CO_2 cooling/compression cost downstream of the stripper gas outlet. This type of degradation is normally controlled at a temperature of about 110 – 120 °C [63]. Oxidative degradation on the other hand results due to the presence of oxygen in the flue gas. Alienating of O_2 in the flue gas via Dissolve Oxygen Removal Apparatus (DORA) is investigated to limit oxidative degradation. [43],[68].

2.5   PROCESS MODIFICATION IN PCC

A number of techniques have been examine to address the fundamental challenge of the SCCP, i.e. reduction in energy consumption and include Exhaust Gas Recirculation (EGR), Selective-Exhaust Gas Recirculation (S-EGR), Supplementary firing and humidification of Gas turbine [69]. These techniques have the benefit of enhancing the partial pressure of CO_2 in the flue gas and consequently, reduction of solvent regeneration energy requirement of the SCCP. These technologies are discussed as follows.

2.5.1. ROTATING PACKED BED (RPB)

In recent years, high gravity-based (HiGee) process intensification technology called the RPB has been proposed to enhance gas-liquid absorption, heat transfer, liquid-liquid extraction and multi-phase separation process in the process and chemical industries. More recently, pilot-scale experimental campaigns are underway as a prelude to its possible commercialization. In principle, the RBP utilizes a packed bed, which is rotated to simulate a centrifugal force from about 200 – 1000 times greater than standard gravity in order to enhance physio-chemical processes. The solvent is been split into thin films of about 100μm (depending the on hyper-gravity fields, consequently enhancing mass transfer efficiency and absorption reaction rates [70],[71],[72]. Due to anticipated increased mass transfer, lower MEA concentration can be afforded to be utilized to restrict equipment corrosion, solvent decay and physical footprint. A simple schematic of the RBP is represented in fig. 2.2.
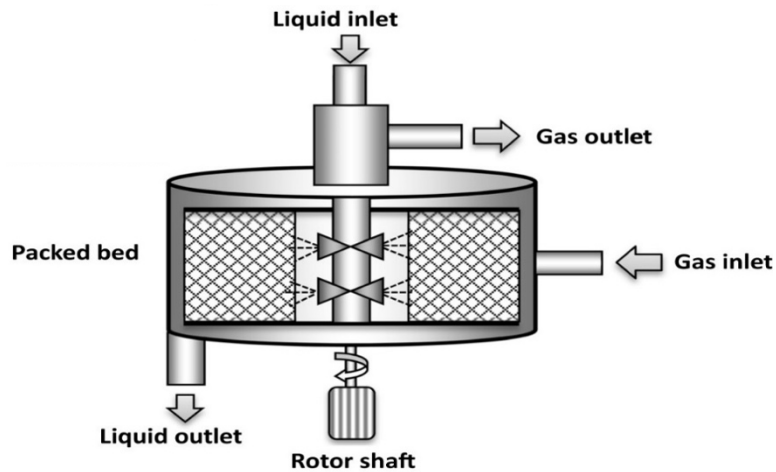
Fig. 2.2   A simple schematic of a RPB showing the process scheme [70].

RPB is beyond the scope of this study because this research is concentrated on the carbon capture technology that is most likely to be deployed earlier than other forms of CCS technologies. Furthermore, the thermodynamics of RPBs favours the miniaturization of the CO_2 capture unit. Thus, as a result negates higher volumetric flow of the amine solvent and flue gas, except if multiple units are to be installed, then this is likely to attract more CapEx. In addition, maintenance issues are envisaged to be higher due to the high axial rotational (mechanical) operation of the technology and the increased likelihood of the erosion-corrosion of the internal structures, RPB favours higher rich loading than fixed columns under the same operational conditions, thus, this it is likely to further facilitate the corrosion of the internal equipment because of the higher concentration of the acid gas in the solvent, additionally, performance response of the RPB under the influence of varying load changes of the power plant is uncertain.

2.5.2   EXHAUST GAS RECIRCULATION

Exhaust Gas Recirculation (EGR) was first proposed as an anti-icing process for a compressor because the exhaust gas stream is normally recirculated at an elevated thermal gradient than the ambient air and additionally as a technique towards offsetting the NOx emissions because of the attenuation of the fuel-air ratio or firing temperature which weakens the NOx formation [73]. EGR is currently proposed to increase CO_2 partial pressure in a bid to reduce the Specific Reboiler Duty (SRD) of the PCC process. CO_2 enrichment technique entails recirculating a certain volume of the exhaust gas after the Heat Recovery Steam Generator (HRSG) back to the compressor of the gas turbine. The CO_2 concentration of natural gas is relatively low, in the order of 3 – 4 vol% [74], the

diminutive occurrence of CO_2 hinders the carbon capture efficiency and necessitates more stripping steam requirement for solvent regeneration, considering high CO_2 purity is required.
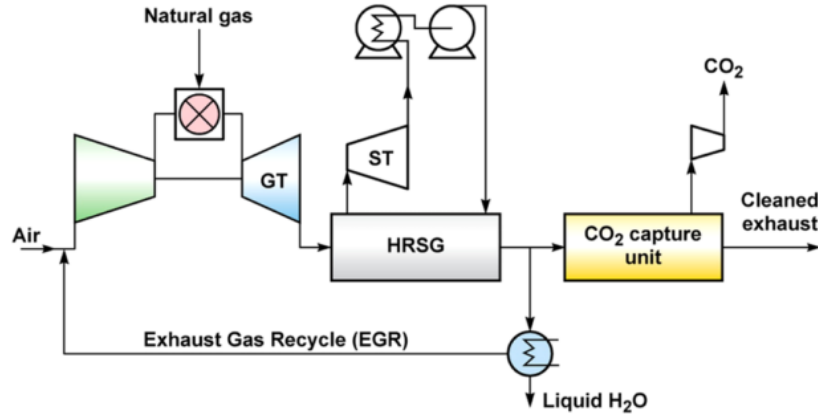
Fig 2.3. A simplified schematic of the EGR system [74].

The EGR is made possible because the recycled flue gas can technically replace the large air volume of about 250% stoichiometric oxygen needed for combustion, with little aberration on the performance of the gas compressors and turbines. The increasing CO_2 concentration in the flue gas via flue gas recirculation will contribute to the reduction of high electrical penalty impacted on the power plant by the ACP. Thus, EGR in theory is a novel way to reduce such a penalty that is responsible for the slow pace of commercializing reactive based CO_2 capture technologies. Not only does EGR enhances the CO_2 concentration of the flue gas upstream of the absorber column but it reduces its flow rate, and reduction of the flow rate reduces the work done by the CO_2 capture plant. However, the limit as to how EGR can be employed has a threshold as it constrains the oxygen availability, hence affecting the efficiency of combustion unless additional oxygen is introduced in the combustor. Increasing the CO_2 concentration also inevitably leads to risks of unburnt hydrocarbons (UH) and CO [75], [76].

The EGR ratio is established from the relation (after condensation) [75] as follows:

$$EGR\ ratio = \frac{\text{Volume flow of recirculated exhaust gas}}{\text{Volume flow of exhaust gas}} \qquad (2.7)$$

Li [75] reported from a simulation result an optimum EGR ratio of 0.5 will reduce the flow rate upstream to the ACP by 51% and increase the CO_2 content from 3.8 - 7.9 mol(%), under which the SRD reduces, thus effectively reducing the electrical energy penalty. However,

Elkady et al., Sipocz and Assadi [76] reported an optimum EGR ratio of 0.35 and 0.4, respectively. A study carried out at the UKCCSRC PACT facility, Sheffield with a mGT by Ali et al. [76] reported a 0.55 EGR ratio under which the CO_2 content in the flue gas increases from 1.6 - 3.7 mol%. Variations from these studies reflects the different system configurations and operating conditions used to carry out the various research work. Ali et al. [76] also concluded that the oxygen concentration at the combustor inlet can be decreased to as low as 14 mol%, but this is not recommended for reasons mentioned earlier in this section. An oxygen concentration of at least 16 mol(%) is recommended for flame stability and combustion efficiency [76].

The decrease in mass flow rate to the capture plant in the case of EGR and SEGR in parallel modes mean that more steam is available to drive the ST, thus improving the net efficiency of the steam cycle. An increase from 174 MWe (NGCC-CCS) to 181.1 MWe and 184.7 MWe for EGR(39%) and S-EGR in parallel (53%), respectively, was reported [74],[39],[73].

In terms of the possible impact on the gas turbine at different positions of the flue gas introduction, three locations were studied which include:

i.   before the compressor,
ii.   after the compressor, and
iii. at the combustion.

A study by Akram [77] has established that the location of the flue gas introduction does not affect the CO_2 content in the capture system. However, implications of the location of the CO_2 enrichment exist and includes extra component requirements, e.g. compressors and blowers to introduce flue gas into the system, which is likely to cause distress to the default control [77], [78].

The overriding benefit of the CO_2 recirculation, irrespective of the aforementioned 3 configurations, is the increasing of the partial pressure of the CO_2 in the turbine's exhaust gas, which consequentially reduces the Specific Reboiler Duty of the CO_2 capture process.

Flue or Exhaust Gas Recirculation before the compressor increases the compressor inlet temperature and a higher exhaust temperature as compared to air-based combustion at ISO ambient conditions. Higher temperatures reduce the gas density, however, with increasing the CO_2 concentration in the flue gas, the gas density increases. A decrease in the gas density leads to a lower mass flow rate and which subsequently leads to a decrease in the

open cycle thermal efficiency gas turbine net power output. With the EGR, the flue gas partially replaces air as a combustor moderator and lowers the O_2 concentration at the combustor. Lowering the combustor O_2 concentration risks the occurrence of flame extinction, onset of thermo-acoustic instability, combustion instability and alteration of the heat transfer distribution. Low O_2 also lowers reaction rates and allows the combustion process to spread over a large region and thereby reducing the peak flame temperature. This phenomenon limits the oxidation of the CO to CO_2 and increases the unburnt hydrocarbons [73],[75],[79].

Irrespective of the point where the CO_2 is introduced into the gas turbine, increasing the EGR ratio restricts the NOx formation and consequently limits the degradation of the amine solvents and its by-products which leads to the corrosion of the internal equipment of the capture plant. This also results in minimizing the need for introducing corrosion inhibitors. However, the limitation of the O_2 concentration in the flue gas due to increasing the EGR ratio reduces the severity of the oxidative degradation of the amine solvent, potentially reducing the CapEx of the CO_2 capture process. It is important to note that only slight deviations from design operation in the compressor and combustor is attained with EGR ratio up to 40% [73],[75],[79].

2.5.3 SELECTIVE EXHAUST GAS RECIRCULATION

Diluent gaseous specie abound in natural gas combustion flue gas stream with regards to its CO_2 content, and these gases are accommodated in the process of recirculating the flue gas to the compressor of the turbine to have a higher CO_2 concentration for carbon capture purposes. As a result, this negates the higher CO_2 concentration at higher O_2 prevalence. To attain a 16 mol% of O_2 for flame stability in the combustor, while accomplishing higher CO_2 concentration, Selective Exhaust Gas Recirculation (S-EGR) has been proposed, where CO_2 is selectively extracted from the flue gas and recirculated back into the combustor. This process benefits the CO_2 absorption efficiency and capture rate in the absorber packed column due to the increase in higher partial pressure of CO_2. Thus, enhancing the driving forces behind the CO_2 mass transfer, consequently reducing the desorption energy requirement of the CO_2 capture plant [74].

A study conducted by Merkel et al. [74] proposes a technique where CO_2 in the flue gas is selectively alienated via a membrane. This transpires by transporting the flue gas through a section of a membrane with air passing through the other half of the membrane. The membrane discriminates against all the gaseous species while having an affinity for CO_2, the CO_2 rich stream is thereafter fed into the compressor [39]. The CO_2 concentration fed

to the compressor of the turbine can be increased from 4vol% (without CO_2 recirculation) to as high as 19vol% (with SEGR). A study by Diego [39] reported a resulting decrease in CO_2 capture energy requirement from 3.95MJ/kg (NGCC-CCS) to 3.71 MJ/kg (NGCC-Parallel S-EGR) [74]. Due to alienation of gaseous specie in the flue gas except CO_2, S-EGR can attain a CO_2 concentration of about 20 % at 16 mol(%) of O_2 while conventional EGR will attain the same, at about 6.5% CO_2 [74].

The S-EGR ratio (after the HRSG outlet) is established using the relationship below [74]:

$$S\text{--}EGR \ ratio = \frac{\text{Mass flow of flue gas to selective CO2 transfer system}}{\text{Mass flow of exhaust flue gas}} \tag{2.8}$$

Merkel et al. [80] proposed parallel and series configurations of NGCC with the CO_2 selective membrane represented in Fig 2.4.
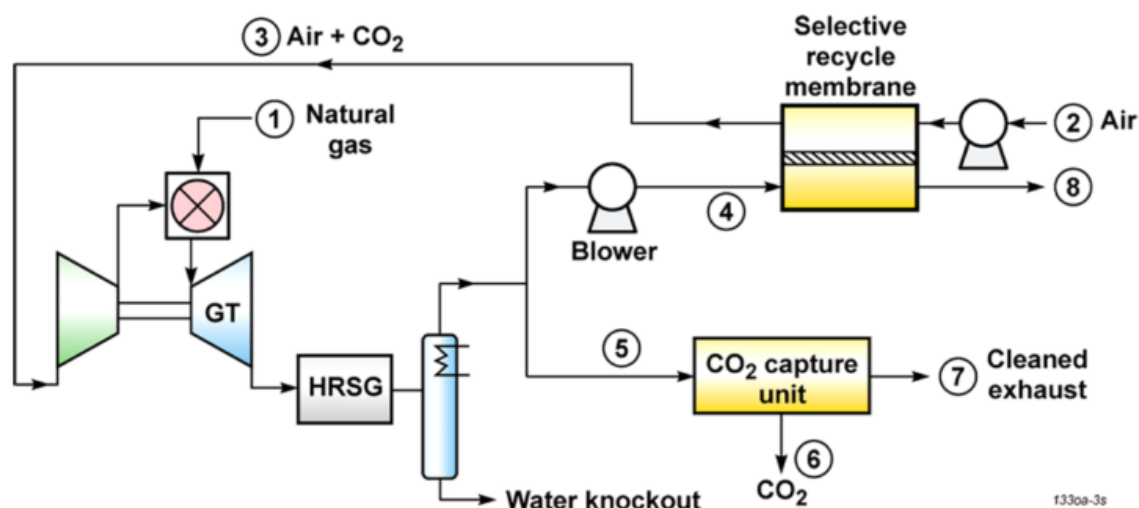
Fig. 2.4 Simplified schematic of a NGCC plant with a membrane-based S-EGR CO_2 capture unit in parallel [74].

The parallel configuration separates the flue gas downstream of the HRSG into two streams, one part is transported to the selective membrane while the other half is ushered to the CO_2 capture plant. The capture plant is in this case able to operate at a lower L/G ratio, which can be translated into lower OpEx and CapEx. A lower regeneration energy is achieved as a result.
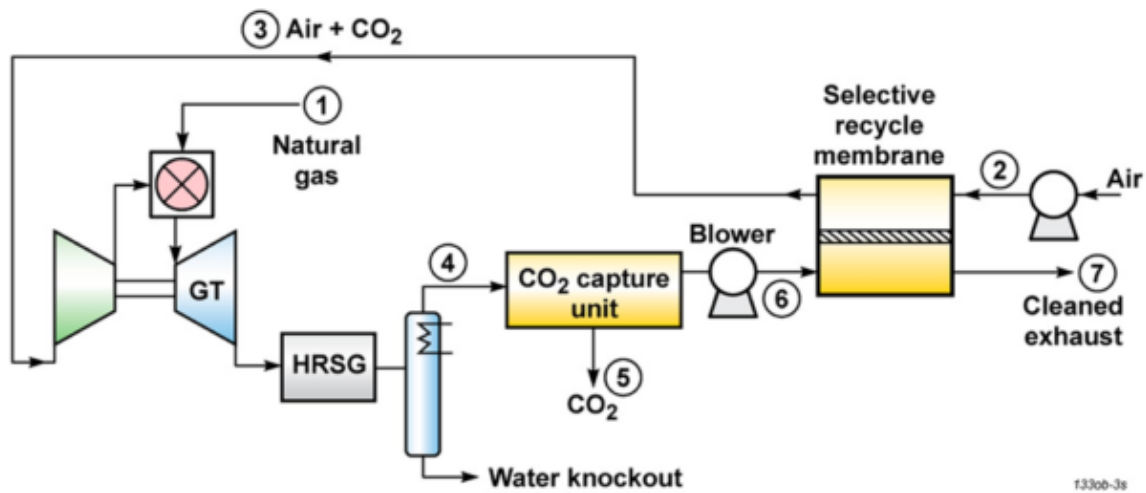
Fig. 2.5: Simplified schematic of a NGCC plant with a membrane-based S-EGR CO2 capture plant in series [74].

The series configuration channels the entire exhaust gas stream to the CO2 capture unit and positions the selective membrane after the carbon capture unit. The CO2 capture efficiency is able to be lessened or relaxed in this scenario. The membrane downstream of the capture plant will capture the remnant CO2 downstream of the CO2 capture plant [80].

Both the parallel and series configurations can be combined together on a NGCC for a double-edged advantage of reducing the flue gas flow rate to the carbon capture unit and an eased CO2 capture efficiency requirement respectively.

2.5.4 SUPPLEMENTARY FIRING

Supplementary Firing (SF) is a process that enriches CO2 concentration in the flue gas to amplify the performance of PCC, SF is fast becoming a viable option in the NGCC-CCS industry to increase the amount of CO2 generated from the NGCC combustion, thus facilitating CO2 absorption and consequently reducing the SRD [40],[81]. This concept necessitates the combustion of the exhaust gas downstream of the GT and upstream of the HRSG using the remaining 12 – 13 vol% of O2 resident in the exhaust gas [69],[81],[82],[83]. Furthermore, the idea of this supplementary combustion using biomass instead of instead of fossil fuel can additionally reduce the carbon footprint of the process towards a state of negative emission [82].

SF has the benefit of lowering the CapEx of an ACP as the process reduces the flowrate of flue gas entering the CO_2 capture system [82]. Furthermore, the consequential reduction of O_2 concentration will additionally have a positive effect by reducing oxidative degradation of the solvent in SCCP [69]. An illustration of the supplementary firing route for NGCC coupled with SCCP and Compression and Purification Unit (CPU) is shown in fig. 2.6.
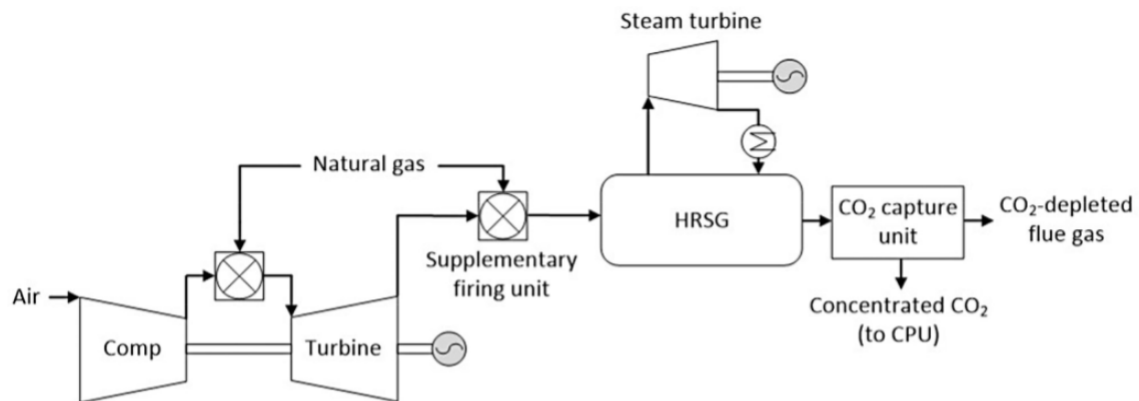
Fig. 2.6 Supplementary firing with NGCC coupled with SCCP [82].

2.5.5   HUMIDIFICATION OF GAS TURBINES

This technique increases the water content of the working fluid to amplify the energy output of turbines and reduction of NOx emissions. However, this technique has been studied as a process of increasing CO_2 concentration in the flue gas for CO_2 capture benefit because the water content has the tendency of replacing the air content, which can be removed via condensation. Operational stability with regards to the H_2O/fuel ratio however need to be achieved so as reduce incomplete combustion to reduce the emission of CO and unburnt hydrocarbons [69],[84], [85]. Schematically represented in the following figure is the humid air gas turbine (HAT) system or evaporative gas turbines (EvGT). HAT system is reported to achieve an electrical power output of up to 52% and decreasing to about 42% when integrated with SCCP [69].
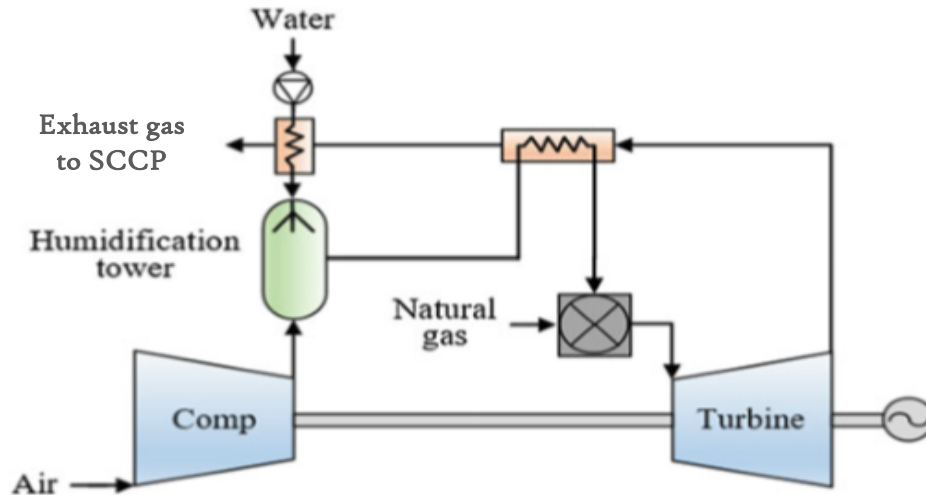
Fig. 2.7 Schematic of a HAT process configuration [69]

Whereas steam injected gas turbine (STIG), a form of humidified gas turbine system introduce steam directly into the combustion chamber. STIG (Fig. 2.7) electrical power output is about 37 – 41 %, which makes it uneconomically viable in the current climate of technical advances especially when integrated with a SCCP. These are the two of the simplest configurations of flue gas CO_2 enhancement via humidification mechanism. A cocktail of other more complex configurations are under study and include but not limited to semi-closed humidified cycles, part-flow evaporative gas turbines, recuperated and intercooled-recuperated cycles, recuperative heating of the flue gas after condenser, regenerated water injected cycles, inverted brayton cycle and integrated bottoming cycle [69],[82].

It is widely agreed across the academia and industry that humidification has benefits with regards to increase in CO_2 concentration in the flue gas especially for HAT and STIG. However, the CO_2 enhancement is limited to about 5 vol%, meaning other techniques may need to be employed to boost the CO_2 concentration in the flue gas, with an expected increase in parasitic energy consumption on the turbine system when coupled with SCCP [69]. Interest of humidified system as a result is currently not a viable option unless novel technologies are established to counter these challenges [86].
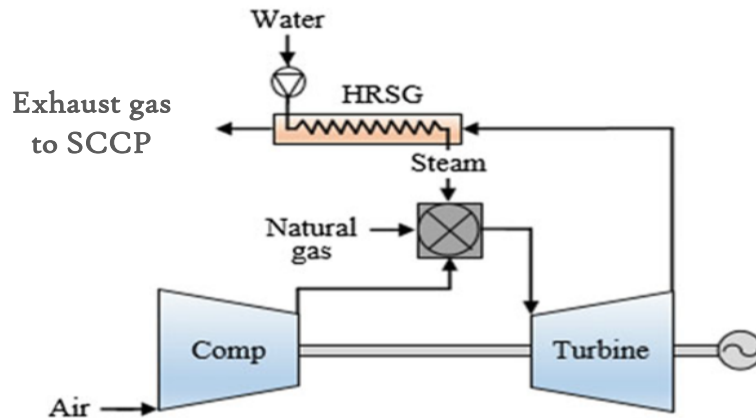
Fig. 2.8 Schematic of a STIG [69].

2.6 AMINES FOR CARBON CAPTURE

Post Combustion CO_2 capture employs the aid of Amines (chemicals that are spin-offs of NH_3, in which an alkyl or aryl group has taken over one or more of the H_2 atoms) to absorb CO_2 via a chemical reaction process when the aqueous amine solution converges with the process or flue gas. The CO_2 laden solvent is regenerated under the influence of thermal energy in a Desorber. Based on whether one, two or three of the H_2 atoms of the NH_3 are substituted by organic functional group; Amines are categorized into primary, secondary and tertiary amine. Amines commonly used for Carbon Capture include, but not limited to, Monoethanolamine (MEA), which is considered as the benchmarked Amine solvent, Diethanolamine (DEA), Triethanolamine (TEA) Methyldiethanolamine (MDEA), 2-Amino-2-Methylpropanol (AMP), Piperazine (PIPA) [87]. The CO_2 absorption capacity of solvent (maximum molar amount of CO_2 recovered per mole of MEA) is influence by the concentration of the solvent. The process of CO_2 absorption capacity of solvents is however relegated by the presence of trace gases, e.g. O_2, NOx, SOx, as these gases produce irreversible derivatives that negates CO_2 absorption reaction rate and solvent regeneration process [88],[56].

It is ironic that the production process of MEA (solvent widely employed to capture CO_2) involves direct or indirect CO_2 emission as well, ultimately increasing the carbon footprint of CO_2 capture process when the life cycle assessment is considered. MEA production kick-starts from NH_3 production as described in the following equation [89].

$$N_2 + 3H_2 = 2NH_3 \tag{2.9}$$

N2 is readily sourced from atmospheric air whereas H2 is sourced from steam reforming or partial oxidation of fossil fuel. Ethylene oxide (EO) is produced by oxidation of ethylene under the influence of silver catalyst as provided in equation 2.8 [89].

$$H_2C=CH_2 + 1/2O_2 = EO \qquad\qquad (2.10)$$

MEA production is an exothermic, high pressure, non-catalyst reaction between NH_3/H_2O and EO. NH_3 molecule reacts with one, two or three molecules of EO to form MEA, DEA and TEA respectively [89].

2.7 NOVEL SOLVENTS

The type of solvent used for CO_2 captured has a fundamental influence on the performance of CO_2 capture rate and day-to-day running of the plant. MEA (30 wt%) is widely utilized as the benchmark solvent for SCCP however, a variety of novel solvents are studied and tested to offset the limitations of the MEA. This includes high reboiler duty of about 3.2 - 4.2 MJ/kg CO_2, increased thermal degradation of between 120 – 135°C and tendencies of degrade under the presence of O_2 and high solvent flow rate requirement, thereby necessitating both higher CapEx and OpEx [82],[90],[91].

To address these challenges, solvents are blended together to compensate for each weakness in a symbiotic relationship. Novel solvents that have shown great viability also include ammonia-based solvents, amino-acid solvent, ionic liquid-based solvent and biphasic solvents [91]. Approximately 20% less regeneration energy requirement has been reported with CESARI, Econamine FG Plus and Praxair (new solvents) as against MEA at between 3.2 – 3.0 MJ/kg of CO_2. Cansolv (A shell proprietary solvent) has further reported 40% decrease in energy requirement as compared to Econamine [82],[92]. C-Capture has claimed to have engineered the most cost-effective and energy efficient solvent that uses amine-free proprietary solvent which utilizes about 1.5 GJ/tonne of CO_2 as compared to about 3.5 GJ/tonnes of CO_2 currently achieved with MEA [93].

2.8 BIOENERGY WITH CARBON CAPTURE AND STORAGE (BECCS)

CCS has an even more promising yardstick as a Negative Emission Technology (NETs), i.e. BECCS, when biomass is employed as all or part of the fuel mix for energy generation. This ambitious NETs is promoted to guarantee deep cut-back in global CO_2 emissions and a pathway towards meeting global warming goals of below 2°C. The context of BECCS gravitates towards the phenomenon of CO_2 absorption in the course of biomass growth (Natural Direct Atmospheric Capture), this CO_2 which is released into the atmosphere during combustion is captured, signifying not only a permanent removal of CO_2 from the atmosphere but a negative carbon balance [94], [95].

The fuel composition of biomass varies with that of conventional fossil fuel and as a result, system modifications is needed to counteract these limitations, which include lower HHV and higher water content than e.g. coal. Co-combustion of biomass appears to cause fouling in reactors. These reduces the energy productivity of power plant and even increased parasitic energy scenario when coupled with an ACP [94]. A number of climate change mitigation scenarios have shown that BECCS stands to be a great decarbonisation pathway, as illustrated in the Fig. 2.9 [96].
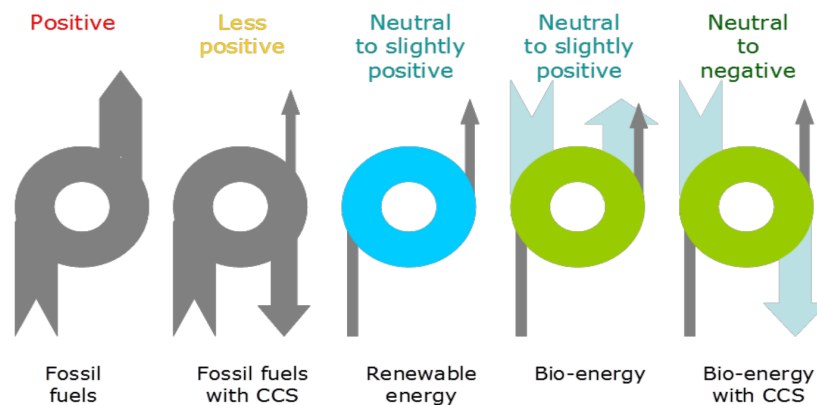
Fig. 2.9 Illustration of climate change mitigation pathways including CCS and BECCS.

Lack of conclusive information however prevails with regards to CCS operational performance with Bio-energy. The full potential of BECCS is being studied, Drax is currently trialling the first BECCS pilot project of its kind in the world using C-Capture's amine-free proprietary solvent. Six (6) major study pathways within two (2) major sectors tabulated as shown in table 2.1 have been identified for comprehensive investigation.

Table 2.1 BECCS study pathways [96].

Study pathway	Technological description	Feedstock share
Electricity generation		
PC-CCS co-combustion	Pulverized coal power plant with biomass co-firing **Post-Combustion**	30% co-firing (2030) 50% co-firing (2050)
CFB-CCS	Circulating Fluidized Bed Combustion power plant **Post-Combustion**	100% biomass
IGCC-CCS co-combustion	Integrated Gasification Combined Cycle with co-gasification of biomass **Pre-Combustion**	30% co-firing (2030) 50% co-firing (2050)
BIGCC-CCS	Biomass Integrated Gasification Combined Cycle **Pre-Combustion**	100% biomass
Biofuel production		
Bio-ethanol generation	Production of Bio-ethanol via hydrolysis and fermentation	100% biomass
FT biodiesel	Biodiesel based on gasification and Fischer-Tropsch-synthesis	100% biomass

Commercial BECCS has however come under much scrutiny with regards to the possible increases in food costs due to land grab to grow biomass, increases in evapotranspiration with unknown consequences and loss of biodiversity. These ethical concerns must be addressed alongside the technical limitations before BECCS eventually take-off on a commercial scale.

2.9 GLOBAL CCS FACILITIES

Carbon Capture has come a long way since the technology was first used back in the 1920's for separating CO_2 from methane gas discovered in commercial quantities. The 1970 ushered in a viable application when captured CO_2 was utilized for Enhanced Oil Recovery (EoR), which has proven to be profitable. Gas processing industries further developed this

technology by removing CO_2 from natural gas in order to have a value as a commodity. Climate change has necessitated the employment of this technology to reduce CO_2 emission and since then facilities from bench/pilot-scale to commercial ones has been constructed towards decarbonizing the energy as well as the heavy chemical industries [97].

Expeditious stride in CCS development projects are currently taking off. There are at least currently 7 test centres (tabulated in Table 2.2) including the UKCCSRC-PACT facility where my research experiments were carried out and an additional 16 centres which are in public consultation stage, ongoing or awaiting commission [98].

Table 2.2 Operational CCS test centres.

Name	Location	Focus
UKCCSRC Pilot-scale Advanced Capture Technology (PACT)	United Kingdom	Capture
CMC Research Institutes (CMCRI)	Canada	Full chain
National Carbon Capture Centre (NCCC)	United States	Capture
National Geo-sequestration Laboratory (NGL) Australia	Australia	Storage
Shand Centre Test Facility (CCTF)	Canada	Capture
Technology Centre Mongstad	Norway	Capture
Post-Combustion Capture (PCC) @ CSIRO	Australia	Capture

There are operational Pilot & Demonstration scale CCS facilities across power generation, cement, chemical, ethanol, fertilizer, iron & steel production and hydrogen production industries across the world that are under construction, in an advanced stage of development and awaiting commissioning [98]. Table 2.3 highlights demonstration plants that are directly incorporated to live power plants via a flue gas slipstream.

Table 2.3 Trials of SCCP integrated with live power plants [91].

Project	Location	Consortium	Cost	Capacity
Pleasant Prairie	Wisconsin, USA	Alstom Power/Electric Power Research Institute /We Energies	US$8.6 M	15,000 tCO$_2$/year
E.ON Karlshamn	Malmo, Sweden	E.ON Thermal Power/Alstom Power	US$15 M	15,000 tCO$_2$/year
AEP Mountaineer	West Virginia, USA	American Electric Power (AEP)/ Alstom Power/RWE/NETL/ Battelle Memorial Institute	US$668 M	100,000 tCO$_2$/year
Brindisi	Brindisi, Italy	Enel and Eni.	€20 M	8000 tCO$_2$/year
Plant Barry	Alabama, USA	Southern Energy/ Mitsubishi Heavy Industries/Southern Company/U.S. DOE's Southeast Regional Carbon Sequestration Partnership and EPRI	Unknown	500 tCO$_2$/day
Gaobeidian	Beijing, China	Huaneng Power Group/CSIRO	Unknown	3000 tCO$_2$/year
Shidongkou	Shanghai China	Huaneng Power Group	US$24 M	120,000 tCO$_2$/year
Shenhua	Mongolia, China	Shenhua Group	Unknown	100,000 tCO$_2$/year
Sinopec	Shangdong, China	Sinopec Group	Unknown	40,000 tCO$_2$/year
Boryeong	Boryeong, S.Korea	Korea Electric Power Company (KEPCO)	US$42 M	2 tCO$_2$/day (Phase 1) 200 tCO$_2$/day (Phase 2)
Wilhelmshaven	Bremen, Germany	Fluor/E.ON Kraftwerke	Unknown	70 tCO$_2$/day
CCSPilot100+	Ferrybridge, UK	SSE/Doosan Babcock/Vattenfall	£21 M	100 tCO$_2$/day
ECO$_2$	Burger	First Energy/ Powerspan/Ohio Coal Development Office	Unknown	20 tCO$_2$/day
Aberthaw	Wales	RWE npower/ CanSolv Technologies Inc.	Unknown	50 tCO$_2$/day

Pikes Peak	Saskatchewan	Husky Energy Inc. /CO_2 Solutions	US$12.13 M	15 tCO_2/day
EDF	Le Havre, France	EDF/Veolia/Alstom Power/Dow Chemical	€22 M	25 tCO_2/day

Large-scale CCS facilities are currently in an operational, ongoing, planning or cancelled around the world. The Caledonia Clean Energy PPC plant in the UK is expected to be completed in 2024. Large-scale facilities are defined as projects that process at least 800,000 and 400,000 tonnes of CO_2/year for coal and gas based power plants respectively [98]. Table 2.4 highlights the major CCS projects across the globe.

Table 2.4 Large-scale chemical absorption CCS projects [91].

PCC process	Developer	Solvent	Demonstration	Project
CanSolv	Shell	Amine-based	TCM Norway Aberthaw PCC Wales	Boundary Dam Canada (Operational) Bow City Canada (Planning)
Advanced Capture Process	Aker Clean Carbon	Amine-based	TCM Norway	Longannet UK (Cancelled) Porto Tolle Italy (Cancelled)
PostCap	Siemens	Amino acid salt	TCM Norway Big Bend PCC Florida	ROAD Netherlands (Planning) Masdar Abu Dhabi (Planning)
Econamine FG Plus	FLOUR	Amine-based	TCM Norway Wilhelmshaven PCC Germany	Trailblazer, Texas (Cancelled)
Advanced Amine Process	Alstom Power/ Dow Chemical	DOW UCARSOLTM FGC 3000	EDF PCC Le Havre, France Charleston PCC, West Virginia	Elektownia Belchatow, Poland (Planning) GETICA Romania (on-hold)
CAP	Alstom Power	Chilled ammonia	TCM Norway Pleasant Prairie	AEP Mountaineer

			PCC Milwaukee Karlshamn PCC Sweden Mountaineer CCS Phase I, West Virginia	CCS Phase II, West Virginia (Cancelled) Project Pioneer Alberta (Cancelled)
KM-CDR	MHI/KEPCO	KS-1 (Hindered amine)	Plant Barry, Alabama Plant Yates, Georgia	Petro-Nova CCS, Texas (Operational) 1.4mtpa
ECO2	Powerspan	Amine-based	Burger PCC, Ohio	
HTC	HTC Purenergy/ Doosan Babcock	Amine-based	International Test Centre, Canada	Antelope Valley CCS, North Dakota
CO2 Solution	CO2 Solutions Ltd	Enzyme-based solvent	Pikes Peak South PCC, Saskatchewan, Canada	
DMX	IFPEN/PROSERNA	Biphasic solvent	ENEL's Brindisi Pilot PCC, Italy	
RSAT	Babcock and Wilcox	OptiCap		

2.10 DYNAMIC OPERATION OF POST-COMBUSTION CO2 CAPTURE

Fossil fuel power plants will have to adapt to changes in electricity demand and operate more often to flexible (dynamic) loads in energy production due to the primarily increasing role the renewable forms of energy, such as wind and solar energy, has taken in the energy production mix. If CCS is to play an important role towards meeting its potential of decarbonizing the carbon-based energy industries in the near future, it must also adapt to these changes to make it techno-economically viable. The SCCP must be able to adapt to fast load changes without relegating the performance of the plant. The dynamic operation of a SCCP does have a direct impact on electricity pricing and CO_2 emissions, necessitating a close collaboration between the industry and government. This is so, because at high electricity demand, when electricity pricing is high, CO_2 capture system may have to be operated at low reboiler heat duty or shut down completely (consequently releasing CO_2) to avoid unacceptable high electricity costs. Research, demonstration and development is underway across the academia and industry to better understand how the performance of SCCP will fare under dynamic operations [99],[100],[101].

Tait et al. [102] conducted a CO_2 study to assess the performance of a pilot-scale CO_2 capture plant to a gas turbine shut down & start up including 3 operational dynamic conditions that include i. power output intensification by bypassing capture plant (steam to the reboiler and flue gas to the absorber stopped), ii. Power output intensification by bypassing the reboiler only (steam to the reboiler stopped) and iii. Thermal energy intensification to the reboiler (by increasing steam flow by 200%). Tait concluded that no major constraints were observed however, solvent inventory study and management is needed for increased performance of the CO_2 capture plant e.g. the proposed solvent storage tanks. A storage tank could be used to feed the CO_2 capture plant with lean solvent during seizure of reboiler steam input and/or to feed the plant with rich solvent when reboiler steam is intensified.

2.11   KEY CHAPTER DEDUCTIONS

- To curtail the energy utilization of PCC due to low CO_2 partial pressure, a number of the CO_2 enhancing mechanism were examined. These techniques are intended to increase the driving force behind CO_2 absorption towards saving the SRD.

- Emerging technologies like the Rotating Pack Beds (RPB), novel solvent development and government incentives to capture CO_2 via enabling favourable provision of policies and services to utilize CO_2 is expected to facilitate the creation of opportunities for the global deployment of commercial CO_2 capture. Sustainable BECCS is also expected to intensify deep decarbonisation campaigns in the energy industries.

CHAPTER III

EXPERIMENTAL CAMPAIGN SCHEME

INTRODUCTION:

The UKCCSRC Pilot-Scale Advanced Capture Technology facility is discussed in this chapter. This comprises the PACT CO_2 capture plant (which was used for experimental campaigns). The micro gas turbine, the gas mixing facility, instrumentations used for this experiment are also discussed. Methods and materials for evaluating data are also conveyed in this chapter.

3.1   THE PACT (PILOT-SCALE ADVANCED CAPTURE TECHNOLOGY) FACILITY

The UKCCSRC PACT national core facility parades a wide-ranging and integrated research facilities that closes the gap between research & development and large-scale industrial pilot evaluation, thus empowering engineers to run trials of their novel research models towards validating and proving its commercial certitude [103].

Facilities include two CHP Turbec T100 micro-gas turbines (mGT). These turbines have the capability of being integrated with the in-house Solvent-based Carbon Capture Plant (SCCP). The Plant is utilized for optimization processes using varying MEA and CO_2 concentrations while modifying a number of input variables and parameters. A Gas Mixing Skid (GMS) supports formulating of a desired synthetic gas for the SCCP when required. Other facilities within the centre also include a 250kW Air/Oxyfuel Combustion Plant, Biomass Grate Combustion Plant as well as a host of process and system modelling platforms. The PACT National Core Facilities is represented in Fig. 3.1.
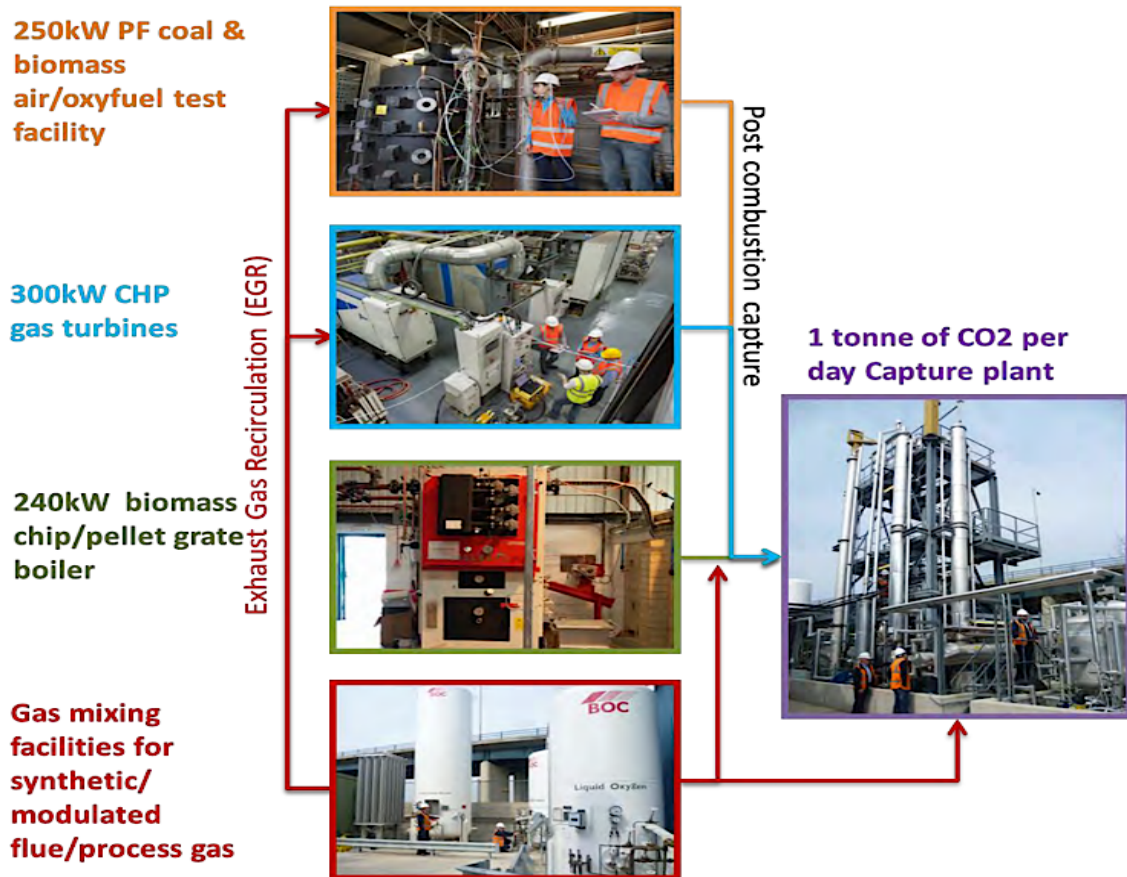
Fig. 3.1 UKCCSRC PACT National Facilities, Beighton. UK.

3.2 UKCCSRC-PACT TURBEC T100 MICRO GAS TURBINE

The experimental campaigns were performed at the United Kingdom Carbon Capture and Storage Research Centre (UKCCSRC) Pilot-scale Advanced CO_2 Capture facilities, Sheffield. The Brayton cycle natural gas fuelled Turbec T100 mGT based at the Facility are schematically represented in Figure 3.2 and this is configured so that the compressor, turbine and generator are positioned on the same shaft. Electricity production of up to 100 kW and ~165 kWth is produced from the mGT and this equates to 30% electrical efficiency with a total natural gas thermal input of 333 kW which increases to 80% efficiency when heat recovery is measured or utilized [64],[104],[105]. A centrifugal compressor is utilized to compress the ambient air (oxidant), which is routed to a recuperator to gain heat energy from the hot exhaust gas leaving the gas turbine. The compressed heated air is then combusted in the presence of natural gas in a lean pre-mixed combustor and consequently this produces 1.6 % (molar basis) of CO_2 [90]. The mGT generates low CO, UHC and NO_X emissions from the expanding exhaust gases at the turbine outlet, low enough that it

can be operated in greenhouses to provide CO_2 to facilitate plant growth [106]. A slipstream from the flue gas produced by the mGT is transmitted to the on-site SCCP for CO_2 capture. [63], [107]. A schematic of the Turbec T100 mGT specifications is given in Fig. 3.2.
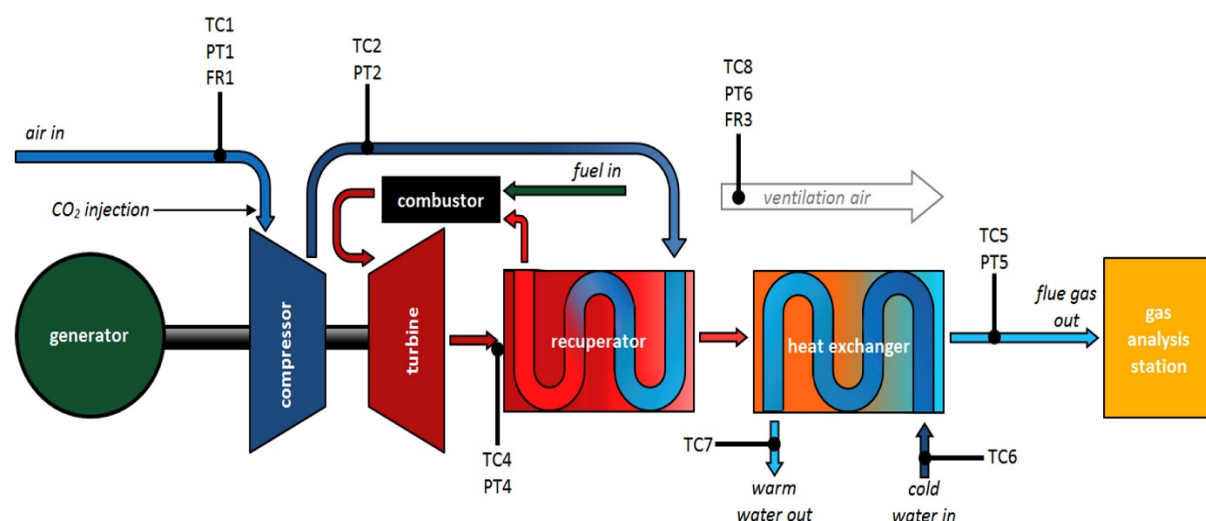
Fig: 3.2 Schematic of the Turbec T100 UKCCSRC PACT mGT modules showing CO_2 injection modifications. TC: Thermocouples, PT: Pressure transducers and FR: Flow rate monitors [108].

The main modules and configuration of the mGT is represented in Fig 3.2, a centrifugal compressor is employed to compress ambient air to an optimal pressure ratio of about 4.5:1 at maximum energy output. The capability to introduce CO_2 has been installed to simulate EGR and S-EGR to enhance CO_2 absorption and consequently reduction in energy consumption for every unit weight of CO_2 captured at the downstream SCCP. The influence of enhanced CO_2 concentration on the mGT linked with Computational Fluid Dynamics (CFD) study has however been studied by Finney and Clements et al. [105],[109]. To gain more electrical energy output, the compressed air acquires thermal energy from the recuperator, which is channelled to the swirl-stabilised combustion unit. The exhaust gases exit the combustion chamber at a temperature and pressure of about 950 °C and 4.5 bar, respectively and expands via the turbine, which drives the compressor as well as the generator. The exhaust gases losses it momentum at the turbine exit with both temperature dropping by approximately 300 °C and pressure plummeting to approximately atmospheric pressure. The exhaust gases further losses its temperature in the recuperator by transferring thermal energy to the combustor inlet air. Heat recovery from the exhaust is further exploited by passing it via a counter current water-gas heat exchanger to generate

hot water of about 70 – 90°C [105]. The main turbine operating specifications at full load is presented in table 3.1.

Table 3.1 Turbec T100 mGT specifications (nominal conditions), PACT Facility, UK. [40].

Parameter	Value
Exhaust gas flow	0.8 kg/s
Electrical output	100 kW
Hot water	165 kW
Combustion outlet temperature	1223 K
Turbine outlet temperature (TOT)	923 K
Compressor ratio	4.5
Fuel flow	39 Nm^3/h

3.3   PACT CO$_2$ CAPTURE PLANT: PROCESS DESCRIPTION

The UKCCSRC-PACT CO$_2$ Capture Plant is pictured in Fig. 3.3 is designed in concordance to a conventional model of reactive absorption with an aqueous solution of amines in an absorber-stripper configuration. The solvent based CO$_2$ Capture is designed to capture up to 1 tonne of CO$_2$ per day from coal combustion flue gas using 30wt% MEA as the reference solvent [63]. The ACP can be connected to the combustion facilities to permit for PCC studies from the flue gas stream of gas turbines, biomass grate boiler and as well as pulverized fuel combustion plant [107]. Furthermore, the CO$_2$ capture plant can also be coupled to dedicated gas mixi ng facility to enable carbon capture of a designated synthesized flue gas composition [103],[110].

Fig. 3.3 Photograph of the UKCCSRC PACT CO2 capture plant, Beighton, UK.

The PACT CO2 capture plant comprises of two reactors (the absorber and stripper) which are 8m in height and 0.3m in diameter featuring a Sulzer Mellapak CC3 structured packing of 6.5m. The absorber column has 10 thermocouples located at intervals of approximately 0.68m and at 0.56, 1.25, 1.93, 2.62, 3.30, 3.99, 4.67, 5.36, 6.04 and 6.73m whereas the stripper has 9 thermocouples located at approximately 0.9m interval at 0.39, 1.34, 2.19, 3.04, 3.89, 4.84, 5.69, 7.09 and 7.59m. These temperature points are plotted to gain an insight of the column temperature profiles under different process input variables. Pressure sensors, flow meters and solvent sampling orifices are also fitted to the columns. A desulphurization wash column is also installed upstream the absorber to remove the sulphur content that exists in

the flue gases in the coal combustion, and this can be taken offline when natural gas is employed. A condenser is fitted downstream of the stripper to enable rich stream of CO_2 at the end of the process. Fig. 3.4 shows the process flow illustration of the PACT CO_2 capture plant while Table 3.2 presents the plant's key specifications.

Table 3.2. The UKCCSRC ACP key design specifications as of September 2018 [63],[110],[111].

Parameters	Specifications
Flue gas source	Turbec T100 MGT + CO_2 feed
Absorber (packed) dimension	300 mm diameter, 6.5m height
Desorber (packed) dimension	300 mm diameter, 6.5m height
Packing type	Sulzer Mellapak CC3 packing
Water wash (packed) column	300 mm diameter, 1.2 m height
Flue gas flow rate (max)	$230 Nm^3/h$ (263kg/h)
Solvent flow rate	400 – 1200 kg/h
CO_2 Stripping energy	Pressurized hot water (PHW)
CO_2 removal rate (>85% capture using MEA)	1 tonne CO_2/day

The applications of the PACT facility include but not limited to:

i. Standardizing, testing and developing of different solvents with regards to the solvent regeneration energy requirement

ii. Performance of the plant under dynamic and flexible operational tests

iii. Performance of the plant based on different flue gas types from coal, natural gas to biomass

iv. Study of the solvent degradation mechanism

v. Study of the different and novel process optimization processes of the CO_2 capture
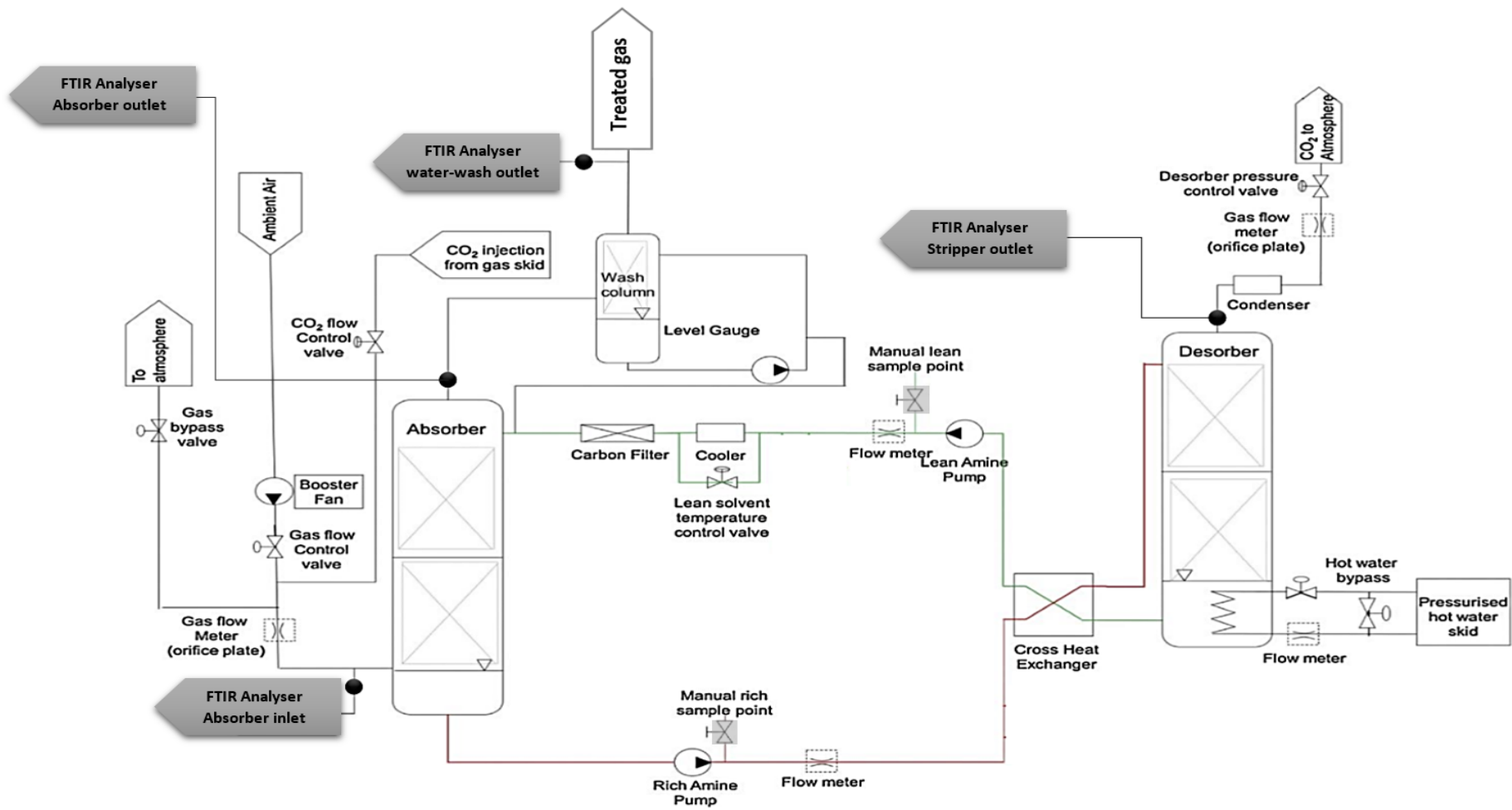
Fig. 3.4 Process flow scheme of the PACT CO2 capture plant as of September 2018 [112].

3.4 PERFORMANCE OF CO₂ CAPTURE

Fig.3.5 shows CO₂ flows in the SCCP. The flue gas (FG) entering the CO₂ capture system has technically 3 outputs and include the captured CO₂ stream (xCO₂ rich stream), cleaned gas (xCO₂ lean stream), CO₂ leaked into the atmosphere (xCO₂ leaked stream) and CO₂ holdup within the SCCP (xCO₂ accumulation) as diagrammatically presented below. xCO2.in is the Molar flow of CO₂ in the FG. CO₂ leaked is considered negligible and as a result is not included in the calculation, i.e. xCO₂ is assumed to be 100% CO₂ [113].
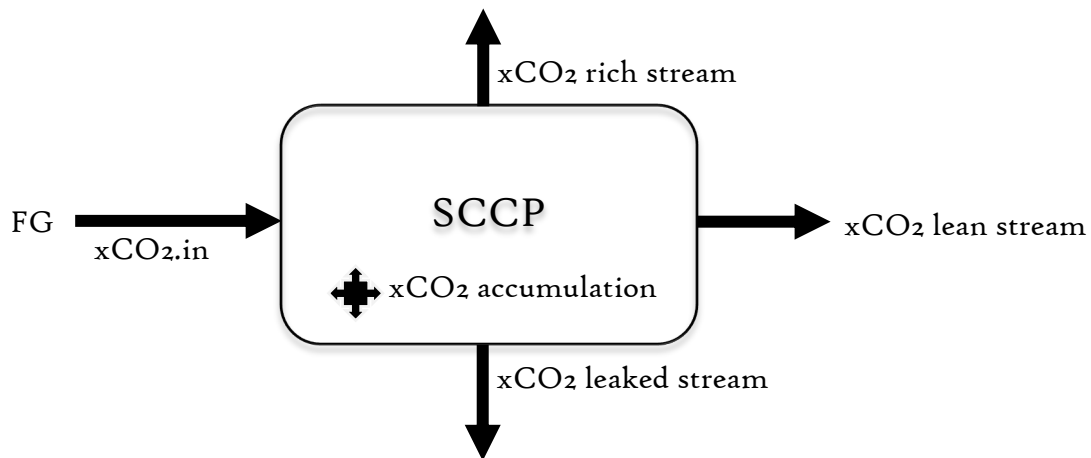
Fig. 3.5 CO₂ flow pathways in the SCCP.

The CO₂ capture efficiency (%) is given as follows:

$$= \frac{\text{xCO2 rich stream}}{\text{xCO2.in}} \text{ mol/hr} \tag{3.1}$$

$$= \frac{\text{xCO2 rich stream}}{(\text{xCO2 lean in stream} + \text{xCO2 rich stream})} \text{ mol/hr} \tag{3.2}$$

$$= \frac{\text{xCO2.in} - \text{xCO2 in lean stream}}{\text{xCO2.in}} \text{ mol/hr} \tag{3.3}$$

The captured CO₂ flow rate on the other hand can be calculated by the difference of the flow rate of CO₂ at the inlet and outlet of the absorber column which is mathematically presented as follows, or directly measuring the flow rate of the CO₂ rich stream.

$$\text{CO2 captured (mol/hr)} = \text{xCO2.in} - \text{xCO2 lean stream} \tag{3.4}$$

The absorption capacity (c_{abs}) which is the ratio of the flow rate of CO₂ captured (mCO₂) by flow rate of solvent amine (mL) and given as follows [90].

$$c_{abs} = mCO2/mL \ (g/kg) \tag{3.5}$$

The degree of solvent regeneration (x_{reg}) is directly influenced by the reboiler heat duty as well as the rich loading and is given as follows, where x_{CO2}^{rich} is the rich CO₂ loading and x_{CO2}^{lean} is the lean CO₂ loading [90].

$$x_{reg} = x_{CO2}^{rich} - x_{CO2}^{lean} \ / \ x_{CO2}^{rich} \tag{3.6}$$

3.5   PACT REBOILER

The Reboiler (heat exchanger) at the PACT enables the transfer of thermal energy from the PHW to the rich solvent for the purpose of reversing the absorption reaction between amine solvent and CO₂ (stripping) as schematically illustrated as follows in fig. 3.6.
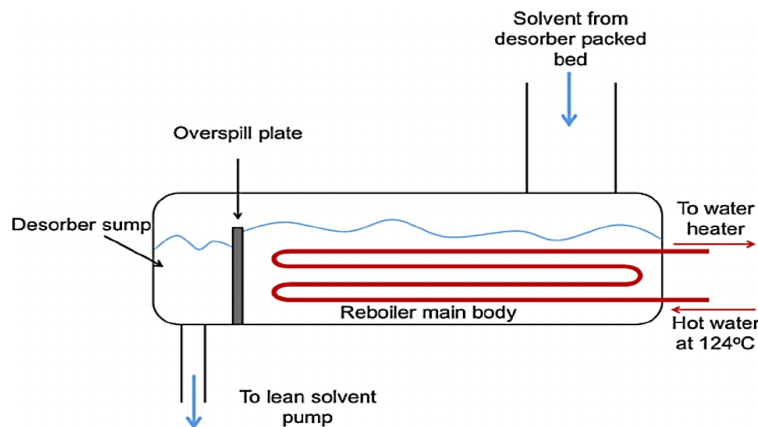
Fig. 3.6 Schematic of the PACT Reboiler design [112].

PHW is introduced into the Reboiler at a certain temperature and flow rate. The lean solvent stream is channelled through the lean outlet and pumped (recycled) back to the absorber to capture more CO₂. Whereas the stripped CO₂ and H₂O rises up through the stripper located above the reboiler, condensed and contained if need be. A photograph of the PACT reboiler is shown in fig. 3.7.
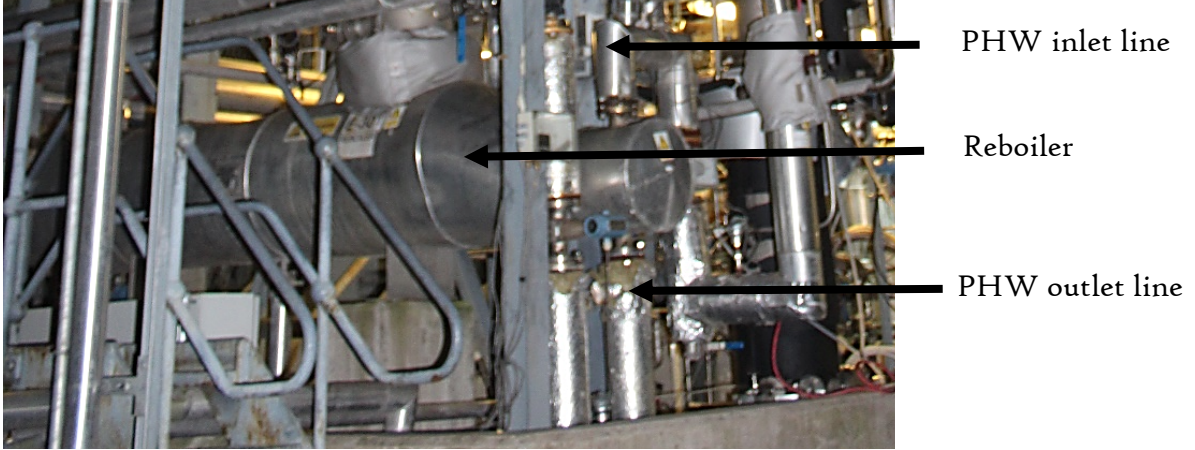
Fig. 3.7. Photograph of the PACT reboiler as of November 2019 [110].

At least 70% of the energy consumption of the SCCP is solvent regeneration energy requirement [90]. Recall that this factor underscores the research work of this thesis. The Specific Reboiler Duty (SRD) is calculated as the energy utilized to regenerate the rich solvent stream for every unit weight of CO_2 captured and mathematically given as follows:

where Q (MJ/hr) = Energy consumption, m_w (kg/hr) = mass flow of the PHW, Cp (mJ/kgK) = Specific heat capacity of PHW, $T_{in} - T_{out}$ (K) = Change in temperature of the PHW going in and out of the reboiler, $n_{co2.in}$ = moles of CO_2 at the absorber gas inlet, $n_{co2.out}$ = moles of CO_2 at the absorber gas outlet and MW_{CO_2} is the molecular weight of CO_2. Normalized Specific Reboiler Duty (N-SRD) is employed in this study and calculated as a ratio of the SRD to the base-case SRD.

$$Q = m_w * C_p * (T_{in} - T_{out}) \tag{3.7}$$

$$SRD \ (MJ/kg \ of \ CO_2) = Q / (n_{co2.in} - n_{co2.out}) * MW_{CO_2} \tag{3.8}$$

The solvent regeneration energy requirement (Q_{reg}) is characterized into four part, i.e. i. CO_2 desorption energy(Q_{des}), ii. Stripping steam generation energy or solvent vaporization energy(Q_{vap}), and iii. Solvent sensible heat(Q_{sh}) and reflux condensate sensible heat. The reflux condensate heating energy requirement is negligible and often not considered in some studies. The solvent regeneration energy requirement is mathematically expressed as follows [65],[114],[115],[116]:

$$Q_{reg} = Q_{des} + Q_{vap} + Q_{sh} \tag{3.9}$$

$$= m_{CO2}\Delta H_{CO2} + m_{H2O}\Delta H_{H2O}^{vap} + m_s\, C_p\, (T_1\text{-}T_2) \qquad (3.10)$$

where ΔH_{CO2} is the enthalpy of the CO₂ desorption, m_{H2O} is the mass flow of H2O vaporized from the desorber, ΔH_{H2O}^{vap} is the latent heat of water, m_s is the solvent flow rate, C_p is the heat capacity of the rich solvent, T_1 is the temperature of the rich solvent exiting the reboiler and T_2 is the temperature of the rich solvent entering the stripper.

The percentage decrease in energy consumption E_{dcr} is the amount of energy saved from an operating condition normally the baseline condition (E_1) to the modified operating condition (E_2) and this is given as follows [64]:

$$E_{dcr} = \frac{E_1 - E_2}{E_1} * 100 \qquad (3.11)$$

3.6   GAS MIXING SKID (GMS)

The desired flue gas blend is formulated in the GMS. The GMS is fed directly from N2 and CO2 large cisterns stored at a pressure of 9 and 15 bar, respectively, as pictorially shown in Fig. 3.8.

Liquid CO₂ cistern

Liquid N₂ cistern

Di-mineralized H₂O for water-wash

Fig. 3.8 Photograph of the gas storage facilities [110].

The liquid N2 is routed via a cryogenic vaporizer for depressurization prior to the GMS as shown in Figs. 3.9 and 3.10.

Fig. 3.9 Photograph of the cryogenic liquid N2 routed via a vaporiser prior to the GMS [110].

The flow rates of the gases from the cisterns are adjusted using flow control valves, which are pictorially shown in Fig. 3.10 until a desired gas composition is achieved.
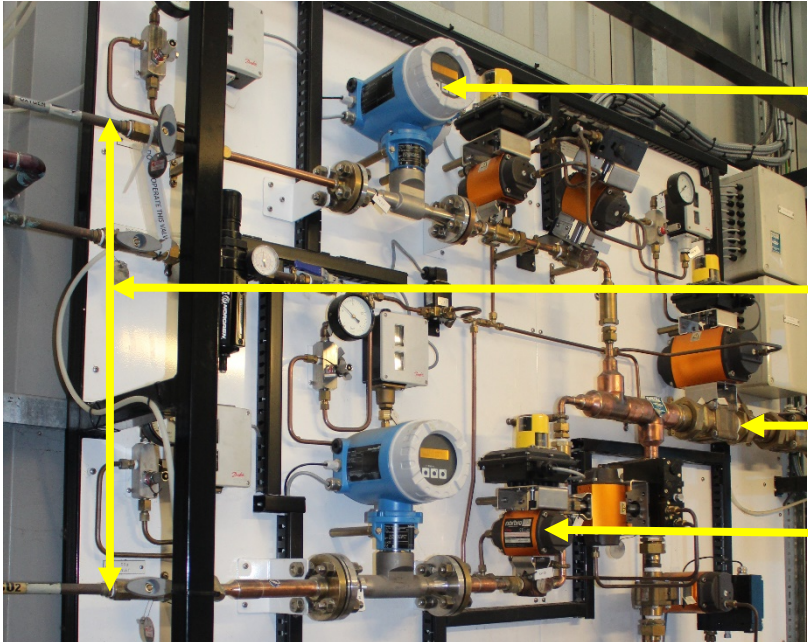
Fig. 3.10 Photograph of the CO2 and N2 lines from the pressurized tanks to the CO2 capture plant [103].

The synthetic gas is then directly fed to the CO2 capture plant. This connection between the ACP and the GMS enables a commanding capability to study the impact of different power generation process gases as well as the emissions from heavy industries, e.g. steel

and cement under any operating conditions on the performance of the CO_2 capture [103]. A booster fan at the base of the capture plant thereafter introduces the gas into the absorber.

3.7 GAS ANALYSIS: FOURIER-TRANSFORM INFRARED SPECTROSCOPY (FTIR)

Five (5) sampling lines are located across the length and breadth of the plant which are routed to the FTIR analyser as pictorially shown in Fig. 3.11. These lines are springy, heated and devised for incessant transmission of the gaseous media. Gas samples are taken from five different points and include i. Flue gas desulphurizer inlet, ii. Absorber reactor inlet, iii. Absorber reactor outlet, iv. Water-wash outlet, and v. Stripper reactor outlet. CO_2, O_2, NO_x, SO_x, VOC, HF, HCl are among about 50 different gases that the analyser can vet and have to passed through a heated oven unit at 180°C to ensure sampled gases do not experience condensation.

Heated oven unit

Sampling gas lines

Line to FTIR analyzer
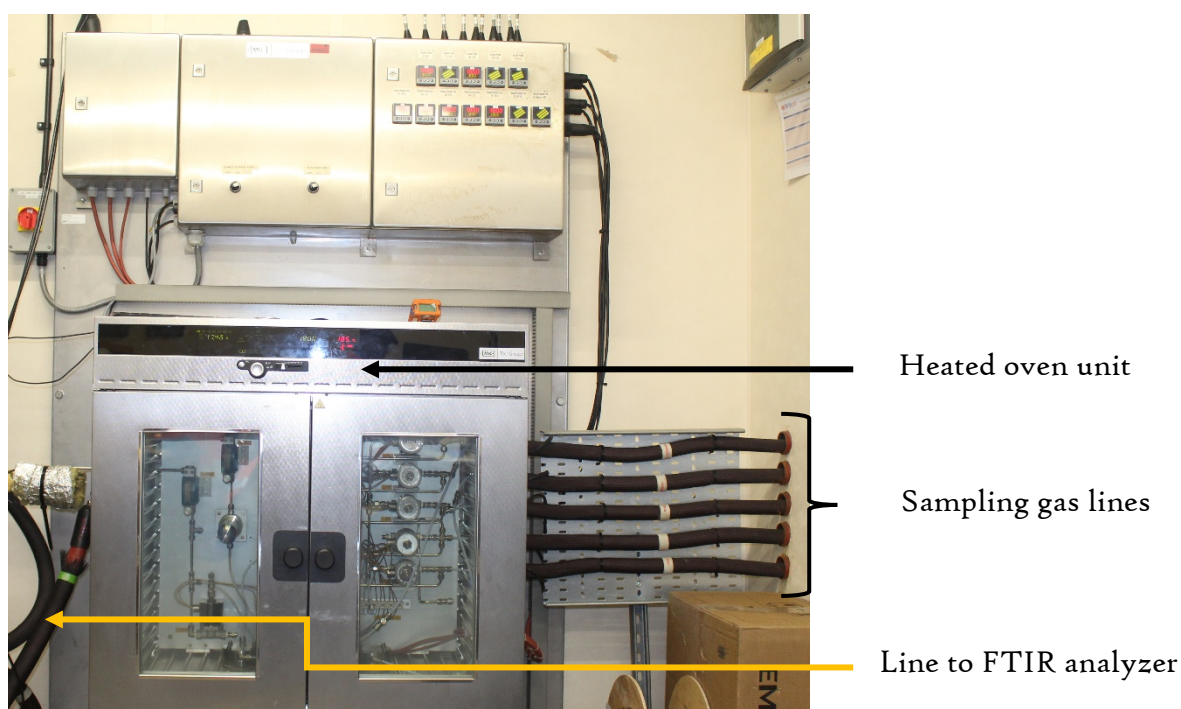
3.11 Photograph of the gas samples en route to the FTIR via the heated oven [110].

These lines are interchangeably connected to the Gasmet FTIR DX4000. The FTIR gas analyser, which is an effective means of fast multi-component measurement of the gas concentration is employed for analysis of the gaseous samples transmitted via the Gasmet heated sampling lines from the CO_2 capture plant onsite. A unique absorption signature is established based on the chemical construct of the gaseous molecule, thus every gaseous

specie does have a unique signatory profile and as a result the FTIR analyser computes the concentration of individual gases based on their absorption traits or characteristic vibrational frequency. This is also referred to as the fingerprinting of the gaseous specie.

Presented in Fig. 3.12 is a simple schematic of the principle behind the FTIR where an infrared radiation is generated via the Michelson interferometer. A beam-splitter splits the infrared beam to both the moving and stationary mirrors, where they are reflected back and detected. The Calcmet (computer program) records the result of the FTIR spectra [117], [118]. Gasmet has the capacity to simultaneously analyse up to 50 gas compounds with a response time of less than 120 seconds subject to the flow rate of the sampled gas designated, which is normally between 120 – 600 Litres/hr [119]. The image of the Gasmet FTIR DX4000 system employed in this experimental campaign is presented in Fig. 3.13.
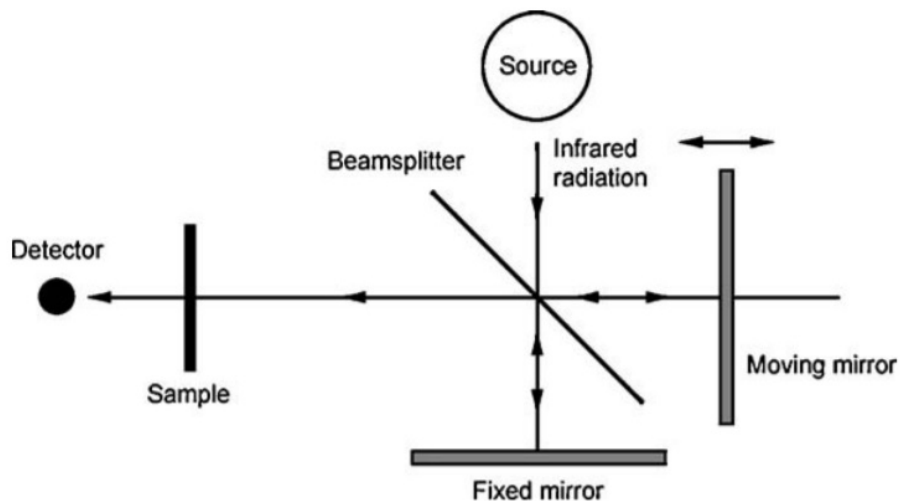
Fig. 3.12 Schematic illustration of the principles of the FTIR [120].
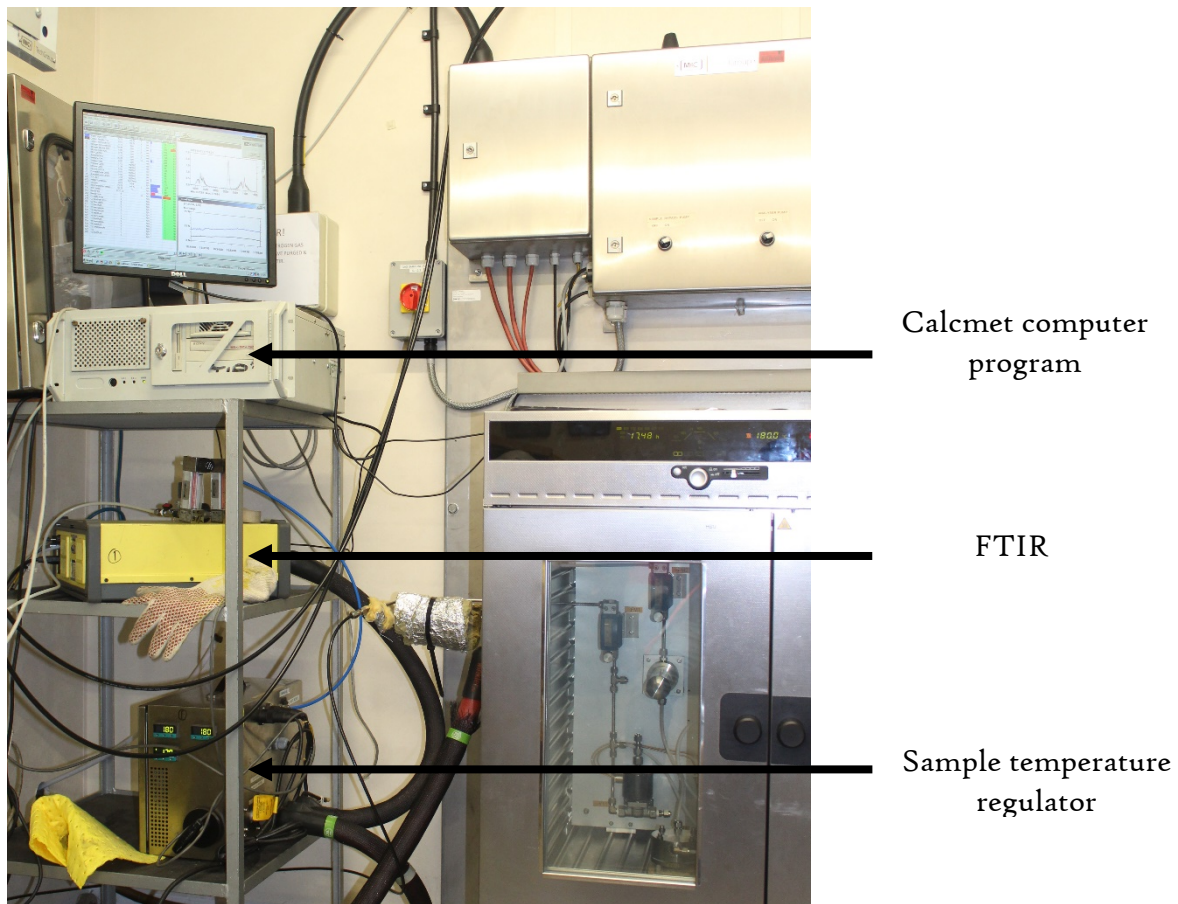
Fig. 3.13 Photograph of the FTIR system [110].

3.8   CONTROL SYSTEMS

The Motor Control Centre (MCC) accommodates the electrical switches, which are employed to distribute power to the electrical motors at the CO_2 capture plant. The Programmable Logic Controller, referred to as the Human Machine Interface (HMI), at the PACT ACP is a computerized workstation that is employed to control the flow of the liquid and gas across the CO_2 capture plant, flow control valves and reboiler temperature. Experimental data is recorded on the LabVIEW and PLC logs. Thus, the operator has access to all important process variables together with the FTIR log that enables a decision with regards to make a sound judgement in the course of the experiment, e.g. whether steady state operation has been attained. This is assessed by calculating the desired CO_2 capture efficiency; modifications are made if dependant parameters are not attained by modifying the input variables, e.g. the PHW temperature. It takes about two hours to run the CO_2 capture plant to reach steady state and liquid samples are manually collected 20-30 minutes after reaching steady state from the designated sampling points shown in Fig 3.4.

However, for the solvent degradation experiment, samples are collected at regular intervals regardless.

The HMI is able to be mirrored on a personal computer allowing the plant to be remotely operated. An image of one of the control screens shown in Fig. 3.14. This control platform enables the operator to designate and operate the control valve position, flow rate, pressure of the solvent and control the liquid levels in the column sumps.
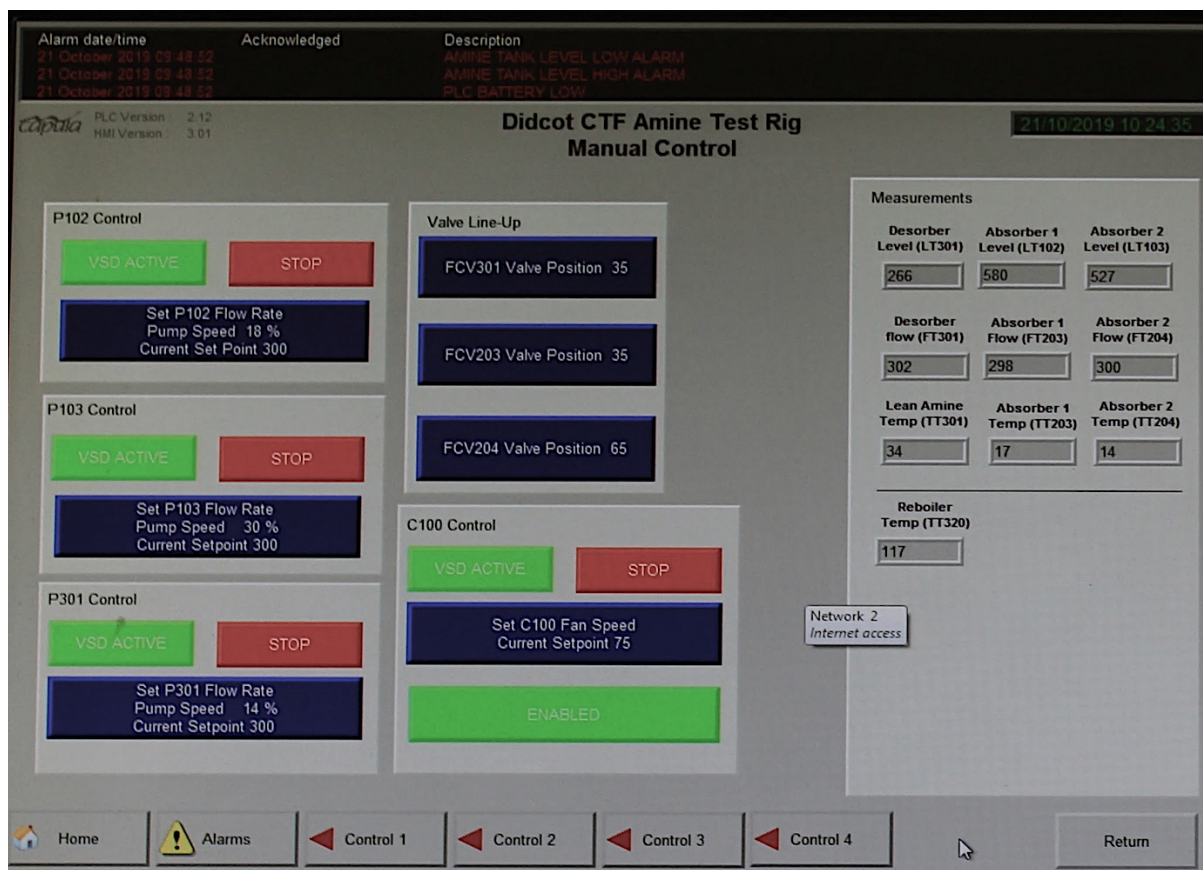
Fig. 3.14 An image of the main control platform on the Human Machine Interface.

The analysis of the recorded data of operations of the CO_2 capture plant is embarked on a designed spreadsheet with the emphasis on the key operating conditions, e.g. liquid and gas flow rates, operating temperatures and CO_2 concentration. Values of the measured input process variables from the LabVIEW, PLC and FTIR logs at the end of the steady state test time are averaged. Similarly, the analysis of the liquid samples are collated.

10 and 9 Resistance Temperature Detectors (RTDs) are distributed across the absorber and the stripper reactors, respectively, see Fig. 3.15, to gain an insight into the temperature behaviour within the columns during the study of the CO_2 absorption and desorption of

the different process flue gases under different operating circumstances. The RTD were also fitted at the reboiler inlet and outlet to calculate the amount of energy utilized for solvent regeneration.
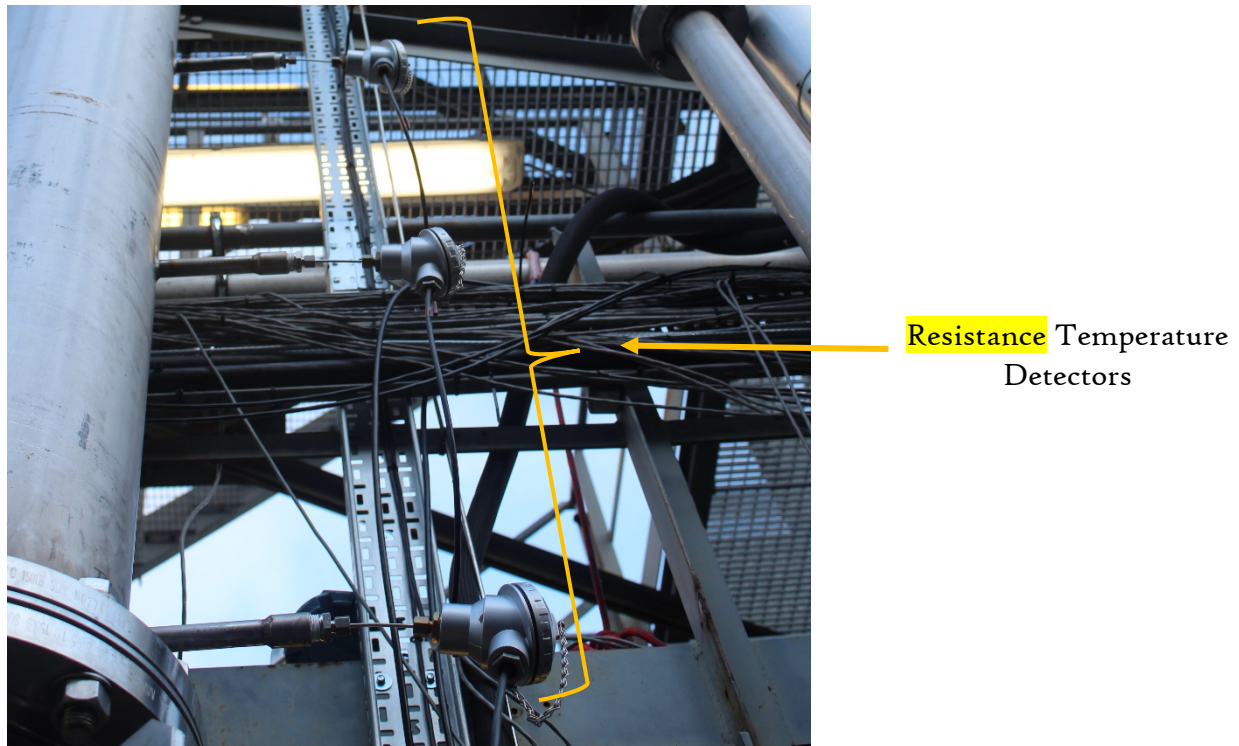
Fig. 3.15   Photograph of the RTDs on the PACT plant [110].

Grundfus centrifugal flow pumps were fitted at the CO_2 capture plant, which are responsible for pumping solvents across the absorber and stripper captioned in 3.16. Emerson flow meter with a liquid mass flow accuracy of ±0.10% was used to measure the flow rate, temperature and density of the fluid [121].
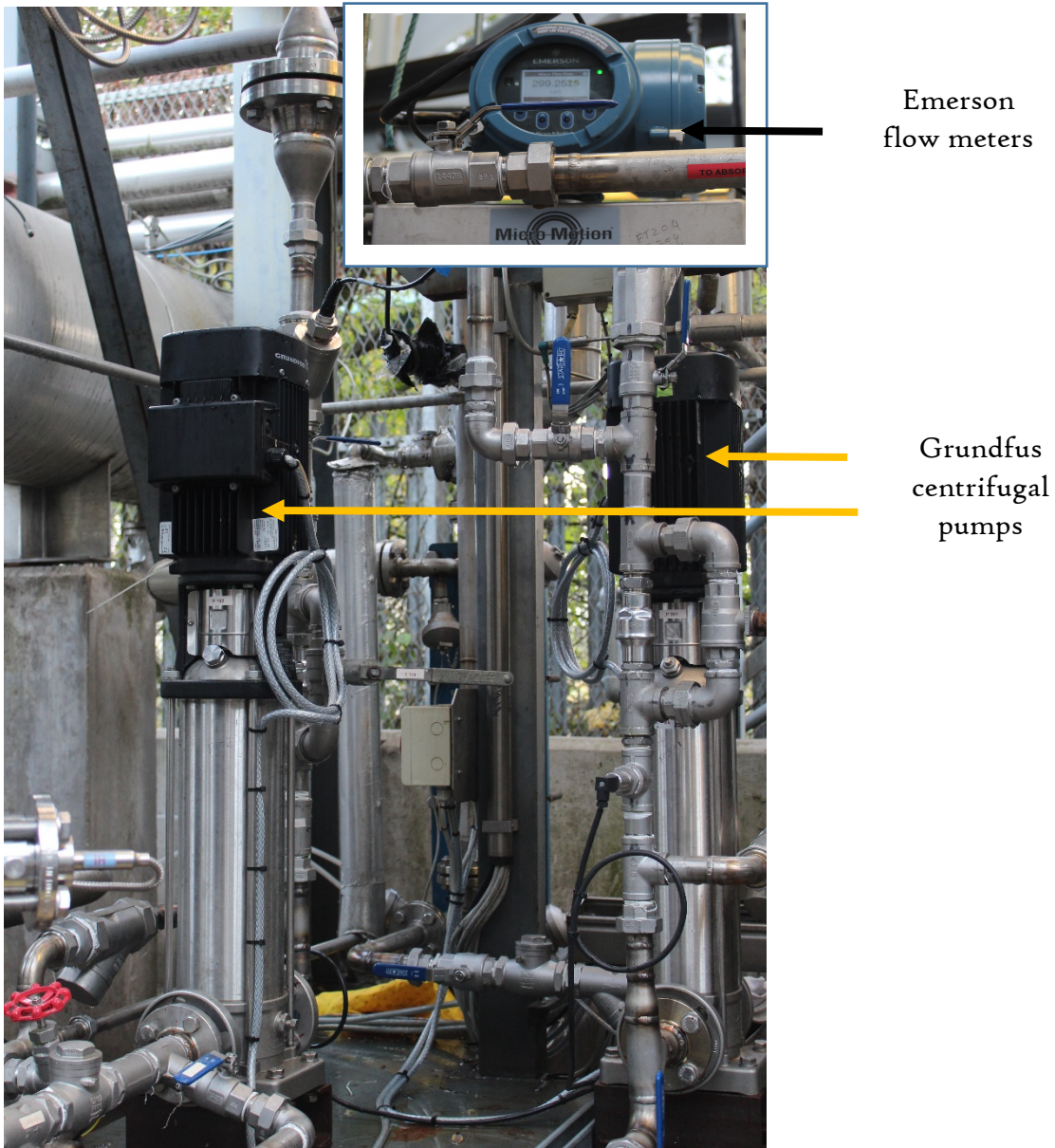
Fig. 3.16 Photograph of the centrifugal pumps and flow meters at the PACT plant [103],[122].

3.9   SOLVENT ANALYSIS

A Mettler Toledo T90 Auto-Titrator was used to analyse the MEA and CO_2 contents of the sampled solvents [123]. The CO_2 loadings, as well as solvent concentrations in the lean, semi-rich and rich solvent streams, were measured for every sampled solvent using the equation (3.12) and (3.13).

$$Active\ solvent\ (\%) = \frac{mL\ of\ HCl*0.1*61.08*100}{weight\ of\ sample\ in\ g*1000} \qquad (3.12)$$

The MEA content was determined by titrating ~1ml of the sampled solvent with 0.1M HCl in a beaker of 50ml deionized water [64].

$$CO2 \ content \ (\%) = \frac{mL \ of \ NaOH * NaOH \ molarity * 0.044 * 100}{weight \ of \ sample \ in \ g} \tag{3.13}$$

The CO_2 loading (%) was resolved by regulating the pH of 50ml methanol solution which is loaded into the analyser port to 11.2 using 0.5M NaOH. 1ml of the sampled solvent was then inserted into the pH regulated (alcoholic solution) methanol. The pH is then titrated back to pH of 11.2.

The CO_2 loading is then determined by the relationship given as follows.

$$CO2 \ loading \ (mol/mol) = \frac{CO2(wt\%) * 1.39}{weight \ (\%) \ of \ MEA} \tag{3.14}$$

A colorimeter test equipment was employed to measure the Fe concentration (mg/l) in the solvent due to the corrosion of the internal equipment of the PACT plant. This measurement has a sensitivity of 0.01 mg/l through the 1.10-phenanthroline method. A 50ml of sample is introduced into the port of the test kit were a background reading is taken, thereafter which the phenanthroline reagent is added to the sample, the reagent reacts with the Fe content and changes colour based on the concentration of the Fe present. and reintroduced back into the test kit where a second reading gives the amount of Fe content in the sample [124],[125],[126].

3.10 DEPENDENT AND INDEPENDENT OPERATING PARAMETERS FOR THE CO_2 CAPTURE

Table 3.3 presents the operating conditions that affect the key outcome performances, i.e. dependent parameters such as the CO_2 capture efficiency, CO_2 capture rate, degree of solvent regeneration, lean and rich CO_2 loadings as well as the SRD. It is in the interest of the operator to obtain the right cocktail of operating conditions that will ultimately run the plant at a low SRD while maximizing the CO_2 capture rate.

Table 3.3 lists the independent parameters that are influential in the performance of a CO_2 capture plant.

Table 3.3 Measured independent parameters of CO₂ capture process.

Parameter		Instrument/Remark
Flue gas	Composition	Sourced (synthetic) from the GMS/mGT
	flow rate	Plant instrumentation
	temperature	Plant instrumentation
	pressure	Plant instrumentation
Amine solvent	Composition	Vendor supplied (MEA)
	Concentration	40wt%
	Solvent flow	lab analyses
	Lean solvent temperature	Plant instrumentation
	Rich solvent temperature	Plant instrumentation
Columns	Absorber	6.5m, Sulzer Mellapak: Structured packing
	Stripper	6.5m, Sulzer Mellapak: Structured packing
	Stripper outlet pressure	Plant instrumentation
Reboiler	PHW temperature	Plant instrumentation
	flow rate	Plant instrumentation
	pressure	Plant instrumentation

The averaging of the FTIR and Labview data was done over a timescale of about 30 minutes under steady state conditions and the reference point of the steady process conditions used in this study is based on attaining a desired CO₂ capture efficiency. Calibration of the flow data measurement instruments were carried out. Mock experimental operation was thereafter carried out to ensure the control and measurement systems in all its ramification are thoroughly synchronized. The volumetric flow rate is monitored on the Programmable Logic Controller (PLC) screen to closely monitor and control that the flue gas and amine solvent flow rates are stabilized. This also necessitates close monitoring of the flow control valves, temperature and pressure sensors to identify any anomaly that may prevail in the course of the experiment. The sampled flue gases are firstly passed through a heated oven enroute to the FTIR to avoid condensation of the gas sample and enable the sample to be analysed in the physical state in which it is sampled. This FTIR enables for the determination of the difference of the CO₂ concentrations in the flue gas at the absorber

flue gas entry and exit point and used to calculate the CO_2 capture flow rate and the efficiency of the CO_2 capture process. This value is ultimately utilized in the calculation of the SRD. The Reboiler skid piping was also fully insulated in order to minimize the leakage of the heat energy through the piping work. Temperature sensors are also installed very close to the reboiler hot water entry point and exit point to ensure appropriate determination of the consumed thermal energy. Sampling of the amine solvent was done by flushing the amine solvent through the sampling orifice so as to remove any contaminants that may be lodged in the passage and the amine is finally sampled and securely enclosed in a plastic bottle.

3.11 THE PACT PLANT (WITH TWIN ABSORBERS): PROCESS DESCRIPTION

The PACT plant was fitted with an extra absorber to enhance the CO_2 capture towards reducing the SRD. This upgrade was embarked upon prior to oxidative degradation experimental tests. The two-absorber columns were both fitted with Structured Flexipac 350X packing with 12 thermocouples on absorber 1. A liquid distribution mechanism was also fitted at the top and mid-way through the columns to enhance the redistribution of the solvent with the aimed to facilitate the mass transfer of CO_2 from the gas to the liquid phase through enabling a higher inter-facial region for liquid phase. Gas distributors at the bottom of the columns were installed to expedite the even distribution of the gas as it rises along the columns. The aforementioned modifications are expected to improve the CO_2 capture and ultimately reduce the SRD. The updated advanced PACT plant configuration is given in Fig. 3.17.
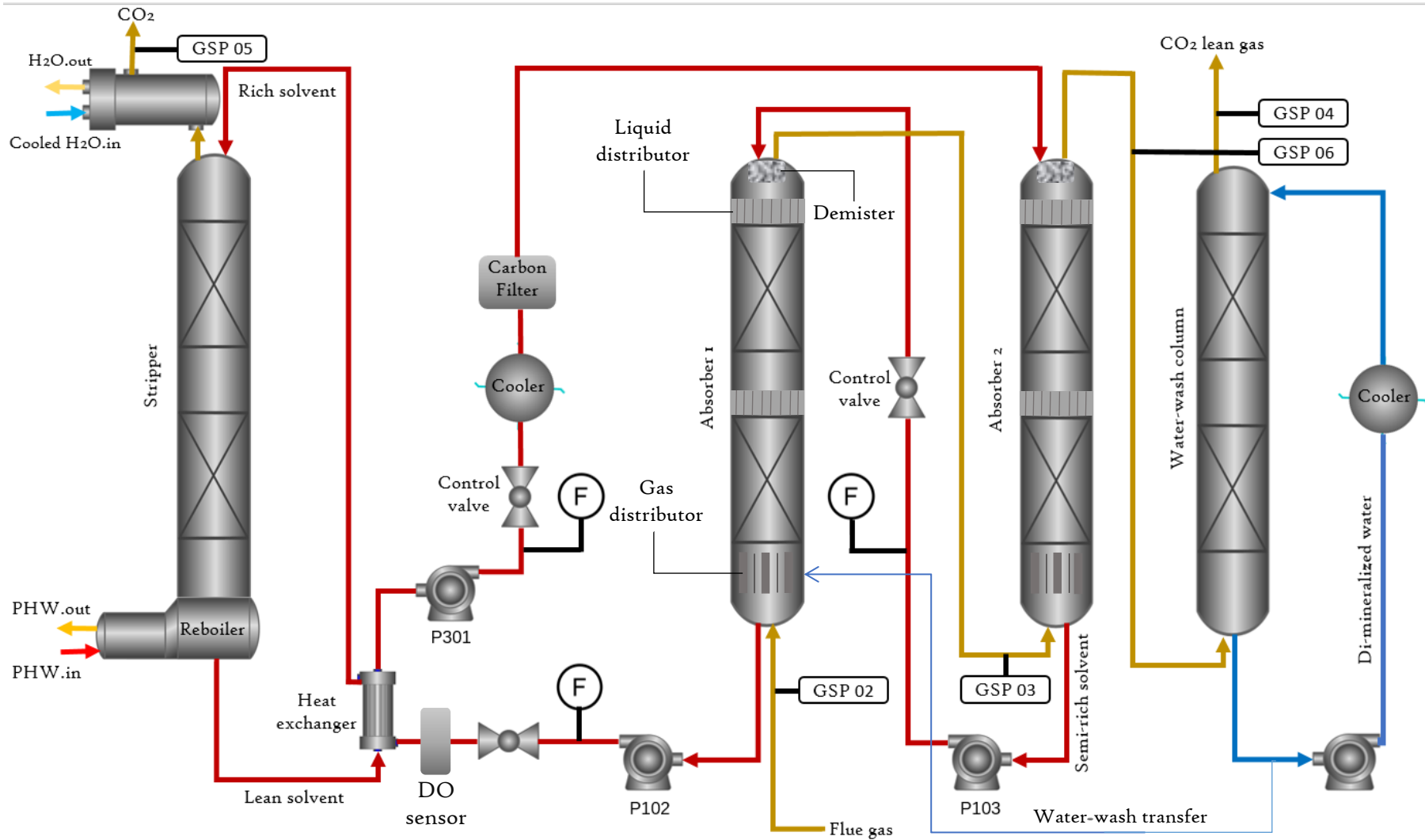
Fig. 3.17   A schematic of the PACT CO2 capture plant with twin absorber columns (Created from gCCS modules).

[GSP - Gas sampling point]

3.12   KEY CHAPTER DEDUCTIONS

- A brief outline of the UKCCSRC - Low Carbon Combustion Centre twin absorber PACT plant was presented with detailed illustration of the specifications, key components and process description. The plant is equipped with the GMS to enable for simulation of S-EGR. HMI and the MCC to enable for the control of the plant and data recorded at the LabVIEW, PLC and FTIR programmes to enable the study of how varying independent parameters affect key performing parameters of the CO_2 capture process. Thus, this capability will enable investigation of the process and operational conditions that influence the SRD and subsequently to design the process aimed at reduce the operating and overnight expenditure of the SCCP.

- Key performing independent and dependent parameters crucial to the performance of the pilot-scale capture plant were presented in this chapter.

- Methods of evaluating the performance of the SCCP, namely the SRD, CO_2 capture efficiency, CO_2 capture rate, CO_2 loadings, Fe concentration, degree of solvent regeneration and solvent absorption capacity are presented to enable for the analysis and an informed decision by an operator to optimally design the process conditions of the SCCP.

CHAPTER IV

EXPERIMENTAL INVESTIGATION OF THE INFLUENCES OF SELECTIVE EXHAUST GAS RECIRCULATION AND PRESSURIZE HOT WATER TEMPERATURE ON THE PERFORMANCE OF THE PACT PLANT

4.1   INTRODUCTION

Recent developments have proposed S-EGR as a technique to reduce the solvent regeneration energy requirement of the SCCP. The study in this chapter experimentally investigates how simulating S-EGR impacts on the performance of the pilot-scale advanced CO_2 capture plant with two absorber columns and under the influence of 40wt(%) MEA with regards to key performing parameters such as the SRD, CO_2 loadings and CO_2 capture rate in experiment 1. Whereas experiment 2 evaluates the impacts of varying Pressurized Hot Water (PHW) temperature on the performance of the CO_2 capture process with the aim of determining the lowest SRD while maximising the highest CO_2 rate. The results from this study is expected to make available data and information with regards to the process and operational parameters that are envisaged to strengthen the global deployment of CO_2 capture technologies by reducing the high reboiler heat duty.

This study is based on experimental study carried out at the UKCCSRC-PACT National Core Facility as described in figure 3.4.

4.2   APPRAISAL OF THE PACT PLANT WITH S-EGR UNDER THE INFLUENCE OF 40 wt(%) MEA

The experiment under the influence of S-EGR examines the performance of the pilot-scale PCC plant using 40wt% MEA and across a range of CO_2 concentrations from 5.5 to 9.1 vol(%). The flue gas mass flow for the CO_2 concentrations was kept at approximately 170 m^3/hr while the CO_2 flow rate at the absorber inlet was increased to achieve the aforementioned CO_2 concentration. The solvent flow rate was increased from 476.4, 570.7, 853.4 to 975.0 kg/hr for the 4 test cases so as to maintain the same CO_2 capture efficiency at approximately 90%. This is due to a long-established but unwritten consensus across the

academia and industry in standardizing 90% as the capture efficiency, which enable capturing of CO_2 at a high capture efficiency without exorbitantly increasing the capture cost. Tables 4.1 and 4.2 presents the key tests data of the dependent as well as the independent process conditions utilized in experiment 1 (simulating S-EGR) and experiment 2 (varying PHW temperature).

Table 4.1   Experiment 1: Summary of the test data (varying CO₂ concentrations).

Parameter	Unit	Test 1	Test 2	Test 3	Test 4
CO₂ concentrations	vol(%)	5.0	6.6	7.7	9.1
FG flowrate	m^3/hr (STP)	170.1	171.1	169.3	171.4
FG inlet temperature	∘C	41.7	39.4	39.7	39.3
FG outlet temperature	∘C	48.1	49.1	42.4	41.0
Lean solvent flowrate	kg/h	476.4	570.7	853.4	975.0
L/G ratio	-	2.1	2.5	3.8	4.2
Amine flow/CO₂ captured	-	12.3	11.2	14.2	13.5
PHW in temperature	∘C	125.7	125.6	125.7	125.7
PHW out temperature	∘C	122.7	122.6	121.6	121.4
Rich loading	mol CO₂/mol MEA	0.378	0.379	0.392	0.399
Lean loading	mol CO₂/mol MEA	0.262	0.267	0.304	0.319
CO₂ captured	kg/hr	14.9	19.9	23.0	26.9
Capture efficiency	%	89	89	89	88
Absorption capacity	g(CO₂)/kg(Solvent)	81.4	89.6	70.4	74.0
Normalized Specific Reboiler Duty (SRD)	-	1.00	0.75	0.92	0.86
decrease in energy consumption	%	-	25.1	8.2	16.3

| Degree of solvent regeneration | % | 30.69 | 29.55 | 22.45 | 20.05 |

Table 4.2 Experiment 2: Summary of the test data (varying PHW temperature).

Parameter	Unit	Test 1	Test 2	Test 3	Test 4
CO_2 concentration	vol(%)	9.1			
FG flowrate	m^3/hr (STP)	168.9	170.2	171.4	169.5
FG inlet temperature	∘C	40.9	40.1	39.3	41.0
FG outlet temperature	∘C	41.8	41.8	41.0	41.5
Lean solvent flowrate	kg/h	986.1	981.3	975.0	976.7
Amine flow/CO_2 captured	-	15.5	14.1	13.5	13.4
PHW in temperature	∘C	123.8	124.8	125.7	126.8
PHW out temperature	∘C	119.6	120.5	121.4	122.2
Rich loading	mol CO_2/mol MEA	0.414	0.419	0.399	0.373
Lean loading	mol CO_2/mol MEA	0.344	0.328	0.319	0.277
CO_2 captured	kg/hr	23.4	25.4	26.9	27.7
Capture efficiency	%	78	83	88	91
Absorption capacity	g(CO_2)/kg(Solvent)	64.5	71.2	73.9	74.6
Normalized Specific Reboiler Duty (SRD)	-	1.00	0.94	1.07	1.12
Change in energy consumption	%	-	6.2	-3.7	-12.3
Degree of solvent regeneration	%	16.91	21.72	20.05	25.74

The backdrop of the experimental process variables in experiment 1 showing trend of the flue-gas flow rate and L/G across varying CO₂ concentrations and experiment 2 showing

the process characteristics across varying PHW temperature are graphically represented in Figs. 4.1 and 4.2 as follow.
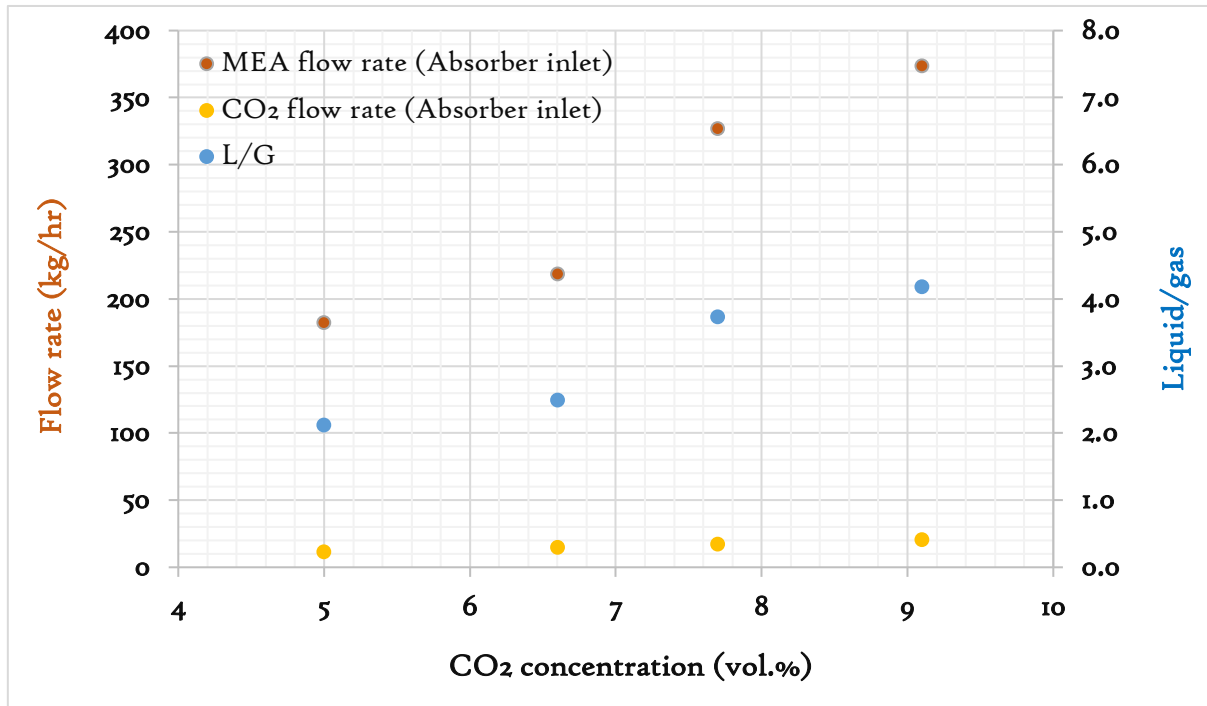
Fig. 4.1 Outline of the operating conditions of mimicking S-EGR at 40 wt% MEA

In the second set of tests, the PHW flow rate, CO_2 flow rate at inlet of the absorber were maintained at 11.4 m³/hr and 21 kg/hr while the PHW was increased from 124, 125, 126 to 127°C as shown in Fig. 4.2.
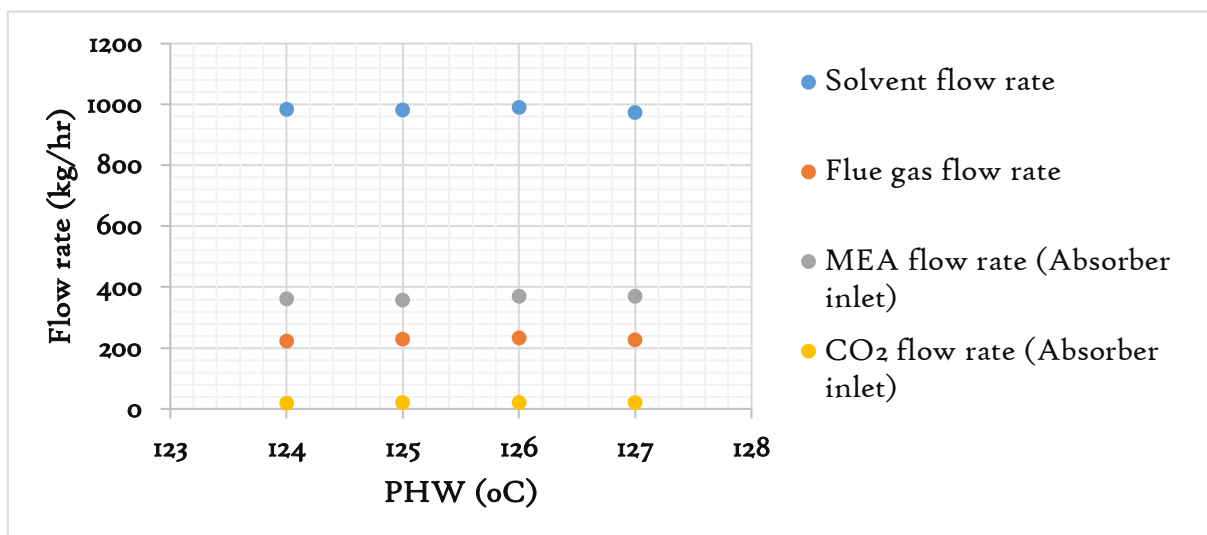
Fig. 4.2 Outline of the operating conditions with varying PHW temperature.

4.3 (a) INFLUENCE OF VARYING THE CO_2 CONCENTRATIONS ON THE CO_2 LOADINGS

Lean loading has a significant effect on the CO_2 capture process. The higher is the reboiler heat duty then the lower is the lean loading and consequently the degree of solvent regeneration is increased. Solvent regeneration is influences by: (i) the sensible heat, which is necessary to increase the temperature of the aqueous solution of amine to the desired temperature of the reboiler inlet temperature. (ii) the heat of absorption/desorption that is required to reverse the CO_2-solvent chemical bonding and this is influenced by the amount of CO_2 captured, amine type and its concentration. (iii) the heat of vaporization, which is responsible for the production of the steam required to sustain the driving force, this is influenced by the partial pressure of CO_2 and H_2O vapour that is in equilibrium with the solvent phase [127],[128].

The lean CO_2 loadings were observed to increase from 0.262, to 0.319 with increasing CO_2 concentrations from 5.0 to 9.1. This behaviour represents a percentage increase of 21.8 % between the aforementioned CO_2 concentrations. This trend was as a result of increasing the CO_2 concentration in the CO_2 rich solvent stream and solvent flow rate entering the stripper and reboiler as the reboiler thermal input was kept constant. As the lean CO_2 concentration increases, so does the rich CO_2 loading. The rich loading was further facilitated by increasing the CO_2 partial pressure in the flue gas with increasing the CO_2 concentration. A percentage increase of 5.56 % in the rich loading was observed from 0.378, to 0.399 between the aforementioned CO_2 concentrations. The rich loading would have been higher in the absence of increasing the solvent flow rate, which was increased in order to maintain the CO_2 capture efficiency of approximately 90 %. Notz et al. (2010), Akram et al. (2016) and Rezazadeh et al. (2016) all reported increasing CO_2 loadings of the solvent with increasing CO_2 concentrations. While Akram et al., 2016 reported a 14.2 % increase in the rich loading between 5.5 to 9.9 vol(%) CO_2 and which translates to 2.8 % increase for every unit percentage increment in CO_2 concentration with 30wt% MEA. A 5.5 % increase of rich loading from 5.0 to 9.1 vol% CO_2 was observed with 40wt% MEA in these tests. Running the same process conditions at the same plant with higher MEA concentration is expected to produce a much higher rich loading for every unit percentage increment in CO_2

concentration, enhance CO_2 capture recovery and reduce the N-SRD. Brigman et al; (2014) has reported a reduction of SRD by 14% when the amine concentration was increased from 30 to 40 wt(%). This is in line with a studies by Abu Zahra et al., 2007 and Akram et al 2020., which established that higher MEA concentrations translates into a higher rich loading due to the increasing driving force for the CO_2 absorption [129],[130]. Higher CO_2 loading was however, reported to facilitate corrosion of the plant's equipment, the products of such corrosion is reported to facilitate solvent degradation especially in the presence of oxygen [131]. Fig. 4.3 presents the relations between the CO2 concentration and the CO2 loadings.
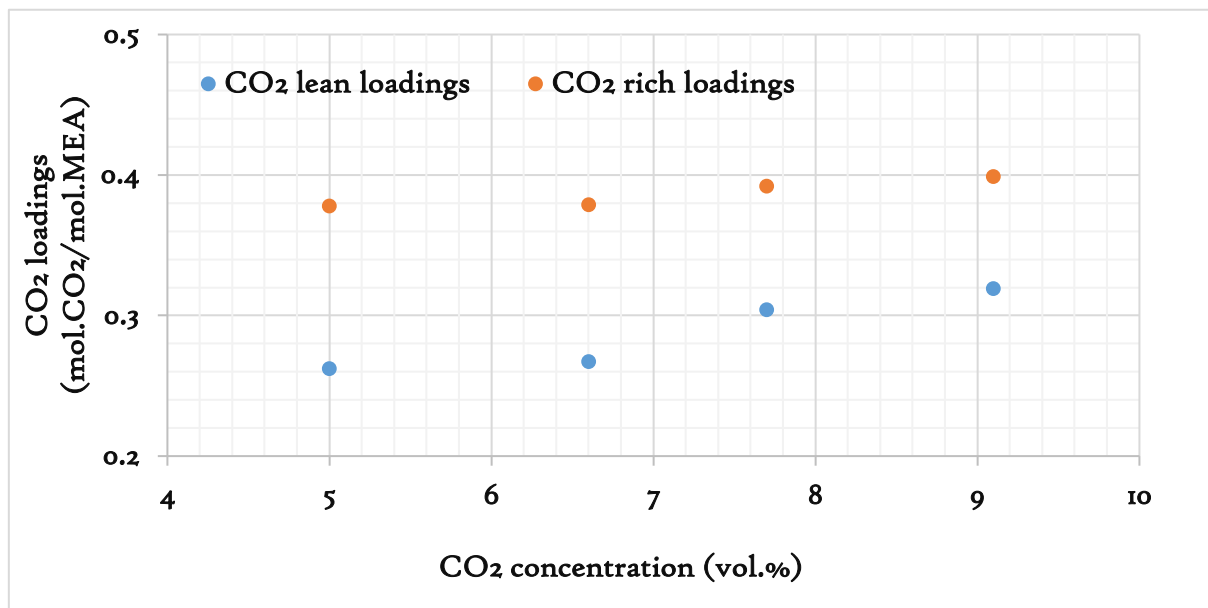
Fig 4.3   The CO2 loadings as a function of the flue-gas CO2 concentrations.

4.3 (b)   INFLUENCE OF THE PHW TEMPERATURE ON THE CO2 LOADINGS

The lean and rich CO_2 loadings at a fixed CO_2 concentration of 9.1 vol(%) were observed to decrease with increasing PHW temperature. Both the lean and rich loadings decreased from 0.344 to 0.277 and 0.414 to 0.383, respectively. This represents a decrease of 19.48 % and 7.49 % for the lean and rich loadings, respectively. By increasing the PHW temperature, regeneration of the solvent intensifies, provided that the solvent flow rate and the CO_2 partial pressure remains constant, and consequently this produces a lower lean loading. The lean loading was observed to decrease by about 19.48% as noted earlier with increasing PHW temperature, thus suggesting the influence of increasing the PHW temperature from 124 to 127 $^\circ$C on the CO_2 desorption. As the lean CO_2 decreases, so does the rich loading with increasing the PHW temperature, thus signifying an increasing capacity to capture

more CO_2 as the PHW temperature is increased. This behaviour is in agreement with the study by Sakwattanapong et al (2005) [132]. For the reason that studies have reported thermal degradation to be facilitated above 130 °C, PHW inlet temperature was kept below the thermal degradation threshold at 127 °C [90],[133]. This finding was on the backdrop of a study by Rochelle et al; 2009 who established that MEA degrades at a pace of about 2.5 – 6 % weekly when held at 135 °C [90],[132],[133],[134].
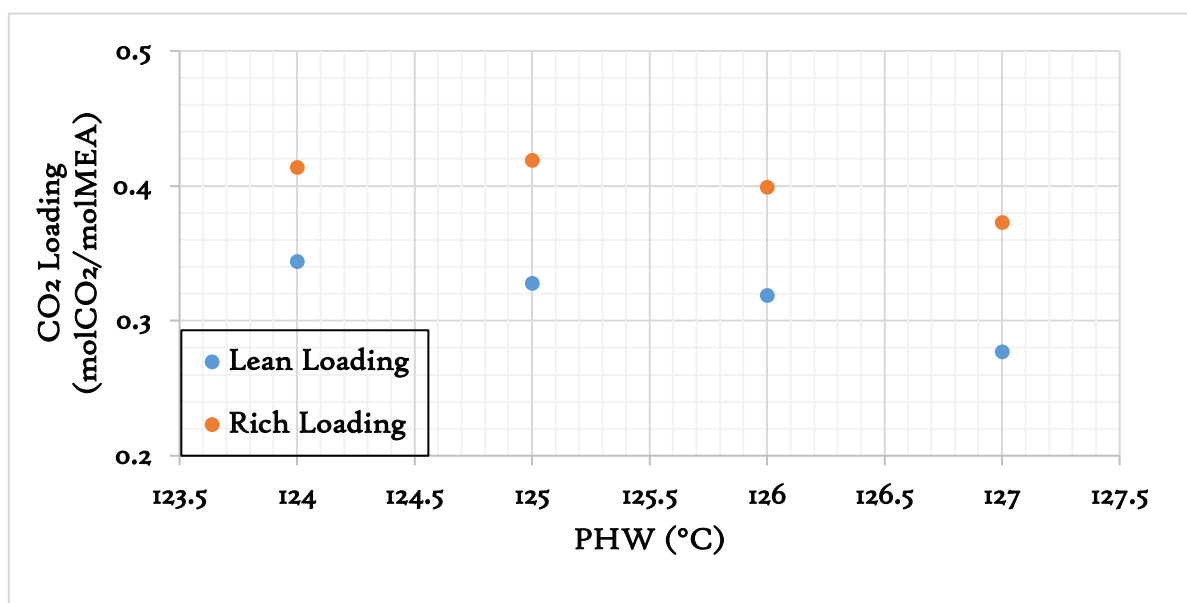
Fig. 4.4   The CO_2 loadings as a function of the PHW temperature.

4.4 (a)   INFLUENCE OF VARYING THE CO_2 CONCENTRATIONS ON THE N-SRD

The N-SRD is expected to decrease with increasing the CO_2 concentrations in the flue gas stream prior to introduction at the absorber gas inlet. More CO_2 is captured with increasing the CO_2 concentration in the flue gas due to the higher driving force for the CO_2 absorption, thus increasing the value of the SRD [64],[65],[75]. However, the N-SRD in these tests was observed to behave in a sinusoidal manner as demonstrated in Fig. 4.5. With increasing the CO_2 concentration from 5.0 to 9.1 vol(%), the solvent flow was increased by 19.8% to maintain a CO_2 capture efficiency at 90% and as a result increases the amount of CO_2 captured. This reduces the N-SRD in spite of the increase in the reboiler heat duty utilization. With increasing CO_2 concentration in the flue gas (above a CO_2 concentration of 5.0 vol(%) and the solvent flow rate, the solvent residence time in the reboiler drastically reduces, and more reboiler thermal energy is consumed for CO_2 desorption to accommodate

the increased solvent flow rate. This increase in reboiler duty utilization causes a higher N-SRD despite the higher CO_2 captured. The marginal decrease in N-SRD from 7.7 to 9.1 vol(%) of CO_2 was due to the increased CO_2 capture at a slightly higher CO_2 partial pressure. Also, it was noted that a good indicator of the behaviour of the N-SRD and the ratio of the solvent flow rate to CO_2 capture as shown in Fig. 2. The higher is the ratio of the solvent flow rate to CO_2 captured, the higher is the N-SRD when both are represented as a function of the CO_2 partial pressure. This finding is on the backdrop of a study by Akram et al., 2020 who reported a decrease in the N-SRD as the MEA concentration was increased from 30 to 40 wt(%) by about 14 %. Increase in the CO_2 recycle ratio is expected to further deliver lower N-SRD due to increasing capacity of the amine solvent to absorb more CO_2.
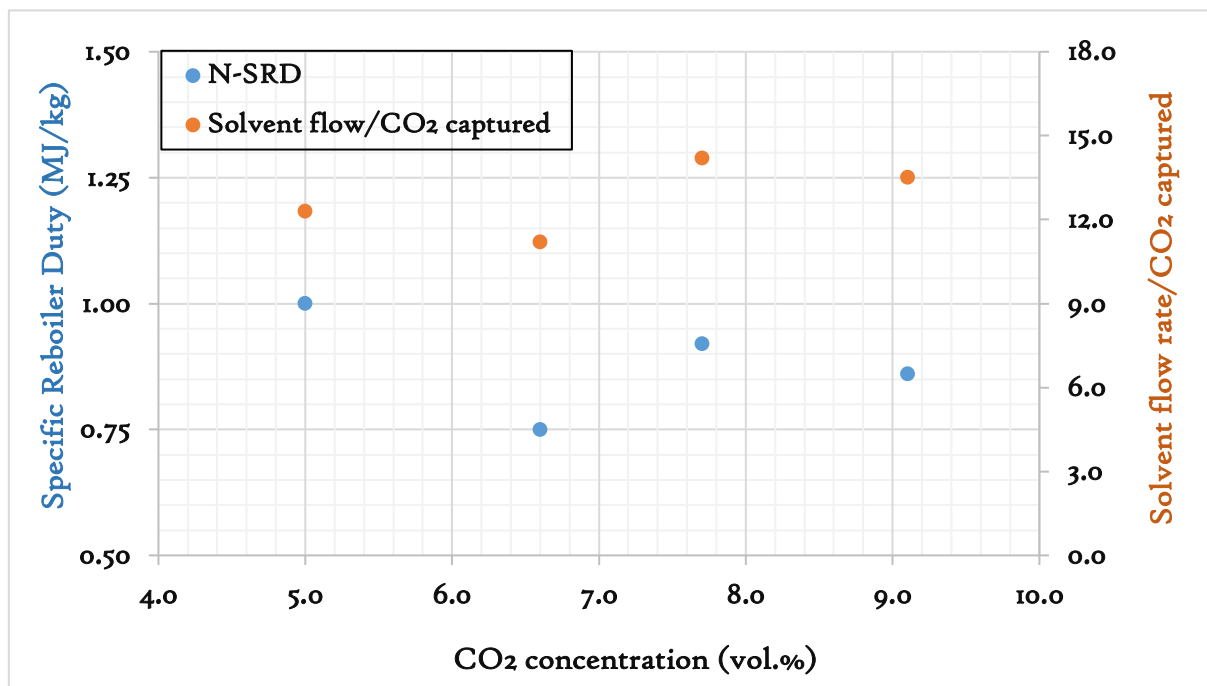
Fig. 4.5 The N-SRD and solvent flow/CO₂ captured ratio as a function of the CO₂ concentration

Figure 4.6 gives an insight into the behaviour of the N-SRD in experiment 1. From 5.0 to 9.1 vol(%) of CO₂, the absorption capacity increased from 81.4 to 89.6 g/kg and the energy consumption reduced by 25.1%, thus prompting a decrease in the N-SRD from 1.0 to 0.75. The operational conditions at CO_2 concentration of 6.6 vol(%) is thus observed as the CO₂ concentration with the lowest SRD in these tests, this value is also where the absorption capacity and reduction in energy consumption were highest. The absorption capacity and

reduction in the energy consumption both decreased thereafter CO2 concentration at 6.6 vol(%) as shown in Fig. 3, and this is due to the increased reboiler heat duty utilization with increasing the solvent flow rate to maintain the CO_2 capture efficiency at approximately 90 %.

Within the course of the CO2 capture process, the highest value of the absorption capacity signifies the process conditions that value gives the lowest reboiler heat duty and this is to be achieved via process optimization campaigns.
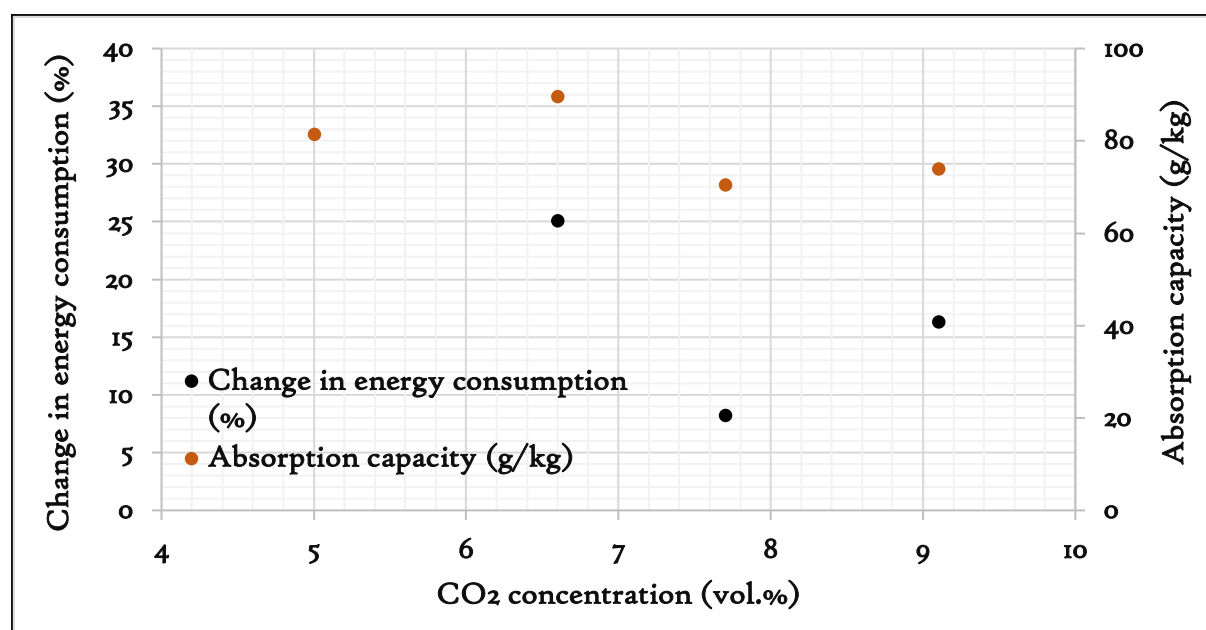
Fig. 4.6 Change in the energy consumption against the base-case NSRD and the absorption capacity as a function of the CO_2 concentrations.

4.4 (b)   INFLUENCE OF THE PHW TEMPERATURE ON THE N-SRD

The N-SRD was observed to decrease from 124 °C of PHW temperature to 125 °C and increase thereafter from 125 °C to 127 °C as demonstrated in Fig. 4.7 The first phase in the decreasing N-SRD is suggestive of increasing the CO_2 capture due to the increasing capacity of the leaner solvent to capture more CO_2, this behaviour was also reported by a study by Akram et al, 2020. However, from 125 to 127 °C, the reboiler duty was high to translate into a decrease in the N-SRD despite capturing more CO_2. 125 °C was observed to be the PHW temperature with lower value of the N-SRD in this study. Also, the PHW temperature has a pronounced impact on the CO_2 capture efficiency which was increased from 78 to 91 % when PHW temperature was increased from 124 °C to 127 °C. This result is

also in agreement with a study report by Akram et al 2020, who also observed an increment of capture efficiency from 72 to 88 %. A leaner solvent, due to the increasing PHW temperature, has a greater capacity to capture the CO_2 and consequently has a better CO_2 capture efficiency. The ratio of the solvent flow to CO_2 captured in these tests took a decreasing linear trend because the liquid-gas ratio and the flue gas CO_2 concentrations were kept constant. Fig. 4.7 shows the N-SRD and the ratio of the solvent flow to CO_2 captured as a function of the PHW temperature.

PHW temperature is thus not recommended to be kept above 125°C according to the test campaign carried out because it only diminishes the SRD, furthermore, risking facilitated thermal degradation which consequently will increase the cost of the running expenditure.
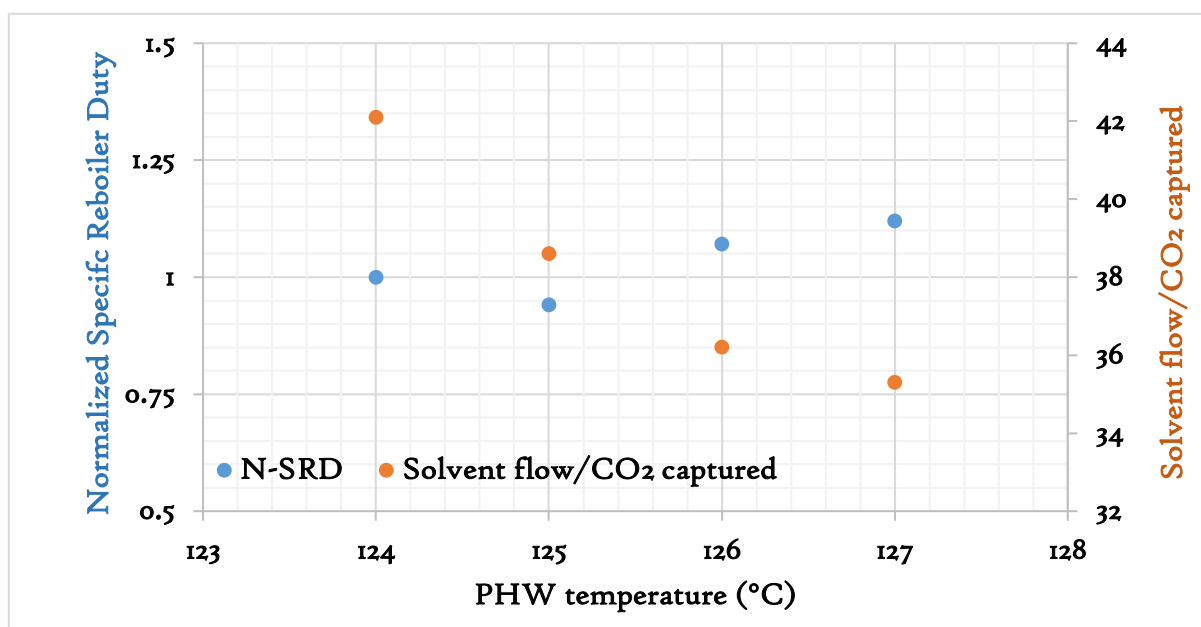
Fig. 4.7   N-SRD and solvent flow/CO2 captured as a function of the PHW temperature.

An increase in the absorption capacity from 64.5 to 74.6 g/kg was observed as the PHW temperature increased from 124 °C to 127 °C, thus signifying an increase by 15.7% as presented in Fig. 4.8. As the PHW temperature increases from 124°C to 125°C, a decrease in energy consumption by 6.2% was observed, whereas an increase in the energy consumption by 12.3% was observed at a PHW temperature of 127°C as against 124°C. Above the PHW temperature of 125°C, the reboiler heat duty is high to attain any reasonable reduction in N-SRD. Whereas, below this temperature, the CO2 captured is low in order to gain a value in the N-SRD, thus the PHW temperature at 125°C has been found based on the process conditions and plant specifications employed for these tests to give

the lowest N-SRD. Fig. 4.8 presents the change in the energy consumption and absorption capacity as a function of the PHW temperature.
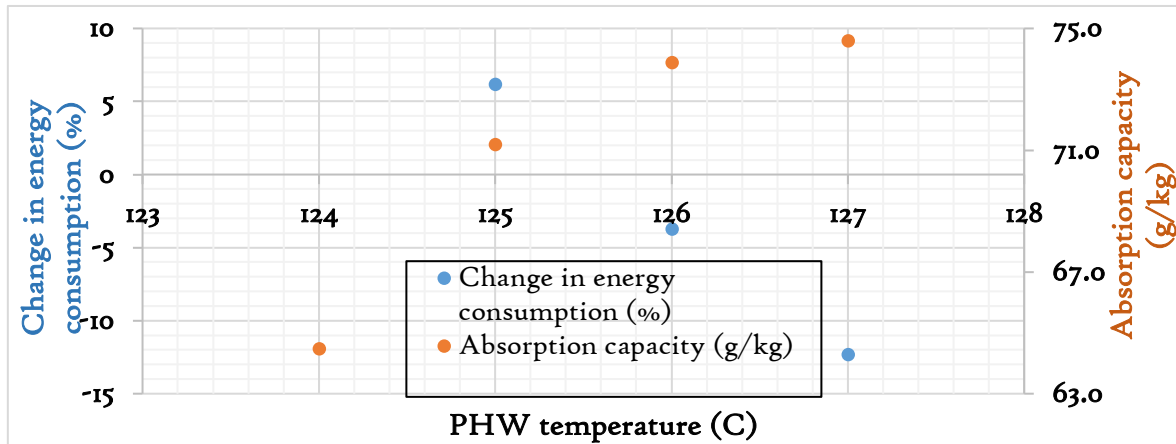
Fig. 4.8 Change in energy consumption against the base-case SRD and absorption capacity as a function of the PHW temperature.

4.5 (a) INFLUENCE OF VARYING THE CO_2 CONCENTRATION ON THE CO_2 CAPTURE EFFICIENCY AND CAPTURE RATE

Approximately 90% capture efficiency was maintained in Experiment 1 as the CO_2 concentration was increased. The CO_2 captured was observed to significantly increase by 80.5% from 14.9 to 26.9 kg/hr. This behaviour underscores the impact behind increasing the S-EGR ratios to facilitate the driving force for the CO_2 absorption. Diego et al; 2017, Li et al 2011 and Akram et al; 2016 have reported in their published studies a similar trend [39], [64],[65]. The increase underscores the influence of the driving forces for the CO_2 capture as the CO_2 partial pressure increases and under the influence of higher solvent concentration at 40 wt(%) MEA. Fig 4.9 presents the CO_2 capture efficiency and capture rate as a function of the CO_2 concentration.
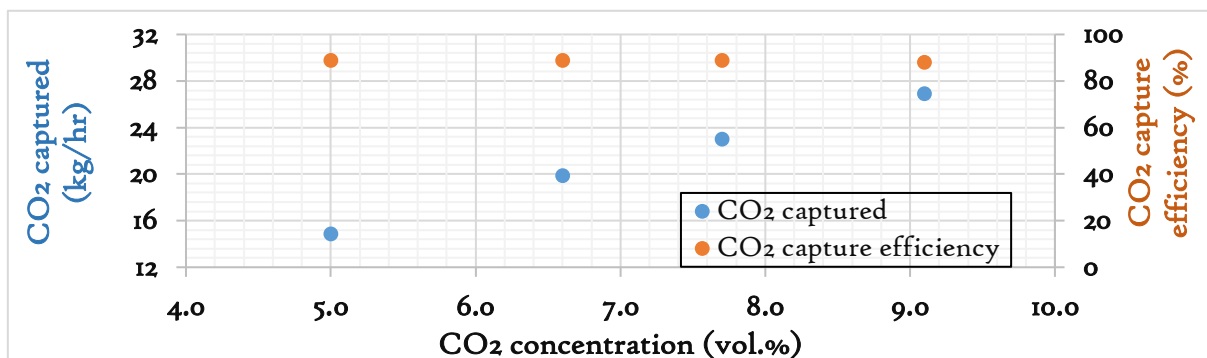
Fig. 4.9 The CO_2 capture efficiency and capture rate as a function of the CO_2 concentration.

4.5 (b) INFLUENCE OF THE PHW TEMPERATURE ON THE CO_2 CAPTURE EFFICIENCY AND CAPTURE RATE

CO_2 captured efficiency was observed to increase from 78% to 91% as the PHW temperature was increased from 124°C to 127°C, signifying the production of a leaner solvent, which has enhanced the CO_2 absorption capacity. With increasing the PHW temperature, the CO_2 captured was also monitored to increase from 23.4 to 27.7 kg/hr. Prior study [130] has also noted on the importance of PHW temperature on the CO_2 capture efficiency. These results signify the impact of increasing the PHW temperature on the amount of CO_2 recovery. However, the higher the PHW temperature, the higher the risk of thermal degradation of the solvent.

Thermal degradation is more likely to transpire in regions of an elevated temperature in the CO_2 capture plant and this includes the reboiler (stripper sump) and lower part of the stripper [134],[135]. Thermal degradation is however beyond the boundary of this study. Increase of PHW temperature, which certainly increases the CO_2 capture does more harm than good because of the risk of thermal degradation and associated cost of solvent management
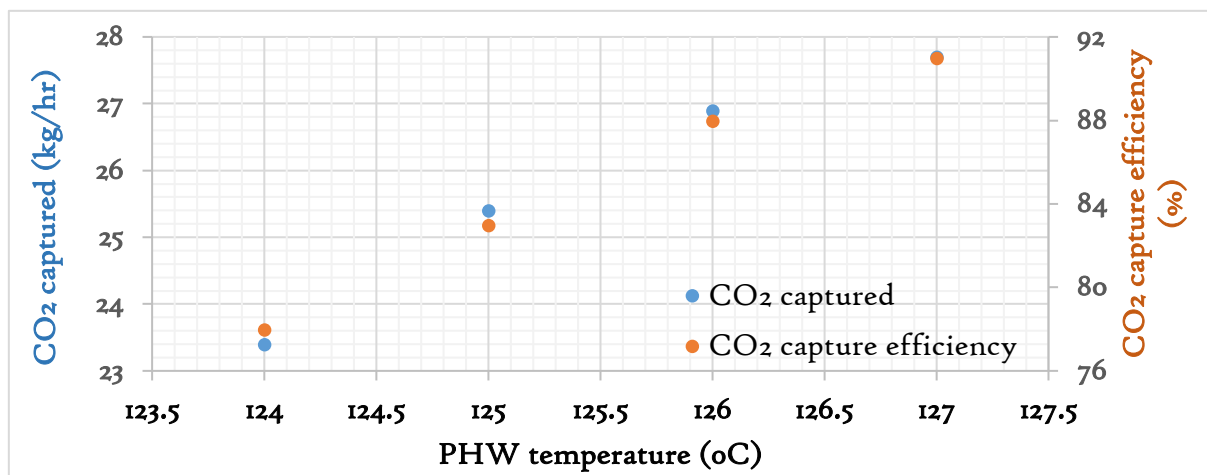
Fig. 4.10   The CO_2 captured (kg/hr) and capture efficiency (%) as a function of the PHW temperature.

4.6 (a) INFLUENCE OF VARYING THE CO_2 CONCENTRATIONS ON THE DEGREE OF SOLVENT REGENERATION

An approximate 34.67% decrease in the degree of the solvent regeneration was observed after it was monitored to reduce from 30.69% to 20.05% as the CO_2 partial pressure

increased under the test conditions utilized in these experiments. The reduction in the solvent regeneration was credited to the reducing residence time of the solvent in the stripper reactor and reboiler as the L/G significantly increased by 100% from 2.1 to 4.2. It should be recalled that the increase in the L/G was to curb the CO_2 capture efficiency at 90%. A similar behaviour in the solvent regeneration with increasing CO_2 partial pressure was also reported by Rezazadeh et al; 2016 [90]. Fig. 4.11 shows the degree of the solvent regeneration and L/G as a function of the CO_2 concentration.

These tests have demonstrated that increasing the L/G with increasing the CO_2 partial pressure decreases the degree of solvent regeneration. Hence, a trade-off exists as a result between the L/G and solvent regeneration. Thus, the point at which the degree of solvent regeneration intersects the L/G represents an optimisation scenario (based on the process conditions in the experiment) where there is no trade-off between the solvent regeneration and L/G. In other words, the point of intersection (at about 7.17 vol(%) of CO_2 in the flue gas) represents the point at which any increase in the L/G will be detrimental to the degree of solvent regeneration.
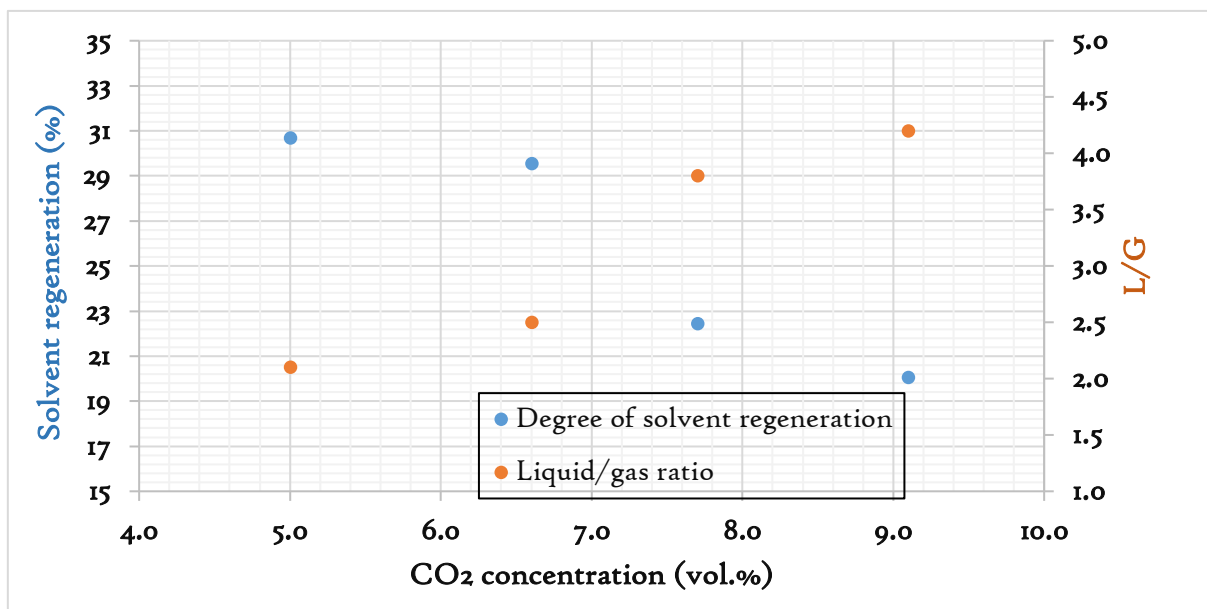
Fig. 4.11   Solvent regeneration as a function of the CO_2 concentration.

4.6 (b) DEGREE OF SOLVENT REGENERATION AS A FUNCTION OF THE PHW TEMPERATURE

The degree of solvent regeneration took a different dimension when influenced by varying the PHW temperature from 124°C to 127°C as the CO_2 concentration and L/G were kept constant at 9.1 vol(%) and 4.3, respectively. Regeneration of the solvent, as expected, was increased due to the increasing reboiler heat duty for CO_2 stripping. This behaviour is presented in fig. 4.12.

Irrefutably the higher the PHW temperature at the reboiler inlet, the higher the degree of solvent regeneration and consequently the higher the CO_2 recovery when the CO_2 partial pressure is kept constant, however, at the risk of increasing the thermal decay of the amine solvent. In as much as PHW temperature at 127°C has benefits in both solvent regeneration and CO_2 capture, the long term implication of solvent degradation outweighs these benefits and PHW temperature should be kept below the thermal degradation threshold.
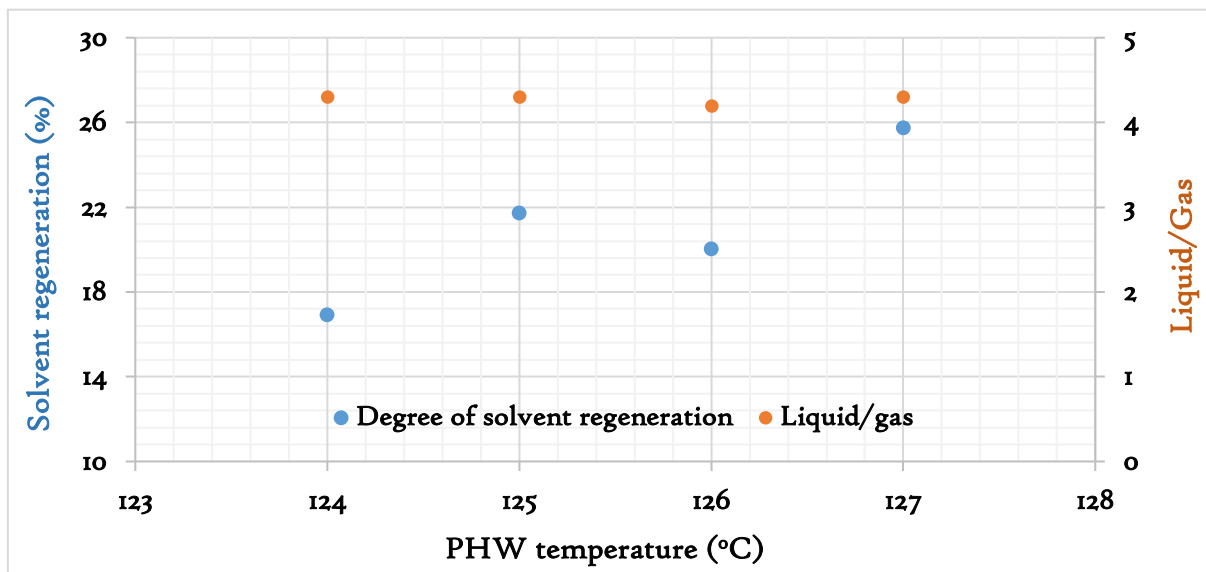
Fig 4.12   Solvent regeneration as a function of the PHW temperature

4.7 (a) INFLUENCE OF VARYING THE CO₂ CONCENTRATION ON THE ABSORBER TEMPERATURE PROFILE

The absorber temperature profile gives an insight into the temperature behaviour of the fluid across the length of the absorber reactor. About 6.6% increase in temperature was observed in the absorber temperature profile at the peak region when the CO_2 concentration

was increased from 5.0 to 9.1 vol(%) as shown in Fig 8. This suggests increasing exothermic CO_2 absorption reaction as the CO_2 partial pressure increases. Also, a noticeable temperature bulge around the middle section of the absorber is also an indicator that gas-liquid in the bulge region is close to equilibrium with regards to the CO_2 concentration [136],[137],[138],[139],[140]. However, the temperature profile at the thermocouples located at the top of the absorber column appears to decrease with increasing CO_2 concentration. This could be attributed to cooler and higher solvent flows into the absorber, which diminishes the rate at which the temperature builds up due to the CO_2-solvent reaction. This phenomenon is also behind why the flue gas outlet temperature decreases with increasing CO_2 concentration. Identifying region of highest temperature bulge could be valuable with regards to enhancing CO_2 absorption via withdrawing part of the solvent from the bulge region and transporting it to the top of the absorber column or routing a fraction of lean amine solvent to the bulge region [141]. The temperature profile at CO_2 concentration at 6.6 vol(%) appears to be higher than 9.1 vol(%) CO_2 due to the likelihood that higher flow rate at 9.1 vol(%) CO_2 may have impacted a cooling effect on exothermic CO_2 absorption. Higher CO_2 recycle ratio is to be avoided to prevent risking reaching high absorber thermal prominence, which is expected to reduce the solvent capacity of CO_2 capture. Higher recycle ratio also promote the tendency of reaching equilibrium pinch, which informs of the better ways to manage the absorber reactor via enabling the driving force of CO_2 absorption [130].
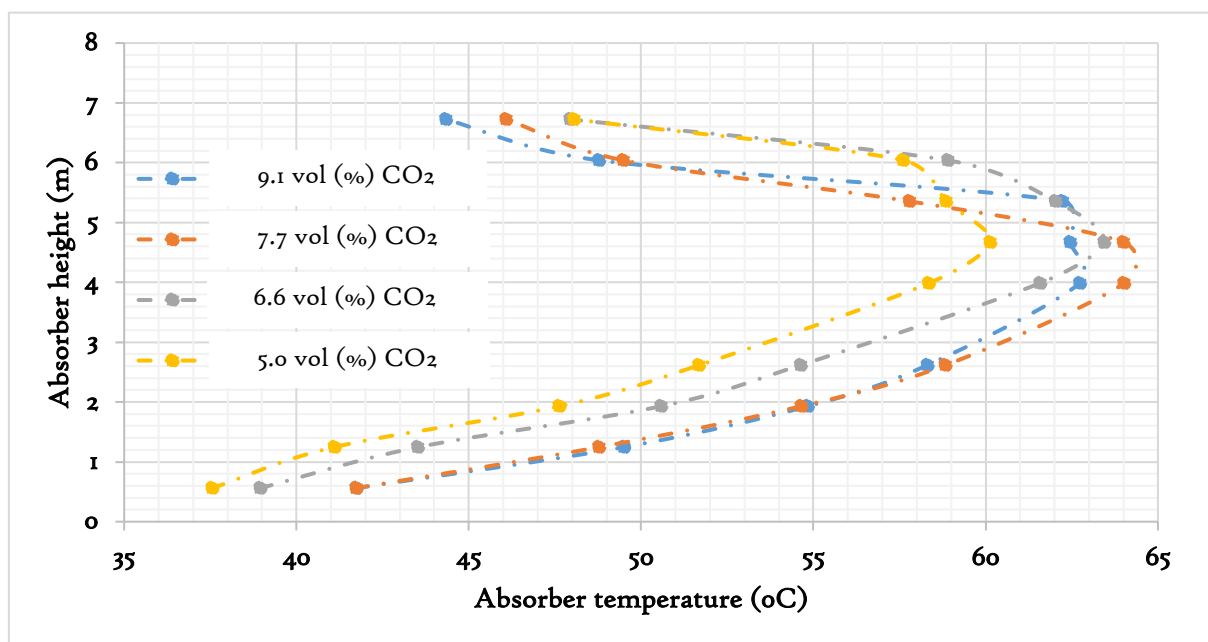
Fig. 4.13 Absorber temperature behaviour with increasing CO_2 concentrations

4.7 (b)   INFLUENCE OF VARYING THE PHW TEMPERATURE ON THE ABSORBER TEMPERATURE PROFILE

As the PHW temperature increases, so does the lean loading provided that the process conditions are kept constant and as a consequence of lower lean loading, the solvent absorption capacity increases. This facilitates an increased CO_2 absorption and its consequential temperature build-up due to an increased exothermic reaction. Therefore, as anticipated, a higher PHW temperature leads to a higher temperature bulge in the absorber as presented below in Fig. 4.14 and this manifestation of the temperature profile with increasing PHW temperature promotes amine emission into the atmosphere. Absorber intercooling may be needed to restrict temperature build-up in the absorber due to increasing PHW temperature at the reboiler.
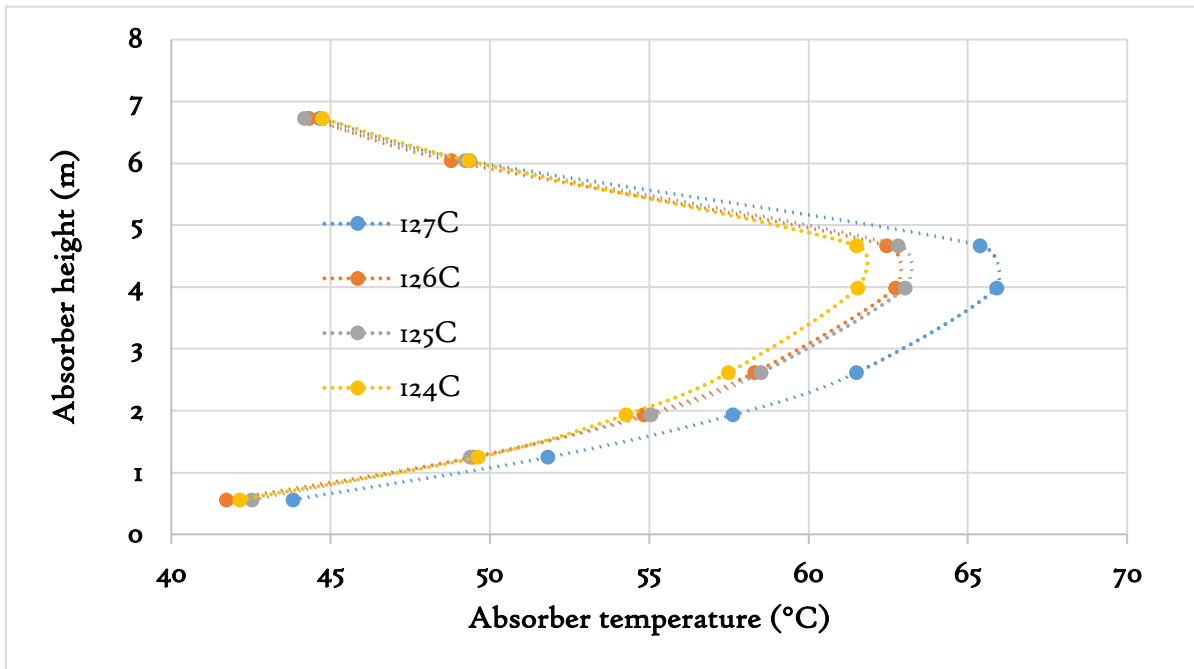
Fig. 4.14   Influence the PHW temperature on the absorber temperature profile

4.8 (a)   INFLUENCE OF VARYING CO₂ CONCENTRATION ON THE STRIPPER TEMPERATURE PROFILE

The CO_2 desorption is an endothermic reaction and high reboiler heat duty is needed to strip the CO_2 from the solvent [64],[114],[142],[127]. The stripper temperature profile was monitored to have reduced from approximately 3% – 9% as the CO_2 concentration increased from 5.0 to 9.1 vol(%), which is probably due to the result in the endothermic

solvent regeneration. The temperature at the base of the stripper was also observed to have a higher temperature profile as a result of the impact of the hot captured CO_2 and H_2O vapour exiting the reboiler gas outlet and entering into the stripper. The stripper temperature did not appear to have a smooth curve and this is likely to be due to changes in the fluid properties under the influence of thermo-chemical environment. This may include preferential pathways along the Sulzer Mellapak (CC3) structured packing, changes in the solvent concentration, vapour pressure, viscosity, surface tension and changes in the concentration of solvent degradation products along the length of the stripper. The clear reduction of temperature at the top of the column may be attributed to the cooler rich solvent that is being introduced into the top of the stripper column. The noticeable increase in the temperature at the base of the stripper is probably due to the location of the facilitated CO_2 desorption, due to the incoming hot stripped CO_2 and its accompanying water vapour. Fig. 4.15 presents the absorber temperature profile under the influence of varying CO_2 concentrations.
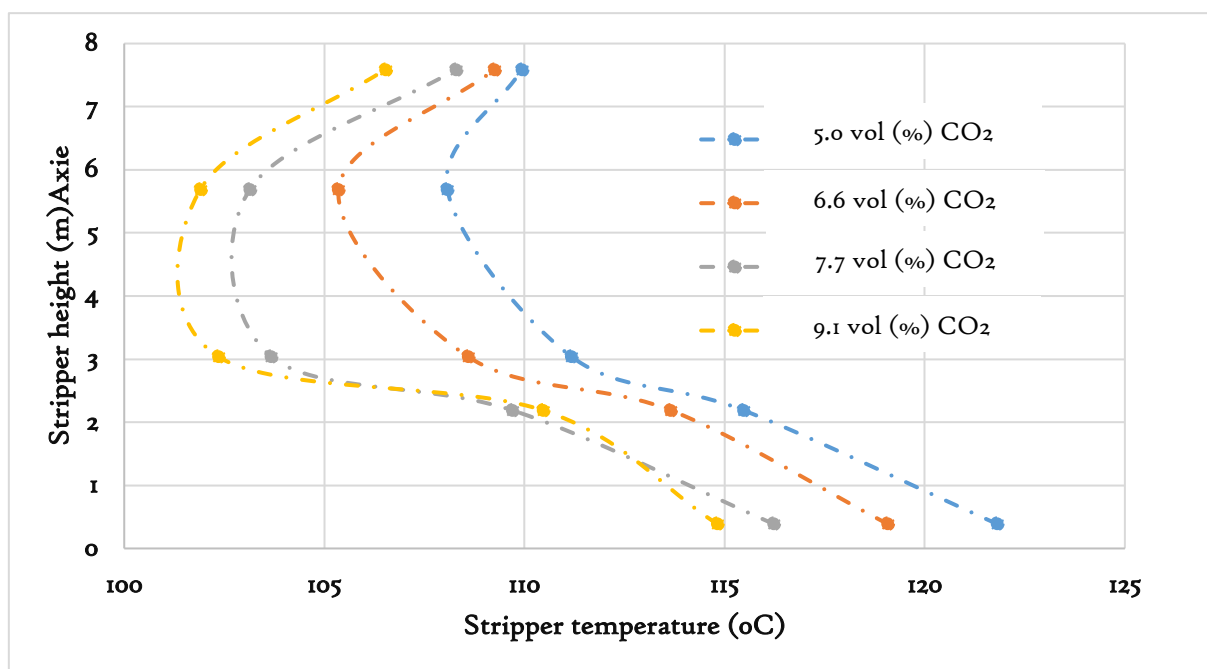
Fig. 4.15 Effect of CO_2. concentrations on stripper temperature profile

4.8 (b)   INFLUENCE OF THE PHW TEMPERATURE ON THE STRIPPER TEMPERATURE PROFILE

The temperature bulge region of the stripper column was observed to increase by about 10% with increasing the PHW temperature from 124°C to 127°C. As anticipated, the hotter the

stripped CO_2 and water vapour exiting the reboiler, the higher is the temperature prevalence in the stripper and vice versa. A significant temperature decrease was observed from the base of the stripper until about 2m, suggesting a region of facilitated endothermic reaction. This is the location where the temperature in the stripper is highest, whereas the noticeable cooling at the top of the stripper signifies a cooling effect as a result of the cooler solvent being introduced via the stripper solvent inlet. This temperature profile clearly suggests that to attain a lower lean loading and desorb more CO_2 from the rich solvent, higher PHW temperature is needed which is likely to increase the reboiler heat duty but consequently increase CO_2 capture.
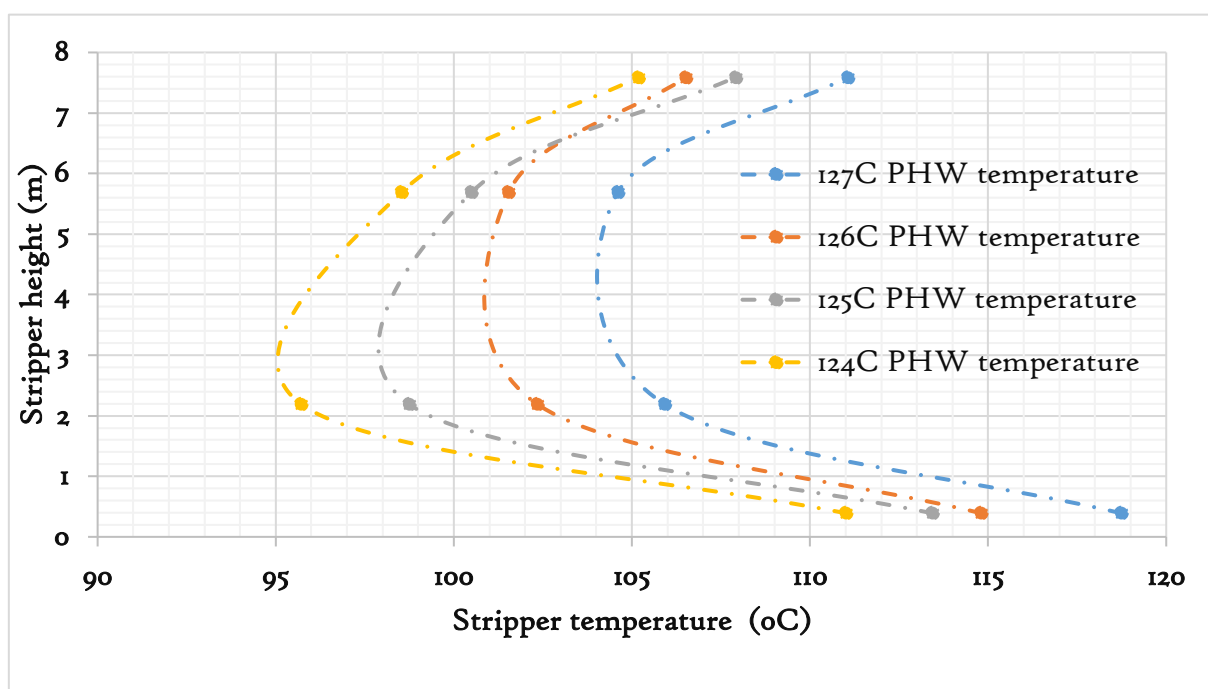
Fig. 4.16   Effect of the PHW temperature on the stripper temperature profile.

4.9 (a)   MEA EMISSION AS A FUNCTION OF THE CO₂ CONCENTRATION

Traces of MEA at the absorber outlet was observed to decrease from 40.9 to 19.6 ppm as the CO_2 concentration increases. This suggests there is a lower residence time of the solvent in the absorber, as the solvent flow rate increases with increasing CO_2 concentration, and this restricts the amine molecules to be carried over into the water-wash column. Furthermore, the temperature at the top of the absorber with increasing CO_2 concentration decreases due to cooling effect of increasing solvent flow rate and thus restricts evaporation and emission

of the MEA. It is anticipated that MEA is emitted in form of a gas into the atmosphere at the absorber outlet while accompanying the treated flue gas in moisture droplets [143]. The MEA recorded at the water-wash outlet was approximately 2 – 3 ppm and this signifies an MEA capture efficiency of the water-wash at approximately 92 %. The MEA emission profile at the water-wash inlet and outlet is presented in Fig. 4.17. Emission can be restricted by employing lower amine concentration as studies have reported lower amine and associated volatile compounds emissions up to 10 times with 40 as opposed to 30 wt(%) MEA [130].
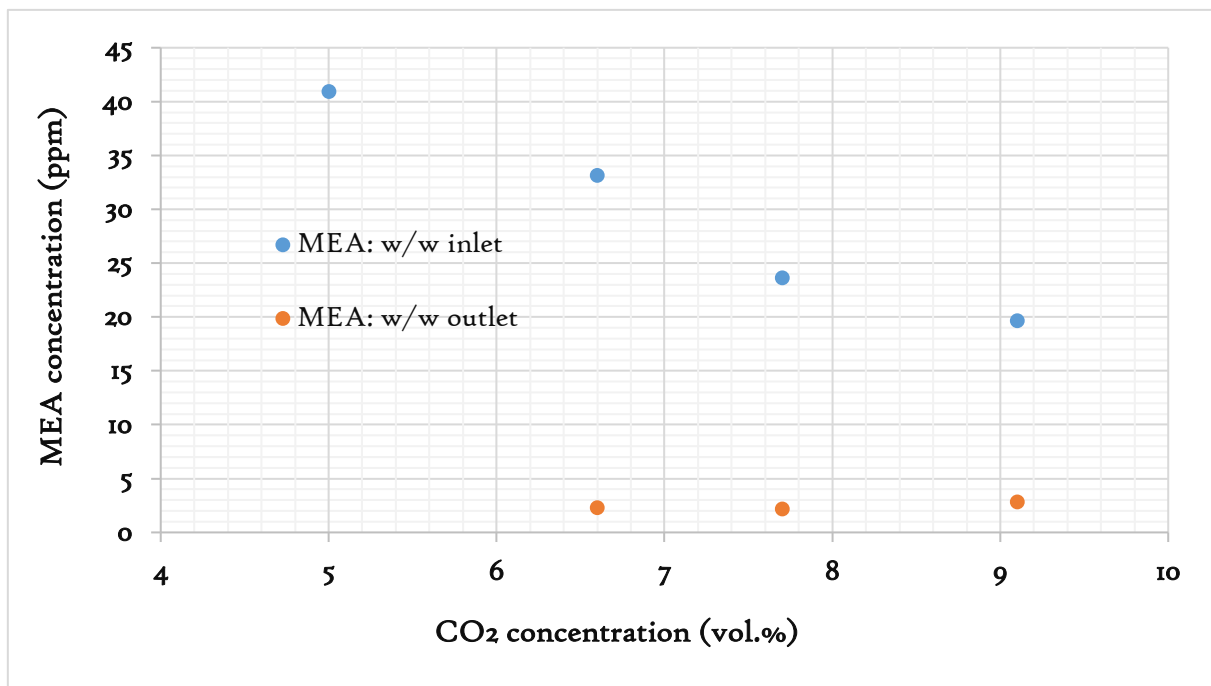
4.17   The MEA concentration as a function of the CO_2 concentration.

4.9 (b)   MEA EMISSION AS A FUNCTION OF THE PHW TEMPERATURE

It is expected that the higher is the temperature in the absorber column, the higher is the amine emission due to the reduced solvent solubility. The MEA was thus observed to increase by 60.7% from 12.2 to 19.6 ppm as the temperature of the PHW was increased from 124°C to 127°C. As stated before, the leaner is the solvent, the higher is the solvent absorption capacity and as a consequence the higher is the exothermic CO_2 absorption. This promotes amine emission. The MEA concentration at the water-wash outlet was monitored to be between 2.8 and 4.7 ppm which signifies an MEA emission capture efficiency of about 76%. To limit amine emission, the operating temperature of the reboiler

heat input is required to be decreased, which also have benefits in the SRD, however, with a reduced CO_2 capture.
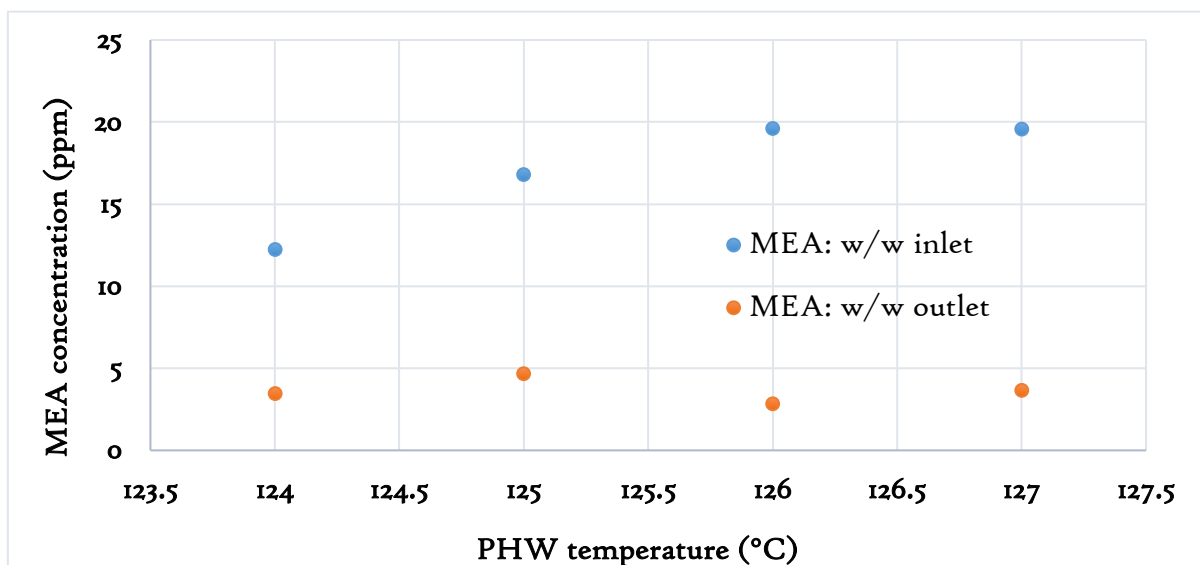
Fig. 4.18   The MEA concentration as a function of the PHW temperature

4.10   CORROSION IN POST-COMBUSTION CARBON CAPTURE

Corrosion is a key challenge in an aqueous solution of amine-based carbon capture installations, and this is envisaged to increase the OpEx as well as the CapEx of the SCCP. Recent research has suggested that this phenomenon is caused as a result of anodic (iron dissolution) and cathodic (reduction of oxidisers present in the solution) electrochemical reactions on metal surfaces [144]. Furthermore, higher levels of CO_2 loadings, elevated levels of amine concentration, higher levels of operating temperature, higher levels of O_2 concentration, presence of Heat Stable Salts (HSS) and mobile solid particles are all observed to facilitate corrosion [131],[144],[145]. The result from this study appear to support the hypothesis that increase in Fe concentration is a key indicator of corrosion of the carbon capture internal equipment and a gauge to how the amine solvent has degraded as Fe concentration was observed to increase by 70.7% (from 9.16 to 15.64 mg/L) within the course of the two experiments. This noticeable amplification of Fe concentration in these experiments underscores the impact of the corrosion in the carbon capture using an aqueous solution of amines. However, employing lower MEA concentration at 30 wt(%) MEA has been demonstrated on a pilot-scale study to corrode the plant's internal equipment slower than higher MEA concentration at 40 wt(%) MEA [130].

The treatment of flue gas in order to get rid of exhaust impurities, reduction of oxygen levels via Dissolve Oxygen Removal Apparatus (DORA) [146], designing corrosion resistant equipment and using the corrosion inhibitors are expected to reduce the severity of corrosion processes.

This study has demonstrated that the rate of about corroded Fe increases in the CO_2 capture plant is approximately 0.1 (mg/l)/hr using synthesized natural gas flue gas over a course of approximately 500 hours of CO_2 capture operation. This value is expected to increase with live industrial flue gas because of the higher amount of impurities in the actual combustion exhaust. However, what is more important when addressing the degree of corrosion irrespective of the flue gas is the identifying of the type of corrosion occurring, be it uniform, Galvanic or bimetallic, crevice, pitting, intergranular/intercrystalline or erosion corrosion [147]. This is to enable identify the type of corrosion and subsequently the best approach for the corrosion treatment. However, the identification of a type of corrosion may entail dismantling of the internal structure for a structural investigation and subsequently to administer the appropriate treatment. Identifying and diagnosing the type of corrosion in this study is likely to be constituted in the future work.

4.11   KEY CHAPTER DEDUCTIONS

To curtail the energy utilization of PCC due to low CO_2 partial pressure, S-EGR ratios was investigated in this study with 40 wt(%) MEA.

- Simulating the S-EGR ratios has benefits in terms of reducing the SRD of SCCP, however to a certain CO_2 concentration in the flue gas, above which the SRD increases due to increased solvent flow rate to cap the CO_2 capture efficiency at 0.9. Enhancing CO_2 capture due to increasing of the S-EGR ratio does have the potential to reduce the OpEx and CapEx of PCC.
- The PHW temperature at 125°C has been identified in this study as the value to yields the lowest N-SRD, above and below which the N-SRD begins to lose its value.
- Higher solvent flow rate captures more CO_2, reduces the absorber temperature build-up at a constant CO_2 concentration and reduces the amine emissions.

However, this is at the expense of decreasing solvent regeneration, increasing running expenditure and risks of increasing the system corrosion.

- Water-wash is an effective mechanism for reducing the amine emissions into the atmosphere.

4.12   NOVEL CONTRIBUTION TO KNOWLEDGE

The novel contribution to knowledge in experimental investigation of S-EGR ratios is as follows:

- The influence of the partial pressure of CO_2 based on increasing S-EGR ratio with 40wt(%) of MEA on the performance of the solvent-based CO_2 capture process with the primary aim of decreasing the high energetic operating cost. The performance indices of the pilot-scale SCCP evaluated include the N-SRD, CO_2 capture efficiency and capture rate, CO_2 loadings, degree of solvent regenerations, amine emission, Fe corrosion, absorber and stripper behaviours based on simulating S-EGR ratios.

CHAPTER V

EXPERIMENTAL STUDY OF THE OXIDATIVE DEGRADATION OF MONOETHANOLAMINE AT A PILOT-SCALE CO₂ CAPTURE FACILITY

5.1   INTRODUCTION

MEA is employed in this experimental study due to its high CO_2 cyclic capacity at low CO_2 partial pressure. Furthermore, its degree of solubility in water, low viscosity and ability to be cheaply produced makes it a good candidate for CO_2 capture on an industrial scale, however, this operational advantages of MEA is accompanied by its tendency to readily degrade via irreversible side reactions in the presence of O_2, CO_2, NOx, SOx and high thermal energy [131]. Advanced knowledge of the amine degradation in the CO_2 capture process is critical in advancing global deployment of commercial scale CO_2 capture facilities in the energy and heavy chemical industries. Thus, this study evaluates the oxidative degradation of MEA with synthesized natural gas combustion flue-gas and against 40wt% MEA to gain a much better insight into the intricacies of solvent degradation based on a pilot-scale CO_2 capture facility. Part of the motivation of this test campaign also stems from the liability of the process equipment to corrode under the influence of CO_2-saturated amines and which, as a consequence, is likely to increase the operational expenditure of the CO_2 capture process.

5.2   AMINE DEGRADATION: NARRATIVE

Polderman and Steele, 1956 [148] first carried out an investigative study into amine solvent degradation *(chemical breakdown into unfavourable products)* [131]. Since then, solvent degradation has been identified as one of the most important challenges in acid gas recovery, especially when the capture process is employed over a prolonged period and under the influence of high solvent regeneration energy. The consequence of the solvent degradation in post-combustion CO_2 capture has been established to impact on the energy and environmental performance of the CO_2 capture process via amine loss, foaming,

corrosion, high solution viscosity, increased volatile emissions and equipment fouling. Consequently increasing the running expenditure and the potential to decrease the plant's life span [131],[149],[150]. Accordingly, MEA replacement due to solvent loss via degradation is reported to cost approximately 10% of the capture process and 4% of the total cost of the CO_2 sequestration [131],[151].

Discourse of the two major pathways of solvent degradation in amine CO_2 capture process are as follows:

5.2.1 THERMAL DEGRADATION
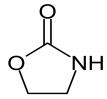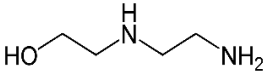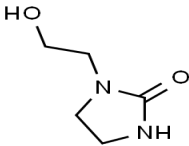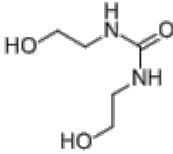
This is the chemical breakdown of the amine solvent in CO_2 capture process due to high thermal energy application. Therefore this form of degradation, prominently takes place in the stripper and reboiler (thermal reclamation unit) of the CO_2 capture plant, thus, the loss of MEA and the degree of degradation products is dependent on the reboiler duty [152]. However, studies by Rezazadeh et al. (2016) [90] have reported that thermal degradation is restricted at about 110°C of solvent regeneration fluid but accelerates above 130°C. Therefore, to maintain an acceptable level of CO_2 capture efficiency and reduce the energetic cost of the process while controlling thermal degradation, a temperature threshold of about 120°C must not be exceeded. Davis and Rochelle have calculated the rate of degradation to be between 2.5 to 6% per week at 135°C [134]. A number of degradation compounds are produced due to high temperature and high CO_2 concentration but the main thermal degradation products are highlighted in Table 5.1 [150].

5.2.2 OXIDATIVE DEGRADATION

Oxidative degradation: Dioxygen (O_2) presents a major challenge in PCC from gaseous industrial effluents, e.g. gas-fired flue gas, because it induces oxidative decay (*irreversible chemical mutation into unwanted compounds that is triggered in the presence of oxygen*) of aqueous solution of amines and breed degradation products of the amine solvent, which limit the efficiency of CO_2 capture process via primarily decreased solvent absorption capacity, enhanced solvent viscosity, corrosion of the system and production of minute solid deposits. Furthermore, the study by Goff and Rochelle, 2004 has estimated that between 0.29 – 0.73 kg MEA/tCO_2 captured is consumed in the oxidation of amine solvent [143],

consequently this is expected to prompt the rise in OpEx and CapEx. Further, some studies has also quantified that the process operating cost may increase to about 10 to 22% from MEA replacement due to amine loss via solvent degradation. [150],[153],[154],[155].

Table 5.1 Primary thermal degradation products [131].
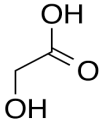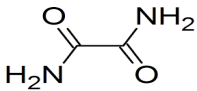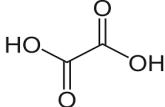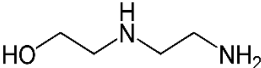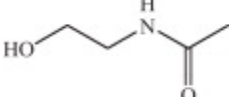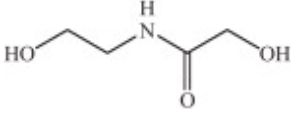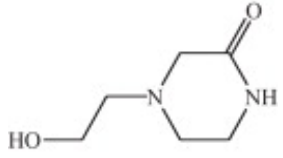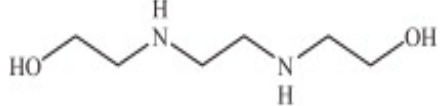
Chemical structure	Name	MW (g/mol)
	Oxazolidin-2-one (OZD)	87
	N-(2-hydroxyethyl) ethylenediamine (HEEDA)	104
	N-(2-hydroxyethyl) imidazolidin-2-one (HEIA)	130
	N,N′-bis-(2-hydroxyethyl) urea	148
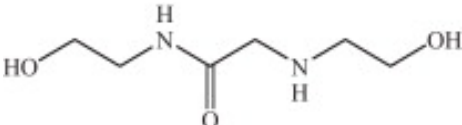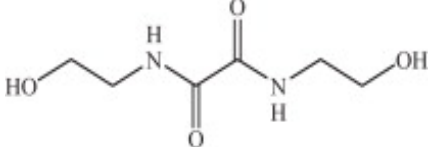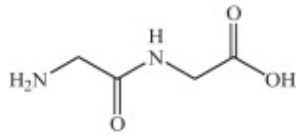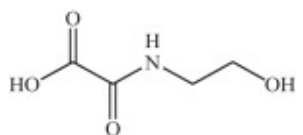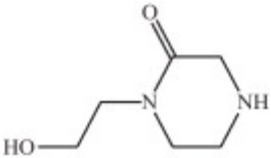
In the course of the last few decades, a broad spectrum of studies on the oxidative solvent degradation was embarked on and include investigation into the rate of solvent degradations, solvent stability, influence of oxidation catalysts, amine concentration as well as CO_2 loadings, inhibitors, operating temperature and O_2 concentration. The degradation rate is normally established based on the evolution of NH_3, which is one of the primary degradation products [156]. Primary products also include aldehydes, carboxylic acids and glycine. These primary oxidative products reacts with the MEA solvent to form secondary degradation products, e.g. HEF, HEA, HEGly [157]. The absorber harbours most of the oxidative degradation process due to the higher concentration of O_2 in the flue gas where Fe^{3+}, Fe^{2+} or Cu^+ acts as catalysts [158]. ReactionsK between the oxidized states of the dissolved metals, e.g. Fe^{3+}, and the solvent may also prompt degradation in the absence

of oxygen and at high temperature in the stripper [159]. The major oxidative degradation products are provided in Table 5.2, while the reaction mechanisms proposed by the authors can be found in [150].

Table 5.2 Major oxidative degradation products [150],[160].

Chemical structure	Name	mw (g/mol)
	Ammonia	17
	Acetaldehyde	44
	Acetic acid	60
	Formic acid	46
	Formamide	45
	Formaldehyde	30
	Glyoxal	58
	Glycine	75

Structure	Name	MW
	Glycolic acid	76
$H_2N—CH_3$	Methylamine	31
	Oxalamide, oxamide	88
	Oxalic acid	90
	N-(2-hydroxyethyl) ethylenediamine (HEEDA)	104
	N-(2-hydroxyethyl)acetamide (HEA) (ou N-acetylethanolamine)	103
	N-(2-hydroxethyl)imidazole (HEI)	112
	2-Hydroxy-N-(2-hydroxyethyl)acetamide (HHEA)	119
	N-(2-hydroxyethyl)piperazin-3-one (HEPO)	114
	N,N'-bis(2-hydroxyethyl)ethylenediamine (BHEEDA)	148

	N-(2-hydroxyethyl)-2-(2-hydroxyethylamino)acetamide (HEHEAA)	162
	N,N'-bis(2-hydroxyethyl)oxalamide (BHEOX)	176
	N-glycylglycine	132
	N-(2-hydroxyethyl)oxamic acid	133
	N-(2-hydroxyethyl)piperazin-2-one	144

Amine degradation mechanisms and emissions are complex and governed the by flue gas composition, flow regimes and operating temperature as a result there are limited validated kinetic model data to-date that is capable of predicting the degradation on an industrial scale [161].

While, the complex and catalytic nature of the oxidative degradation mechanisms of the amine solvents for CO_2 capture have been broadly studied [150],[155],[157],[161],[151], [160],[162],[159],[131],[163],[164],[165],[166] there is limited knowledge with regards to how O_2 concentration of natural gas combustion (~15 vol% O_2) can affect the breeding of degradation products at 5 vol(%) of CO_2, i.e. (*CO_2 concentration of gas turbine exhaust gas*) on a pilot-scale CO_2 capture plant, in order to evaluate the rate of degradation under the aforementioned flue gas characteristics.

This chapter experimentally investigates the oxidative degradation of the MEA which normally occurs in the absorber column at lower temperatures of about 40 to 60°C [64],[167] using synthesized gas turbine combustion flue-gas with the aim to demonstrate and gain a much more knowledgeable insight and behavioural acumen into the oxidative solvent degradation of (Post-combustion Carbon Capture) for Natural Gas Combined Cycle Power Plant at a Pilot-scale Advanced CO_2 Capture Plant. This experimental campaign also presents an alarming rate of the equipment corrosion with regards to the rate of key degradation products produced in the course of the experimental campaign.

5.3   EXPERIMENTAL INVESTIGATION

The UKCCSRC-Pilot-scale Advanced CO_2 Technology Plant is fitted with two absorber columns and it is located near Sheffield, UK (Fig 3.3 and 3.17). It was operated for approximately 525 hours over the course of the experimental campaign in order to study the effect of the oxidative degradation of 40wt% MEA. The synthesized natural gas combustion flue gas, solvent and PHW characteristics are provided in Table 5.3. The simulated flue gas was concocted using the aid of the Gas Mixing Skid (GMS) (Fig. 3.10), the 40wt% aqueous solution of amine solvent was procured from a licensed operator and the solvent regeneration thermal energy was produced from an onsite PHW skid [103].

Table 5.3   The experimental investigation: independent process conditions

Parameter	Characteristics		Flow rate	Temperature	Pressure
FG	N_2	0.79 vol%	~200m3/hr	40°C	1bar
	O_2	0.15 vol%			
	H_2O	0.01 vol%			
	CO_2	0.05 vol%			
Solvent	MEA	40wt%	~400kg/hr	40°C	2bar
PHW	H_2O			124°C	4 bar

An aqueous solution of the lean, semi-rich and rich amine solvent was sampled via conduit valves located at the base of the rich and semi-rich absorber columns and the lean solvent stream line, where it is used to analyse the CO_2 loadings and for the quantification of the solvent metal (Fe) concentration (Section 3.9). The FTIR (Section 3.7 and Fig. 3.13) was utilized for the gas sample analyses from the absorber inlet and absorber, water-wash and stripper outlets. The results of the process variables and conditions were recorded on the FTIR, LabVIEW and PLC logs. Dissolved Oxygen (DO) was measured with an oxygen sensor which was fitted downstream of the absorber 1.

5.3.1   IMPACT OF CORROSION ON IRON UPSURGE

MEA as a stable compound that is not readily susceptible to decomposition or degradation below its boiling point of 170°C, furthermore, pure and aqueous amines are not readily corrosive due to the high pH and/or low conductivity, however, it is in practise prone to gradually corrode the amine plant with increasing acid gas loadings [168],[169],[170]. Classically, rich solvents display belligerent corrosion capabilities and studies have identified a number of reasons behind the corrosion of steel in the CO_2 capture structural framework that include amine type, high acid gas loadings, amine solution concentration, process temperature, degradation products, process contaminants and fluid turbulence [171].

A number of electrochemical reactions demonstrates that a number of oxidizing agents present are liable for corrosion of carbon steel as follows [170],[171].

Anodic half reaction. This process produces ferrous ion via the oxidation of Fe

$$Fe \leftrightarrow Fe^{2+} + 2e^-$$ (5.1)

Cathodic half reaction. This process reduces hydrogen from the +1 oxidation state to the element as follows:

$$2H^+ + 2e- = H_2$$ (5.2)

The net chemical reaction is given as follows:

$$Fe + 2H^+ = H_2 + Fe^{2+}$$ (5.3)

Reduction of hydronium ion: Cathodic reaction

$$2H_3O^+ + 2e^- \leftrightarrow H_2O + H_{2(g)} \quad\quad (5.4)$$
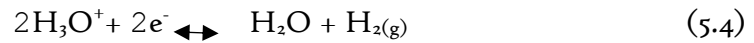
Reduction of bicarbonate ion

$$2HCO_3^- + 2e^- \leftrightarrow 2CO_3^{2-} + H_{2(g)} \quad\quad (5.5)$$
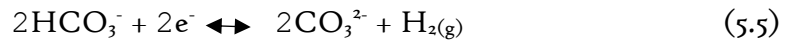
Reduction of undissociated water

$$2H_2O + 2e^- \leftrightarrow 2OH^- + H_{2(g)}$$

Reduction of protonated amine

$$2R_2NH_2^+ + 2e- \rightarrow 2R_2NH + H_{2(g)} \quad\quad (5.6)$$
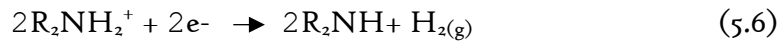
In PCC, it is likely that the steel corrosion is partly due to the CO_2 liberated from the amine to form an aqueous CO_2 solution that promptly reacts with the bared carbon steel to produce iron carbonate as follows [170]:

$$Fe + H_2O + CO_2 = FeCO_3 + H_2 \quad\quad (5.7)$$
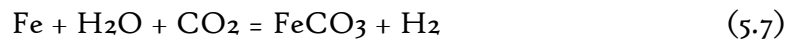
A key advantage of the process (5.3) is that iron carbonate is marginally soluble and thus creates a film over the metal surface resulting in a protective mechanism from aggravating corrosion [170].

The Fe concentration as a function of the experimental campaign time was observed to staggeringly increase by about 10 times (Fig 5.1). This underscores the severity in the corrosion in PCC systems with a natural gas combustion flue gas. A dip in the Fe concentration in Fig. 5.1 was observed from about 160 to 260 hours from the beginning of the test campaign due to the amine top-up, which was necessitated as a result of inadvertent amine leakage. This enabled us to maintain the MEA concentration at 40 wt(%).
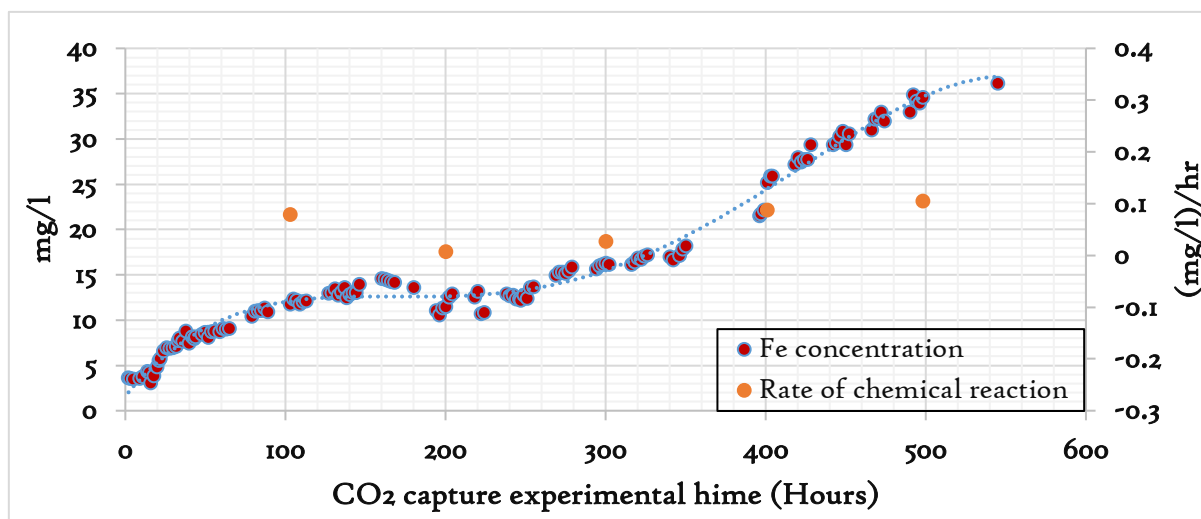
Fig. 5.1 Fe concentration as a function of test campaign hours

Reactions to produce Fe in this phenomenon is irreversible and thus the rate of reaction is dependent on the species on the left-hand side of the equation (5.3). The relative stability of the rate of reaction after 200 hours (Fig. 5.1) may be attributed to the protective thin layer of iron carbonate covering the metal surfaces coupled with the dilution of the amine solvent due to leakage in that period of time. The upsurge in the Fe concentration, which is a product of the carbon steel corrosion will also ultimately depend on different PCC process conditions and this includes the quality of the flue gas, DO concentrations, CO_2 loading, operating temperature, ratio of the solvent to the flue gas flow rates and duration of the CO_2 absorption campaigns as demonstrated in the test campaigns on 3 different CO_2 capture systems [167]. While the test campaigns at both TNO and ENEL's CO_2 capture plants in the Netherlands and Italy, respectively, reported Fe concentrations of less that 3mg/l, the EnBW CO_2 capture plant in Germany reported Fe concentration of more than 900mg/l. This fundamental difference in Fe concentration between the TNO and ENEL, as against EnBW, and may be attributed to the longer operating hours and erosion-corrosion at EnBW. This form of corrosion is influenced by the solution turbulence caused by the high solvent flow velocities, high gas flash and injection rates and impingement of liquid-gas on the steel surface. A higher liquid/gas ratio may also facilitate the tearing apart of the protective film of iron carbonate [168]. These scenarios may have attributed to a considerable Fe iron content in the EnBW test campaign as opposed to TNO and ENEL. Information on the process conditions of all three of the capture plants used, that include the CO_2 loadings, operating temperatures, rate of water-wash transfer, solvent top-up,

amine contaminants, amine solution concentration is limited to exert a feasible conclusion on why the Fe concentration was much higher in the EnBW plant. However, the considerably higher CO_2 capture operating time and lower flue gas temperature at the EnBW is likely to be the main contributing factor of the higher Fe concentration. Assuming that Fe upsurge due to corrosion continues at approximately 0.062 (mg/l)/hr, the Fe concentration at the PACT CO_2 capture plant will be about 90 mg/l, alike to EnBW's campaign over the course of similar time and higher than what has be reported at the TNO and ENEL plants.

Fig. 5.2 presents the degree of coloration due to the Fe concentration in the sampled solvents. Observed coloration of the solvent is the first insignia of solvent degradation and an apparent change was observed soon after interaction with the flue gas at the end of the first day. The amine solvent sampled on a daily basis distinctly shows the intensifying coloration of the solvent from light peach to dark brown colour over the course of the experimental campaign. Fig. 5.2 supports the behaviour of the rate of reaction where the Fe concentration increased by about 220% within the first 100 hours of running the plant and this is reflected on the solvent colour across the first 9 sample bottles. The colour of the amine solvent appeared to be relatively steady after the first 100 hours and can this can be attributed to the low rate of reaction; the corrosion however, is expected to continue but at a slower pace (Fig 5.1.). Employing the same solvent without solvent top-up for the CO_2 capture and for about 5 months will eventually transform the solvent colour to raisin black, as observed by a study conducted by the CO_2 Technology Centre Mongstad (TCM) [160]. Under this state, the solvent is likely to lose its primary capacity to capture the CO_2 and the solvent treatment for recycling purposes is diminished. The solvent colour can thus be utilized as a means of gauging the solvent degradation. The degree of how a solvent changes colour and the rate of discoloration will ultimately rely on the flue gas characteristics, L/G, rate of corrosion, concentration of the aqueous solution of the amine and reboiler duty. Solvent make-up accounts for up to 10% of the solvent management (using MEA as a benchmark solvent) and this underscores the importance of maintaining the solvent quality in the PCC [172].
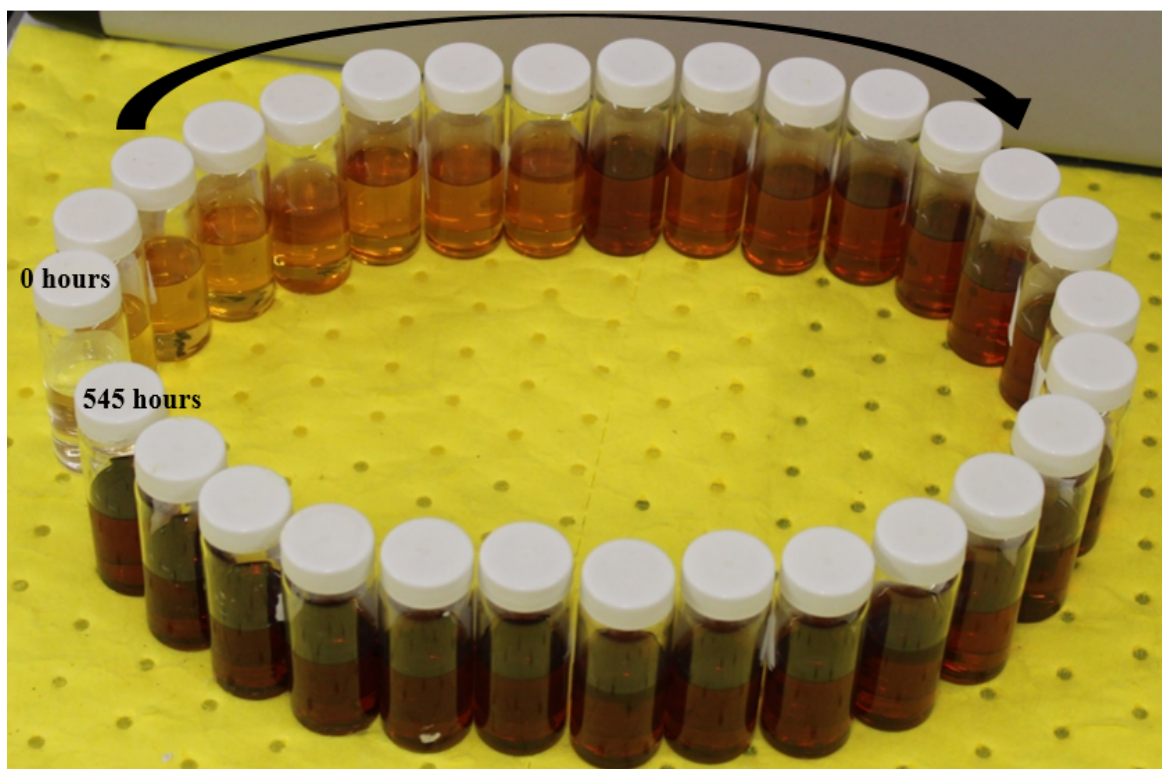
Fig 5.2   Degree of dicoloration of the amine solvent over the course of the experiment.

5.3.2   AMMONIA EMISSIONS

Ammonia is one of the major volatile product of oxidative amine solvent degradation. The ammonia emission was observed to be within the range of 18 to 58 ppm over the course of the data recorded in the experimental campaign at the 1 tonne of CO_2 capture/day PACT plant. The ammonia data points presented in Fig. 5.3 were taken at the solvent sampling times. In addition, the Fe is reported to catalyse oxidative degradation of the amine [143] and from Fig. 5.3, it can be observed that the behaviour of the NH_3 emissions bear slight similarities with the rate of the chemical reaction of Fe (Fig. 5.1) and the degree of solvent coloration (Fig. 5.2). This indicates a relationship between the corrosion (Fe production) and NH_3 emission. The ammonia emissions were also reported according to the investigation by Kolderup et al., 2012 to increase due to the increasing concentration of O_2 in the flue gas [173].

Volatile emissions will ultimately depend on the size and the operational and process conditions of the plant as studied by khakharia et al. (2014) on a 6 tonnes CO_2/day plant and Knudsen et al. (2013) on a 4.8 tonne/day plant and both reported the ammonia emissions within the range of 14.4 to 100.5 ppm and 4 – 7 ppm respectively [173].

Furthermore, investigation at Heriot-Watt University has established that dynamic operation of the CO_2 capture plant leads to higher amount of emissions by about 200 % [176]. These emissions are important in the CO_2 capture plant because they significantly contribute to the MEA loss due to oxidative degradation of the amine solvent, which is reported to be about 1.6±0.1 kg/ton of the CO_2 captured by a study conducted at the TCM plant [146],[174]. As a result, to counteract the amine degradation via oxidation, measures are thus needed to reduce the amount of DO from the solvent, especially in the absorber sump, i.e. where the DO is expected to be higher. In response to restrict the oxidative degradation, TNO has developed the Dissolved Oxygen Removal Apparatus (DORA), based on a gas-liquid contactor, where a sweep gas of mainly N_2/CO_2 or N_2/air is used to retract oxygen from the rich solvent. Secondly, an oxygen scavenger (liquid-liquid contactor) is employed using an aqueous Na_2SO_3 solution as a sweep liquid. The performance of this technology is determined based on the O_2 removal efficiency the and amount of the NH_3 emissions [68].

Fig. 5.3   Ammonia emissions as a function of days of operation.

Ammonia and other volatile amine emissions are governed via three major mechanisms namely vapour emission, liquid entrapment and formation of mist [173]. The gas phase emission is transpired via the evaporation of the aqueous solution of the amine solvent. Therefore the higher the volatility of the solvent, the higher the likelihood of vapour-phase emissions. A higher absorber operating temperature is thus unfavourable for the restriction of the gas-phase emission because the amine's vapour pressure increases with higher temperature. The ammonia emission has been reported to increase from 30 to 50 ppm when

the lean solvent temperature was increased from 30 to 50 °C [173]. However, higher CO_2 loadings restrict the solvent vapour pressure, thus the higher the CO_2 loading and consequently the formation of carbamate and bicarbonate lowers the volatile emissions [175]. Furthermore, the cooling effect of higher L/G in the absorber column is considered to be favourable in to restricting the amount of vapour-phase emissions.

Whereas the liquid (aqueous solution of amine solvent) entrapment is caused due to volatile liquid droplets that are being carried by the vertically rising gas flow in the absorber. This phenomenon can be mitigated via an increased L/G that will consequently favour higher CO_2 capture efficiency but at the expense of increased operational expenditure. The NH_3 as a volatile compound can also be absorbed and hosted in an amine mist, especially at suitable locations where the hot flue gas comes in contact with the colder solvent stream [173].

Employing the acid-wash mechanism has been reported to improve and considered to be the state-of-the-art in the abatement of NH_3 emissions from CO_2 capture systems and test campaigns at TNO's capture plant at Maasvlaakte when this technology has achieved NH_3 emissions of lower than 7.2 ppm [143]. A water-wash system is nevertheless an effective method of NH_3 removal and increasing the water make-up of the water-wash column by $14 dm^3/hr$ reduces the ammonia emission by 35.7% [173].

In as much as a number of operational and process procedures can be employed to restrict the solvent Fe accumulation due to corrosion of the internal components of the CO_2 capture plant, curbing corrosion in the first place is expected to mitigate against volatile solvent degradation emissions, such as NH_3. Stainless steel has an excellent corrosive resistance in comparison to carbon steel and as such has a tendency to reduce the Fe accumulation especially in regions of highest corrosivity where the temperature is highest, i.e. in the reboiler, stripper, and the rich stream line to and from the heat exchanger [176],[167]. Introducing corrosion inhibitors e.g. sodium metavanadate and copper carbonate, can reduce the corrosion, however the long-time effect of inhibitors, is likely to increase foreign chemicals, which may inhibit the CO_2 capture efficiency of the amine solvent [168]. The influence of the corrosion inhibitors and solvent treatment is however beyond the scope of this study.

5.3.3 IMPACT OF OXIDATIVE DEGRADATION ON CO_2 CAPTURE

There has not been any experimental studies on a pilot-scale facility to my knowledge, that has focused in the influence of oxidative solvent degradation on the CO_2 capture efficiency using natural gas combustion flue gas. As such, there is limited data to reference on the above subject title of Section 5.3.3. It is however, well understood that the decay of the solvent subjects it to build-up of unwanted contaminants and as a consequence degrades the solvent capacity of the capture efficiency as discussed in Section 5.2.2. In this pilot-scale experimental campaign, the CO_2 capture efficiency and capture rate were observed to be relatively steady on a scale of 1 to 100% over the course of about 545 hours of running the PACT plant as presented in Fig. 5.4, and the differences in the CO_2 recovery observed was a result of changes in operational conditions. The CO_2 recovery (Fig. 5.4) indicates that within about 500 hours of operating a CO_2 capture plant, the solvents CO_2 capacity does not meaningfully degrade with the flue gas characteristics used in this test (Table 5.1) which has an Fe concentration not exceeding 40mg/l and NH_3 emissions less than 70 ppm. This does not suggest that there is no solvent degradation but alludes to the theory that the degree of degradation is not severe to devalue the CO_2 capture process. Also, This result underscores the importance of removing flue gas impurities/contaminants prior to the introduction into absorber column in order to maintain the performance of the amine solvent.
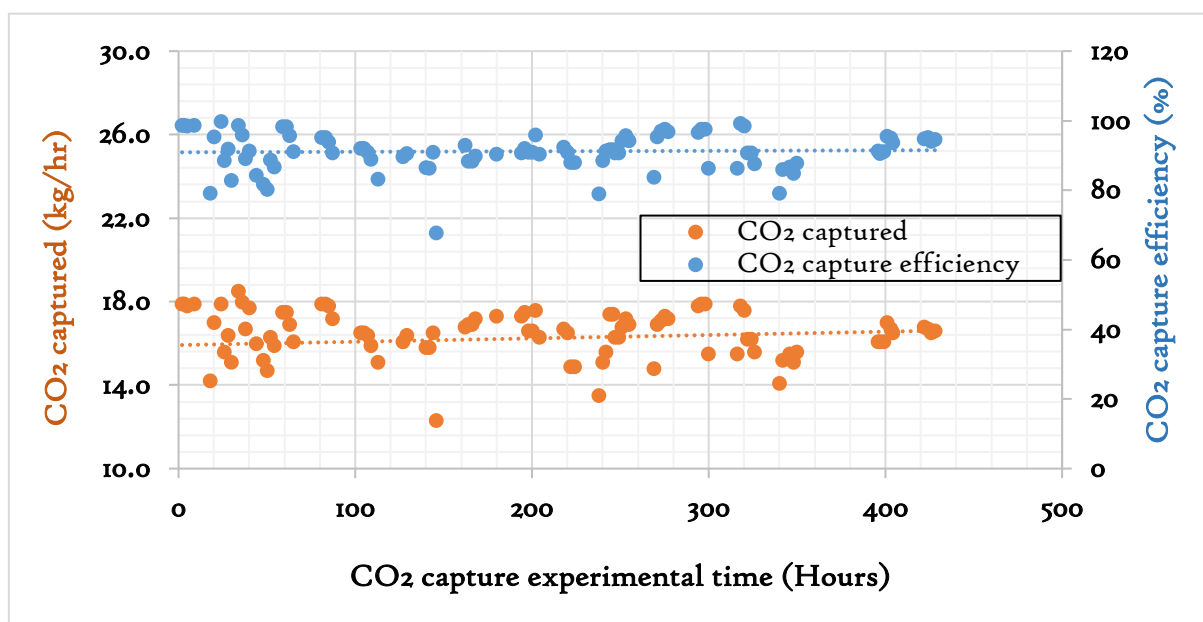
Fig. 5.4 CO_2 capture efficiency and capture rate as a function of days of operation.

At what point does the solvent start to appreciably lose its capacity to capture CO_2 will ultimately depend on a number of scenarios, which includes but is not limited to, the duration of the CO_2 capture process, concentration of Dissolved Oxygen (DO), flue gas characteristics, solvent hold-up residence time, CO_2 loadings, absorber, stripper and reboiler operating temperatures and pressures, L/G, concentration and type of the aqueous amine and also the rate of corrosion. Therefore to identify a solvent's 'breaking point' can only be evaluated and identified based on the CO_2 capture plant specifics.

5.3.4 IMPACT OF OXIDATIVE DEGRADATION ON THE N-SRD

The NSRD during the course of the CO_2 capture is expected to eventually increase as the solvent losses its CO_2 capture capacity because of the build-up of impurities due to the solvent degradation, this is a direct consequence of the increase in the ratio of the reboiler duty to the mass flow of the CO_2 capture. Because, the specific heat capacity of the solvent is likely to increase due to the degradation products in the solvent, it is probable that the sensible heat energy requirement of the solvent will increase, thus negatively impacting on the NSRD. The NSRD in this study was observed to non-linearly vary as presented in Fig. 5.5, which is a direct consequence of the CO_2 capture efficiency and capture rate in the course of the experimental campaign. Also, the variation of the NSRD was thought to be mainly as a result of changes in the enthalpy of the PHW which was caused due to changes in the PHW inlet temperature. Under a test campaign, where, the CO_2 capture process is continued for a much longer time (several months) and at relatively steady state, then this is likely to provide valued information and a much better understanding on the influence of the solvent degradation on the N-SRD.
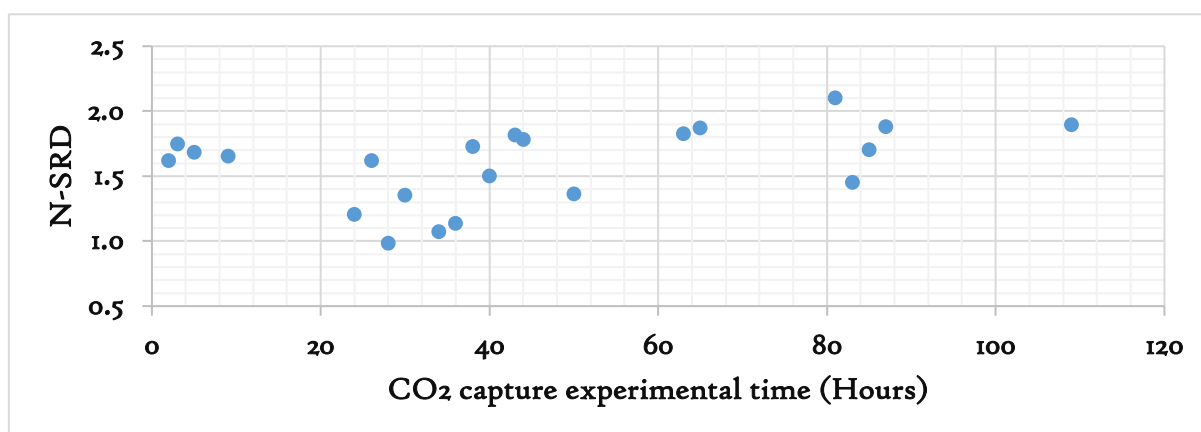
Fig. 5.5   N-SRD as a function of the hours of operation.

5.3.5 INFLUENCE OF WATER-WASH TRANSFER ON THE DISSOLVED OXYGEN (DO) PEAKING

The term DO is commonly employed to refer to the amount of oxygen dissolved in a unit volume of water and which is governed by [177].

- The pressure that the atmospheric O_2 exerts at the air-H_2O interface
- The temperature of the H_2O and
- The amount of other substances dissolved in the H_2O

The DO concentration is expected to be influenced by the pH of the solvent, the higher the pH, the higher the DO and vice versa [178]. This means the higher the rich CO_2 loadings, the lower the pH and the lower the DO concentration of the solvent [179]. In the event of water wash transfer to the absorber sump (as in the case of the PACT facility), the pH is expected to slightly decrease due to the lower pH value of water as compared to the 40 wt(%) amine, consequently expected to diminish the spiking of DO levels as water is transferred as seen in 5.6. However, the DO spiking is very prominent in these tests, suggesting that the overriding influence of water-wash as a carrier of DO as oppose to the influence the pH value that the solvent plays. A trade-off thus arises as to manging the pH of the solvent, as a lower pH will promote corrosion of the plant equipment whereas higher pH will promote higher DO prevalence and consequently oxidative degradation of the solvent.

DO measurement is being fundamentally influenced by temperature as lower temperature impacts higher O_2 dissolution than higher temperature. Also change in temperature impacts on the rate of diffusion of the oxygen through the membrane of the DO sensing element which can be up to 4%/°C. The DO measurement error was minimized in this study by utilizing an optical sensor designed for aqueous solution and that automatically compensates for temperature changes [180]. Further, an extrapolated plot of O_2 saturation against the operating solvent temperature of 40 wt(%) in Fig. 5.7 was used to calculate for the weight of DO for unit volume of the aqueous solution.

The oxygen content in the flue gas of natural gas combustion is approximately 15 vol(%), nonetheless, the Dissolved Oxygen (DO) concentration which is critical in oxidative degradation of amine solvent is likely to vary based on the operating temperature of CO_2

absorption process. Thus, the higher temperature and CO2 loading is expected to reduce the oxygen solubility [159],[162], [164],[167].

As about 7.1 litres of water from the water-wash column was automatically transferred at approximately 70 minutes intervals to the absorber column 1 (Fig. 3.17) to maintain the water balance in the PCC system and also avoid increasing the concentration of MEA, peaks of DO were detected by the DO sensor which was fitted downstream of the absorber column 1. The DO in the rich solvent stream was observed to peak up to 2 mg/l from about 0.1 mg/l at the onset of the water-wash transfer. This observed phenomenon of the DO peaking as the water is transferred (Fig. 5.6) suggests that water-wash transfer may be an instrumental carrier of the DO into the CO₂ capture system.
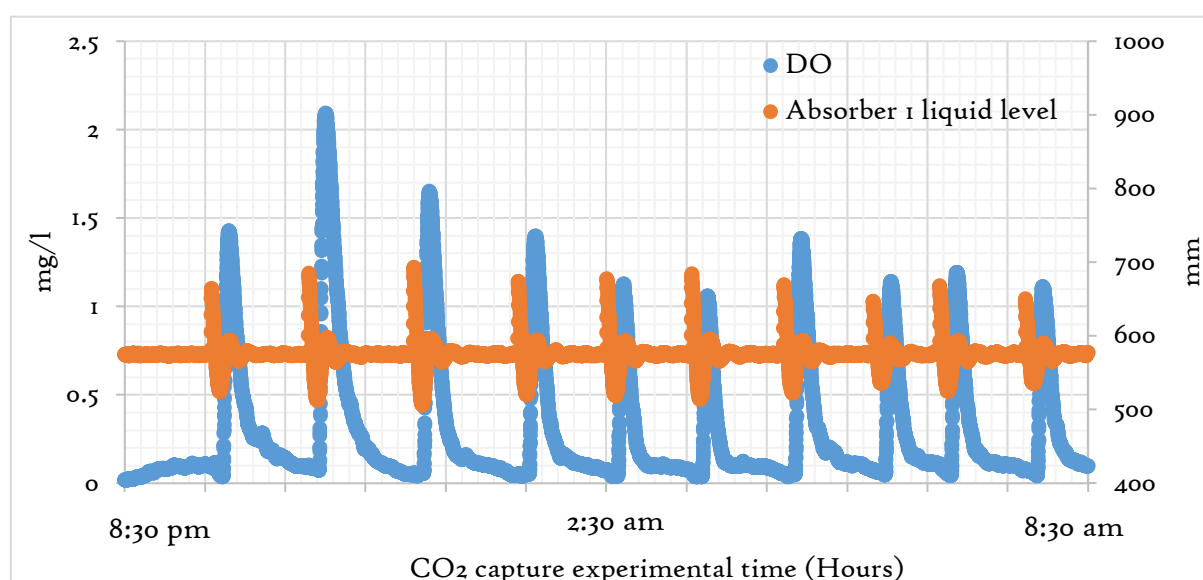
Fig 5.6   The DO and absorber column liquid height as a function of the CO₂ experimental time.

A study into the oxidative degradation of the amine solvent at 3 different CO₂ capture plants, namely; EnBW (Germany), TNO (Netherlands) and ENEL (Italy), using similar oxygen concentrations in the flue gas observed that the EnBW has a higher DO concentration in the rich solvent. This was due to the lower rich solvent stream temperature at EnBW due to lower flue gas temperature and absorber intercooling mechanism and this leads to a higher rate of solvent degradation at the plant. Furthermore, EnBW has a higher residence time of the solvent in the reboiler or stripper sump, therefore aggravating more degradation of the solvent, especially in the presence of oxygen. On the other hand, ENEL has the highest rich solvent stream temperature and lowest absorber sump residence time,

consequently experienced the lowest concentration of DO and this is thought to be responsible for the lower NH_3 emissions at the plant [167]. The experiment at PACT plant produced NH_3 concentration similar to the EnBW plant at about 500 hours of their operation. Based on the operation of the aforementioned 3 CO_2 capture plants briefly discussed, it is apparent to come to the understanding that the duration of CO_2 capture process, operating temperature, absorber sump residence time, characteristics of the flue gas affects and DO concentration in the solvent are primary factors lead to facilitated solvent decay. To suppress oxidative degradation at the PACT plant, most importantly, the amount of DO must be restricted. This can be achieved via higher absorber operating temperature (but of course to be kept way below the solvents CO_2 stripping temperature), reduction of the amount of water-wash transfer to the plant and the reduction of the residence time of the absorber sump; however, it is worth noting that higher absorber temperature is likely to influence the amount of CO_2 capture and absorber effluent emissions.

It was also observed from this study that the DO peaks coincide with the density dips of the amine solvent as presented in Fig. 5.7. The transfer of water from the water-wash column to the absorber is thought to slightly reduce the temperature of the solvent, which advances the DO solubility of amine solvents and water as presented in Fig. 5.7 [181]. Density of the aqueous solution of amine in the absorber 1 sump is further reduced after the water-wash transfer due to accompanying dissolved volatile gases e.g. NH_3 in the water, which is 1000 times less dense than water. The resultant decrease in the density further enhances the O_2 solubility in the fluid.
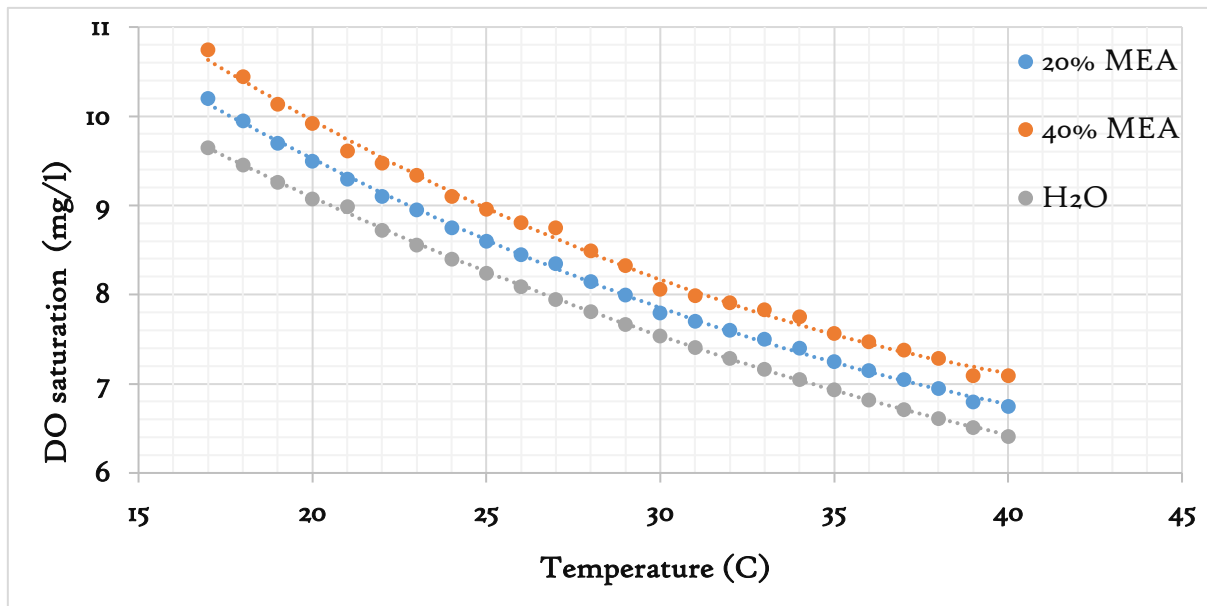
Fig 5.7 DO saturation as a function of temperature.

The sporadic and intermittent reduction of the solvent density by about 10 kg/m³ (Fig. 5.8) in the rich solvent stream due to water-wash transfer within about 30 minutes is expected to have a slight effect on the reboiler duty performance. This is because the water-wash transfer promotes a leaner rich solvent stream and lower rich loading leads to lower equilibrium partial pressure of CO_2, more reboiler energy is thus required to generate more H_2O vapour to enable the driving force for mass transfer, consequently increasing heat duty as a result [114],[132]. This means the higher the operating temperature of the CO_2 capture process, the higher the water loss via evaporation and the higher the water-wash transfer to maintain the water content in the process. As a consequence, the lower the solvent density, the prospect of lowering the temperature of the rich solvent, the higher the risk of DO peaking in the rich solvent.
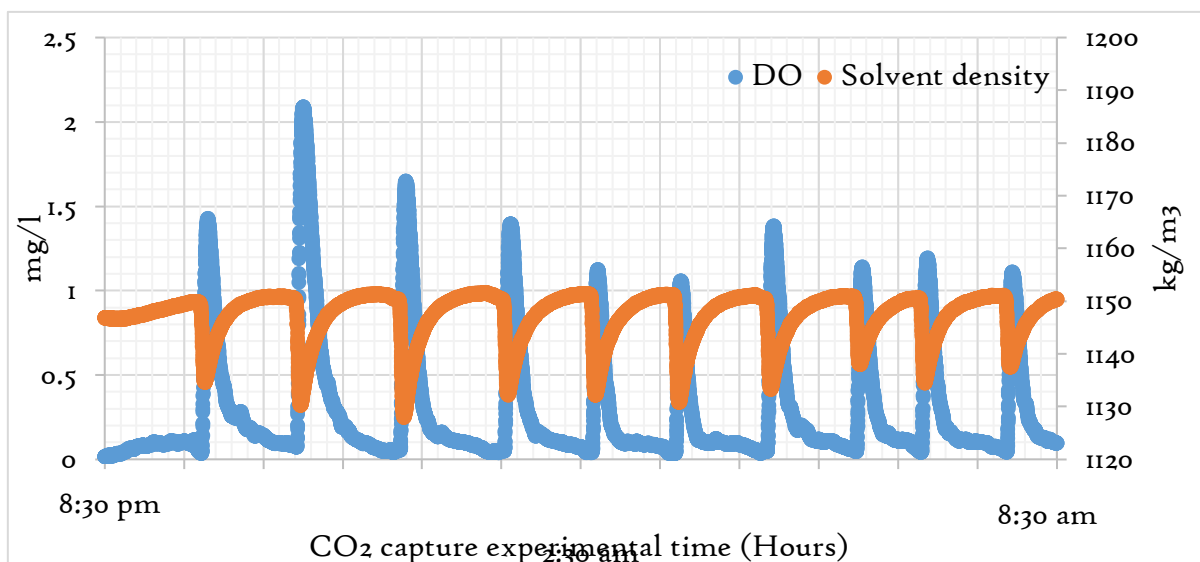
Fig. 5.8   The DO and solvent density as a function of CO_2 capture time.

The trade-off is unavoidable when the intricacies of operating a CO_2 capture process to limit the oxidative degradation of the amine solvent is considered. The higher the operating temperature, the lower the solvent density, the lower the O_2 solubility, the lower the oxidative degradation of the amine solvent, however, at the expense of enhanced CO_2 capture rate.

5.4   KEY CHAPTER DEDUCTIONS

In the course of the experiment to investigate the oxidative degradation of 40 wt(%) of MEA at 15 vol(%) O_2 and 5 vol(%) CO_2, key conclusions made are as follows:

- The NH_3 emission (a primary degradation product) was observed to have increased to about 40 ppm and the rate of Fe corrosion was about 0.062 (mg/l)/hr based on the operational and process conditions employed in the course of about 500 hrs in this investigative study. However, the control or severity of the amine solvent degradation is liable to plant specifics and based on the operational and process conditions employed.

- Solvent discoloration as the solvent degrades can be utilized as a scale to gauge the severity of the solvent degradation based on its discoloration from light peach to raisin black.

- Maintaining the operating temperature of the absorber column low, essentially avoiding high temperatures and increasing the liquid-gas ratio is expected to

constrain the NH3 and associated volatile emission but at the expense of increasing O2 solubility in the amine solvent.

- There was no dramatic variation in the CO2 recovery rate and NSRD based on about 500 hours of the experimental campaign. This suggests that the solvent performance was maintained within the period of the tests and thus has not reached its breaking point.

5.6 NOVEL CONTRIBUTION TO KNOWLEDGE

- Investigation into oxidative degradation of 40 wt(%) MEA under the influence of synthesized natural gas combustion flue gas at a pilot-scale CO2 capture plant. This study is based on the accumulation of metal content, NH3 emissions and possible role to water-wash transfer on the dynamics of Dissolved Oxygen (DO) peaking and solvent density. This study has also revealed that under 500 hours of CO2 capture operation under the test specifications employed does not subject the MEA to a breaking point in such a manner as to significantly affect the NSRD or the CO2 recovery rate.

CHAPTER VI

SIMULATION STUDY OF
POST-COMBUSTION CARBON CAPTURE PROCESS

6.1   INTRODUCTION

This chapter covers the modelling and simulation study of the building and validating of a CO_2 capture process that gives a confident and reliable representation of the PACT Pilot-scale Carbon Capture Plant using gCCS. This software is a process-modelling approach under the auspices of PSE's gPROMS (General PROcess Modelling System) advanced modelling platform. The gCCS is the 'world's first whole-chain system modelling' platform support tool that enables the design, system modifications and optimization processes across the entire CCS chain that include fuel combustion, CO_2 capture, transport, compression, transmission and injection [182]. For the purpose of this research project, the gCCS carbon capture-modelling ecosystem was employed (see Fig. 6.1) to build and simulate models of solvent-based CO_2 capture process. This process-modelling platform empowers engineers to construct complex and graphic models to study the steady and dynamic state of operation of the Post-Combustion Carbon Capture (PCC) process, optimization of the fraternization between the power plant and the Amine Capture Plant (ACP) and the evaluation of the performances of the process based on changes in the upstream or downstream operating parameters.

This chapter validates the experimental study on the performance evaluation of the UKCCSRC-PACT plant (Fig. 3.4) carried out by Akram et al. [64] using gCCS. The close conformity of the simulation (gCCS) against experimental [64] and a second simulation (ASPEN: based on the same experiment) result gave the confidence and conviction to perform offline process optimization process of the CO_2 capture process. This chapter further evaluates the performance of the PACT plant with two-absorber columns (to increase the solvent-CO_2 absorption process residence-time) under the influence of varying CO_2 concentrations (mimicking S-EGR), lean CO_2 loadings and L/G ratios with the aim of reducing the solvent regeneration energy requirement of the process. This chapter finally closes by giving a conclusion based on the generated results, namely if S-EGR is important or not as an energy reducing mechanism.
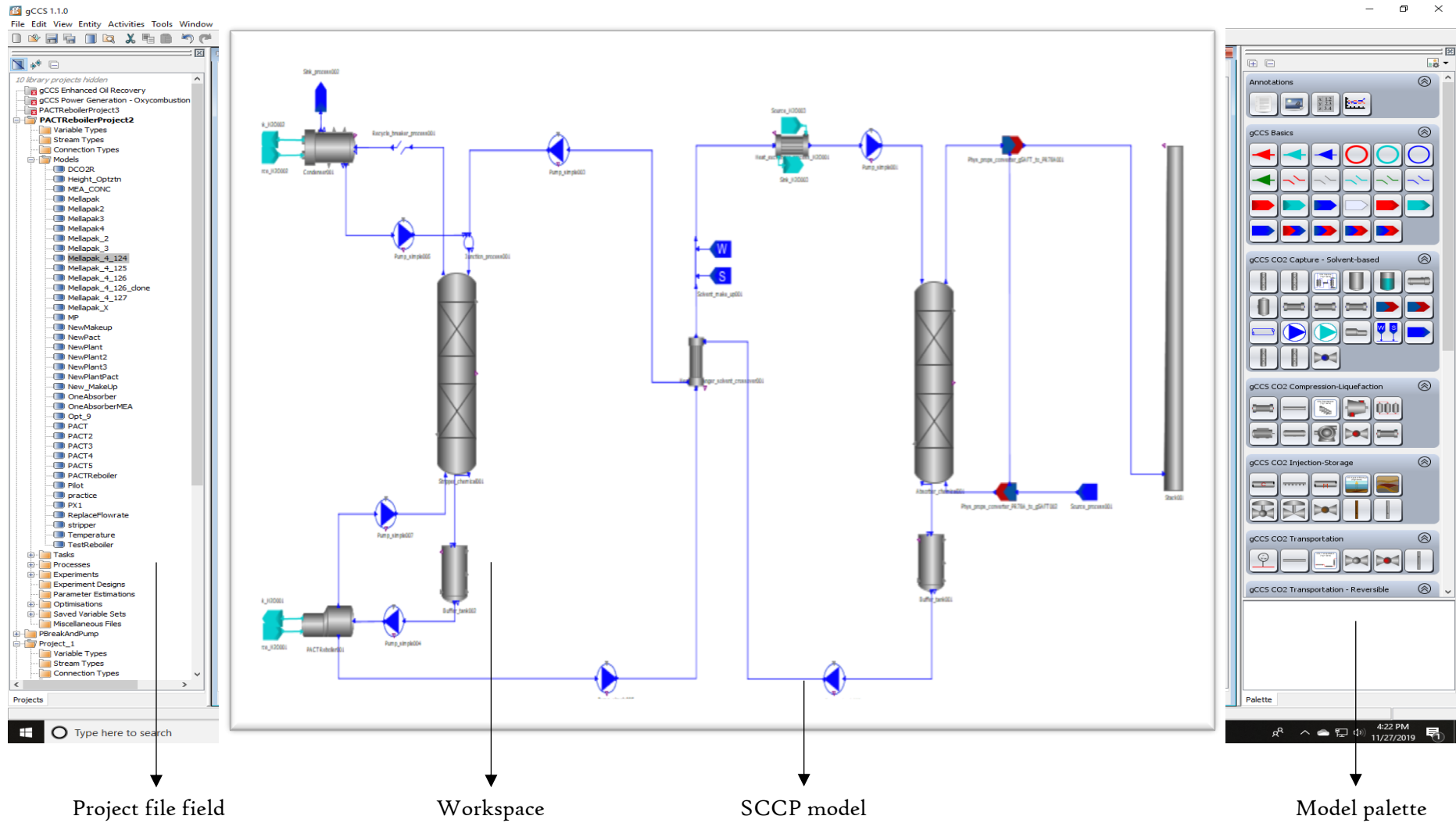
Fig 6.1 The main screenshot of gCCS system modelling workstation containing a classic modelled amine loop configuration [183]

6.2   gCCS CO₂ CAPTURE MODEL LIBRARY

A model (set of equations expressing the physical as well as chemical characteristics of the component unit) was created in the workspace topology, which was sourced from the model palette (a field that graphically the exhibit model component units) shown in Fig. 6.1. An operational and process flow scheme is thus created by connecting the individual models via designated ports. The component units and ports of the model modules are specified to build a functional process model, which utilizes the gSAFT advanced thermodynamics to model the behaviour of the gas-liquid phases. Model specification is embarked on using a dialogue box, and this task assigns values to the gPROMS language [182],[184]. The CO₂ absorption and stripping models are based on the two-film theory, discussed in chapter 2.11 and in Fig. 2.10.

Figs. 6.2 to 6.4 presents the most important components utilized in the building of the solvent-based CO₂ capture plant used in the validation process of the published experimental campaign at PACT starting with the source process model as provided in Fig 6.2 [185].
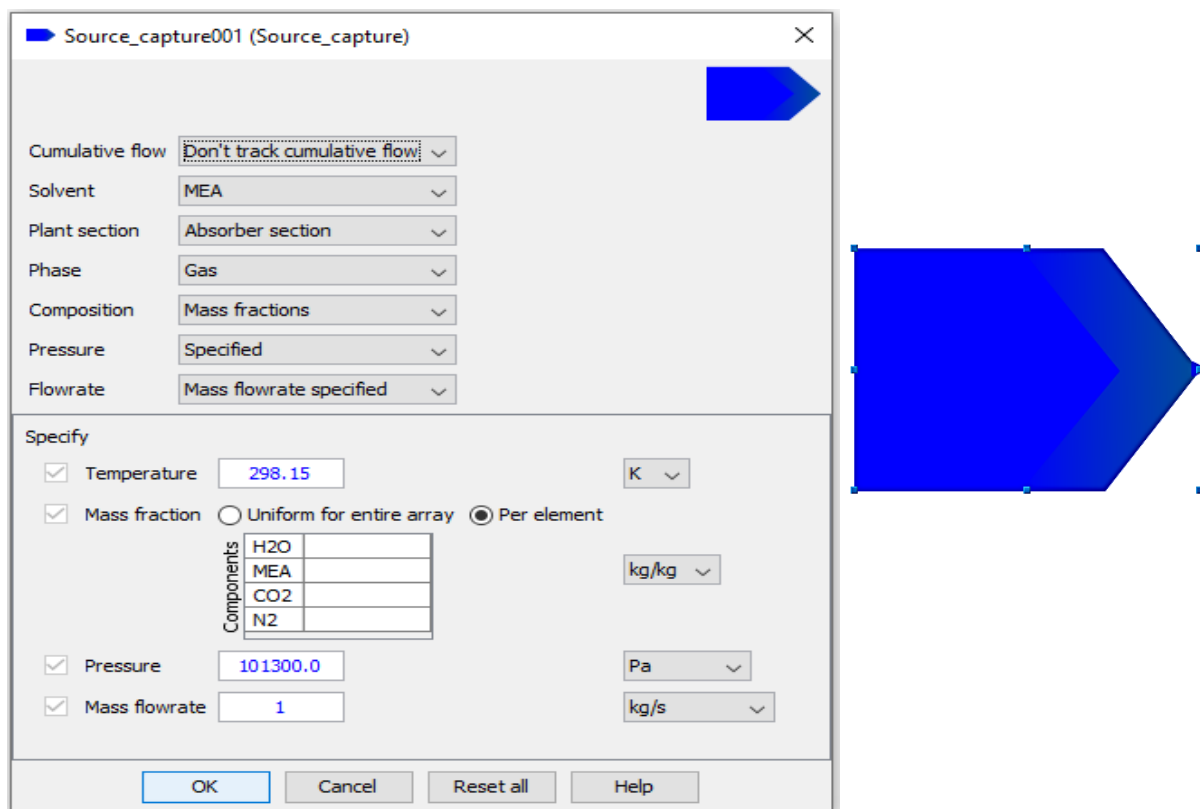
Fig. 6.2 The gCCS source process model.

The source process model makes provision for feeding a material flow into a flowsheet. It is utilized in introducing a generic source into an energy system and thus no inlet. It is as a result equipped with only an outlet port. The source-process model assumption is that it has infinite potential to perform work.

Both the absorber and stripper model (Fig 6.3) are governed by the rate-based absorption/desorption of CO_2 for a number of amine solvents that can operate under a steady or dynamic state. This model has two inlet ports and two outlet ports for the 'flue gas & lean amine solvent' and 'CO_2 lean gas & rich amine solvent', respectively.

Model assumption:

i.   Phase equilibrium is attained at the interface between the thin film of the gas and liquid phases.

ii.   The two-film model gives an acceptable prediction with regards to the mass transfer between the liquid and vapour bulk phases.
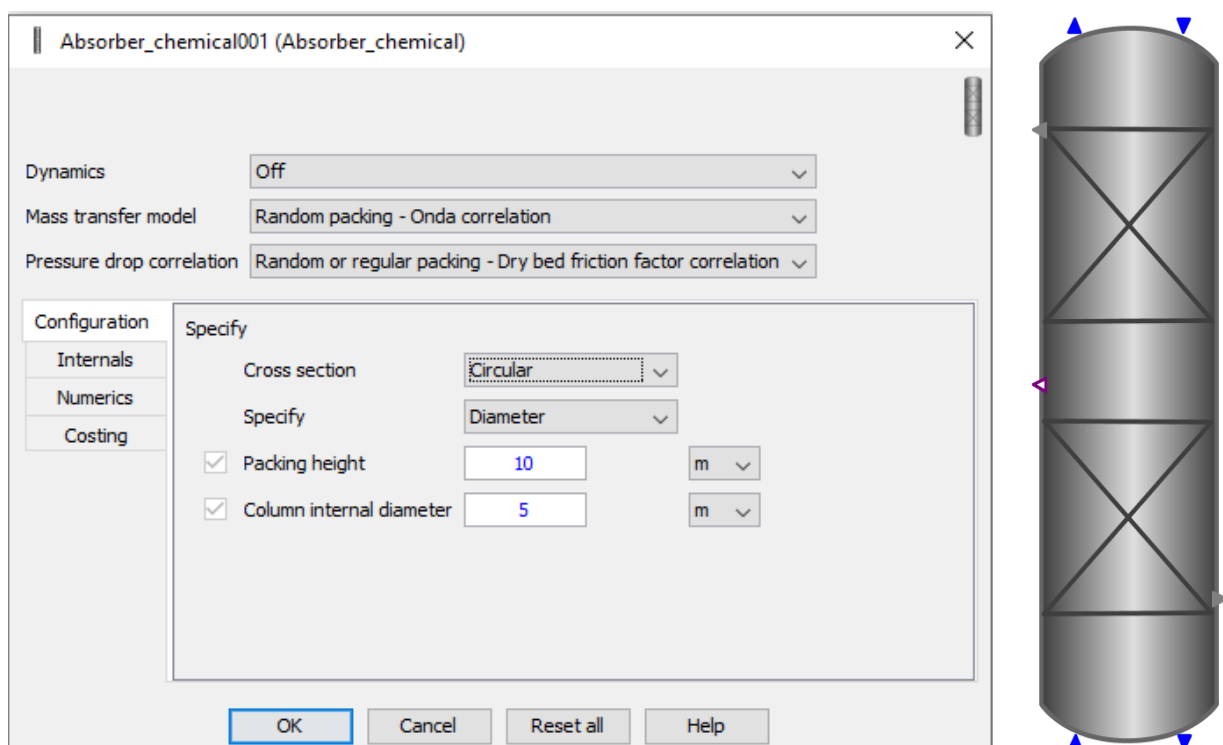
Fig. 6.3   The gCCS absorber and stripper.

The reboiler model operates as a dynamic unit that heat up the CO_2 laden amine solution (rich solvent) for regeneration. The reboiler has a number of inlets and outlets as follows; process fluid inlet, liquid & vapour outlets and Inlet and outlet water streams. Temperature is specified and flow rate computed by the model under the calibration mode whereas the user specifies flow rate of the water and temperature computed in the operational mode.
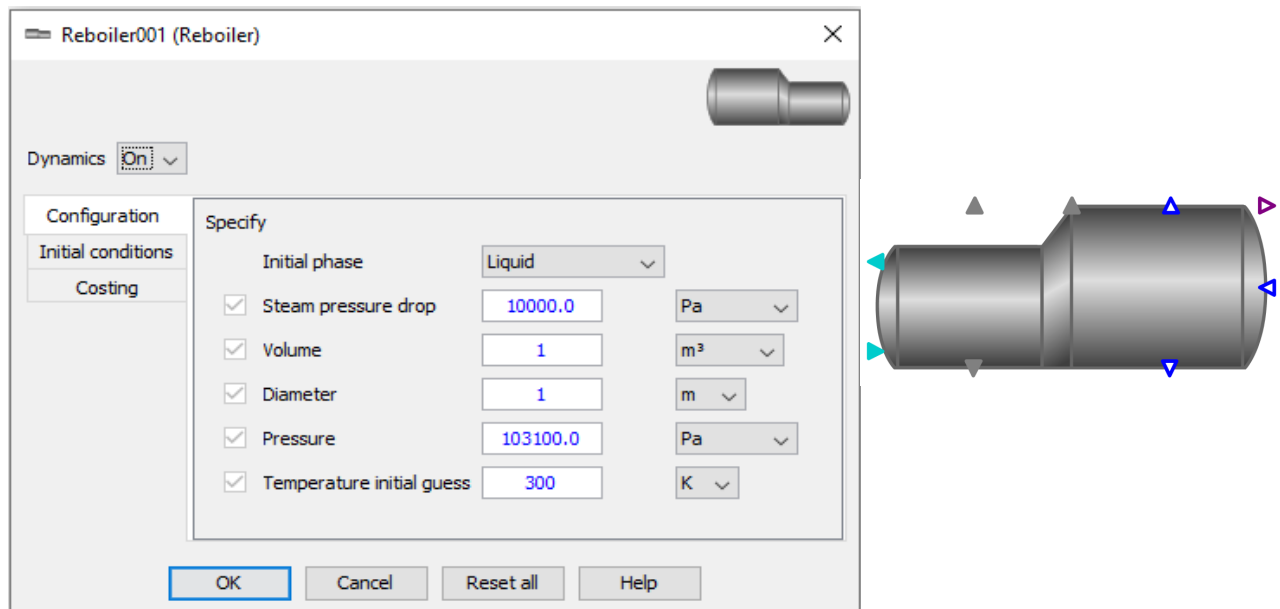
Fig. 6.4 The gCCS reboiler model.

Reboiler model assumption:

- A state of equilibrium exists between the liquid and gas phases
- There is complete mixing of the liquid and gas phases
- There is no thermal energy lost to the environment
- Complete condensation of the steam occurs

6.3   gPROMS LANGUAGE

The input liquid and gas characteristics are specified at the source models of the flue gas, amine solvent and PHW source (Fig 6.2) and thereafter connected to the primary model components including the absorber, stripper, condenser, heat exchangers and the reboiler. Variables are then created, which gives a trademark identification to the parameters to be calculated, example of the variables are given as follows:

- VARIABLE

Lean_loading AS no_type_gCCS

rich_loading AS no_type_gCCS

Specific_reboiler_duty AS no_type_gCCS

CO_2_regeneration AS no_type_gCCS

CO_2_captured AS no_type_gCCS

Liquid_to_Gas AS no_type_ gCCS

gCCS designated equations are then created based on the variables defined and are as follows: These equations are the gCCS clones or manifestations of the basic equations for calculating the desired dependable variables which are given in Section 3.4.

- EQUATION

Lean_loading = Pump_simple005.mass_fraction('CO_2') * 1.39 / Pump_simple005.mass _fraction('MEA');

Rich_loading = Pump_simple002.mass_fraction('CO_2') * 1.39 / Pump_simple002.mass_ fraction('MEA');

Specific_reboilerduty = (PACTreboiler001.Q * 1e-6) / (Source_process001.F * Source_ process001.w('CO_2')) - (Stack001.F * Stack001.w('CO_2'))* 3600;

CO_2_regeneration = (Stripper_chemical001.InletLiquid.F * Stripper_chemical001. InletLiquid.w('CO_2') - PACTReboiler001.OutletLiquid.F * PACTReboiler001.OutletLiquid.w('CO_2')) / (Stripper_chemical001.InletLiquid.F * Stripper_chemical001.InletLiquid.w('CO_2'));

CO_2_captured = (Source_process001.F * Source_process001.w('CO_2') - Stack001.F * Stack001.w('CO_2')) * 3600;

Liquid_to_Gas = Absorber_chemical001.InletLiquid.F / Absorber_chemical001. InletVapour.F;

- ASSIGN

The model is then assigned with the required dependable parameter to keep fixed in the course of the simulation. Examples are as follows, where the SRD was kept at 4.5 MJ/kg. The model will hence be simulated modifying the reboiler process input based on the gas and liquid chracteristics to attain the required set SRD.

#Lean_loading := 0.244;

#CO_2_captured := 0.9;

Specific_reboiler_duty := 4.5;

- SAVE VARIABLE SET

The save variable set saves all the process characteristics of the gCCS models in a save variable set folder so it can be re-used in later time and simulated in a short period of time. The process is carried out as follows:

```
SCHEDULE
    SEQUENCE
      CONTINUE FOR 1
        SAVE 'give name of model'
            END
```

The calibration data file is then copied and pasted in the 'Save Variable Set' folder. The Schedule is delete, the process is modified to 'read this file', which is carried out at the PRESET section via introducing

```
PRESET
    RESTORE 'name of the model'
```

The model is then simulated.

6.4   VALIDATION OF THE gCCS PACT MODEL

A 100kW$_e$ Turbec T100 mGT (see Fig. 3.2) was integrated into the 1 TPD PACT plant (see Figs. 3.3 and 3.4) in such a configuration that a slipstream of the flue gas from the mGT was used to furnish the CO_2 pilot-scale capture plant [64]. The gas turbine exhaust characteristics are presented in Table 6.1.

Table 6.1 The flue gas characteristics from the mGT at the PACT facility [64].

H_2O	vol (%)	3.32
CO_2	vol (%)	1.52
CO	ppm	90.73
N_2O	ppm	0.37
NO	ppm	2.84
NO_2	ppm	0.3
Methane	ppm	5.86
Ethane	ppm	0.64
Ethylene	ppm	0.49
Formaldehyde	ppm	0.51
TOC	mgC/Nm^3	4.72

As the onsite mGT is a lean pre-mixed combustor, the CO_2 from a cryogenic tank was introduced at a flow rate of from 17 to 31.5 kg/hr in addition to the slipstreamed flue gas at the absorber inlet in order to mimic the CO_2 concentration in the flue gas of the gas turbine combustion of about 4 – 6 vol% as the base-case test [72],[90]. The operating conditions employed for the mGT-PACT plant campaign are given in Table 6.2 [64].

Table 6.2   The operating conditions utilized for the experimental campaign.

Parameters	Unit	Test 1	Test 2	Test 3	Test 4	Test 5
CO_2 injection	Kg/hr	17	21	24.5	27	31.5
CO_2 in FG (after injection)	vol%	5.5	6.6	7.7	8.3	9.9
FG flow rate	Nm^3/hr	210	210	210	210	210
FG temperature	°C	37	39	38	38	40
Solvent flow rate	Kg/hr	400	488	567	604	721
Lean solvent temperature	°C	40	40	40	40	40
Liquid to Gas ratio	Kg/kg	1.55	1.88	2.17	2.30	2.73

PHW flow rate	m^3/hr	7.43	7.43	7.43	7.43	7.43
PHW inlet temperature	°C	120.62	120.41	120.77	120.46	120.52
PHW outlet temperature	°C	115.79	114.54	115.33	114.50	114.66

The UKCCSRC-PACT plant specification (see Table 3.2 and illustrated in Fig. 3.4) was employed to capture the CO_2 at varying concentrations in order to evaluate its performance under these conditions against 30wt% of MEA using Koch Intalox Metal Tower Packing (IMTP) No. 25 random packing in the columns [90].

The experimental operating conditions (see Table 6.2) was utilized to validate the PACT model using the gCCS by comparing the simulation results against the experimental data. The results generated by gCCS was also compared against the simulation results obtained using ASPEN for the same experiment. The basis of which the validated model will be utilized for further process simulation studies on the modification of the operating conditions with the aim of reducing the high energetic cost of the CO_2 capture process.

Table 6.3 Model validation using gCCS.

Process variables	Unit	A	B	C	A	B	C	A	B	C	A	B	C	A	B	C
CO_2 concentration	vol%		5.5			6.6			7.7			8.3			9.9	
Lean loading	mol/mol		0.165			0.172			0.183			0.180			0.204	
Rich loading	mol/mol	0.388	0.386	0.394	0.399	0.405	0.411	0.411	0.401	0.414	0.417	0.417	0.426	0.443	0.432	0.443
CO_2 captured	Kg/hr	20.2	20.3	20.3	23.8	24.4	24.3	26.9	28.2	28.7	29.2	30.7	30.6	33.2	36.1	36.1
Degree of regeneration	%	57.5	57.6	58.1	56.9	57.9	58.2	55.5	54.6	55.8	56.8	57.1	57.7	54.0	53.0	54.0
SRD	MJ/hr	7.1	7.3	7.3	7.4	6.6	6.8	6.0	6.4	6.1	5.9	6.1	5.8	5.3	5.2	5.0

A: Experimental campaign at PACT [64]

B: Simulation results using gCCS

C: Simulation results using ASPEN [90]

The simulation lean loading was set as that of the experimental loading as a reference for the simulations on the models. The percentage deviations in the simulation results using gCCS against the experimental and simulation studies (ASPEN) was found to be within 0 – 2.5%, which indicates that the rich loadings simulation results compare very favourably with both the previous experimental and simulation (ASPEN) investigations.
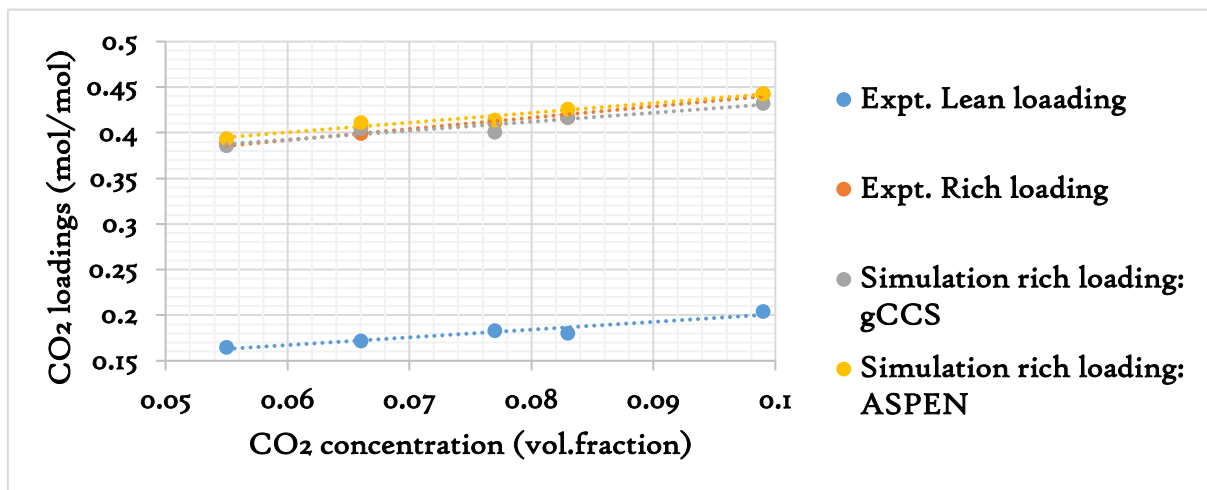
Fig. 6.6   The gCCS vs Experiment vs ASPEN: The CO_2 loadings as a function of the CO_2 concentration.

The CO_2 captured simulation results are in very close agreement with the experimental data and the ASPEN simulation results as observed in Fig. 6.7. The percentage deviations between the gCCS simulation results against the experimental data and ASPEN simulation results were observed to be from about 0 to 8.7 %.
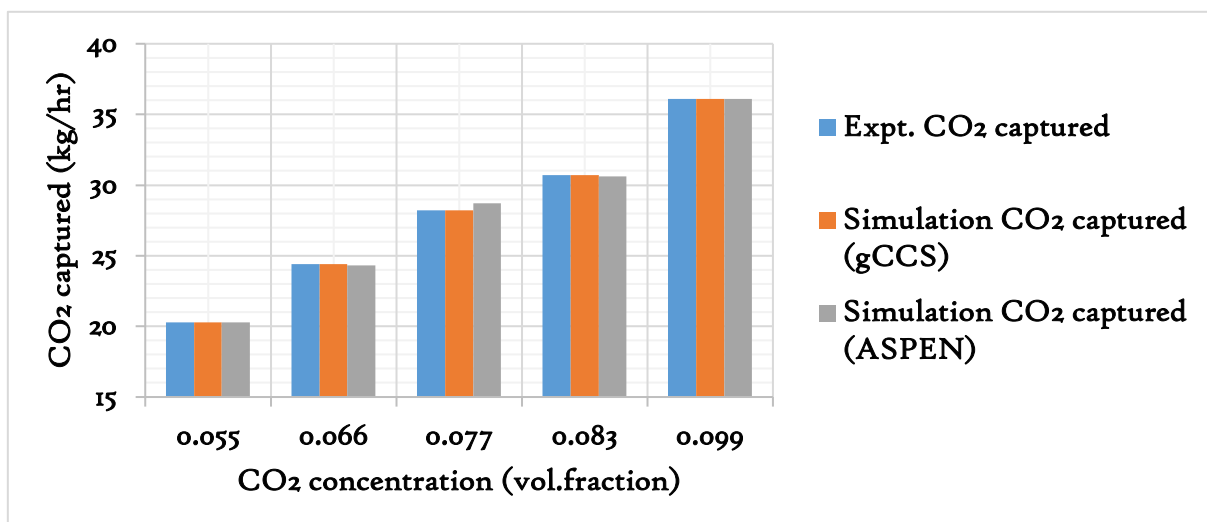
Fig. 6.7   The gCCS vs Experiment vs ASPEN: The CO_2 captured as a function of the CO_2 concentration.

The SRD in the gCCS was also observed to be in close agreement with the experimental data and ASPEN simulation. The percentage deviation between the gCCS predictions against the experimental data were observed to be within the range of about 1.8 – 10.8%.
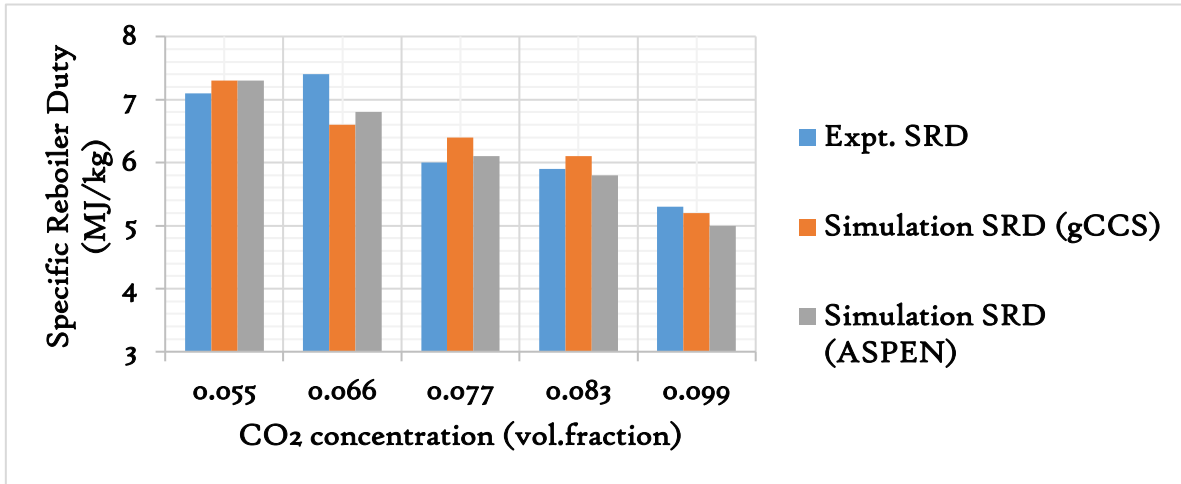
Fig. 6.8   The gCCS vs Experiment vs ASPEN: The SRD as a function of the CO_2 concentration

Differences in the results by up to about 10% is not unusual due to the postulations that have been highlighted in the assumptions in Figs. 6.3 and 6.4. Furthermore, the structural and operational constraints that are normally experienced during the course of the experimental investigations are almost non-existent when compared with the modelling and simulation software environments. As a result of having a validated gCCS model that has a very favourably confirmed trends and the behaviour of the pilot-sale CO_2 capture experimental data, the gCCS is thus employed in the study of the key performing parameters in the subsequent sections.

6.5   INFLUENCE OF TWO ABSORBER COLUMNS ON THE PERFORMANCE OF THE CO₂ CAPTURE PROCESS

A higher residence time of the amine solvent and flue gas in the absorber column in principle increases the CO_2 capture efficiency, thus a structural modification of the capture plant that increases the residence time of both the solvent and flue gas in the absorber column offers a valuable option for reducing the solvent regeneration energy requirement of the Solvent-based CO_2 Capture process. This approach can be attained by equipping a second absorber column as an extension to the main the CO_2 capture plant [186]. Thus, a

process simulation study was embarked on in order to evaluate the key performances of the PACT plant (Fig.3.4) as if it were to be fitted with two absorber columns in a counter-current flow configuration as shown on the gCCS simulation environment in Fig. 6.15. The key performing indices studied include the CO_2 loadings, CO_2 capture efficiencies and the SRD. The first test case with one-absorber column (denoted by A), the two-absorber column (denoted by B) was conducted with the same input process variables as test case (A), whereas test case (C) with two absorber columns was undertaken while fixing the lean loading and CO_2 capture efficiency as in test case (A). Table 6.4 and 6.5 presents the process conditions and the results obtained for the three test cases.

Table 6.4 Process conditions of the tests A, B and C.

Flue gas flow rate	250 kg/hr
Flue gas temperature at inlet of absorber	40°C
Flue gas pressure at absorber inlet	1.04 bar
PHW flow rate at inlet of reboiler	5652 kg/hr
PHW inlet temperature	124°C
Cold outlet approach	19.03°C
MEA concentration	40wt(%)

Table 6.5 Operating simulation test results of an SCCP with one and two (A and B) absorber columns.

Parameter	Unit	A*	B	C	A	B	C	A	B	C	A	B	C	A	B	C
CO_2 conc.	vol%	0.04			0.055			0.07			0.085			0.10		
Lean loading	mol/mol	0.231	0.228	0.231	0.251	0.255	0.251	0.271	0.275	0.271	0.301	0.307	0.301	0.321	0.347	0.321
Rich loading_1	mol/mol	0.369	0.391	0.449	0.375	0.390	0.445	0.383	0.397	0.44	0.394	0.410	0.434	0.404	0.437	0.435
Rich loading_2	mol/mol	-	0.258	0.367	-	0.28	0.367	-	0.306	0.367	-	0.341	0.372	-	0.39	0.385
CO_2 capture eff_1	%	-	79.81	33.54	-	78.89	36.05	-	72.66	38.86	-	65.34	41.83	-	49.94	39.32
CO_2 capture eff_2	%	-	89.69	84.95	-	88.68	84.36	-	91.0	83.64	-	94.59	82.81	-	93.63	83.52
CO_2 capture eff_T	%	90.0	97.9	90	90.0	97.6	90.0	90.0	97.5	90.0	90.0	98.1	90.0	90.0	97.0	90.0
CO_2 capture rate	kg/hr	13.5	14.7	13.5	18.5	20.0	18.43	23.3	25.2	23.3	28.0	30.6	28.0	32.7	35.2	32.7
Solvent regeneration	%	38.0	42.0	49.0	33.6	35.0	44.0	29.6	31.0	39	24.0	25.0	31.0	20.7	21.0	26.0
L/G_1	kg/kg	1.4	1.3	0.9	2.1	2.1	1.4	2.9	3.0	2.0	4.1	4.3	3.0	5.5	5.6	4.1
L/G_2	kg/kg		1.2	0.9		2.0	1.4		2.8	1.9		4.0	2.8		5.5	3.7
SRD	MJ/kg	6.94	6.37	5.05	6.34	5.83	4.71	5.86	5.39	4.47	5.40	4.95	4.32	5.30	4.67	4.33
mCO_2_FG	kg/hr	15.0			20.5			25.9			31.1			36.3		
mCO_2_TG	kg/hr	1.5	0.3	1.5	2.05	0.5	2.05	2.59	0.6	2.59	3.11	0.6	3.11	3.63	1.2	3.63
Reboiler duty	MJ/hr	96.0	96.0	69.77	119.5	119.5	88.67	139.23	139.2	106.4	154.5	154.5	123.7	177.0	167.7	144.6
mSolvent	kg/hr	341		216	515		330.8	723		478	1037		730	1370		993.9

A denotes the test case with one absorber column while A* is the baseline case study.

B denotes the test case with two absorber columns

C denotes the test case with two absorber columns while fixing the lean and CO_2 capture

   efficiency as test case A

_1 denotes absorber 1

_2 denotes absorber 2

_ T denotes total CO_2 capture efficiency in the SCCP with two-absorber columns and

where conc., mCO2_FG, mCO2_TG, eff and mSolvent, refers to concentration, mass flow rate of CO_2 in flue gas, mass flow rate of CO_2 in treated gas, efficiency and mass flow rate of the amine respectively.

6.5.1 IMPACT OF THE CO_2 CONCENTRATION ON THE CO_2 LOADINGS FOR TESTS A, B AND C

The CO_2 loadings with increasing CO_2 concentration with two absorber columns, irrespective of the test cases, were observed to generally increase due to the increasing driving forces for the CO_2 absorption and this trend is in line with the results that have been reported in the published research papers [64],[90]. However, what is new in this study is that the CO_2 loadings in absorber 1 (Rich loading) are noticeably higher by about 11 – 34% (with increasing CO_2 concentration) than the CO_2 loadings in absorber 2 (Semi-rich loading) because of complimentary CO_2 capture in absorber 1. Furthermore, fresh flue gas is first introduced into absorber 1, which also enhances the rich loadings. Interestingly, the difference between the CO_2 loadings in the first and second absorbers appears to diminish with increasing CO_2 concentration (Fig. 9) and this behaviour can be attributed to increasing the semi-rich loadings due to increasing the L/G. By implication, this restricts the solvent absorption capacity in absorber 1. An additional absorber column in this study has increased the rich loading by 6.0% and 1.6% for cases B and C respectively. This has the tendency to increase the CO_2 capture and consequently reduce the SRD, however at an initial increase in the capital cost. A graphical representation of the CO_2 loadings (rich, semi-rich and lean loadings) is shown in Fig. 6.9. Hence, two absorber columns have value with regards to increasing the rich loading of the CO_2 capture process with the potential to reduce the SRD.

Fig. 6.9 Profile of the CO₂ loadings for tests A, B and C across varying CO₂ concentrations.

6.5.2 IMPACT OF THE CO₂ CONCENTRATION ON THE CO₂ CAPTURE EFFICIENCY FOR TESTS A, B AND C

The two-absorber column as against one has a pronounced impact on the CO_2 capture efficiency as shown in 6.10. It was observed that the CO_2 capture efficiency increased to 98% in test B as compared to 90% in test A, irrespective of the CO_2 concentration. However, the capture efficiency was kept at 90% in test C (same as test A) and therefore, it does not have any effect on the capture efficiency. This test has demonstrated that when the SCCP is fitted with the two-absorber column the there is an unrivalled influence on the efficiency of the CO_2 capture process. A general trend, observed in Fig. 6.10, has established that most of the CO_2 capture takes place in the absorber 2, i.e. where the thermally regenerated (lean solvent) in firstly introduced into the CO_2 absorption column. Increasing the CO_2 concentration increases the CO_2 capture efficiency in absorber 2 by about 4.4% and this is because of the increasing L/G. The CO_2 capture efficiency in absorber 1 (test B) was observed to decrease by 37.5% with increasing the CO_2 concentration (see Fig. 6.10) and this is due to the reducing of the CO_2 absorption capacity of the semi-rich solvent, which underscores the impact of the lean solvent that is being introduced into the absorber 2 at a higher solvent flow rate.

Due to the fact that the CO_2 capture efficiency was restricted to 90% in test C (Fig. 6.10), the behaviour of the CO_2 capture efficiency in both the absorbers 1 and 2 appears not to show any meaningful deviation as the CO_2 concentration increases because the CO_2 capture

efficiency was capped to 90%. It is found that about 60%, more CO_2 absorption takes place in the absorber 2 in test C, which is thought to be due to the introduction of the regenerated (lean) solvent.

Fig. 6.10 presents the CO_2 capture efficiencies as a function of the CO_2 concentrations. It is not surprising to discover that the rich loading is higher in absorber 1 (see Fig. 6.9) while the CO_2 capture efficiency is higher in absorber 2 (see Fig. 6.10), and this is because absorber 1 acts as a complimentary CO_2 absorption mechanism.
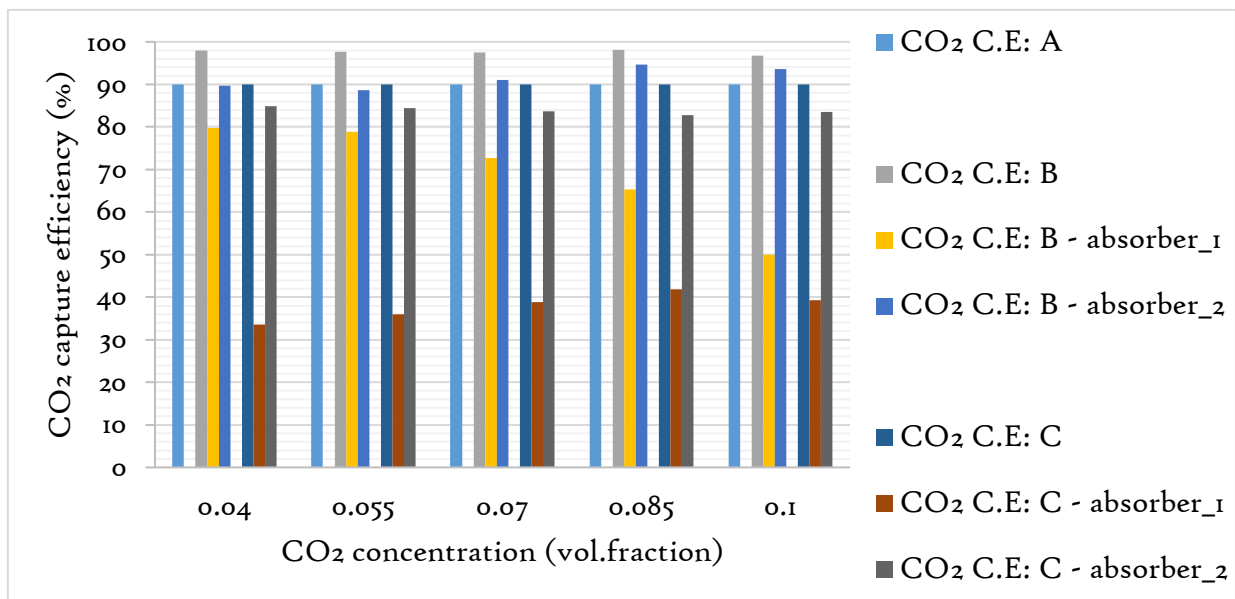
Fig. 6.10 Profile of the CO_2 capture efficiencies for tests A, B and C across varying CO_2 concentrations.

6.5.3 IMPACT OF THE CO_2 CONCENTRATION ON THE CO_2 CAPTURE RATE AND SOLVENT REGENERATION FOR TESTS A, B AND C

With increasing the CO_2 concentration in the flue gas, the higher is the mass transfer of CO_2 from the gaseous to the liquid phase, and this is due to the increasing tendency of the CO_2 to escape from the gas phase resulting from the higher CO_2 partial pressure [65],[187]. The behaviour of the CO_2 captured in tests A, B and C confirmed this theory. Test B was however, observed to have a higher CO_2 capture rate by about 8% across the varying CO_2 concentrations and this due to the influence of the increased residence time of the CO_2-solvent association in the two-absorber columns configuration. Test C was capped at 90% CO_2 capture and therefore the CO_2 captured is the same as in test A. The SCCP should be

operated for a long-term if it is to yield the benefit of about 8% increase in the CO_2 capture rate in order to offset the initial capital cost of the second absorber. Restricting the CO_2 capture efficiency to 90% with two absorber columns as in the case of one absorber do not give value in the CO_2 captured. Fig 6.11 shows a graphical representation of the CO_2 captured as a function of the CO_2 concentration for the tests A, B and C.
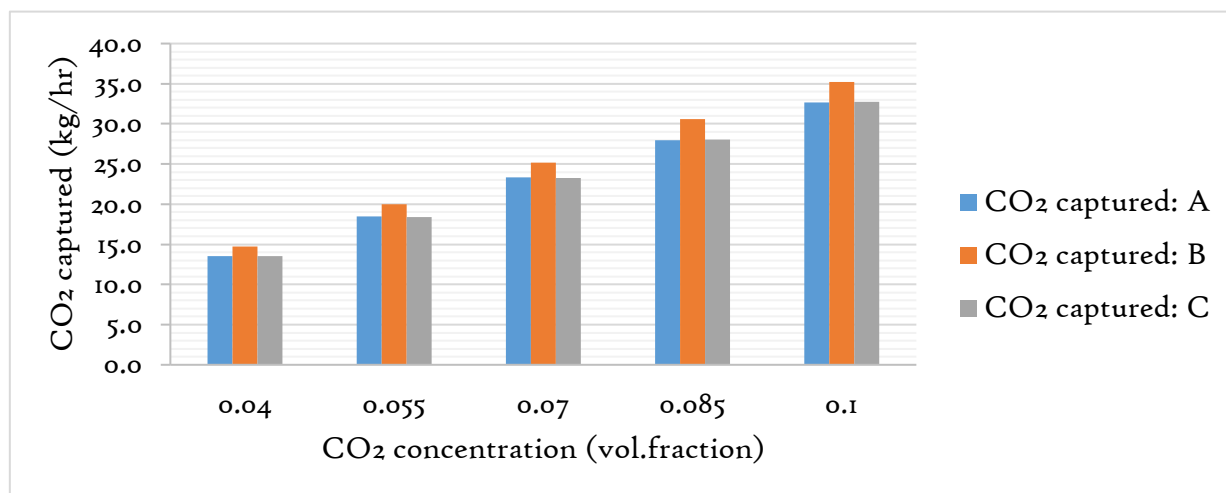
Fig. 6.11   Profile of the CO_2 capture rate for tests A, B and C across varying CO_2 concentrations.

The solvent regeneration decreases with increasing CO_2 concentration and this is due to the lower residence time of the solvent in the reboiler and stripper column as the L/G is increased to accommodate for the increasing CO_2 concentration. The solvent regeneration in test B was observed to be higher than test A and this is because it is probably due to that more solvent regeneration (thermal) energy in the form of CO_2 desorption energy playing a more active role than the solvent sensible heat because the solvent is richer in test B [188]. Whereas test C has the highest solvent regeneration energy, because it has the lowest L/G in the test cases, and this is due to the higher solvent residence time in the reboiler and stripper. The lower L/G in test C was as a result of setting the lean loading as in test A, which means that a lower solvent flow is needed for the required lean loading and the capped at 90% CO_2 capture efficiency. Fig 6.12 shows the degree of solvent regeneration against the CO_2 concentration for tests A, B and C. Thus, L/G has a remarkable influence on the degree of solvent regeneration, which can potentially affect the solvent regeneration energy requirement.
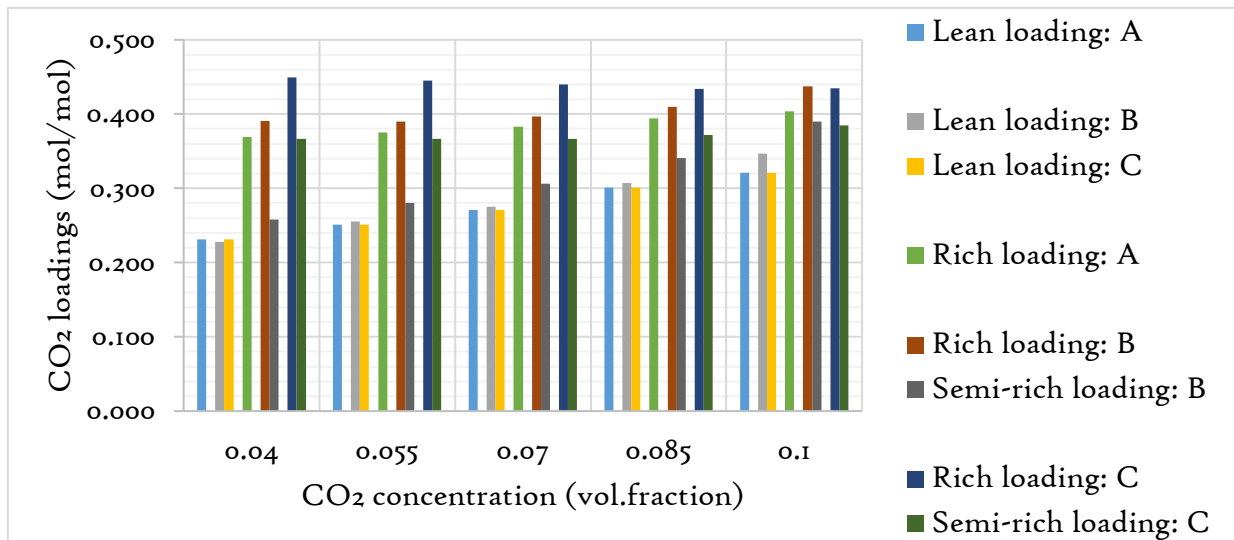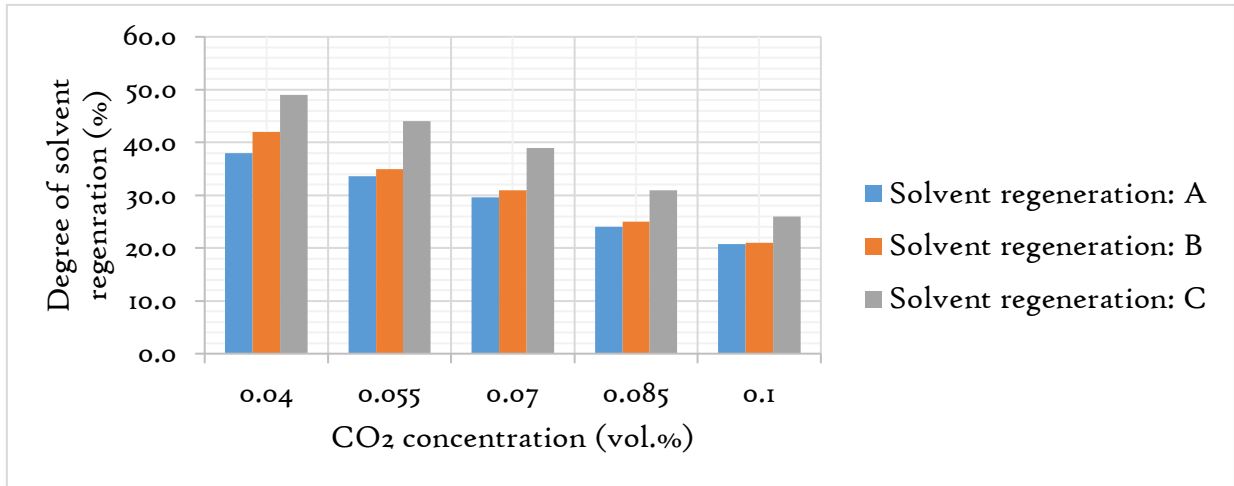
Fig. 6.12   Profile of the CO₂ capture rate for tests A, B and C across varying CO₂ concentrations.

6.5.4   IMPACT OF THE CO₂ CONCENTRATION ON THE SPECIFIC REBOILER DUTY FOR TESTS A, B AND C

The primary aim of these tests was to evaluate the reduction of the reboiler duty per every kg of CO_2 captured. As expected, there was a notable decrease of the SRD by an average of 9% across the varying CO_2 concentration when the SCCP was fitted with two absorber columns, indicating higher interaction time between the solvent and CO_2. Thus, leading to more CO_2 being captured. However, when the lean loading was fixed in test C, as the same as test A and the CO_2 capture efficiency fixed at 90%, the SRD further experiences a remarkable decrease in its SRD, reducing by an average of about 20% across the varying CO_2 concentration. This striking reduction is due to the higher solvent regeneration (see Fig. 6.12) which due to the reduced L/G to cap the CO_2 capture efficiency at 90%.
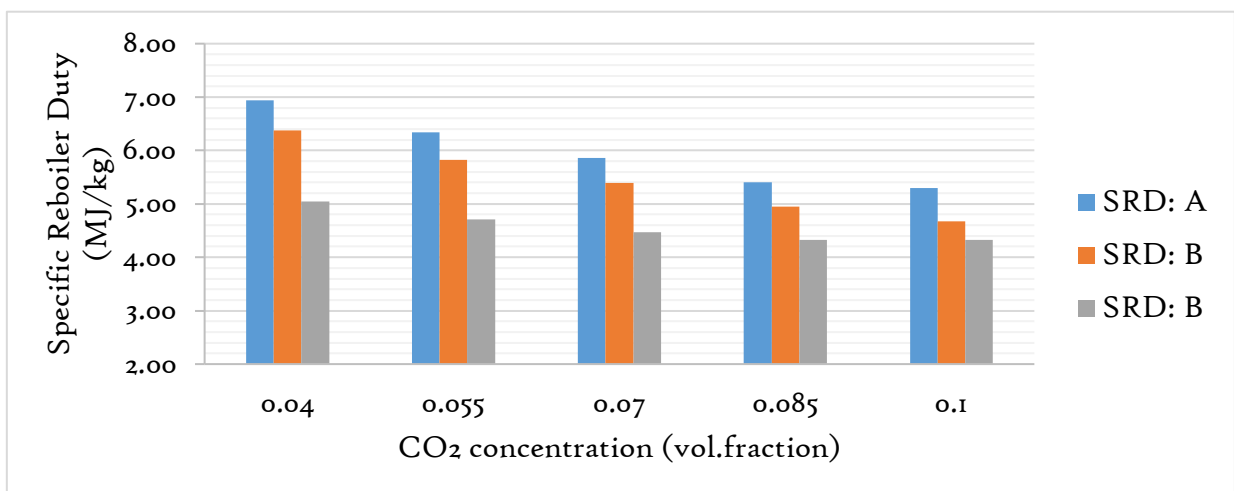
Fig. 6.13   Profile of the SRD for tests A, B and C across varying CO₂ concentrations.

132

Tests A, B and C offer an exciting opportunity to better understand the energy reduction of the solvent-based CO_2 capture process when fitted with two absorber columns. A reduction of about 20% in SRD is a very worthwhile investment in the additional absorber. Furthermore, two absorber columns can be better operated due to the dynamic load changes of the NGCC by bypassing one absorber if required.

6.6 EVALUATION OF TWO MAJOR CONFIGURATIONS OF THE 2-ABSORBER COLUMNS

Following tests to establish the performance of two-absorber column (test B: uncapped at 90% and test C: capped at 90%), this section seeks to evaluate the two major configurations of two absorber columns all capped at 90% because it has shown to yield lower SRD, i.e. the split-stream flow configuration and the counter-current flow configuration (used in the preceding section). The two configurations are presented in Figs. 6.14 and 6.15 as captioned with the gCCS simulated environment.

From Table 6.5, the lean loading was fixed for the same two configurations and for the same CO_2 concentration, while the rich loading decreased by 15 to 5% from the counter current-current to the split-stream flow with increasing CO_2 concentration. The reduction in loadings is postulated to be due to the fact that there is more residence time of the solvent in the absorber columns than the split-flow configuration which accounts for up to 50% of the solvent residence time for the counter-current configuration. While the rich loading of the split-stream flow configuration was monitored to have increased by 8.1% with increasing CO_2 concentration, the rich loading of the counter-current flow configuration was observed to decrease by 3.1%. This is due to the increase in the semi-rich loading by 4.9% and as a result restricting the solvent absorption capacity with increasing CO_2 concentration. The CO_2 loading representation of the two configurations is given in Fig. 6.16.
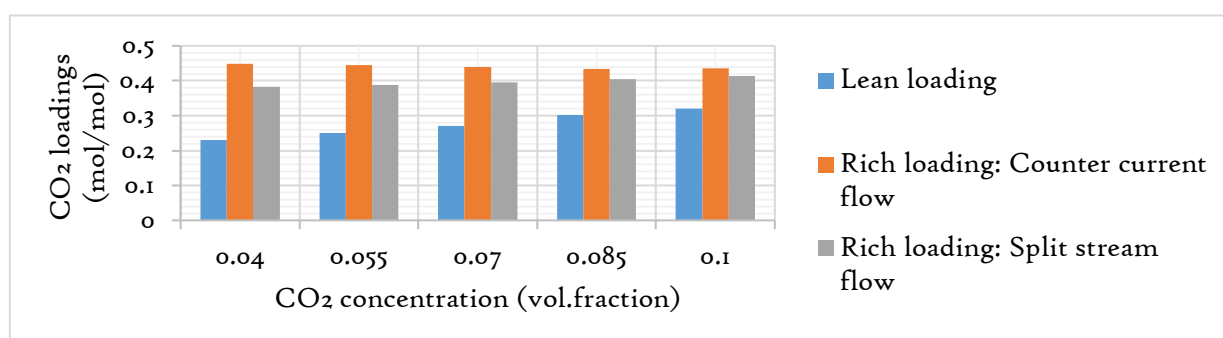
Fig. 6.16   The loadings across counter-current and split-stream flow configurations.
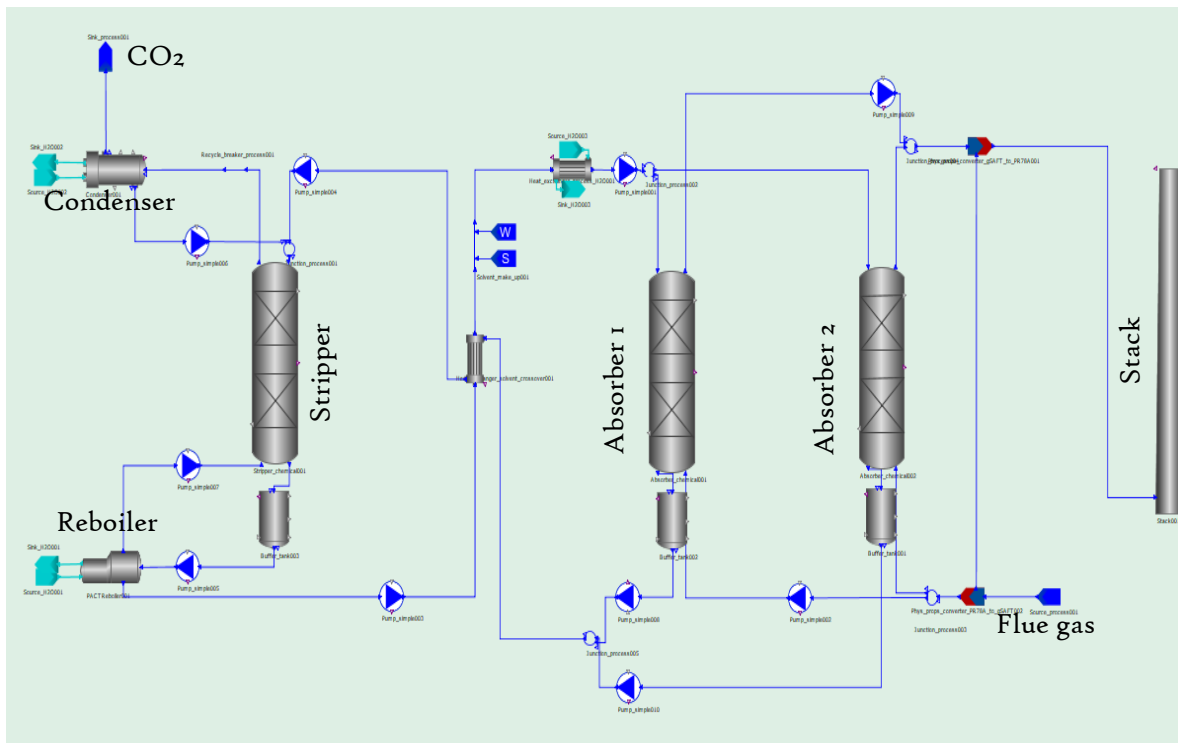
Fig. 6.14   Two absorber columns in the split-stream flow configuration.
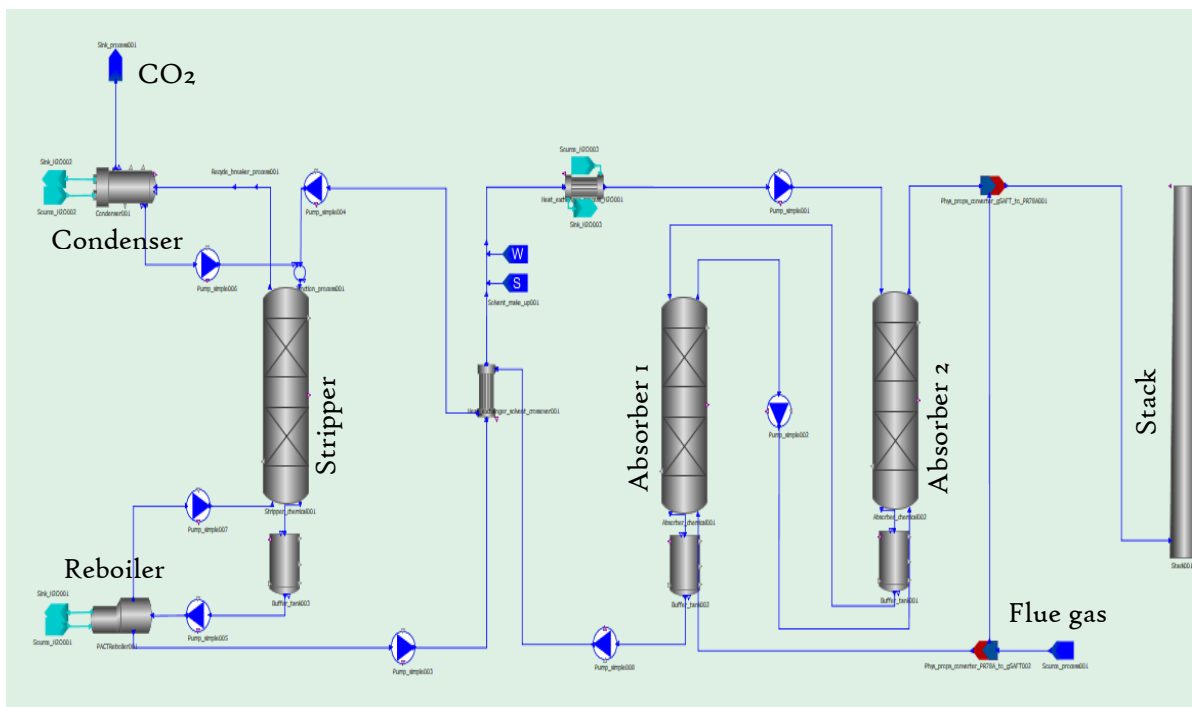
Fig. 6.15   Two absorber columns in the counter-current flow configuration.

The same flue gas, solvent and PHW characteristics used for test C was utilized for the split-stream flow configurations. Table 6.6 gives the results obtained for the two tests.

Table 6.6   The data table for counter-current and split flow CO₂ capture configuration.

Parameters	Unit	Counter-current flow	Split stream flow	Counter-current flow	Split stream flow	Counter-current flow	Split stream flow	Counter-current flow	Split stream flow	Counter-current flow	Split stream flow
CO_2 conc.	vol.%	0.04		0.055		0.07		0.085		0.1	
Lean loading	mol/mol	0.231		0.251		0.271		0.301		0.321	
Semi-rich loading	mol/mol	0.367	0.382	0.367	0.388	0.367	0.395	0.372	0.405	0.385	0.413
Rich loading	mol/mol	0.449	0.382	0.445	0.388	0.440	0.395	0.434	0.405	0.435	0.413
CO_2 capture eff_1	%	33.54	90	36.05	90	38.86	90	41.83	90	39.32	90
CO_2 capture eff_2	%	84.95	90	84.36	90	83.64	90	82.81	90	83.52	90
CO_2 capture eff_T	%	90									
CO_2 capture	kg/hr	13.5		18.43		23.27		28.02		32.7	
Solvent regeneration		49	40	44	36	39	32	31	26	26	22
L/G_1	kg/kg	0.9	1.3	1.4	1.9	2.0	2.6	3.0	3.7	4.1	4.9
L/G_2	kg/kg	0.9	1.3	1.4	1.9	1.9	2.6	2.8	3.7	3.7	4.9
SRD	MJ/	5.05	6.54	4.71	5.96	4.47	5.5	4.32	5.06	4.32	5.06
mCO₂_FG	kg/hr	15.0		20.5		25.9		31.1		36.3	
mCO₂_TG	kg/hr	1.50		2.05		2.59		3.11		3.63	
Solvent flow	kg/hr	216	313	331	468	478	655	730	936	993.9	1229

Due to the fact that the CO_2 capture efficiency was capped at 90%, both configurations captured the same amount of CO_2. However, the degree of solvent regeneration was higher in the counter-current configuration because of lower the L/G, which was possible because it enables a longer residence time than the split-stream flow configuration. As a result the L/G has as a result proven to be a key factor that affects the solvent regeneration energy requirement. Consequently, yielding a much lower SRD, by as low as about 20%, as against the split-flow configuration (see Fig. 6.17).
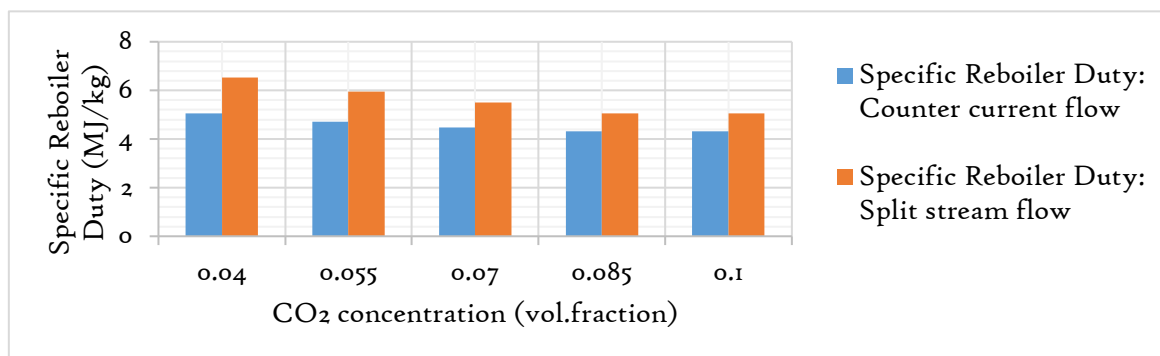
Fig. 6.17   The SRD across counter-current and split-stream flow configurations.

Having studied these two different structural configurations, the split-stream flow configuration has the better advantage of readily been adapted to the dynamic operation of the power generation. The dexterity for carbon capture plant to flexibility adapt to changes to varying thermal loads is critical to the long-term implementation of carbon capture [102]. In the event of high energy demand and when CoE is high, the thermal input to the reboiler may significantly be curtailed and it may be operationally appropriate to utilize the services of an additional absorber column to enable the continuing capture of CO_2 in the flue gas for rich solvent storage, pending the resumption of thermal input. During the period of thermal energy maximization, two absorber columns may also have huge benefit to the CO_2 capture process in regulating the lean loading to a desired value. However, the flexibility in controlling the residence time of the solvent in the absorption column in response to a required CO_2 recovery rate, solvent regeneration or desired solvent loading may be an overriding advantage of implementing two absorption columns configuration. Lower CO_2 capture requirement may call for utilizing of one absorber configuration. Furthermore, the flexibility in the absorber maintenance regime is better achieved via operating the capture plant by taking one absorber offline while utilizing the other one. More about dynamic/flexible operation is presented in section 2.10.

6.7 IMPACT OF THE LEAN LOADINGS AND L/G UNDER THE INFLUENCE OF CO_2 CONCENTRATIONS WITH TWO ABSORBER COLUMNS

The lean loading is a key factor that affects the performance of the CO_2 capture process because it is a manifestation of the consequence of solvent regeneration and dictates the solvent absorption capacity in the absorber column. On the other hand, L/G influences the amount of CO_2 captured and the operating expenditure of the CO_2 capture process. As a result, having an understanding of how this key parameter impacts on the performance of the CO_2 capture process under the influence of S-EGR is critical in the PCC for NGCC power plants.

Previous studies on S-EGR [64],[80],[82], [90],[187] gravitate towards increasing the L/G to maintain a CO_2 capture efficiency of 90%. This study evaluates how the performance of the CO_2 capture process will fare while maintaining the same L/G across varying S-EGR ratios. These tests evaluate the impact of the liquid to gas ratio based on different lean loadings on the test cases highlighted as follows.

- Test A: Case 1:   Liquid-gas ratio of 1.1 at 0.271 lean loading

    Case 2:   Liquid-gas ratio of 1.1 at 0.231 lean loading

- Test B: Case 1:   Liquid-gas ratio of 2.1 at 0.271 lean loading

    Case 2:   Liquid-gas ratio of 2.1 at 0.231 lean loading

Results in all test cases is tabulated in table 6.6 and 6.7.

The CO_2 lean loadings of 0.271 (Case 1) and 0.231 (Case 2) were utilized against the L/G of 1.1 and 2.1 under the influence of S-EGR to assess the performance of the PACT plant as presented in Tables 6.6 and 6.7.

6.7.1 CO_2 CONCENTRATION UNDER THE INFLUENCE OF VARYING LEAN LOADINGS AT A FIXED L/G

As the L/G is kept constant against varying the CO_2 concentration and at fixed CO_2 lean loadings of 0.271 (Case 1) and 0.231 (Case 2), the rich and semi-rich loadings in Cases 1 and 2 were all observed to noticeably increase (see Fig. 6.18) and this is due to the influence of increasing the CO_2 partial pressure [65]. However, the curve was observed to begin to

flatten after about 6.0 vol% of CO_2, thus indicating that the solvent absorption capacity is beginning to waiver due to insufficient solvent inventory with increasing CO_2 concentration. This study has been established based on the process conditions utilized that inadequate inventory of the amine solvent to accommodate the increase in the CO_2 concentration in the flue gas does not yield to a reasonable boost in the rich loadings which is expected to ultimately reduce the SRD.
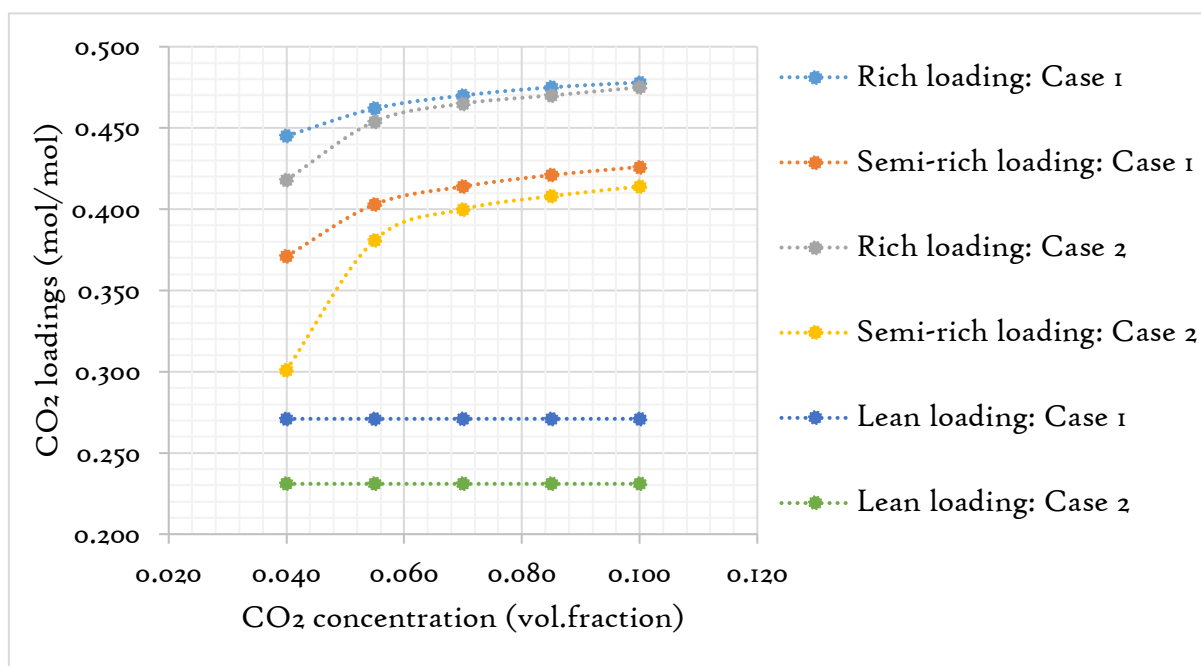
Fig. 6.18   The CO_2 loadings as a function of the CO_2 concentrations under L/G of 1.1 for Case 1 (0.271) and Case 2 (0.231).

Table 6.7   Test Case 1 and Case 2 with the L/G of 1.1.

Parameter	Unit	Case 1	Case 2	Case 1	Case 2	Case 1	Case 2	Case 1	Case 2	Case 1	Case 2
CO$_2$ conc.	vol%	0.04		0.055		0.07		0.085		0.1	
Lean loading	mol/mol	0.271	0.231	0.271	0.231	0.271	0.231	0.271	0.231	0.271	0.231
Rich loading_1	mol/mol	0.445	0.418	0.462	0.454	0.470	0.465	0.475	0.47	0.478	0.475
Rich loading_2	mol/mol	0.371	0.301	0.403	0.381	0.414	0.400	0.421	0.408	0.426	0.414
CO$_2$ capture eff_1	%	38.34	60.48	22.27	27.65	16.49	19.33	13.27	15.32	11.17	12.8
CO$_2$ capture eff_2	%	83.78	92.07	64.74	78.46	51.71	62.66	43.19	52.04	37.22	44.65
CO$_2$ capture eff_T	%	90	96.87	72.59	84.41	59.67	69.88	50.73	59.39	44.24	51.73
CO$_2$ captured	kg/hr	13.5	14.5	14.9	17.3	15.4	18.1	15.8	18.49	16.08	18.8
Solvent regeneration	%	39.0	45.0	42.00	50.00	43	51	43	51	44.00	52.00
L/G_1	kg/kg	1.1									
L/G_2	kg/kg	1.1	1.1	1.1	1.1	1.1	1.1	1.1	1.1	1.1	1.1
SRD	MJ/kg	4.33	5.63	4.07	5.00	3.97	4.85	3.90	4.78	3.86	4.72
CO$_2$ in fuel	kg/hr	15.0	15.0								
CO$_2$ in FG	kg/hr	15.0	15.0	20.48	20.48	25.85	25.85	31.14	31.14	36.3	36.3
CO$_2$ in TG	kg/hr	1.5	0.5	5.61	3.2	10.42	7.79	15.34	12.65	20.27	17.54
Solvent flow rate	kg/hr	270.31	270.91	270.31	269.14	270.0	268.7	269.77	268.49	269.6	268.31
FG flow rate	kg/hr	250									
PHW flow	kg/hr	5652									
PHW inlet T	°C	124.0									
PHW outlet T	°C	121.5	120.5	121.4	120.3	121.4	120.3	121.4	120.2	121.4	120.2

Table 6.8   Test Case 1 and Case 2 with L/G of 2.1.

CO_2 conc.	vol%	0.04		0.055		0.07		0.085		0.1	
Lean loading	mol/mol	0.271	0.231	0.271	0.231	0.271	0.231	0.271	0.231	0.271	0.231
Rich loading_1	mol/mol	0.369	0.33	0.405	0.367	0.434	0.403	0.449	0.432	0.456	0.447
Rich loading_2	mol/mol	0.278	0.233	0.308	0.245	0.356	0.285	0.382	0.340	0.394	0.37
CO_2 capture eff_1	%	90.24	96.13	69.52	88.07	44.03	67.01	31.05	43.01	24.75	30.82
CO_2 capture eff_2	%	74.61	64.55	88.92	86.83	86.46	92.82	76.21	89.86	66.4	80.77
CO_2 capture eff_T	%	97.52	98.63	96.62	98.43	92.42	97.63	83.59	94.22	74.71	86.69
CO_2 captured	kg/hr	14.6	14.81	19.8	20.15	23.9	25.24	26.03	29.34	27.15	31.51
Solvent regeneration	%	27.0	31	33.00	38	38	43	40	47	41.00	49
L/G_1	kg/kg	2.1									
L/G_2	kg/kg	2.1	2.1	2.0	2	2.0	2	2.0	2	2.1	2.0
SRD	MJ/kg	6.37	8.69	5.19	7.04	4.59	6.07	4.35	5.51	4.23	5.27
CO_2 in fuel	kg/hr	15.0									
CO_2 in FG	kg/hr	15.0	15.0	20.48	20.48	25.85	25.85	31.14	31.14	36.3	36.34
CO_2 in TG	kg/hr	0.4	0.21	0.69	0.32	1.96	0.61	5.11	1.8	9.19	4.84
Solvent flow rate	kg/hr	520.04	522.08	513.72	515.35	510.5	510.21	509.41	507.44	508.8	506.46
FG flow rate	kg/hr	250									
PHW flow	kg/hr	5652									
PHW inlet T	°C	124.0									
PHW outlet T	°C	120.0	118.5	119.6	117.9	119.3	117.5	119.2	117.1	119.1	116.9

When the L/G is increased by about 90% to 2.1, there appears to be a more significant rise in the rich and semi-rich loadings from 23.6 to 35.5% and 7.4 to 13.6%, respectively, as compared to when the L/G was kept at 1.1. This test has further underscored the prominence of increasing the L/G under the influence of S-EGR to increase the CO_2 loading of the lean solvent stream, this has the implication of reducing the solvent regeneration energy requirement of the CO_2 process, however, at the expense of the increased operating expenditure.
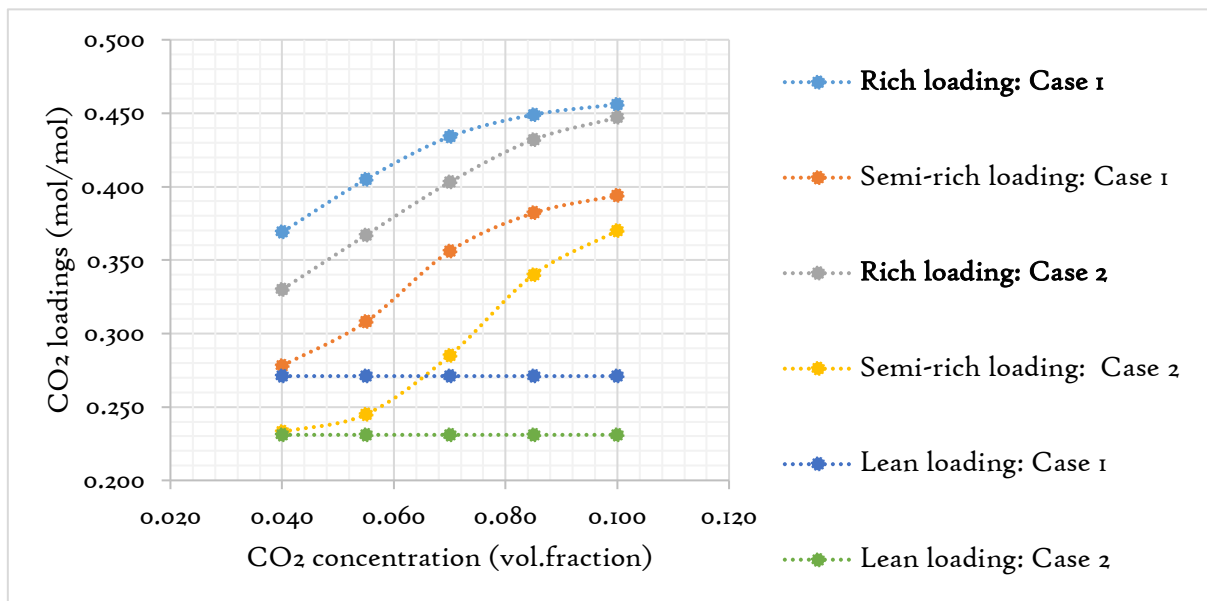
Fig. 6.19   The CO_2 loadings as a function of the CO_2 concentrations under L/G of 2.1 for the Case 1 (0.271) and Case 2 (0.231).

6.7.2   CARBON CAPTURE EFFICIENCY AS A FUNCTION OF THE CO_2 CONCENTRATION UNDER THE INFLUENCE OF VARYING LEAN LOADINGS AT A FIXED L/G

The CO_2 capture efficiency was observed to drastically decrease with increasing CO_2 concentration when the L/G was fixed at 1.1. This trend mirrors the behaviour of the lethargic rise in rich loadings with increasing CO_2 concentration in the flue gas when kept at a constant L/G (6.18). It can be stated, with confidence, that with a fixed L/G, the absorption capacity of the solvent diminishes, leading to a decrease in the CO_2 capture efficiency from 90 to 44% and 96.9 to 51.7% for the cases 1 and 2, respectively. Case 2 appears to overall have a higher CO_2 capture efficiency and this is because it has a lower lean loading. This means a better solvent absorption capacity.
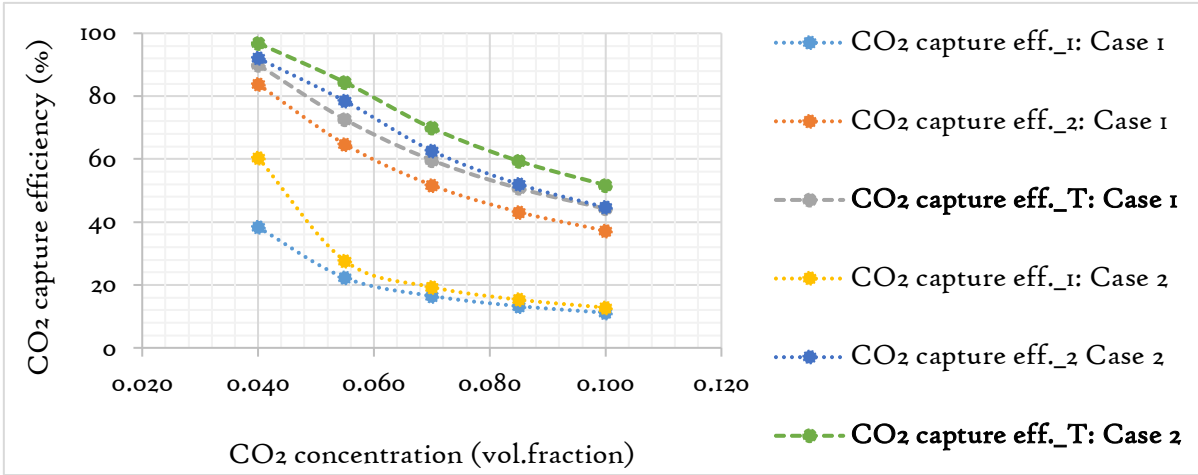
Fig. 6.20   The CO2 capture efficiency as a function of the CO2 concentrations under a L/G of 1.1 for Case 1 (0.271) and Case 2 (0.231).

The CO2 capture efficiency decreased in less than a dramatic manner when the L/G is increased to 2.1 as compared to 1.1 and this is due to the fact that there is a higher solvent inventory within the SCCP to absorb the CO2 with increasing the CO2 concentration. However, a peculiar behaviour was observed with the CO2 capture efficiencies in absorbers-2 for both test cases of different lean loading (see Fig. 6.21). This behaviour in the initial increase of the CO2 capture efficiency and decreasing in absorbers-2 can be postulated to be due to the boost in the CO2 capture due to the increase in the flow rate of the regenerated (lean) solvent to 2.1. After which it reaches saturation and starts to decline due to the inability of the CO2 saturated solvent to capture more CO2. This test further demonstrates that to keep the CO2 capture efficiency high under EGR or S-EGR, an increase in solvent inventory requirement is necessary.
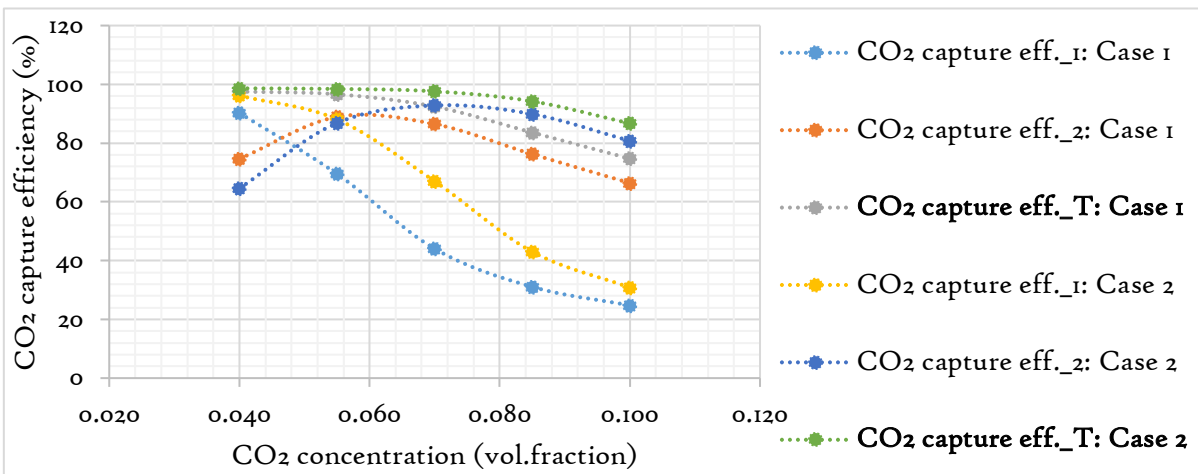
Fig. 6.21   The CO2 capture efficiency as a function of the CO2 concentrations under L/G of 2.1 for Case 1 (0.271) and Case 2 (0.231).

6.7.3 CAPTURE RECOVERY AND SOLVENT REGENERATION AS A FUNCTION OF THE CO_2 CONCENTRATION UNDER THE INFLUENCE OF VARYING LEAN LOADINGS AT A FIXED L/G

The CO_2 captured with increasing CO_2 concentration was observed to increase up to 5.5 vol% of CO_2 (see Fig. 6.22) before it starts to stagnate and marginally increase for Case 1, at this concentration, the solvent absorption capacity diminishes due to an insufficient solvent flow to accommodate for the increasing CO_2 concentration in the flue gas stream.
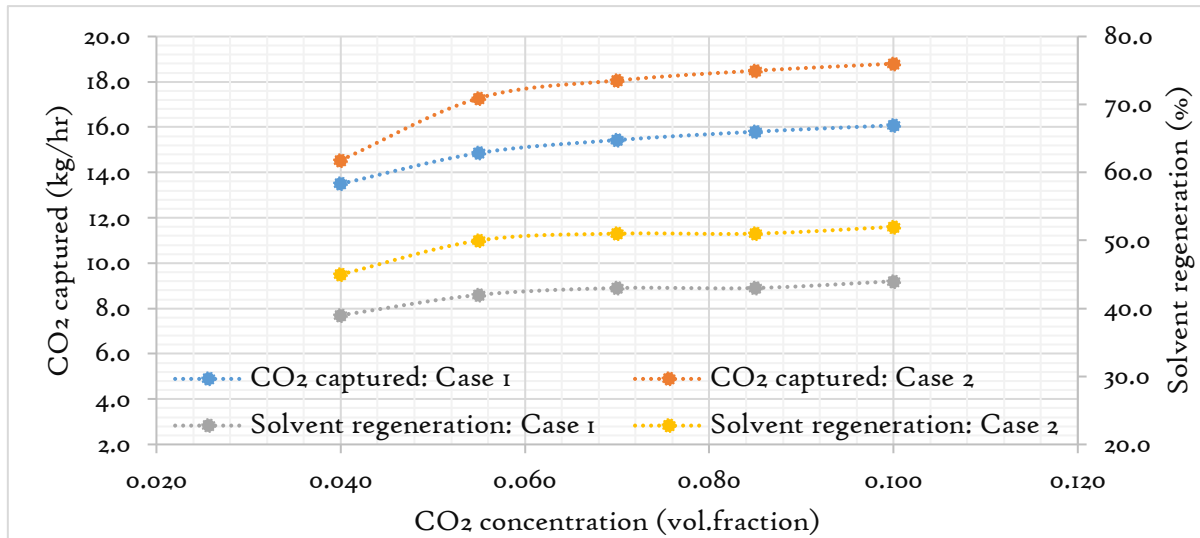
Fig. 6.22   The CO_2 capture rate as a function of the CO_2 concentrations under L/G of 1.1 for Case 1 (0.271) and Case 2 (0.231).

The degree of solvent regeneration was also observed to be relatively steady after 5.5 vol% of CO_2 because the rich loading after this concentration has also seized to appreciably increase and as a result, embarking on S-EGR with limited solvent flow to accommodate for the increase CO_2 concentration is not worth employing the CO_2 recirculation technique because it has little value in increasing the amount of CO_2 captured.

With increasing L/G to 2.1, the CO_2 captured was observed to appreciably increase for both test cases (see Fig. 6.23). Also the solvent regeneration was monitored to noticeably increase. This suggests that the introduction of more solvent with increasing CO_2 concentration at the absorber gas inlet translates to a higher absorption capacity of the solvent, which was also reflected in the amplified rich and semi-rich loading in Fig. 6.19, However, it should be bourne in mind that an increased solvent inventory increases the cost of the solvent management.
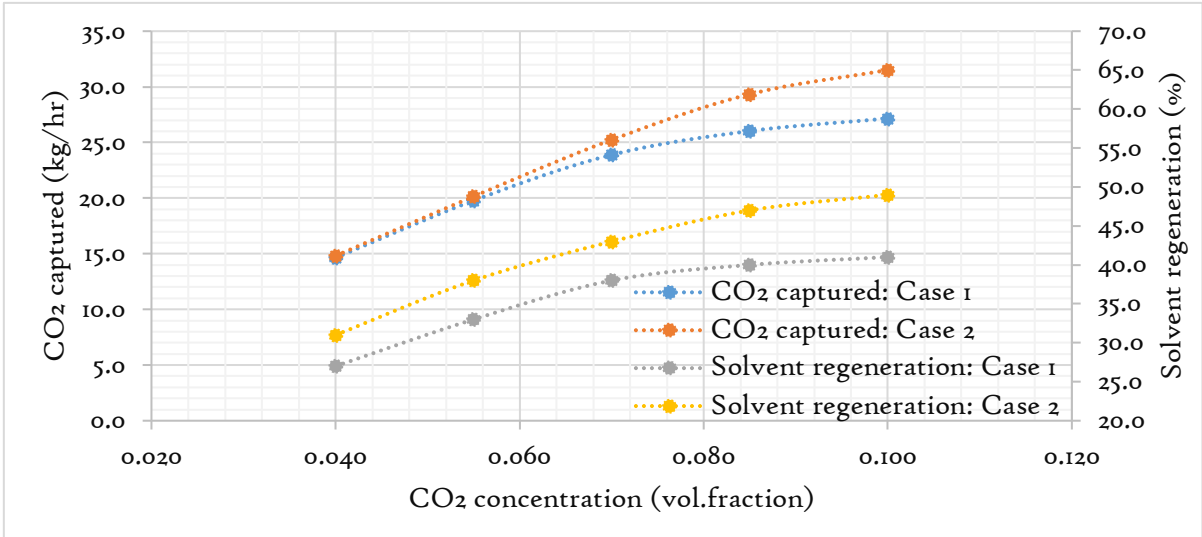
Fig. 6.23   The CO2 capture rate as a function of the CO2 concentrations under L/G of 2.1 for Case 1 (0.271) and Case 2 (0.231).

6.7.4 SRD AS A FUNCTION OF THE CO2 CONCENTRATION UNDER THE INFLUENCE OF VARYING LEAN LOADINGS AT A FIXED L/G

The thermal energy utilized to capture every unit weight of CO_2 in the flue gas has an influence on the CO_2 captured and the degree of solvent regenerated. Across all the test cases investigated, the solvent regeneration energy requirement decrease with increasing the CO_2 concentration [64],[65]. The test Case 1 (0.271) appears to be lower in SRD than in the test Case 2 (0.231). This is as a result of the direct implication of the higher loading which is manifested due to lower reboiler duty, thus lower the SRD as shown in Fig. 6.2 but as a consequence the CO_2 capture efficiency was lower.
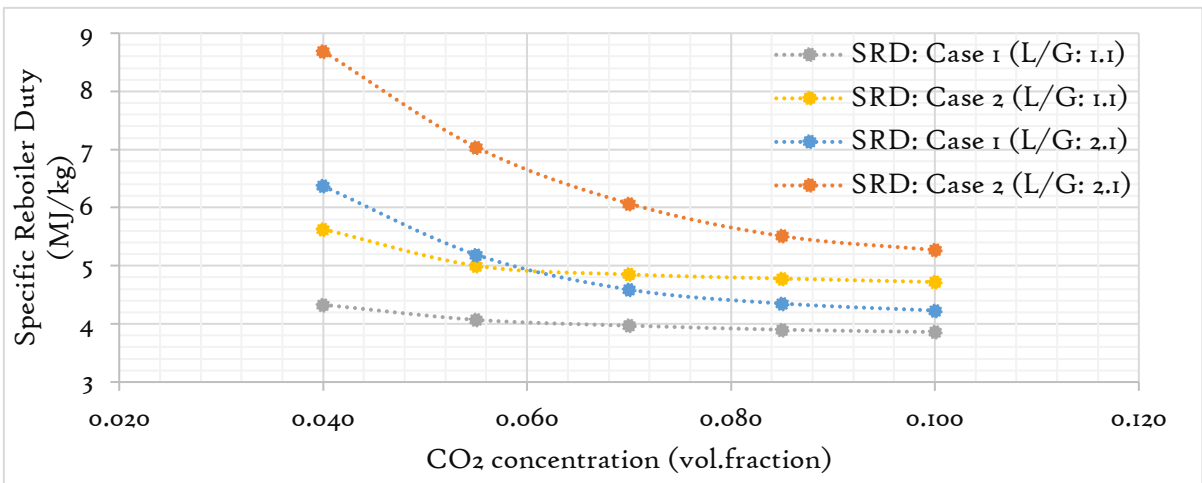
Fig. 6.24   The SRD as a function of the CO2 concentrations under L/G of 2.1 for case 1 (0.271) and Case 2 (0.231).

The lowest SRDs were observed to be 3.86 and 4.23 MJ/kg of CO_2 for Case 1 (L/G: 1.1) and Case 1 (L/G: 2.1). These tests demonstrate how higher lean loading is fundamental in generating lower SRDs, however, at the risk of compromising the CO_2 captured. A trade-off thus exists as a result, which is decided by the operator of the CO_2 capture process. To gain value in the CO_2 capture process with regards to the SRD, the lowest reboiler heat duty that yields the highest CO_2 captured is deemed to be the point of the optimization. This test has also established that a lower L/G is necessary for a lower SRD. The S-EGR, in order to attain a lower SRD is debunked according to Case 1 (L/G: 1.1) as the difference between the base case SRD and one at 10 vol% CO_2 (the lowest SRD) is 10.9%. This saving can be negated by the additional cost of the operating and capital expenditure of operating the S-EGR technology, especially at high CO_2 capture efficiency of the CO_2 selective membrane.

6.8 IS S-EGR WORTH IT ?

The key concept of Selective Exhaust Gas Recirculation (S-EGR) is to enhance the CO_2 concentration at the gas inlet of the absorber column via recycling of the CO_2 from the exhaust gas or CO_2 captured back to the turbine plant via the aid of Nano Materials Enhanced Membranes for the CO_2 capture (NANOMEMC[2]) to enhance CO_2 absorption [189],[190], see Section 2.52 and Figs 2.4 and 2.5. The test results in this section evaluate the worthiness of the S-EGR. Cases 1 and 2 refer to tests under CO_2 capture efficiency of the solvent-based CO_2 capture process and the CO_2 capture efficiency of the CO_2 in the fuel combustion gas, respectively. The process data is given in Table 6.8.

Table 6.9 Process data of the CO_2 capture process of 90% capture efficiency of the SCCP and that of the CO_2 content in the fuel combustion.

Parameters	Units	Case 1	Case 1	Case 2	Case 1	Case 2	Case 1	Case 2	Case 1	Case 2	Case 1	Case 2	Case 1	Case 2
CO_2 conc.	vol%	0.04	0.055		0.07		0.085		0.1		0.125		0.15	
Lean loading	mol/mol	0.231												
Rich loading_I	mol/mol	0.449	0.447	0.441	0.445	0.434	0.443	0.428	0.442	0.423	0.440	0.418	0.438	0.415
Rich loading_II	mol/mol	0.367	0.365	0.352	0.363	0.340	0.361	0.331	0.360	0.325	0.358	0.319	0.357	0.317
CO_2 capture eff_I	%	33.54	33.91	38.89	34.22	43.1	34.46	46.36	34.61	48.73	34.72	50.91	34.72	51.4
CO_2 capture eff_II	%	84.95	84.87	88.01	84.8	89.8	84.74	91.02	84.71	91.95	84.68	93.18	84.68	94.19
CO_2 capture eff_T	%	90	90	92.67	90	94.2	90	95.18	90	95.87	90	96.65	90	97.18
CO_2 captured	kg/hr	13.5	18.4	18.98	23.3	24.35	28.02	29.64	32.70	34.84	40.35	43.34	47.8	51.61
Solvent regn.	%	49.0	49.0	48	49	47.00	48	47	48.00	46	48.00	45.00	48.00	45.00
L/G_1	kg/kg	0.9	1.2	1.3	1.6	1.7	1.9	2.2	2.2	2.6	2.8	3.4	3.4	4.1
L/G_2	kg/kg	0.9	1.2	1.2	1.5	1.6	1.8	2.0	2.1	2.4	2.8	3.0	3.0	3.6
SRD	MJ/kg	5.05	5.15	5.25	5.22	5.43	5.30	5.59	5.37	5.73	5.46	5.90	5.54	6.01
CO_2 in fuel	kg/hr	15.0												
CO_2 in FG*	kg/hr	15.0	20.5	20.50	25.9	25.9	31.1	31.1	36.3	36.3	44.8	44.84	53.1	53.1
CO_2 in TG	kg/hr	1.5	2.05	1.5	2.59	1.5	3.11	1.5	3.63	1.5	4.48	1.5	5.31	1.5
Solvent flow rate	kg/hr	216.3	297	315	378.3	417.98	458.95	523.93	538.99	631.18	670.62	808.02	799.61	977.15
FG flow rate	kg/hr	250												
PHW flow	kg/hr	5652												
PHW inlet T	°C	124.0												
PHW outlet T	°C	121.0	120.0	119.8	118.8	118.8	117.7	116.9	116.5	115.5	114.6	113.1	112.7	110.8

CO_2 in FG*: CO_2 content in flue gas after CO_2 recirculation

Fig. 6.25 shows a background outlook of the simulation tests while considering:

- Case 1: Capture efficiencies of the CO_2 capture process

- Case 2: Capture efficiency of the CO_2 in the exhaust gas prior to CO_2 enhancement
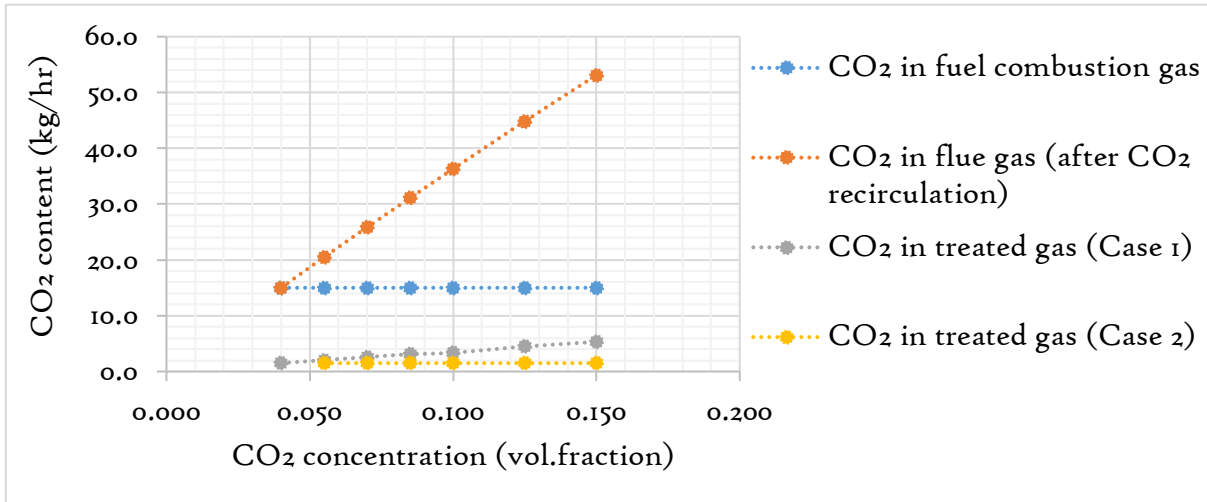
Fig. 6.25   A graphical representation of the CO_2 flow rate in the fuel combustion gas, gas at the absorber inlet and the treated gas streams with increasing CO_2 concentrations.

These tests were conducted while enhancing the CO_2 concentration at the inlet of the absorber column gas inlet of the CO_2 capture process with two-absorber columns from 4 vol% of CO_2 (Base case) to 15 vol% CO_2 as captioned in Table 6.8 and Fig. 6.25. As the CO_2 recycle ratio increases, the CO_2 at the inlet of the absorber column increases by 254% from 15.0 to 53.1 kg/hr across the increasing CO_2 concentration. This also increased the CO_2 emissions into the atmosphere by 254% after capture. The analysis in the next section will shed more light on the intricacies of the S-EGR in the Case 1 and Case 2.

6.8.1   IMPACT OF RICH LOADINGS AGAINST CO_2 CONCENTRATIONS IN CASES I & 2

Figure 6.26 shows a graphical representation of the CO_2 loadings in the Cases 1 and 2.

Case 1: Average rich loading in the absorber I and absorber II are 0.433 and 0.362 respectively across the varying CO_2 concentration. This signifies an increase in the rich loading in absorber I by 19.6%. Fresh solvent was first introduced into the absorber II and consequently most of the loading takes place in absorber II. Absorber I acts as a complimentary absorbing facility as mentioned earlier to enhance the CO_2 rich loading.
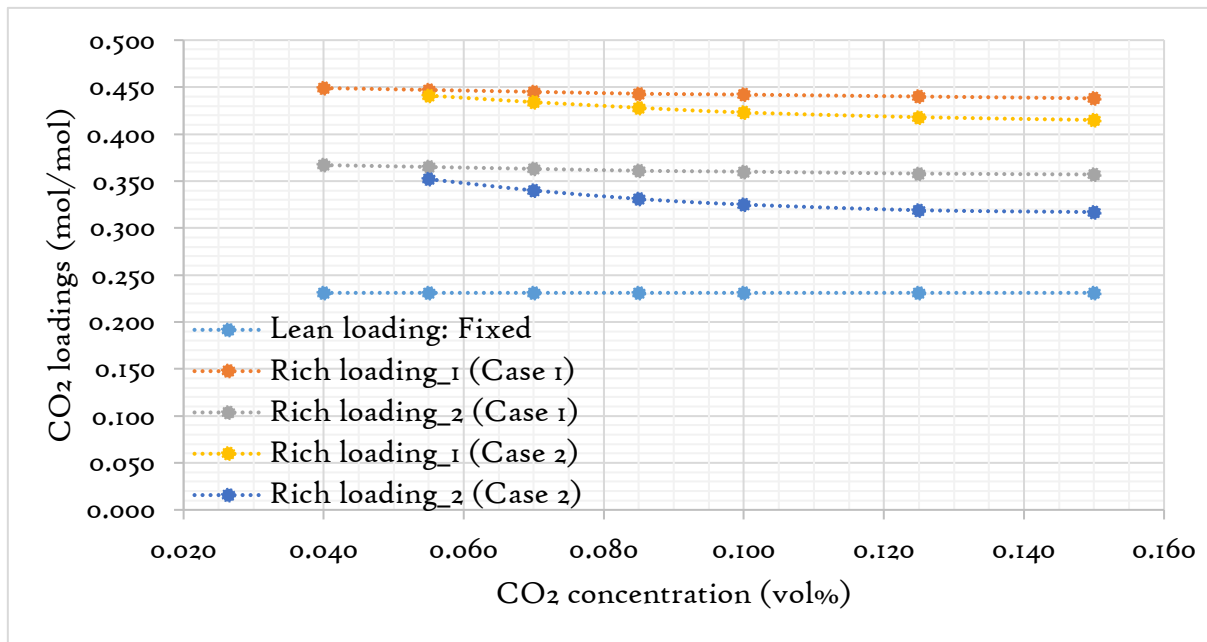
Fig 6.26 A graphical representation of the rich CO_2 loadings of the solvent on twin absorber reactors at a fixed lean loading of 0.231 and at capture efficiencies of the CO_2 capture plant (Case 1) and CO_2 content in the exhaust gas prior to CO_2 enhancement (Case 2).

Case 2: Average rich loadings in the absorbers 1 and 11 are 0.427 and 0.331, respectively, across varying CO_2 concentration, this signifies an increase in rich loading in absorber 1 by 29%. The same observational trend in case 1 holds for case 2.

The average rich loading in case 1 was observed to be higher than Case 2 and this is due to the lower increase in solvent flow rate in case 1 by 270% as compared to 352% in Case 2 across the CO_2 concentration increase by 275%. The yardstick used in suggesting higher rich loading leads to higher CO_2 capture and ultimately lower SRD under the influence of SRD does not hold in this test because the lean loading was kept constant across all the tests.

6.8.2   THE CO_2 CAPTURE RATE AND EFFICIENCY AS FUNCTION OF THE CO_2 CONCENTRATIONS FOR CASES 1 AND 2

Case 1: The average CO_2 capture efficiency in absorbers 1 and 11 are 34.3 and 84.8%, respectively, representing a significant difference in the capture efficiencies between the two columns. This is in line with the behaviour of rich loadings, where most of the loading takes place in absorber 11.

Case 2: The average CO_2 capture efficiency in absorbers 1 and 11 are 46.6 and 91.4% respectively. The same behaviour holds for Case 1.

The total capture efficiency in Case 2 was observed to be higher and this is due to the higher amount of solvent flow rate to capture 90% of the CO_2 in the flue gas prior to CO_2 enrichment. Presented in fig 6.27 is a behaviour of the capture efficiency for the two cases of CO_2 capture efficiencies.
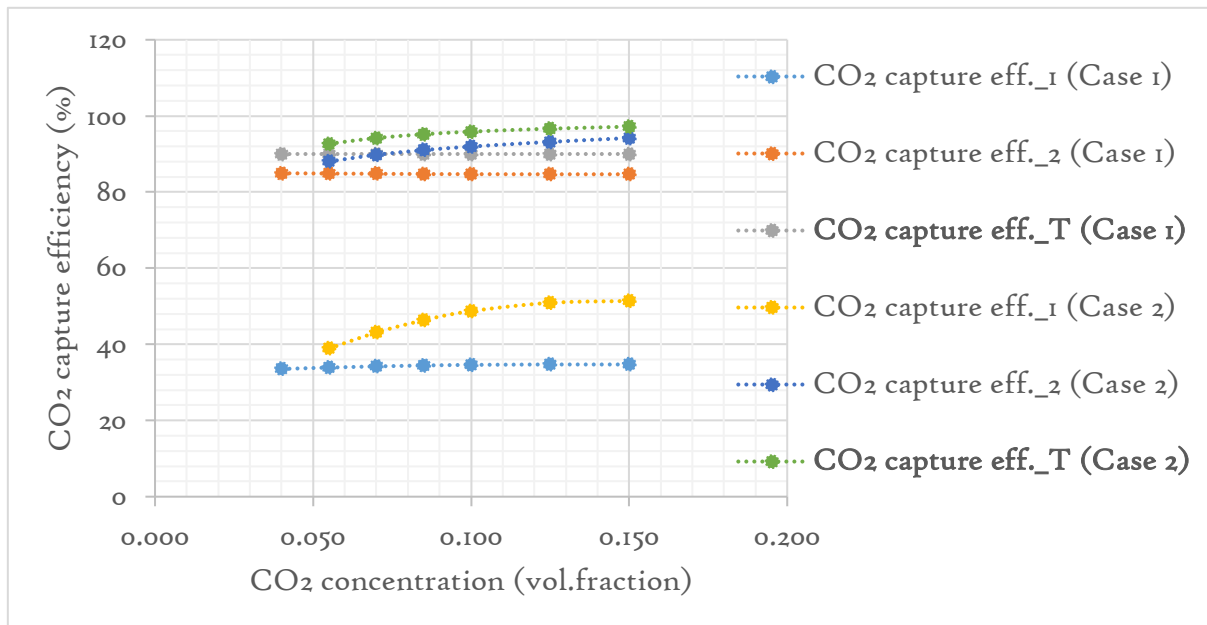
Fig 6.27   The CO_2 capture efficiencies in absorbers 1 and 2 under Case 1 and case 2.

As expected, the CO_2 captured follows the same behaviour as the capture efficiency and was observed to be higher in Case 2 than Case 1. The average CO_2 captured across the CO_2 concentrations was 6% higher in Case 2 than Case 1 and this is because the CO_2 content in the flue gas prior to recirculation was considered and as a consequence may translate to a higher SRD.

6.8.3   SRD AS A FUNCTION OF THE CO_2 CONCENTRATIONS FOR CASES 1 AND 2

More CO_2 was captured in Case 2, however, the SRD was observed to be higher under this condition due to the higher L/G, and more reboiler heat input was utilized to accommodate the higher solvent flow rate for CO_2 stripping in case 2. The increase in the CO_2 captured was not enough to offset the increase in the reboiler heat duty to translate into a lower SRD in Case 2. The difference between the SRD in Case 1 and Case 2 was also observed to

increase as the CO₂ concentration increases, this was due to the widening difference in the solvent flow rate in the two cases as the CO₂ concentration increases.
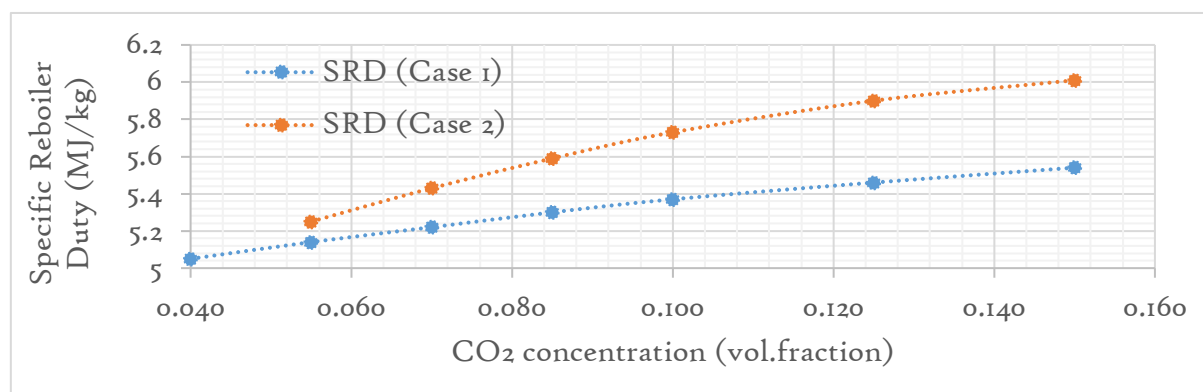
Fig 6.28   The SRD for Case 1 and Case 2 as a function of varying CO₂ concentration.

To wrap up this section, i.e. is S-EGR worth it? It is important to acknowledge that the more CO₂ is recycled to the gas turbine process in the S-EGR scheme, the more CO₂ is emitted into the atmosphere after the CO₂ capture process. However, previous studies on S-EGR have so far failed to mention this aspect [73],[74], [80],[187],[191]. Furthermore, the capture efficiency of the CO₂ capture process does not represent the CO₂ concentration of the CO₂ in the fuel combustion gas-stream because the capture efficiencies are often calculated based on the CO₂ at the inlet of the absorber gas inlet after the CO₂ recirculation [65],[90]. This study has established that the SRD substantially increases with increasing CO₂ recycle ratio when the actual concentration of the CO₂ in the gas combustion is considered.

6.9   KEY CHAPTER DEDUCTIONS

This study has validated the gCCS model based on published data of the PACT plant and employed for the CO₂ capture process optimizations.

- The gCCS has proven to accomplish the reproducibility of the published experimental data.
- Two absorber columns have an unrivalled advantage to reduce the SRD by as much as 20% as compared to a one-absorber plant.
- Two absorber columns in counter-current achieves energy savings as opposed to the split-stream flow configuration, but the latter has a better structural advantage of dynamic operation to load changes.

- The liquid-gas ratio and higher lean loading have been substantiated to be the key independent and dependent parameters, respectively, to achieve lower solvent regeneration energy requirements across a large range of operational conditions.

- The S-EGR based on the operating of the CO_2 capture process at low L/G and high lean loading does not achieve appreciable energy savings and it is not worth executing S-EGR under these conditions.

6.10   NOVEL CONTRIBUTION TO KNOWLEDGE

The novel contribution to knowledge from this simulation studies is as follows:

- Simulation investigation of the performance impact of two-absorber reactors, as against a CO_2 capture plant with one absorption reactor, operating over a wide spectrum of conditions that includes the lean, semi-rich and rich CO_2 loadings, L/G and degree of solvent regeneration. Furthermore, the influence of the CO_2 capture efficiencies of the CO_2 capture process as against that of the CO_2 concentration in the fuel combustion exhaust and the Specific Reboiler Duty (SRD) across varying CO_2 concentrations (mimicking S-EGR) using gCCS as the process modelling platform was also evaluated.

CHAPTER VI

CONCLUSION

BACKGROUND

Combusting fossil fuels to generate energy and its consequential CO_2 emission has been proven beyond reasonable doubt across a broad spectrum of climate scientists in a series of reports by the Intergovernmental Panel on Climate Change (IPCC), which reaffirms CO_2 as the prime driver of climate change. An idealized fossil-fuel free economy is thus required to address climate change; however, since it is not possible to abruptly cut off the lifeline of civilized society, i.e. electricity, without crashing the global economy, a transitional plan is necessary to switch over to cleaner forms of energy generation. Part of the transitional scenario is to create a closed loop approach in which the CO_2 destined to be expelled into the atmosphere is retrieved from large and stationery point combustion effluents and be returned back into the earth where it was initially been exploited. Clearly this how Carbon Capture and Storage was coined.

Investigative studies were undertaken to address some of the imperative challenges and knowledge gaps of PCC, and based on the results generated in the course of these studies, the general conclusions are as follows:

7.1   GENERAL CONCLUSIONS

- In spite of decades of innovative and breakthrough achievements in CCS, its future cannot be said to be without major challenges due to not technological prowess but political determination that will enable the policies to drive the deployment of CCS. This is essential since it is implausible to think that trillions worth of monetary values of energy source that lies beneath our feet will be forsaken (in at least half a century) from now for intermittent sources of energy.

- Increasing the S-EGR ratio with higher amine concentration has the benefit of increasing the performance of the absorber column via increasing the driving force of CO_2 absorption. As a result, decreasing the thermal regeneration energy per unit weight of CO_2 captured and accelerating the global deployment of PCC. The

modalities of S-EGR is however plant specific and optimization campaigns are required to evaluate the S-EGR ratio that gives the lowest reboiler duty.

- It is worth noting to mention that higher S-EGR ratio increases the operational expenditure of the PCC via increasing the solvent inventory especially if the CO_2 capture efficiency is to be maintained or capped at 90%. This is likely to increase the operational maintenance on auxiliary machineries and increase solvent reclamation management. A higher S-EGR ratio inevitably translates to higher rich loadings, which facilitates corrosion of the PCC plant's equipment. A trade-off scenario thus transpires with regards to shorter benefits of higher CO_2 capture, lower volatile emissions and lower reboiler duty or long-term drawbacks of higher capital expenditure.

- Oxidative degradation of the amine solvent is inevitable unless the oxygen content in the flue gas is restricted to limit the degradation process. This can potentially be achieved via EGR, S-EGR, supplementary firing or flue gas deoxygenation techniques.

- The Amine Capture Plant, equipped with two absorber columns, offers an outstanding advantage over one absorber with regards to operational and dynamic flexibility, higher CO_2 capture and lower SRD. Lean loadings and L/G have been determined to be two of the most influential factors affecting the performance of the CO_2 capture plant.

- Operation of a solvent-based CO_2 capture plant requires trade-offs and compromises in all its ramifications. The consequential result of operational and process conditions/modifications to concede over the others will ultimately depend on a cocktail of the power plant's operational, legislative, regulatory and environmental requirements.

Compartmentalized and more detailed conclusions based on the three major research trajectories are as follows:

7.2 INFERENCE ON VARYING CO₂ CONCENTRATIONS AGAINST 40 wt(%) MEA

The experimental campaigns were undertaken at the UKCCSRC-PACT facility in Sheffield, UK to evaluate the performance of the CO_2 capture process using 40 wt(%) MEA by

i. Varying the CO_2 concentrations (simulating S-EGR) with a cap of 90% CO_2 capture efficiency, and

ii. Varying the PHW temperatures at the reboiler (solvent regeneration unit) inlet.

In conclusion

- Increasing the partial pressure of the CO_2 in the flue gas of the gas turbines via increasing the CO2 concentrations under the influence of 40 wt(%) MEA increased the lean and rich CO2 loadings by 21.8 and 5.6 %, respectively. While the CO2 capture efficiency was kept at 90 %, the CO2 capture rate was increased by 80.5 %. The N-SRD was however, observed to behave in a non-linear form. N-SRD is advantageous only up to a certain CO_2 concentration of 6.6 vol(%) based on the process conditions and plant specifications used in this study. Above which the N-SRD begins to increase. A good indicator of the N-SRD trend was observed to be the ratio of solvent flow/CO_2 captured and the absorption capacity, which is lowest and highest respectively when the N-SRD is at its lowest value. Achieving a lower value of the N-SRD via S-EGR and at an elevated amine concentration however comes with the risks of potentially advancing solvent degradation and system corrosion, which consequently translates to increasing the OpEx and CapEx of the CO2 capture process. Higher CO_2 recycle ratios induces a thermal prominence in the absorber column and as a result, risks the possibility of reaching the solvent's flash point and consequently reducing the performance of the CO_2 capture. The temperature bulge was observed to be conspicuous at about the middle part of the absorber column during the steady state operation, indicating a region of exothermic CO2 absorption reaction. The bulge regions suggest a low absorption driving force and near equilibrium state between the liquid-gas phases with regards to the CO2 concentration. This also suggests low absorber performance at the top and bottom levels of the absorber column.

The PHW temperature has a profound effect on the performance of the PCC process and as a result, the lean loadings, rich loadings, CO_2 capture efficiency, CO_2 capture rate and degree of solvent regeneration all increased by 19.5, 9.9, 18.4, 16.7, and 52.2 %, respectively. This study has determined, based on the operating conditions used, that the N-SRD was lowest at a certain PHW temperature, i.e. 125 °C based on the plant's test process conditions utilized; below and above this identified temperature the N-SRD increases. The CO_2 capture absorption capacity increased in an almost linear manner with increasing the PHW temperature from 124 – 127 °C but despite this behaviour, the N-SRD was observed to increase above 125°C. Since previous studies have reported that the reboiler temperature above 130 °C accelerates the thermal degradation of the solvent, the PHW temperature above the thermal degradation threshold should only be utilized for flash CO_2 desorption in order to either promptly increase the CO_2 capture rate or lower the lean CO_2 loading.

- The MEA emission was observed to decrease by about 52 % across the increasing CO_2 concentrations. Higher solvent flow limits the emission of MEA from the absorber gas outlet as it induces a cooling effect at the top of the absorber reactor, thereby negating traces of MEA and associated volatile compounds to be carried out into the atmosphere, where it can degrade to form carcinogenic compounds in the form of Nitrosamines and Nitramines. However, higher liquid/gas leads to higher recurrent expenditure but lower cost of solvent treatment and replacement due to the lower solvent stress.

- The Fe concentration was observed to increase to about 70.7% in the course of the pilot-plant tests, thus underscoring the equipment corrosion as a major challenge in CO_2 capture plants.

7.2.1 RECOMMENDATIONS AND FUTURE WORK

In light of the results generated under the experimental campaign with increasing the CO_2 recycle ratio, the following investigations are recommended as part of the future work to

gain better insight into the intricacies of PCC, with the aim of ultimately accelerating the deployment of this low-carbon technology.

- An exhaustive absorber management study is required, e.g. absorber intercooling, lean stream split flow technique, flue gas compression & expansion and enhance liquid & gas distribution mechanisms to enhance the absorber performance especially under the influence of S-EGR.

- The CO_2 content of the exhaust flue gas is to be taken as a baseline to peg the CO_2 capture efficiency in the course of increasing the S-EGR ratios. As the CO_2 capture efficiency calculated, based on the CO_2 content in the flue gas after the S-EGR, is misleading because it measures the capture efficiency of the CO_2 capture process.

- An investigative study to evaluate the performance of dynamic operation of PCC under the influence of varying CO_2 recycle ratios.

- The utilization of Rotating Packed Beds (RPB) to evaluate its performance under higher S-EGR ratios.

- The employment of multiple live gaseous & liquid sampling techniques to minimize errors, especially in calculating the dependable performance parameters.

- The incorporation of the mGT's heat exchanger to further heat the rich solvent stream prior to the introduction into the stripper column to reduce the work done by the reboiler.

7.3   INFERENCE ON OXIDATIVE DEGRADATION OF MEA

The experimental campaigns were undertaken at the UKCCSRC-PACT facility in Sheffield, UK to investigate the oxidative degradation of 40 wt(%) MEA at 5 vol(%) CO_2 and 15 vol(%) O_2.

In conclusion

- The Fe concentration, which is a key indicator of solvent degradation, was increased approximately 10 times from 3.68 to 3.62 mg/l in the course of about 500 hours of running the PACT plant. The increase in the Fe content was reasonably synonymous with the discoloration of the amine solvent, which changed colour from macaroon peach to raisin black. The colour variation however will be dependent on the flue gas characteristics, plant specifics and process conditions. The

rate at which the amine coloration evolved relatively conforms to the rate of reaction of corrosion which was about 1 (mg/l)/hr.

- The NH3 emission, which is a primary degradation product, increased by about 200 % from 18 to 58 ppm within the period of the experimental campaign.

- The N-SRD was not observed to appreciably increase in the course of the study, suggesting that the amine has not reached its breaking point in the course of about 500 hours of pilot-scale experimental campaign.

- The peaks in the Dissolved Oxygen (DO) of about 1.25 mg/l was observed about 10 minutes after about 100 mm of water-wash was transferred from the water-wash column to the absorber 1 sump of 0.3 diameter. This phenomenon could very well allude to the facilitating influence of the water-wash transfer to the PCC plant on the oxidative degradation of the amine solvent. Solvent density was also observed to coincide with the peaking of the DO, which reduced by 10 kg/m^3, further indicating the expediting inducement of the water-wash transfer on the solvent density and likely to the performance of the PCC.

7.3.1 RECOMMENDATIONS AND FUTURE WORK

Taking into account the results generated under the experimental campaign to study the oxidative degradation of 40 wt(%) MEA at 5 vol(%) O2 and 15 vol(%) O2, recommendations and future work are as follows:

- Further investigation, which is beyond the scope of this study, is required for de-oxygenation techniques of the flue-gas to counteract the facilitating stimulus of oxidative degradation of the amine solvent.

- The investigation into the long-term effect of corrosion inhibitors on the performance of the CO2 capture process is required to gain a deeper insight into the role and dependency of such inhibitors for the advancement of the PCC.

- A study into how the emission of NH3 (a primary oxidative degradation product) can be restricted based on keeping the temperature of the solvent well away from its flash point, higher rich CO2 loading and higher liquid-gas ratio as all these process modifications limits the solubility of O2 in the solvent.

- The fitting of stainless steel as the internal framework of the CO_2 capture plant to evaluate the placidity of the corrosion as against carbon steel.

- A study of the photometry characteristics of the solvent as the solvent degrades. This information can be employed as a gauge and or scale to infer on the degree of the solvent degradation.

- The fitting of Dissolved Oxygen (DO) sensors upstream, downstream before and after of the wash-transfer mechanism of the absorber columns, to exhaustively study the location of DO build-up and independent process conditions that affect DO surge or peaking.

- Investigative study into how EGR, S-EGR, Dissolved Oxygen Removal technique and supplementary firing restricts oxidative degradation of amine solvent.

7.4   INFERENCE ON PROCESS SIMULATION OF THE PCC

The process simulation was undertaken with the gCCS 'version 1.1.0' General Process Modeling Platform (gPROMS) of Process System Enterprise's (PSE) to validate a published experimental campaign at the PACT plant [64] and run a number of process optimization studies towards achieving lower solvent regeneration energy per unit weight of CO_2 captured.

In conclusion

- The generated results from the model validation study with gCCS has demonstrated that the process simulation platform is able to reasonably replicate pilot-scale experimental data and thus gives the confidence to run the model offline.

- The fitting of the CO_2 capture plant with an additional absorber gives unparalleled advantage in reducing the solvent regeneration energy requirement of the PCC by as much as 20%, although at the expense of increased overnight expenditure. This study has also established that the configuration of two absorber columns in a counter-current format achieves lower energy savings than the split-flow configuration; however, it is worth noting that the split-flow configuration gives better operational flexibility when one absorber is to be taken offline for maintenance then a lower CO_2 capture efficiency is required.

- The liquid-gas ratio and lean loadings have been determined to be prime factors that affect the performance of the PCC.

- Implementing S-EGR based on the operating of the PCC system at lower L/G and higher lean loading does not yield noteworthy energy savings and as a result, not worth executing S-EGR under these conditions.

7.4.1 RECOMMENDATIONS AND FUTURE WORK

In light of the process simulation studies with gCCS (v. 1.1.0) on running a broad spectrum of operational and process conditions of the PCC, recommendations and future work are hereby provided as follows:

- The General Process Modeling Platform (gPROMS) of Process System Enterprise's (PSE) should be able to incorporate the chemical kinetics of the oxidative & thermal degradation and metal corrosion within their suite of simulation models. This will enable validation of the models against experimental data. Furthermore, this will empower process engineers to study an array of process and operational conditions that restricts solvent degradation and metal corrosion.

- The solvent reclamation unit systems are also required to be provided within the gPROMS to enable investigative studies of 'infiltrating a percentage of the degrading solvent for treatment and returning the reclaimed solvent back into the system' on the performance of the CO_2 capture system.

- The provision of an absorption and a stripping liquid and gas entry ports at different levels on the column models should also be incorporated to enable engineers run column management and optimizations processes, e.g. solvent split flows and absorber inter-cooling. This structural and operational advancement will enable enhanced column optimizations to ultimately reduce the specific Reboiler Duty of the PCC process.

- The dynamic and intermittent operation of the gPROMS CO_2 absorption models is essential to appropriately model the PCC systems based on varying the liquid-gas ratio and steam or PHW provision in order to gain an advanced insight on how varying the dynamic operations may impact on the performance of the CO_2 capture process. This information will enable operators to make informative decisions to the cocktail of operational conditions to employ under specific circumstances.

7.5 NOVEL CONTRIBUTION TO ORIGINAL KNOWLEDGE

The novel contribution to knowledge in the course of this research endeavour are as follows:

- The influence of the increasing CO_2 recycle ratios (simulating S-EGR) with 40wt(%) of MEA on the performance of the solvent-based CO_2 capture process with the primary aim of decreasing the high energetic operating cost. The performance indices of the pilot-scale SCCP evaluated include the SRD, CO_2 capture efficiency and capture rate, CO_2 loadings, degree of solvent regenerations, amine emission, Fe corrosion, absorber and stripper behaviours.

- Investigation into oxidative degradation of 40 wt(%) MEA under the influence of synthesized natural gas combustion flue gas at a pilot-scale CO_2 capture plant. This study determined the accumulation of the metal content, NH_3 emissions and the possible role of the water-wash transfer on the dynamics of Dissolved Oxygen (DO) peaking and solvent density. This study has also revealed that under 500 hours of CO_2 capture operation under the test specifications employed does not subject the MEA to a breaking point in such a manner as to significantly affect the NSRD or the CO_2 recovery rate.

- Simulation investigation of the performance impact of two-absorber reactors, as against a CO_2 capture plant with one absorption reactor, operating over a broad spectrum of process conditions that includes the lean, semi-rich and rich CO_2 loadings, L/G and degree of solvent regeneration. Furthermore, the influence of the CO_2 capture efficiencies of the CO_2 capture process as against that of the CO_2 concentration in the fuel combustion exhaust and the Specific Reboiler Duty (SRD) across varying CO_2 concentrations using gCCS as the process modelling platform was also evaluated.

7.6 CLOSING STATEMENT

Engineering the CO_2 capture system to gain benefits across a broad spectrum of key dependable parameters e.g. the N-SRD, CO_2 recovery rate, degree of solvent

regeneration or lower solvent degradation via operational and process optimizations necessitates inexorable trade-offs in the performance of one dependable parameter over another. Utilizing 40 wt(%) of MEA has a significant advantage to enhance CO_2 recovery rate and ultimately reduce the solvent regeneration energy requirement of the CO_2 capture process for the same process conditions utilized for the benchmark 30 wt(%) MEA. This benefit is further achieved via EGR/S-EGR. As a consequence, utilizing 40 wt(%) MEA offers the potential of reducing the OpEx of the CO_2 capture plant. However, these benefits come at the detriment of increasing corrosion of the internal components of the plant (in the long term) with increasing solvent concentration which not only advance degradation of the solvent but ultimately increases the CapEx of the capture facility.

In a nutshell, the dynamics of the OpEx and CapEx of the SCCP are not reciprocal.

REFERENCES

[1]   Z. Hausfather, "Analysis: Why scientists think 100% of global warming is due to humans," *Carbon Brief*, 2017. [Online]. Available: https://www.carbonbrief.org/analysis-why-scientists-think-100-of-global-warming-is-due-to-humans. [Accessed: 25-Nov-2019].

[2]   International Energy Agency, "CO2 emissions from fuel combustion," *IEA Statistics*, 2019. [Online]. Available: https://webstore.iea.org/download/direct/2521?fileName=CO2_Emissions_from_Fuel_Combustion_2019_Highlights.pdf. [Accessed: 25-Nov-2019].

[3]   The Shift Project Data Portal, "Breakdown of electrcity generation by energy source," 2015. [Online]. Available: http://www.tsp-data-portal.org/Breakdown-of-Electricity-Generation-by-Energy-Source#tspQvChart. [Accessed: 20-May-2017].

[4]   Institute for Energy Research, "Fossil Fuels," 2017. [Online]. Available: http://instituteforenergyresearch.org/topics/encyclopedia/fossil-fuels/. [Accessed: 09-Aug-2017].

[5]   Atmospheric Chemistry and Physics, "Combustion chemistry and air quality standards," 2006. [Online]. Available: https://ocw.mit.edu/courses/chemical-engineering/10-571j-atmospheric-physics-and-chemistry-spring-2006/assignments/psn_1.pdf. [Accessed: 09-Aug-2017].

[6]   Lenntech, "History of the greenhouse effect and global warming," 2017. [Online]. Available: http://www.lenntech.com/greenhouse-effect/global-warming-history.htm. [Accessed: 29-May-2017].

[7]   C. Central, "Keeling Curve," 2017. [Online]. Available: http://www.climatecentral.org/gallery/graphics/keeling_curve. [Accessed: 29-May-2017].

[8]   United Nations Frame Work Convention on Climate Change, "Kyoto Protocol," 2014. [Online]. Available: http://unfccc.int/kyoto_protocol/items/2830.php. [Accessed: 29-May-2017].

[9]   United States Environmental Protection Agency, "Understanding Global

Warming Potentials," 2017. [Online]. Available:
https://www.epa.gov/ghgemissions/understanding-global-warming-potentials.
[Accessed: 29-May-2017].

[10]   United States Environmental Protection Agency, "Climate Indicators: Climate
       Forcing," 2016. [Online]. Available: https://www.epa.gov/climate-
       indicators/climate-change-indicators-climate-forcing. [Accessed: 29-May-2017].

[11]   Carbon Offset Research and Education, "Radiative forcing," 2011. [Online].
       Available: http://www.co2offsetresearch.org/aviation/RF.html. [Accessed: 09-
       Aug-2017].

[12]   International Panel on Climate Change, "Radioactive Forcing of Climate Change."
       [Online]. Available: https://www.ipcc.ch/ipccreports/tar/wg1/pdf/TAR-06.PDF.
       [Accessed: 09-Aug-2017].

[13]   U. S. E. P. Agency, "Global Greenhouse Gas Emissions Data," 2017. [Online].
       Available: https://www.epa.gov/ghgemissions/global-greenhouse-gas-emissions-
       data. [Accessed: 29-May-2017].

[14]   I. panel on climate Change, "Sixth assessment report cycle," 2017. [Online].
       Available: https://www.ipcc.ch/index.htm. [Accessed: 29-May-2017].

[15]   P. T. Zhiwu Liang, Kaiyun Fu, Raphael Idem, "Review on current advances, future
       challenges and consideration issues for post-combustion CO_2 capture using amine-
       based absorbents," *Chinese J. Chem. Eng.*, vol. 24, no. 2, pp. 278–288, 2016.

[16]   EIA, "The greenhouse effect," *Phys. Teach.*, vol. 21, no. 3, p. 194, 1983.

[17]   U. S. E. P. Agency, "climate-change-basic-information @ www.epa.gov." United
       States Environmental Protection Agency.

[18]   NASA, "NASA: Climate Change and Global Warming," *NASA Official Web Site*.

[19]   U. N. F. C. on C. Change, "The Paris Agreement." United Nations Framework
       Convention on Climate Change, 2014.

[20]   Hannah Ritchie and Max Roser, "CO_2 and Greenhouse Gas Emissions," *Our
       World in Data*, 2018. [Online]. Available: https://ourworldindata.org/co2-and-
       other-greenhouse-gas-emissions. [Accessed: 11-Dec-2019].

[21]   M. R. and E. Ortiz-Ospina, "World Population Growth." OurWorldInData.org, 2016.

[22]   L. Population, "Projection of population growth of the world (2035)," 2017. [Online]. Available: http://www.livepopulation.com/population-projections/world-2035.html. [Accessed: 24-Mar-2017].

[23]   B. Petroleum, "BP Energy Outlook 2035 shows global energy demand growth slowing, despite increases driven by emerging economies, Energy Outlook 2035." 2014.

[24]   I. E. Agency, "IEA Energy Atlas," 2017. [Online]. Available: http://energyatlas.iea.org/?utm_content=buffer6b947&utm_medium=social&utm_source=linkedin.com&utm_campaign=buffer#!/tellmap/-1118783123/0. [Accessed: 20-Apr-2017].

[25]   Internation Energy Agency, "Energy Technology Perspectives," *Iea*, p. 14, 2015.

[26]   International Energy Agency (IEA), "World Energy Outlook 2016," 2016.

[27]   International Energy Agency, *Energy Technology Perspectives: Scenarios & Strategies To 2050*. 2010.

[28]   T. Probert, "Millicent Media," *Millicent Media*, Mar-2012.

[29]   E. and I. S. Emma Owens, Department for Business, "Powering past coal alliance," 2018. [Online]. Available: https://ukccsrc.ac.uk/sites/default/files/documents/event/emma-owens-Powering Past Coal Alliance(PPCA)(1).pdf. [Accessed: 16-Apr-2018].

[30]   I. E. Agency, "IEA finds CO2 emissions flat for third straight year even as global economy grew in 2016," 2017. [Online]. Available: http://www.iea.org/newsroom/news/2017/march/iea-finds-co2-emissions-flat-for-third-straight-year-even-as-global-economy-grew.html?utm_content=buffera4740&utm_medium=social&utm_source=linkedin.com&utm_campaign=buffer. [Accessed: 24-Mar-2017].

[31]   E. & I. S. Department for Business, "Updated Energy and Emissions projections 2016," 2017. [Online]. Available:

https://www.gov.uk/government/uploads/system/uploads/attachment_data/file/599539/Updated_energy_and_emissions_projections_2016.pdf. [Accessed: 18-Apr-2017].

[32]   S. Emmott, "10 billion," 2017. [Online]. Available: https://www.sky.com/watch/title/programme/146d6cb5-ff03-49be-9987-ee7709859e9c. [Accessed: 16-Apr-2018].

[33]   S. Pacala, "Stabilization Wedges: Solving the Climate Problem for the Next 50 Years with Current Technologies," *Science (80-.).*, vol. 305, no. 5686, pp. 968–972, 2004.

[34]   B. Page, "the Global Status of Ccs | 2016 'Time To Accelerate,'" 2016. [Online]. Available: http://hub.globalccsinstitute.com/sites/default/files/publications/201158/global-status-ccs-2016-summary-report.pdf. [Accessed: 11-Jan-2017].

[35]   UKCCSRC, "cross-cutting-issues @ ukccsrc.ac.uk." 2016.

[36]   Global CCS Institute, "The global status of CCS." pp. 1–12, 2015.

[37]   Global CCS Institute, "Capture | Global Carbon Capture and Storage Institute." .

[38]   Global CCS Institute, "The global status of CCS," 2018. [Online]. Available: https://indd.adobe.com/view/2dab1be7-edd0-447d-b020-06242ea2cf3b. [Accessed: 12-Nov-2019].

[39]   M. P. Maria Elena Diego, Jean-Michel Bellas, "Process analysis of selective exhaust gas recirculation for CO_2 capture in natural gas combined cycle power plants using amines," in *Proceedings of ASME turbo Expo 2017*, 2017.

[40]   M. Akram, L. Ls, and S. Blakey, "Influence of Gas Turbine Exhaust CO_2 concentration on the performance of post combustion carbon capture plant," pp. 2–10, 2017.

[41]   M. M. M.-V. Dennis Y.C. Leung, Giorgio Caramanna, "An overview of current status of carbon dioxide capture and storage technologies," *Renew. Sustain. Energy Rev.*, vol. 426–443, p. 428, 2014.

[42]   J. Davidson, "Performance and costs of power plants with capture and storage of

CO2." Elsevier, 2007.

[43] M. Wang, A. Lawal, P. Stephenson, J. Sidders, and C. Ramshaw, "Post-combustion CO2 capture with chemical absorption: A state-of-the-art review," *Chem. Eng. Res. Des.*, vol. 89, no. 9, pp. 1609–1624, 2011.

[44] Y. T. Ligang Zheng, "Overview of Oxy-fuel Combustion Technology for CO2 Capture," *Cornerstone: Official journal of the world coal industry*. [Online]. Available: http://cornerstonemag.net/overview-of-oxy-fuel-combustion-technology-for-co2-capture/. [Accessed: 11-Jan-2017].

[45] Y. Liu *et al.*, *Carbon dioxide capture by functionalized solid amine sorbents with simulated flue gas conditions*, vol. 45, no. 13. 2011.

[46] C. B. Mohamed Kanniche, Rene Gros-Bonnivard, Philippe Jaud, Jose Valle-Marcos, Jean-Marc Amann, "Pre-Combustion, Post-Combustion and oxy-combustion in thermal power plant for CO2 capture," *Appl. Therm. Eng.*, vol. 30, pp. 53–62, 2010.

[47] U. D. of Energy, "Pre-Combustion Carbon Capture Research," *Precombustion carbon capture research*. [Online]. Available: https://energy.gov/fe/science-innovation/carbon-capture-and-storage-research/carbon-capture-rd/pre-combustion-carbon. [Accessed: 10-Jan-2017].

[48] D. Jansen, M. Gazzani, G. Manzolini, E. van Dijk, and M. Carbo, "Pre-combustion CO2 capture," *Int. J. Greenh. Gas Control*, vol. 40, pp. 167–187, Sep. 2015.

[49] Wikipedia, "Oxyfuel combustion process," 2017. [Online]. Available: https://en.wikipedia.org/wiki/Oxy-fuel_combustion_process. [Accessed: 09-May-2017].

[50] National Energy Technology Laboratory, "Oxy-Combustion." [Online]. Available: https://www.netl.doe.gov/research/coal/energy-systems/advanced-combustion/oxy-combustion. [Accessed: 11-Jan-2017].

[51] B. H. Engineering, "Oxy fuel combustion for CO2 capture," 2016. [Online]. Available: http://www.brighthubengineering.com/power-plants/39088-oxy-fuel-combustion-for-co2-capture/. [Accessed: 27-Jul-2017].

[52] V. P. I. P. Koronaki, L. Prentza, "Modeling of CO_2 capture via chemical absorption processes - An extensive literature review," *Renew. Sustain. Energy Rev.*, no. 50, pp. 547–566, 2015.

[53] Process System Enterprise Ltd, "gCCS overview." [Online]. Available: https://www.psenterprise.com/products/gccs. [Accessed: 15-Jan-2017].

[54] Energy Technologies Toolkit, "CCS Systems Modelling Tool-Kit," 2019. [Online]. Available: https://www.eti.co.uk/programmes/carbon-capture-storage/ccs-systems-modelling-tool-kit. [Accessed: 05-Oct-2019].

[55] G. G. Brend Smit, Ah-hyung Alissa Park, "The grand challenges in carbon capture, utilization and storage," *Frontiers in Energy Research*, 2014. .

[56] J. G. Jose I. Huertas, Martin D. Gomez, Nicholas Giraldo, "CO_2 Absorbing Capacity of MEA," 2015. [Online]. Available: https://www.hindawi.com/journals/jchem/2015/965015/. [Accessed: 24-Oct-2018].

[57] F. R. Arthur Kohl, *Gas Purification*, 3rd ed. Houston, Texas: Gulf Publishing Company, 1979.

[58] R. R. Bottoms, "Process for separating acidic gases," 1783901, 1930.

[59] M. Abian, M. Cebrian, A. Millera, R. Bilbao, and M. U. Alzueta, "CS_2 and COS conversion under different combustion conditions," *Combust. Flame*, vol. 162, no. 5, pp. 2119–2127, 2015.

[60] J. Gale, "CCS Now and the Challenge Ahead Post COP21," in *IEA Greenhouse Gas R&D Programme*, 2017.

[61] F. Rezazadeh, "Optimal Integration of Post-Combustion CO_2 Capture Process with Natural Gas Fired Combined Cycle Power Plants," University of Leeds, 2016.

[62] A. B. Rao, "A technical, economic and environmental assessment of Amine-based CO_2 capture technology for power plant Greenhouse Gas Control," Pittsburgh, 2002.

[63] F. Rezazadeh, "Optimal Integration of Post-Combustion CO 2 Capture Process with Natural Gas Fired Combined Cycle Power Plants Fatemeh Rezazadeh Submitted in accordance with the requirements for the degree of Doctor of

Philosophy The University of Leeds School of Chemica," no. September, 2016.

[64] M. Akram, U. Ali, T. Best, S. Blakey, K. N. Finney, and M. Pourkashanian, "Performance evaluation of PACT Pilot-plant for CO_2 capture from gas turbines with Exhaust Gas Recycle," *Int. J. Greenh. Gas Control*, vol. 47, pp. 137–150, 2016.

[65] R. Notz, H. P. Mangalapally, and H. Hasse, "Post combustion CO_2 capture by reactive absorption: Pilot plant description and results of systematic studies with MEA," *Int. J. Greenh. Gas Control*, vol. 6, pp. 84–112, 2012.

[66] E. O. Agbonghae, K. J. Hughes, D. B. Ingham, L. Ma, and M. Pourkashanian, "Optimal process design of commercial-scale amine-based CO_2 capture plants," *Ind. Eng. Chem. Res.*, vol. 53, no. 38, pp. 14815–14829, 2014.

[67] M. Wang, A. S. Joel, C. Ramshaw, D. Eimer, and N. M. Musa, "Process intensification for post-combustion CO_2 capture with chemical absorption: A critical review," *Appl. Energy*, vol. 158, pp. 275–291, 2015.

[68] Roberto Figueiredo, "De-Oxygenation as counter-measure for the reduction of oxidative degradation of CO_2 capture solvents," 2018. [Online]. Available: https://www.sintef.no/globalassets/project/tccs-10/dokumenter/a5/tccs-deoxygenation.pptx.pdf. [Accessed: 14-Nov-2019].

[69] M. P. Maria Elena Diego, Karen N. Finney, "The sustainable Option of Power from Fossil Fuels with Carbon Capture and Storage: An Overview of State-of-the Art Technology," in *Sustainable Energy Technology and Policies*, D. A. M. Sudipta De, Santanu Bandyopadhyay, Mohsen Assadi, Ed. Singapore: Springer, 2018, pp. 195–229.

[70] G. C. Bingtao Zhao, Wenwen Tao, Mei Zhong, Yaxin Su, "Process, performance and modeling of CO_2 capture by chemical absorption using high gravity: A review," *Renew. Sustain. Energy Rev.*, vol. Volume 65, 2016.

[71] "CO_2 Solutions rotating packed bed pilot results," *Carbon Capture J.*, 2017.

[72] M. P. Peng Xie, Xuesong Lu, Xin Yang, Derek Ingham, Lina Ma, "Characteristics of liquid flow in a rotating packed bed for CO_2 capture: A CFD analysis," *Chem. Eng. Sci.*, vol. Vol. 172, 2017.

[73]   Palomino Laura Herraiz, "Selective Exhaust Gas Recirculation in Combined Cycle Gas Turbine Power Plants with Post-combustion Carbon Capture," University of Edinburgh, 2016.

[74]   T. C. Merkel, X. Wei, Z. He, L. S. White, J. G. Wijmans, and R. W. Baker, "Selective Exhaust Gas Recycle with Membranes for CO 2 Capture from Natural Gas Combined Cycle Power Plants," *Ind. Eng. Chem. Res.*, vol. 52, pp. 1150–1159, 2013.

[75]   H. Li, G. Haugen, M. Ditaranto, D. Berstad, and K. Jordal, "Impacts of exhaust gas recirculation (EGR) on the natural gas combined cycle integrated with chemical absorption CO_2 capture technology," *Energy Procedia*, vol. 4, pp. 1411–1418, 2011.

[76]   U. Ali *et al.*, "Process simulation and thermodynamic analysis of a micro turbine with post-combustion CO_2 capture and exhaust gas recirculation," *Energy Procedia*, vol. 63, no. 44, pp. 986–996, 2014.

[77]   M. P. M. Akram, S. Blakey, "Influence of gas turbine exhaust CO_2 concentration on the performance of post combustion carbon capture plant," in *Influence of gas turbine exhaust CO_2 concentration on the performance of post combustion carbon capture plant*, 2015.

[78]   M. P. Usman Ali, Carolina Font Palma, Kevin J Hughes, Derek B Ingham, Lin Ma, "Impact of the operating conditions and position on the performance of a micro gas turbine," 2015.

[79]   TMI, "Impacts of exhaust gas recirculation on gas turbines," 2011. .

[80]   M. L. Erika Palfi, Laura Herraiz, Eva Sanchez Fernandes, "Selective Exhaust Gas Recirculation in Combined Cycle Turbine Power Plants with Post Combustion Carbon Capture," Edinburgh.

[81]   J. Y. Hailong Li, Mario Ditaranto, "Carbon capture with low energy penalty: supplementary fired natural gas combined cycles," *Appl. Energy*, vol. 97, pp. 164–169, 2012.

[82]   M. P. Maria Elena Diego, Muhammad Akram, Jean-Michel Bellas, Karren N. Finney, "Making gas-CCS a commercial reality: The challenges of scaling up," *Greenh. Gases Sci. Technol.*, 2017.

[83] M. L. Abigail Gonzalez Diaz, Eva Sanchez Fernandez, Jon Gibbins, "Sequential supplementary firing in natural gas combined cycle with carbon capture: A technology option for Mexico for low-carbon electrcity generation and CO_2 enhanced oil recovery," *Int. J. Greenh. Gas Control*, vol. 51, pp. 330–345, 2016.

[84] J. Y. Maria Jonsson, "Humidified gas turbines - a review of proposed and implemented cycles," *Energy*, vol. 30, no. 7, pp. 1013–1078, 2005.

[85] D. B. Hailong Li, Mario Ditaranto, "Technologies for increasing CO_2 ceoncentration in exhaust gas from natural gas fired power production with post-combustion, amine based CO_2 system," *Energy*, vol. 36, no. 2, pp. 1124–1133, 2011.

[86] S. R. Avinash Shankar Rammohan Subramanian, Kristin Jordal, Rahul Anantharaman, Brede A. L. Hagen, "A comparison of Post-combustion Capture Technologies for the NGCC," *Energy Procedia*, vol. 114, pp. 2631–2641, 2017.

[87] A. S. Renjie Shao, "Amines used in CO_2 capture; health and environmental impacts," 2009. [Online]. Available: http://bellona.org/assets/sites/3/2015/06/fil_Bellona_report_September__2009_-_Amines_used_in_CO2_capture-11.pdf. [Accessed: 24-Oct-2018].

[88] J. L. N. Ralph H. Weiland, Nathan A. Hatcher, "Benchmarking solvents for carbon capture," *Digital Refining*, 2010. [Online]. Available: http://www.digitalrefining.com/article/1000737,Benchmarking_solvents_for_carbon_capture.html#.W9BOC2hKhaQ. [Accessed: 24-Oct-2018].

[89] P. Luis, "Use of MEA for CO_2 capture in a global scenario: Consequences and alternatives," *Desalination*, vol. 380, pp. 93–99, 2016.

[90] F. Rezazadeh, W. F. Gale, M. Akram, K. J. Hughes, and M. Pourkashanian, "Performance evaluation and optimisation of post combustion CO_2 capture processes for natural gas applications at pilot scale via a verified rate-based model," *Int. J. Greenh. Gas Control*, vol. 53, pp. 243–253, 2016.

[91] A. S. J. Eni Oko, Meihong Wang, "Current status and future development of solvent-based carbon capture," *Coal Sci. Technol.*, 2017.

[92] K. S. Ajay Singh, "Shell Cansolv CO_2 capture technology: Achievement from First Commercial Plant," *Energy Procedia*, vol. 63, pp. 1678–1685, 2014.

[93] C-CAPTURE, "C-Capture," 2019. [Online]. Available: https://www.c-capture.co.uk/. [Accessed: 14-Nov-2019].

[94] N. M. D. Mai Bui, Mathilde Fajardy, "Bio-energy with carbon capture and storage (BECCS): Opportunities for performance improvement," *Fuel*, vol. 213, pp. 164–175, 2018.

[95] Carbon Brief, "The history of BECCS," 2015. [Online]. Available: https://www.carbonbrief.org/beccs-the-story-of-climate-changes-saviour-technology. [Accessed: 24-Oct-2018].

[96] International Energy Agency, "Potentials for Biomass and Carbon Capture and Storage," Cheltenham, UK, 2011.

[97] International Energy Agency, "A brief History of CCS and Current Status." [Online]. Available: https://ieaghg.org/docs/General_Docs/Publications/Information_Sheets_for_CCS_2.pdf. [Accessed: 25-Oct-2018].

[98] Global CCS Institute, "Test centers and other initiatives." [Online]. Available: https://www.globalccsinstitute.com/projects/test-centers-and-other-initiatives. [Accessed: 25-Oct-2018].

[99] E. M. M. Bui, I. Gunawan, T. V. Verheyen, "24 - Dynamic operation of liquid absorbent-based post-combustion CO_2 capture plants," *Absorption-based Post-combustion Capture of Carbon Dioxide*, pp. 589–621, 2016.

[100] M. C. M. Sanoja A. Jayarathna, Bernt Lie, "Development of a Dynamic Model of Post Combustion CO_2 Capture Process," *Energy Procedia*, vol. 37, pp. 1760–1769, 2013.

[101] P. L. F. Jozsef Gaspar, Anne Gladis, John Bagterp Jorgensen, Kaj Thomsen, Nicolas Von Solms, "Dynamic Operation and Simulation of Post-Combustion CO_2 Capture," *Energy Procedia*, vol. 86, pp. 205–214.

[102] P. Tait, B. Buschle, I. Ausner, P. Valluri, M. Wehrli, and M. Lucquiaud, "A pilot-scale study of dynamic response scenarios for the flexible operation of post-combustion CO_2 capture," *Int. J. Greenh. Gas Control*, vol. 48, pp. 216–233, 2016.

[103] PACT, "PACT 'Accelerating The Development Of New Technologies,'" 2018. [Online]. Available: https://pact.group.shef.ac.uk/facilities/. [Accessed: 17-Oct-2018].

[104] UKCCSRC, "Pilot-Scale Advanced Capture Technology: Gas Turbine," 2013. [Online]. Available: http://www.pact.ac.uk/facilities/PACT-Core-Facilities/Gas-Turbine/. [Accessed: 10-Jul-2017].

[105] M. P. Thom Best, Karen. N. Finney, Derek B. Ingham, "Impact of CO_2-enriched combustion air on micro-gas turbine performance for carbon capture," *Energy*, vol. 115, pp. 1138–1147, 2016.

[106] NewEnCo, "Turbec T100 Microturbine," 2018. [Online]. Available: http://www.newenco.co.uk/combined-heat-power/turbec-t100-microturbine. [Accessed: 23-Mar-2018].

[107] UKCCSRC, "Pilot-Scale Advanced Capture Technology," 2013. [Online]. Available: http://www.pact.ac.uk/PACT-Core-Facilities/250kW-Air-Combustion-Plant/. [Accessed: 10-Jul-2017].

[108] M. P. Thom Best, Karen N. Finney, Derek B. Ingham, "CO_2 enhanced and humidified operation of micro-gas turbine for carbon capture," *J. Clean. Prod.*, vol. 176, pp. 370–382.

[109] M. P. Karen N. Finney, Andrea De Santis, Thom Best, Alastair G. Clements, Maria Elena Diego, "Exhaust Gas Recycling for Enhanced CO_2 Capture: Experimental and CFD Studies on Micro-Gas Turbine," *Ind. Combusiton, Int. Flame Res. Found.*, vol. Special Ed, 2018.

[110] U. K. C. C. and S. R. Centre, "Solvent-based carbon capture plant," 2013. [Online]. Available: http://www.pact.ac.uk/facilities/PACT-Core-Facilities/Solvent-based-Carbon-Capture-Plant/. [Accessed: 02-Jul-2017].

[111] E. O. Agbonghae, T. Best, K. N. Finney, C. F. Palma, K. J. Hughes, and M. Pourkashanian, "Experimental and process modelling study of integration of a micro-turbine with an amine plant," *Energy Procedia*, vol. 63, pp. 1064–1073, 2014.

[112] P. Tait, B. Buschle, K. Milkowski, M. Akram, and M. Pourkashanian, "International Journal of Greenhouse Gas Control Flexible operation of post-

combustion CO 2 capture at pilot scale with demonstration of capture-e ffi ciency control using online solvent measurements," *Int. J. Greenh. Gas Control*, vol. 71, no. June 2017, pp. 253–277, 2018.

[113] E. S. H. David Thimsen, Andrew Maxson, Vian Smith, Toine Cents, Olav Falk-Pedersen, Oddvar Gorset, "Results from MEA testing at the CO2 technology centre mongstad. part 1: Post-combustion CO2 capture testing methodology," *Elsevier Energy Procedia*, vol. 63, pp. 5938–5958, 2014.

[114] Y. N. Xu Zhang, Kaiyun Fu, Zhiwu Liang, Zhen Yang, Wichitpan Rongwong, "Experiemental Studies of Regeneration Heat Duty for CO2 Desorption from Aqueous DETA Solution in a Randomly Packed Column," *GHG -12*, vol. 63, pp. 1497–1503, 2014.

[115] Y. Z. and J. L. Jie Gao, Jun Yin, Feifei, Xin Chen, MingTong, Wanzhong Kang, "Experimental Study of Regeneration Performance for CO2 Desorption from a Hybrid Solvent MEA-Methanol in a stripper Column Packed with Three Different Packing: Sulzer BX500, Mellapak Y500 and Pall Rings 16 * 16," *AIChE*, 2017.

[116] C. C. Xiaofei Li, Shujuan, "Experimental study of energy requirement of CO2 desorption from rich solvent," *GHGT - 11*, vol. 37, p. 1843, 2013.

[117] G. Technologies, "Gasmet." [Online]. Available: https://www.gasmet.com/products/category/portable-gas-analyzers/dx4000/. [Accessed: 22-Oct-2018].

[118] ThermoFisher, "FTIR Basics." [Online]. Available: https://www.thermofisher.com/uk/en/home/industrial/spectroscopy-elemental-isotope-analysis/spectroscopy-elemental-isotope-analysis-learning-center/molecular-spectroscopy-information/ftir-information/ftir-basics.html. [Accessed: 22-Oct-2018].

[119] Gasmet, "Gasmet DX4000." [Online]. Available: https://www.gasmet.com/products/category/portable-gas-analyzers/dx4000/. [Accessed: 05-Nov-2018].

[120] Findlight blog, "FTIR: Fourier-Transform Infrared Spectroscopy Principles and Applications," 2019. [Online]. Available:

https://www.findlight.net/blog/2019/03/27/ftir-principles-applications/.
[Accessed: 18-Nov-2019].

[121] Emerson, "Micro Motion 5700 Field-Mount Transmitter," 2019. [Online].
Available: https://www.emerson.com/en-us/catalog/automation-
solutions/measurement-instrumentation/micro-motion-sku-
5700?fetchFacets=true#facet:&facetLimit:&productBeginIndex:0&orderBy:&pageV
iew:list&minPrice:&maxPrice:&pageSize:&. [Accessed: 18-Nov-2019].

[122] Grundfus, "Vertical multistage centrifugal pumps," 2019. [Online]. Available:
https://www.lenntech.com/Data-sheets/Grundfosliterature-CR-serie-GB-L.pdf.
[Accessed: 18-Nov-2019].

[123] Mettler Toledo, "Excellence Titrator T7." [Online]. Available:
https://www.mt.com/gb/en/home/products/Laboratory_Analytics_Browse/Prod
uct_Family_Browse_titrators_main/Titration_Excellence/T7_Titrator.html.
[Accessed: 23-Oct-2018].

[124] HACH, "FerroVer® Iron Reagent Powder Pillows, 10 mL, Pk/100," 2019. [Online].
Available: https://www.hach.com/ferrover-iron-reagent-powder-pillows-10-ml-pk-
100/product?id=7640176719. [Accessed: 12-Jun-2019].

[125] HACH, "POCKET Colorimeter II Colorimeter Test Kit for Iron analysis," 2019.
[Online]. Available: https://uk.hach.com/pocket-colorimeter-ii-colorimeter-test-
kit-for-iron-analysis/product-downloads?id=25114271808. [Accessed: 12-Jun-2019].

[126] HACH, "Pocket Colorimeter II," 2014. [Online]. Available:
file:///C:/Users/Abdul/Downloads/DOC022.L1.80451_1ed.pdf. [Accessed: 12-Jun-
2019].

[127] N. M. D. Salman Masoudi Soltani, Paul S. Fennell, "A parametric study of CO_2
capture from gas-fired power plants using monoethanolamine (MEA) _ Elsevier
Enhanced Reader," *Int. J. Greenh. Gas Control*, vol. 63, pp. 321–328, 2017.

[128] N. S. Ahmed Alhajaj, Niall Mac Dowell, "A techno-economic analysis of post-
combustion CO_2 capture and compression applied to a combined cycle gas turbine:
Part I. A parametric study of the key technical performance indicators,"
InternationalJournalofGreenhouseGasControl, vol. 44, pp. 26–41, 2015.

[129] M. R. M. Abu-Zahra, L. H. J. Schneiders, J. P. M. Niederer, P. H. M. Feron, and G. F. Versteeg, "CO₂ capture from power plants. Part I. A parametric study of the technical performance based on monoethanolamine," *Int. J. Greenh. Gas Control*, vol. 1, no. 1, pp. 37–46, 2007.

[130] M. Akram, K. Milkowski, J. Gibbins, and M. Pourkashanian, "Comparative energy and environmental performance of 40 % and 30 % monoethanolamine at PACT pilot plant," *International Journal of Greenhouse Gas Control*, vol. 95. 2020.

[131] P.-L. C. C. Gouedard, D. Picq, F.Launay, "Amine degradation in CO₂ capture. I. A review," *Int. J. Greenh. Gas Control*, vol. 10, pp. 244–270, 2012.

[132] and A. V. Roongrat Sakwattanapong, Adisorn Aroonwilas, "Behavior of Reboiler Heat Duty for CO₂ Capture Plants Using Regenerable Single and Blended Alkanolamines," *Ind. Eng. Chem. Res.*, vol. 44, pp. 4465–4473, 2005.

[133] Global CCS Institute, "Thermal Degradation of MEA." [Online]. Available: https://hub.globalccsinstitute.com/publications/32-thermal-degradation-mea. [Accessed: 02-May-2019].

[134] Jason Davis and Gary Rochelle, "Thermal degradation of monoethanolamine at stripper conditions," *Elsevier Energy Procedia*, vol. 1, pp. 327–333, 2009.

[135] G. T. Rochelle, "Thermal degradation of amines for CO₂ capture," *Curr. Opin. Chem. Eng.*, vol. 1, no. 2, pp. 183–190, 2012.

[136] G. T. R. Hanne M. Kvamsdal, "Effects of the Temperature Bulge in CO₂ Absorption from Flue Gas by Aqueous Monoethanolamine," *Ind. Eng. Chem. Res*, vol. 47, pp. 867–875, 2008.

[137] P. T. Teerawat Sanparsertparnich, Raphael Idem, "CO₂ absoprtion in an absorber column with series of intercooler circuits," vol. 4, pp. 1676–1682, 2011.

[138] Optimized Gas Treating, Inc., "Improve Deep CO₂ Removal with Intercooling," *The Contactor*, vol. 9, no. 3, 2015.

[139] Digital Refining, "Making sense of amine absorber temperature profiles," 2017. [Online]. Available: https://www.digitalrefining.com/article/1001373,Making_sense_of_amine_absorber

_temperature_profiles.html#.XMshWOhKhaQ. [Accessed: 02-May-2019].

[140] D. S. Fatemeh Rezazadeh, William F. Gale, Gary T. Rochelle, "Effectiveness of absorber intercooling for CO₂ absorption from natural gas fired flue gases using monoethanolamine solvent," *Int. J. Greenh. Gas Control*, vol. 58, pp. 246–255, 2017.

[141] K. A. H. Yann Le Moullec, Thibaut Neveux, Adam Al Azki, Actor Chikukwa, "Process Modifications for Solvent-Based Post CombustiPon CO₂ Capture," *GHGT-12*, vol. 63, pp. 1470–1477, 2014.

[142] X. Luo, K. Fu, Z. Yang, H. Gao, W. Rongwong, and Z. Liang, "Experimental Studies of Reboiler Heat Duty for CO 2 Desorption from Triethylenetetramine (TETA) and Triethylenetetramine (TETA) + N - Methyldiethanolamine (MDEA)," 2015.

[143] Scottish Environment Protection Agency, "Review of amine emissions from carbon capture systems," 2015.

[144] "Corrosion in amine systems - a review," *Carbon Capture J.*, 2012.

[145] S. G. Jean Kittel, "Corrosion in CO 2 Post-Combustion Capture with Alkanolamines – A Review," *HAL archieves-ouvertes*, 2014. [Online]. Available: https://hal-ifp.archives-ouvertes.fr/hal-01085365/document. [Accessed: 05-Feb-2020].

[146] P. Moser *et al.*, "Results of the 18-month test with MEA at the post-combustion capture pilot plant at Niederaussem – new impetus to solvent management, emissions and dynamic behaviour," *International Journal of Greenhouse Gas Control*, vol. 95. 2020.

[147] R. Singh, "Different forms of corrosion in industries," *Counc. Sci. Ind. Res.*, 2011.

[148] R. B. N. Arthur L. Kohl, *Gas purification*, 5th Editio. Houston, Texas: Gulf Publishing Company, 1997.

[149] N. I. Sakinul Islam, Rozita Yusoff, Brahim Si Ali, "Degradation studies of amines and alkanolamines during sour gas treatment process," *Int. J. Phys. Sci.*, vol. 5, pp. 97 - 109, 2010.

[150] P.-L. C. A. Rey, C. Gouedard, N. Ledirac, M. Cohen, J. Dugay, J. Vial, V.Pichon,

L.Bertomeu, D. Picq, D. Bontemps, F.Chopin, "Amine degradation in CO_2 capture. 2. New degradation products of MEA. Pyrazine and alkylpyrazines: Analysis, mechanism of formation and toxicity," *Int. J. Greenh. Gas Control*, vol. 19, pp. 576–583, 2013.

[151]   Stephen A. Bedell, "Oxidative degradation mechanisms for amines in flue gas capture," *Energy Procedia*, vol. 1, no. 1, pp. 771–778, 2009.

[152]   A. J. G. Kali-Stella Zoannou, Devin J. Sapsford, "Thermal degradation of monoethanolamine and its effect on CO_2 capture capacity," *Int. J. Greenh. Gas Control*, vol. 17, pp. 423–430, 2013.

[153]   K. A. H. and A. B. Eirik Falck da Silva, "Emissions from CO_2 capture plants; an overview," *GHGT - 11*, vol. 37, pp. 784–790, 2013.

[154]   and P.-L. C. Helene Lepaumier, Dominique Picq, "New Amines for CO_2 Capture. I. Mechanisms of Amine Degradation in the Presence of CO_2," *Appl. Chem.*, vol. 48, pp. 9061–9067, 2009.

[155]   S. B. Fredriksen and K.-J. Jens, "Oxidative degradation of aqueous amine solutions of MEA, AMP, MDEA, Pz: A review," *GHGT-11*, pp. 1770–1777, 2013.

[156]   H. F. S. Solrun Johanne Vevelstad, Andreas Grimstvedt, Jørund Elnan, Eirik Falck da Silva, "Oxidative degradation of 2-ethanolamine: The effect of oxygen concentration and temperature on product formation," *Int. J. Greenh. Gas Control*, vol. 18, pp. 88–100, 2013.

[157]   C. P.-L.Carrette, "Amine degradation in CO_2 capture. 3. New degradation products of MEA in liquid phase: Amides and nitrogenous heterocycles," *Int. J. Greenh. Gas Control*, vol. 29, pp. 61–69, 2014.

[158]   M. P. Richard Porter, Kevin Hughes, Kris Milkowski, "Amine Degradation Modelling," Leeds, 2015.

[159]   Qian Susan Chi, "Oxidative Degradation of Monoethanolamine," University of Texas at Austin, 2000.

[160]   E. S. H. Anne Kolstad Morken, Steinar Pedersen, Eirik Romslo Kleppe, Armin Wisthaler, Kai Vernstad, Øyvind Ullestad, Nina Enaasen Flø, Leila Faramarzi,

"Degradation and Emission Results of Amine Plant Operations from MEA Testing at the CO₂ Technology Centre Mongstad," *Energy Procedia*, vol. 114, pp. 1245–1262, 2017.

[161] T. V. V. Jillian Dickinson, Andrew Percy, Graeme Puxty, "Oxidative degradation of amine absorbents in carbon capture systems – A dynamic modelling approach," *Int. J. Greenh. Gas Control*, pp. 391–400, 2016.

[162] S. C. Gary Rochelle, "Oxidative Degradation of Monoethanolamine," *Ind. Eng. Chem. Res.*, 2002.

[163] H. F. S. Hélène Lepaumier, Eirik F. da Silva, Aslak Einbu, Andreas Grimstvedt, Jacob N. Knudsen, Kolbjørn Zahlsen, "Comparison of MEA degradation in pilot-scale with lab-scale experiments," *GHGT-10*, vol. 4, pp. 1652–1659, 2011.

[164] Adeola Bello and Raphael O. Idem, "Comprehensive Study of the Kinetics of the Oxidative Degradation of CO₂ Loaded and Concentrated Aqueous Monoethanolamine (MEA) with and without Sodium Metavanadate during CO₂ Absorption from Flue Gases," *Ind. Eng. Chem. Res.*, vol. 45, pp. 2569–2579, 2006.

[165] Andrew J. Sexton and Gary T. Rochelle, "Reaction Products from the Oxidative Degradation of Monoethanolamine," *Ind. Eng. Chem. Res.*, vol. 50, pp. 667–673, 2011.

[166] P. A. V. M. Rahul R. Bhosale1*, Anand Kumar1*, Fares A. Almomani1, Shahd Gharbia1, Darren Dardor1, Mehak Jilani1, Jamila Folady1, Moustafa Ali1, Eman Eid1, Shiva Yousefi1, Diana Abuarja1, "Oxidative degradation of co2 absorbing aqueous amine solvents," 2015.

[167] E. G. Alexander Rieder, Sanjana Dhingra, Purvil Khakharia, Luigi Zangrilli, Bernd Schallert, Robin Irons, Sven Unterberger, Peter van Os, "Understanding solvent degradation: A study from three different pilot plants within the Octavius project," *13th Int. Conf. Greenh. Gas Control Technol. GHGT-13, 14-18 Novemb. 2016, Lausanne, Switz.*, vol. 114, pp. 1195–1209, 2017.

[168] S. G. J. Kittel, "Corrosion in CO 2 Post-Combustion Capture with Alkanolamines – A Review," *HAL*, 2014.

[169] Natural Gas (Second Edition), "Monoethanolamine," *Sci. Direct*, 2019.

[170] D. A. H. R. B Nielson, K. R. Lewis, John G. McCullough, "Controlling Corrosion in Amine Treatment Plants." [Online]. Available: https://www.amine-gas-treatment.com/dbimg/1142527275.pdf. [Accessed: 05-Feb-2020].

[171] R. K. Aida Rafat, Mert Atilhan, "Corrosion Behavior of Carbon Steel in CO_2 Saturated Amine and Imidazolium-, Ammonium-, and Phosphonium-Based Ionic Liquid Solutions," *Ind. Eng. Chem. Res.*, 2015.

[172] I. M. S. S. N. lShaukat A.Mazari, Brahim Si Ali, Badrul M.Jan, "An overview of solvent management and emissions of amine-based CO_2 capture technology," *Int. J. Greenh. Gas Control*, vol. 34, pp. 129–140, 2015.

[173] A. W. T. Spietz, T. Chwola, A. Krotki, A. Tatarczuk, L. Wieclaw-Solny, "Ammonia emission from CO_2 capture pilot plant using aminoethylethanolamine," *Int. J. Environ. Sci. Technol.*, vol. 15, pp. 1085–1092, 2018.

[174] S. P. Anne Kolstad Morkena *et al.*, "Degradation and Emission Results of Amine Plant Operations from MEA Testing at the CO_2 Technology Centre Mongstad," *13th Int. Conf. Greenh. Gas Control Technol. GHGT-13*, vol. 13, pp. 14–18, 2017.

[175] T. Nguyena, M. Hilliard, and G. Rochelle, "Volatility of aqueous amines in CO_2 capture," *Energy Procedia GHGT - 10*, vol. 4, pp. 1624–1630, 2011.

[176] A. B. J. Kittel, R.Idem, D.Gelowitz, P. Tontiwachwuthikul, G. Parrain, "Corrosion in MEA unbits for CO_2 capture: pilot plant studies," *GHGT - 9*, vol. 1, pp. 791–797, 2009.

[177] Omega, "Technical Dissolved Oxygen - The Fundamentals," 2020. [Online]. Available: https://www.omega.co.uk/techref/ph-1.html. [Accessed: 26-Mar-2020].

[178] R. P. Livia Vittori Antisari, A. A.-B. Maddalena Pennisi, Serena Carbone, and G. V. Umberto Aviani, "Potentially toxic element cycles and characterization of multiple sources in the irrigation ditches from the ravenna coastal plains though trace elements and isotope geochemistry," *Environ. Qual.*, vol. 3, pp. 21–32, 2010.

[179] T. Nakagaki, I. Tanaka, Y. Furukawa, H. Sato, and Y. Yamanaka, "Experimental evaluation of effect of oxidative degradation of aqueous monoethanolamine on heat of CO_2 absorption, vapor liquid equilibrium and CO_2 absorption rate," *Energy Procedia*, vol. 63, pp. 2384–2393, 2014.

[180] JUMO, "JUMO ecoLine O-DO - Optical Sensor for Dissolved Oxygen," 2020. .

[181] L. E. Maxime H. Wang, Alain Ledoux, "Oxygen Solubility Measurements in a MEA/H2O/CO2 Mixture," *J. Chem. Eng. data*, no. 58, pp. 1117–1121, 2013.

[182] Process System Enterprise Ltd, "gCCS - Overview," 2017. [Online]. Available: https://www.psenterprise.com/products/gccs. [Accessed: 25-Oct-2017].

[183] Process Systems Enterprise Limited, "gCCS." 2016.

[184] T. H. E. Advanced and P. Modelling, "gCCS – whole-chain CCS system modelling All-Energy Motivation for systems modelling for CCS CCS System Modelling Tool-kit project gCCS overview," no. May, 2013.

[185] Process System Enterprise Ltd, "gCCS Model Documentation." PSE, United Kingdom, 2016.

[186] P. M. Tibor Nagy, Katalin Koczka, Enikő Haáz, András József Tóth, László Rácz, "Efficiency Improvement of CO2 Capture," *Period. Polytech. Chem. Eng.*, vol. 61, no. 1, pp. 51–58, 2017.

[187] M. E. Diego, J.-M. Bellas, and M. Pourkashanian, "Process Analysis of Selective Exhaust Gas Recirculation for Co2 Capture in Natural Gas Combined Cycle Power Plants Using Amines," *J. Eng. Gas Turbines Power*, vol. 139, no. December, pp. 1–10, 2017.

[188] C. C. Xiaofei Li, Shujuan Wang, "Experimental study of energy requirement of CO2 desorption from rich solvent," *GHGT-11*, vol. 37, pp. 1836–1843, 2013.

[189] Energy 2050, "Nano Materials Enhanced Membranes for Carbon Capture (Nanomemc2)." [Online]. Available: http://energy2050.ac.uk/events/nanomaterials-enhanced-membranes-for-carbon-capture-nanomemc2/. [Accessed: 04-Apr-2019].

[190] Nanomemc2, "The Project: Nanomemc2," 2019. [Online]. Available: https://www.nanomemc2.eu/the-project/. [Accessed: 04-Apr-2019].

[191] W. S. W. H. Jin Huang, Jian Zou, "Carbon Dioxide using a CO2-Selective Facilitated Transport Membrane," *Ind. Eng. Chem.*, vol. 47, pp. 1261–1267, 2008.